The Development of the Staking-Ensemble of Methods for Analyzing Academic Data

Indira Uvaliyeva, Zhenisgul Rakhmetullina, Olga Baklanova

East Kazakhstan Technical University, Department of Engineering mathematics, A. K. Protazanov Str. 69, 070004, Ust-Kamenogorsk, Kazakhsta
e-mail: {iuvalieva, zhrakhmetullina, obaklanova}@ektu.kz

György Györök

Óbuda University, Alba Regia Technical Faculty, Budai út 45, H-8000 Székesfehérvár, Hungary, e-mail: gyorok.gyorgy@amk.uni-obuda.hu

Abstract: Within the framework of this article, the Staking-ensemble of methods for analyzing academic statistics is proposed, which makes it possible to increase the effectiveness of implementing academic monitoring tasks. The relevance of the topic is the need to develop a distributed information and analytical system that integrates information resources and general principles of models and methods of monitoring the infrastructures of academic facilities based on education statistics. Education statistics is a system of indicators characterizing quantitative and qualitative changes taking place in the field of education which makes it possible to obtain information for each level of education on the number of educational institutions, the contingent of students, characteristics of the internal efficiency of the learning process, data on admission to educational institutions, graduation of specialists, quantitative and qualitative characteristics of the teaching staff, the state of the material and technical base of educational institutions. The object of the study is the system of formation of statistical data in education. The subject of the study are the approaches of combining intelligent methods of data analysis. The idea of the work is the use of modern methods of data processing in the implementation of academic monitoring in order to successfully solve the tasks of the state program for the development of education. The goal of the study is to develop an algorithm for Staking-ensemble methods for analyzing academic statistics to improve the effectiveness of academic monitoring tasks. The scientific novelty of the research is the staking-ensemble for analyzing education statistics, which aggregated the following 3 types of intellectual models: the Bayes algorithm, the decision tree algorithm, and the neural network. The practical importance of the research results lies in the applicability of the proposed Staking-ensemble algorithm for solving the problems of information and analytical support of management decision-making when tracking the business processes of monitoring, controlling and forecasting the state of distributed academic objects at various levels of training, management and functioning.

Keywords: academic statistics; analysis of indicators; Staking-ensemble algorithm; combination of intellectual methods

Introduction

Great interest in education in society and the need to make effective management decisions aimed at improving the quality of education require the use of prompt and reliable information on the state and development trends of the entire education system, its analysis and adequate interpretation. To solve this problem, it is necessary to use the processing algorithms of the system of indicators characterizing the quantitative and qualitative changes taking place in the field of education. In this study, it is proposed to apply a combination of the following algorithms for intelligent data processing: Bayes algorithm, decision tree algorithm and neural network. Education statistics cational statistics is a system of indicators characterizing quantitative and qualitative changes taking place in the field of education which makes it possible to obtain information for each level of education on the number of educational institutions, the contingent of students, characteristics of the internal efficiency of the learning process, data on admission to educational institutions, graduation of specialists, quantitative and qualitative characteristics of the teaching staff, the state of the material and technical base of educational institutions [1-4]. These data reflect the state, general assessment, trends and dynamics of development, the effectiveness of the education system, which are used to determine the effectiveness of its functioning and forecasts regarding the prospects for the development of its individual components and phenomena, as well as the basis for developing the necessary management decisions. In order to improve the efficiency of decision-making in the field of education, this study proposes a comprehensive application of methods of intellectual processing of educational statistics data.

In recent years, highly specialized data mining packages have appeared. For such packages, orientation to a narrow range of practical problems is often characteristic, and their algorithmic basis is a model using a neural network, solving trees, limited search, etc. Such developments are substantially limited in practical use. First, the approaches inherent in them are not universal with respect to the dimensions of the tasks, the type, complexity and structure of the data, the magnitude of the noise, the inconsistency of the data, and so on. Secondly, created and "tuned" to solve certain problems, they can be completely useless for others. Finally, many tasks of interest to a practical user are usually broader than the possibilities of a separate approach [5].

At the same time, the variety of algorithms for extracting knowledge (Data Mining) suggests that there is no one universal method for solving all problems [6-8]. In addition, the application of various analysis and modeling tools to the

same dataset may have different objectives: either to construct a simplified, transparent, easily interpretable model to the detriment of accuracy, or to build a more accurate but also more complex, and therefore less interpretive model.

Thus, one of the urgent tasks of the modern approach to data processing, including forecasting, is to find a compromise between indicators such as accuracy, complexity and interpretability. Most researchers prefer obtaining more accurate results since for the end users the concept of transparency is subjective. The accuracy of the results depends on the quality of the data source, the subject area and the data analysis method used.

Obtaining more accurate results is more important since in recent years there has been a significant increase in the interest in the accuracy of Data Mining models based on intelligent teaching methods, by combining the efforts of several methods and creating ensembles of predictor models, which allows improving the quality of solving analytical problems [9-12]. The training of the ensemble of models is understood as the training of the final set of basic classifiers, the results of forecasting which are then combined, and the forecast of the aggregated classifier is formed.

When forming an ensemble of models, it is necessary to solve three main tasks [13-15]:

- to choose a basic model;

- to determine the approach to the use of a training set;

- to choose a method of combining the results.

Due to the fact that the ensemble is an aggregated model consisting of separate basic models, two alternatives are possible in its formation:

- the ensemble is made up of basic models of the same type, for example, only from decision trees, only from neural networks, etc.;

- the ensemble is made up of models of different types - decision trees, neural networks, regression models, etc.[16,17].

On the other hand, when constructing an ensemble a training set is used, for the use of which there are two approaches:

- re-selection, i.e., several subsamples are extracted from the initial training set, each of which is used for training one of the ensemble models;

- the use of one training set for the training of all ensemble models.

1 Mathematical Description of the Ensemble Algorithm

Let X be the set of object descriptions, Y is the set of answers, and there is an unknown "target dependence" - the mapping f: $X \rightarrow Y$ whose values are known only for the objects of the final training sample (1):

$$(X, Y) = \{(x_1, y_1), \ldots, (x_{|(X,Y)|}, y_{|(X,Y)|})\} \quad (1)$$

It is required to construct an algorithm a: $X \rightarrow Y$ approximating the target dependence on the entire set X.

Along with the sets X and Y, we introduce an auxiliary set R, called the space of estimates. We consider algorithms having the form of a superposition (2):

$$a(x)=C(b(x)) \quad (2)$$

the function b: $X \rightarrow R$ is called an algorithmic operator, and the function C: $R \rightarrow Y$ is a decisive rule. Many classification algorithms have exactly this structure: first estimates of the object's belonging to classes are calculated, then the decision rule translates these estimates into the class number. The value of the estimate b (x) can be the probability that the object belongs to the class, the distance from the object to the separating surface, the degree of confidence in the classification, and so on.

The composition T of algorithms $a_t(x)=C(b_t(x))$, $t=1,\ldots,T$ is the superposition of the algorithmic operators $b_t : X \rightarrow R$, correcting the operation F: $RT \rightarrow R$ and the decision rule C: $R \rightarrow Y$ (3):

$$a(x) = C(F(b_1(x), \ldots b_T(x))), x \in X \quad (3)$$

The algorithms a_t, and sometimes the operators b_t, are called basic algorithms.

Superpositions of the form $F(b_1, \ldots b_T)$ are mappings from X to R, that is, again, by algorithmic operators.

We denote the set of base classifiers as α. Using the terms formulated above, the idea of stacking is the use as the algorithmic operators b_t of the base classifiers $A \in \alpha$, and as the corrective operation F of some meta-classifier M.

In turn, for combining the results, there are several best-known corrective operations:

Simple Voting:

$$b(x) = F(b_1(x), \ldots b_t(x)) = \frac{1}{T} \sum_{t=1}^{T} b_t(x) \quad (4)$$

Weighted Voting (5):

$$b(x) = F(b_1(x), \ldots b_t(x)) = \sum_{t=1}^{T} w_t \times b_t(x),$$
$$\sum_{t=1}^{T} w_t = 1, w_t \geq 0; \tag{5}$$

Mixture of Experts [18] (6):

$$b(x) = F(b_1(x), \ldots b_t(x)) = \sum_{t=1}^{T} w_t(x) \times b_t(x),$$
$$\sum_{t=1}^{T} w_t(x) = 1, \forall x \in X. \tag{6}$$

It is obvious that Simple Voting is only a special case of Weighted Voting, and Weighted Voting is a special case of a Mixture of Experts. It is also worth noting that, because of the large number of degrees of freedom, the training of a Mixture of Experts takes much longer than other compositional algorithms, so their practical applicability is justified only in the case of a priori information on the competence functions $g_t(x)$, which are most often determined by:

- the sign of $f(x)$ (7):

$$w_t(x;\alpha;\beta) = \sigma(\alpha f(x) + \beta),$$
$$\alpha, \beta \in R; \tag{7}$$

- direction $\alpha \in R^n$ (8):

$$w_t(x;\alpha;\beta) = \sigma(x^{\mathrm{T}}\alpha + \beta),$$
$$\alpha \in R^n, \beta \in R; \tag{8}$$

- distance to $\alpha \in R^n$ (9):

$$w_t(x;\alpha;\beta) = \exp(-\beta\|x - \alpha\|^2),$$
$$\alpha \in R^n, \beta \in R; \quad \text{.....(9)}$$

more complex methods (by means of estimating the density of data distribution, etc.). In the above formulas of functions, the competencies of the sigmoid are equal (10) [19]:

$$\sigma(z) = \frac{1}{1 + e^{-z}}. \tag{10}$$

The use of model ensembles to solve various analysis problems opens up wide opportunities for improving the efficiency of Data Mining models. Therefore, in the past few years, active research has been carried out in this area, resulting in a large number of different methods and algorithms for the formation of ensembles. Among them, the most widely used methods are bagging, boosting and stacking [20].

2 Mathematical Description of the Stacking Algorithm

The Stacking algorithm is not based on a mathematical model. His idea is to use as the base models different classification algorithms, trained on the same data. Then, the meta-classifier is trained on the initial data, supplemented by the results of the prediction of the basic algorithms. Sometimes the meta-classifier uses not the results of the prediction of the basic algorithms, but the estimates of the distribution parameters obtained by them, for example, the probabilities of each class.

The generalized scheme for implementation of the stacking algorithm is shown in Figure 1. The idea of Stacking is that the meta-algorithm learns to distinguish which of the basic algorithms should be "trusted" on which areas of the input data.

The Stacking algorithm is trained using cross-validation: the data are randomly divided into n times, T1 and T2, containing each time (for example, for n = 10) 90% and 10% of the data, respectively. Basic algorithms are trained on data from T1, and then applied to data from T2. The data from T2 is combined with the forecasts of the base classifiers and trains the meta-classifier. Since after n partitions all available data will end up in some one of T1 and in some of T2, the meta-classifier will be trained on full data [21].

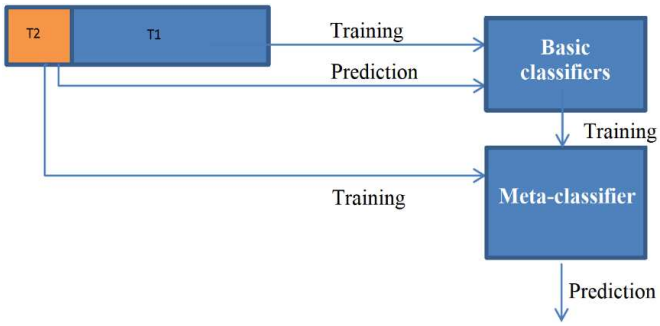

Figure 1
Generalized scheme for implementing the Stacking-ensemble algorithm

The statement of the classification problem is as follows.

Let X be the set of descriptions of objects, Y is a finite set of numbers (names, labels) of classes. There is an unknown "objective dependence" - the mapping f : $X \to Y$ whose values are known only on the objects of the final training sample $(X, Y) = \{(x1, y1), \ldots, (x|(X,Y)|, y|(X,Y)|)\}$.

It is required to construct an algorithm a a: $X \to Y$, capable of classifying an arbitrary object $x \in X$. The notation used in Table 1 is used.

Table 1
Notations and their descriptions

Notation	Description
(X0, Y0)	validation sample
A	basic classifier used to build meta tags
A.fit(X, Y)	function of training classifier A on (X, Y)
A.predict(X)	function predicting the target variable for X by the classifier A
M	some metaclassifier
MF(X, A)	meta-attribute obtained by classifier A for sample X
P	the final prediction of the stack for the validation sample
concatV(Xi , Xj)	concatenation operation Xi and Xj on columns
concatH(Xi , Xj)	concatenation operation Xi and Xj in rows

The idea of stacking is to train the meta-classifier M on (1) the original characteristics, the matrix X, and (2) on the predictions (meta-features) obtained with the help of the base classifiers. The meta-attributes obtained using the classifier A for the sample X will be denoted by MF(X, A).

Figure 2 shows the implementation of the stacking algorithm.

The simplest stacking algorithm for P sample prediction is based on dividing the training sample (X, Y) into 2 parts: (X1,Y1) and (X2,Y2).

A.fit(X1,Y1)
MF(X2;A) := A.predict(X2)
MF(X0;A) := A.predict(X0)
M.fit(concatV(X2;MF(X2;A)); Y2)
P := M.predict(concatV(X0;MF(X0;A)))

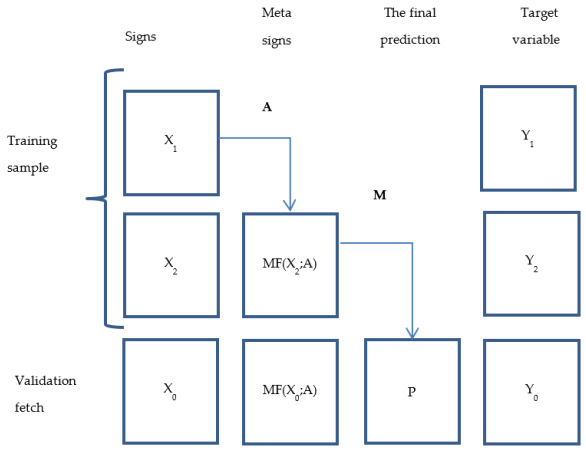

Figure 2
Schema implementation of the staking-ensemble algorithm

This algorithm is less effective because the meta-classifier is trained only on the second part of the sample P. To improve the efficiency of the prediction, you can apply this algorithm several times using different partitions and then average the predictions. The algorithm for this approach is as Fig. 3:

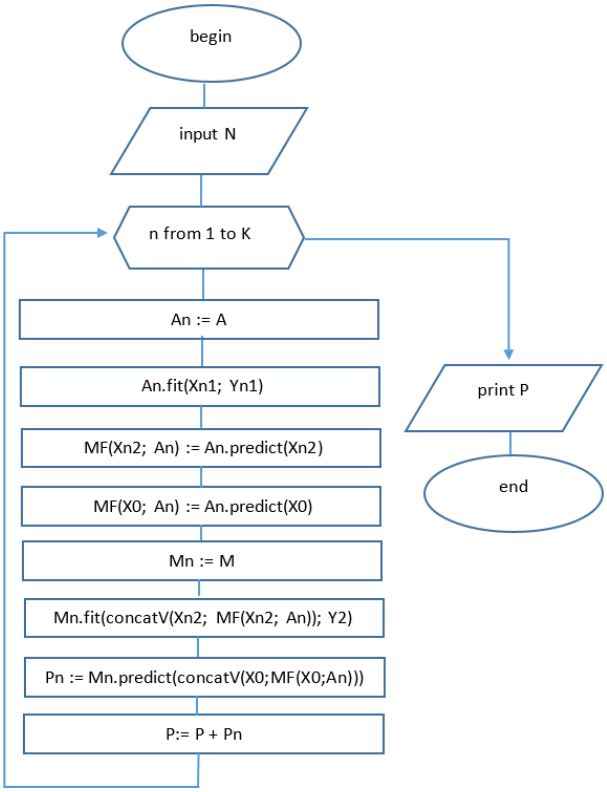

Figure 2
Algorithm of approach

Next, we represent the modification of the second algorithm, which allows us to add a new base classifier for learning set A. To do this, we need to get the meta-feature MF (X, A) for the entire training sample. The algorithm of this approach is as follows:

```
A1 := A
A1.fit(X1; Y1)
MF(X2;A1) := A1.predict(X2)
MF(X0;A1) := A1.predict(X0)
A2 := A
A2.fit(X2; Y2)
MF(X1;A2) := A2.predict(X1)
MF(X0;A2) := A2.predict(X0)
```

```
MF(X;A) := concatH(MF(X1;A2);MF(X2;A1))
MF(X0;A) := (MF(X0;A1) +MF(X0;A2)) / 2

M.fit(concatV(X;MF(X;A)); Y )
P := M.predict(concatV(X0;MF(X0;A)))
```

Thus, the modified Staking algorithm is presented, which allows the meta-classifier M to be used for learning the entire sample X. An accepted one is also a stacking representation in the form of a multilevel scheme where the features are denoted as "Level 0", meta-features obtained by training the base classifiers on the attributes as "Level 1", and so on.

3 Application of the Staking-Ensemble Algorithm for the Tasks of Academic Statistics

To construct an ensemble of models on the data of academic statistics, the Stacking algorithm was used, which aggregated the following 3 types of intellectual models: the Bayes algorithm (BC), the decision tree algorithm (DT), and the neural network (NN). The training was done on a single data set. The meta-level data used to train the meta-model will be the results of predicting models for each of the fields. To be able to be used as a meta-model of the BC, we include in the meta-level data of the class field a number for the BC, DT, and NN. Thus, the stacking-ensemble algorithm tries to train each classifier using the meta learning algorithm, which allows to find the best combination of outputs of base models. The structural scheme of the ensemble on the basis of stacking is presented in Figure 3.

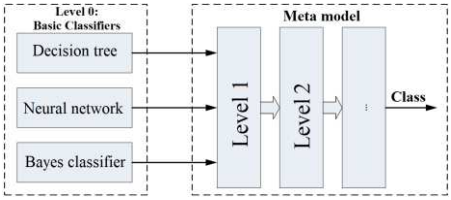

Figure 3
Block diagram of the ensemble on the basis of stacking

The base models form Level 0. At the input of the meta-model, also called the Level 1 model, the results are output from the outputs of the base models. The Level 1 example has as many attributes as there are Level 0 models, and the attribute values themselves are model outputs of the zero level. Then, based on the results obtained by the model of Level 1, a Level 2 model is constructed, etc., until some of the conditions for stopping the training are fulfilled.

Figure 4 shows the scheme of the algorithm for the ensemble of BC, DT, and NN models based on stacking.

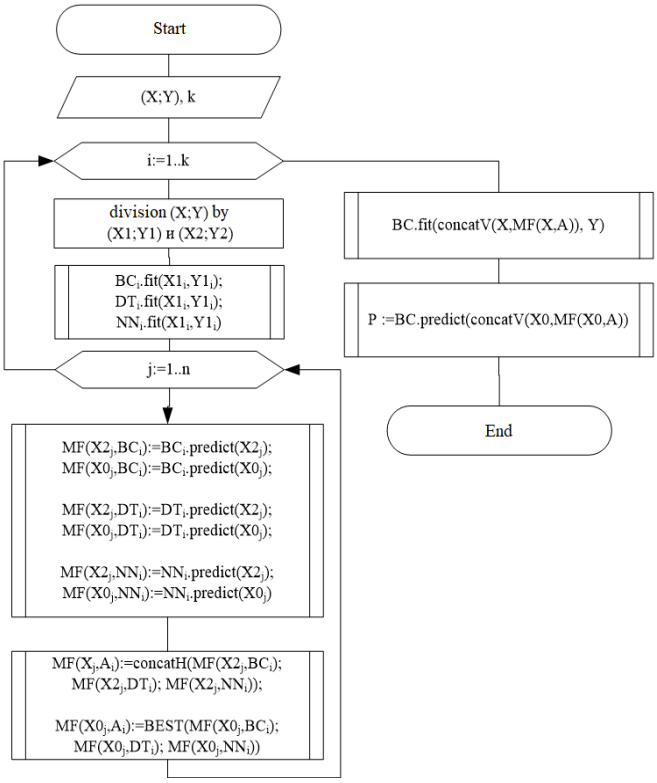

Figure 4
Diagram of an algorithm for the ensemble of BC, DR, and NC models based on stacking

The most common way to reduce the distortions caused by unsuccessful sampling is to repeat the entire learning and testing process several times with different random samples. At each iteration, a certain amount of data (for example, 2/3) is randomly selected for training, and the remaining ones are used for testing. For this, it is necessary to determine the number of iterations of the partitioning of the original data. Next, you specify the vector into which the data for learning the meta-model is collected. For each iteration, the following steps must be taken:

Step 1: Divide the original data into 2 parts: the first part is intended for learning the models, the second is for testing the model forecast. The proportion of the initial data division is chosen proceeding from the fact that as all the initial data after all the iterations are either in the 1st or 2nd part. To accomplish this, several analysis structures have been made in Analysis Services (the version number is added in the name). The sampling variability is specified through the HoldoutSeed property. It is different for different options.

Step 2: We teach the three initial models on the first part of the data.

Step 3: For each data line of the second part, you need: implement a forecast for each model; choose the most accurate of the forecast values; write a row with data and a prediction into a vector. If the vector already has this data line, then a more accurate prediction from the existing and obtained from Step 3 is recorded for it.

Step 4. After implementing all the iterations, the algorithm for constructing the meta-model is chosen. The meta-model is trained on the basis of the data collected in the vector.

To estimate the accuracy of the forecast for all iterations, a forecast accuracy chart, a classification matrix, and a cross-checking were constructed.

In the forecast accuracy chart, the forecasts of all models are compared. In this diagram, you can set the accuracy display for forecasts in general or for forecasts of a certain value. It displays a graphical representation of the accuracy change provided by the mining model. The X-axis of the diagram represents the percentage of the verification dataset used to compare forecasts. The Y-axis of the diagram represents the percentage of predicted values.

The classification matrix is created by sorting all the options into categories: whether the predicted value corresponds to the real one and whether the predicted value was true or false. These categories are sometimes also referred to as a false positive result, a true positive result, a false negative result and a true negative result. Then, all the variants in each category are recalculated, and the quantities obtained are output as a matrix.

During cross-validation, mining structures are split into cross-sections, after which cyclic learning and model checking for each data section is performed. To split the data, several sections are indicated, and each section, in turn, plays the role of verification data, while the remaining data are used to train the new model. Then, for each model a set of standard accuracy indicators is formed. Comparing the indicators of the models created for each section, you can get a good idea of how accurate the mining model is for the entire data set.

4 Implementation of the Staking-Ensemble Algorithm

To implement the experimental study of the Staking-ensemble algorithm of intellectual methods of data analysis, the following 2 objectives of academic monitoring at the higher education level were identified: 1) analysis of academic statistics data for forecasting GPA transfer points; 2) analysis of the data of academic statistics for forecasting the employment of a graduate of a university.

The study was conducted on the basis of the data of academic statistics at D. Serikbayev EKTU for 2017 - 2020 on baccalaureate (the daytime form on the basis of secondary education).

With a credit academic system, GPA (Grade Point Average) is used as the indicator of student's progress. It is a weighted average assessment of the level of the student's academic achievements in the chosen specialty, which is used to transfer the student to subsequent academic courses. Based on the Model Rules for the ongoing monitoring of academic performance, intermediate and final certification of students in higher academic institutions, approved by the #125 order of the Ministry of Education and Science of the Republic of Kazakhstan from March the 18th, 2020 and the Rules for the organization of the academic process on credit technology of education approved by the #152 order of the Ministry of Education and Science of the Republic of Kazakhstan dated 20.04.2011, in D.Serikbaev EKTU, the following transfer values of GPA for bachelor students of the daytime form of education were established on the basis of secondary education in the context of courses: for transfer to the second course - 1.5; for transfer to the third rate - 1.67; for transfer to the fourth course - 2.0; for the transfer to the fifth course - 2.1.

In Kazakhstan, the problem of employing graduates becomes more important every year. Currently, the results of numerous studies show that the current higher education system of training specialists largely does not meet the needs of the labor market. The problem of finding a job in the specialty after graduation, the problem of the first job is exacerbated every year. Even more urgent are these issues for the graduate of the university in the conditions of high socio-economic uncertainty and risks arising during economic downturns and crises. According to the purpose of the activity regulations is the creation of an effective system to facilitate the employment of graduates of the D. Serikbayev EKTU in accordance with the qualification and their adaptation to the labor market.

Thus, 2 objectives of academic monitoring implemented on the basis of the Staking-ensemble algorithm were defined to predict the following indicators of academic statistics: 1) GPA obtainment rate; 2) indicator of employment.

The Staking-ensemble algorithm assumes that data is taken for training and is divided randomly into 2 parts. The first part is used to teach the original models. Part 2 is used to predict data based on the original models and based on this forecast a meta-model is built. This operation is performed several times - so that all the initial data in different breakdowns are in the 2nd part.

To implement this algorithm, several mining structures were created in Analysis Services (the variant number was added in the name). The sampling variability is specified through the HoldoutSeed property. It is different for different options.

For each variant, the probability of occurrence of an event for each model in the ensemble is calculated. For example, for the task of analyzing the data of a transfer point set – the probability that the student will not gain a transfer point,

for the problem with the employment of graduates – the probability that the student will not be employed. From these probabilities we choose the most suitable: maximum – if the student does not score a transfer point / is not employed, and minimal – if otherwise. Based on the probabilities for each test line, a vector is formed that will be used to train the meta-model. To view the received data for learning the meta-model in MS SQL Server Management Studio, one of the following procedures is called:

- CALL SPMining.SPMining.SPortalMiningProc.GenerateTableGPA()
- CALL SPMining.SPMining.SPortalMiningProc.GenerateTableEmployment()

The following algorithm is used to create a metamodel:

```
CREATE MINING MODEL [Staking - Transferable GPA score has been scored]
(
  [ID] LONG KEY,
  [Basic Education] TEXT DISCRETE,
  [Entrance score] LONG DISCRETE,
  [Group of Specialties] TEXT DISCRETE,
  [Type of Financing] TEXT DISCRETE,
  [Year of study] LONG DISCRETE,
  [Total GPA Score For The Previous Course] LONG DISCRETIZED,
  [Specialization] TEXT DISCRETE,
  [Form of Training] TEXT DISCRETE,
  [The Number Of Undeveloped Disciplines For The Previous Course] LONG DISCRETIZED,
  [Language of Instruction] TEXT DISCRETE,
  [Class] TEXT DISCRETE PREDICT
)
USING Microsoft_Naive_Bayes(MINIMUM_DEPENDENCY_PROBABILITY=0.01)
```

Next, this model needs to be trained. Classes are identified for training, which are allocated depending on the probability. Classes are specified by a string when learning a model:

<ClassName1> = <Probability1>; <ClassName2> = <Probability2>; ...

To build a meta-model, we will use the algorithms of BC, DT and NN. Figure 5 shows the subsystem of the data analysis of academic statistics based on the Staking-ensemble algorithm.

Using several models gives the following advantages:

- realize the prediction of the output indicator of academic statistics both in numerical form (NN) and in the form of classification (DT and BC), which determines the variety of possible methods of visualizing the results;

- consistency of the results for all models allows to make a conclusion about their reliability.

The results of the Staking-ensemble algorithm implemented in the data analysis subsystem are presented below.

The training based on the basic classifiers for analyzing the data of the first objective of academic monitoring showed the following results.

The window of the subsystem with learning outcomes of the base classifier based on the BC algorithm contains the following tabs for mapping the interaction between the predicted attributes and the input attributes for the options table: the dependency network; attribute profiles; attribute characteristics; comparison of attributes.

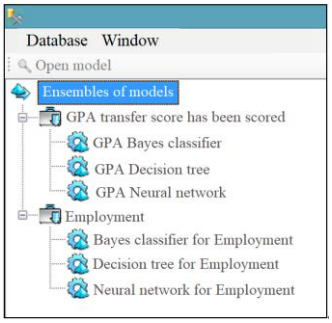

Figure 5

The main menu of the subsystem Staking-ensemble

Based on the data of academic statistics, the results of training the basic classifier on the basis of the BC algorithm for analyzing the data of the GPA set were obtained and are presented in the form of a network of dependencies in Figure 6.

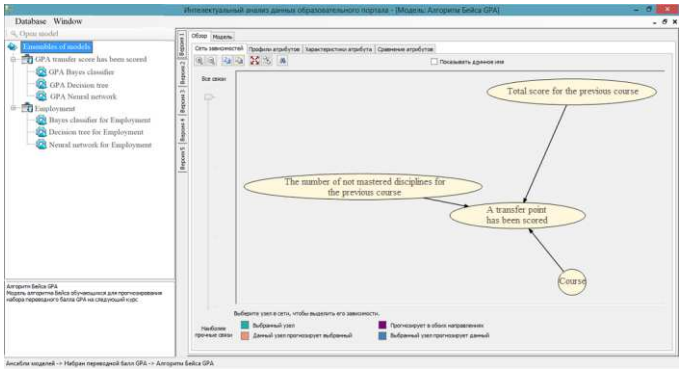

Figure 6

Subsystem window with learning base classifier results based on the BC algorithm for analysis of GPA data

The sub-system window of dependencies network tab displays the dependencies between the input indicators of the university's academic statistics and the predicted indicator that characterizes the GPA. The slider to the left of the viewer acts as a filter, tied to the strength of the dependencies. When you move the slider down, only the strongest ones are displayed. The symbols at the bottom of the subsystem window associate the color codes with the type of dependency on the

graph. As it can be seen in Figure 7, the indicator "Obtained GPA" is influenced by such indicators of academic statistics as the number of unfinished disciplines for a previous year, training, the total GPA score for the previous year of study. The basis of the second basic classifier was the decision tree algorithm, the results of which are shown in Figure 7a. This algorithm supports classification and regression, is used for predictive modeling of discrete and continuous attributes. As you can see from Figure 7b, the subsystem window contains the "Decision Tree" and "Dependency Network" tabs.

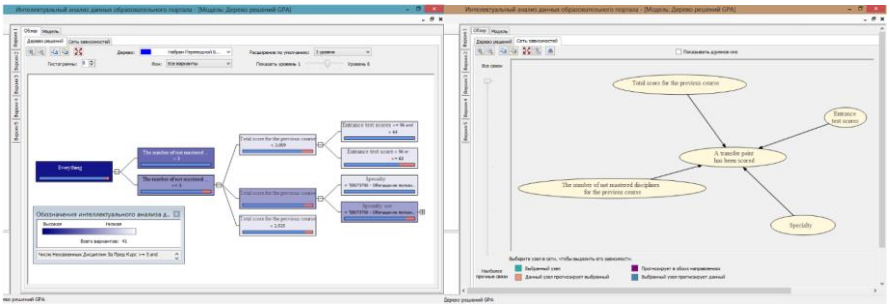

Figure 7
The window with the results of training the base classifier on the basis of the DR algorithm for analyzing the data of the GPA set

The results of training the basic classifier on the basis of the DT algorithm showed that the set of GPA has a dependence on the following indicators of the academic statistics of the university: the number of unfinished disciplines for the previous year, the GPA's total score for the previous year of study, specialty and the UNT score. Figure 8 shows the results of training the basic classifier based on the NN algorithm for analyzing data from the GPA set.

The meta-classifier Staking-ensemble was built on the basis of the BC algorithm. The results of the accuracy of the forecast implementation of Staking-ensemble based on the classification matrix.

The results of the meta-classifier training in the variation sample showed that the indicator of academic statistics "Obtained GPA" has a dependence on such indicators as the number of unfinished disciplines for the previous year, the GPA total score for the previous year, the Basic Education and the Course.

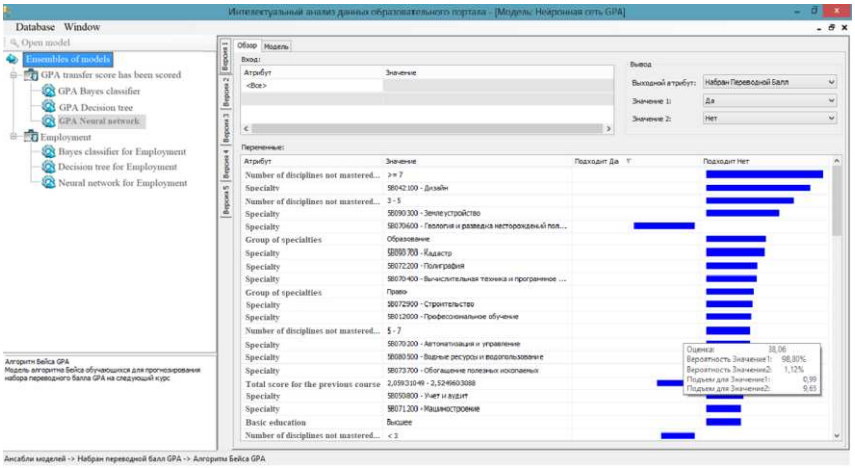

Figure 8

The window with the learning outcomes of the basic classifier based on the NN algorithm for analyzing the data of the GPA set

The windows with the results of the accuracy of the prediction of the implementation of the Staking-ensemble algorithm based on the accuracy chart is presented in Figure 9.

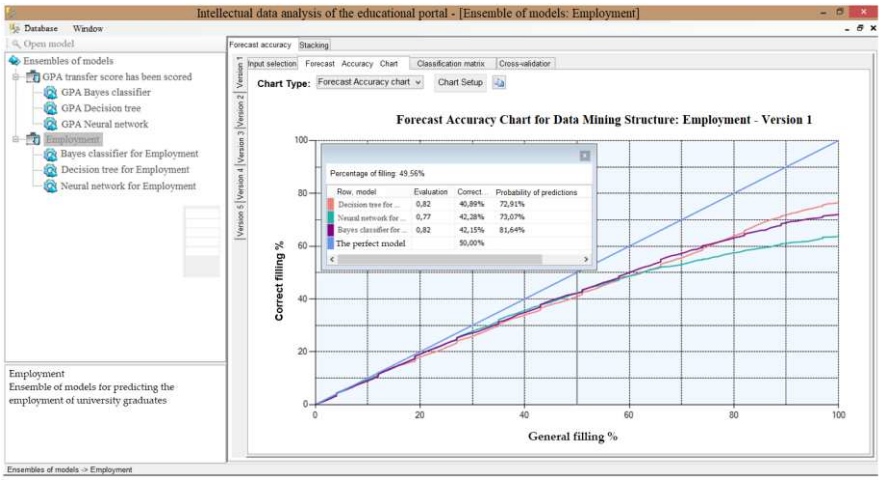

Figure 9

Staking-ensemble algorithm based on the accuracy chart

In this way the scientific novelty of the research is that for the first time the Staking-ensemble of methods for analyzing academic statistics is used to improve the effectiveness of academic monitoring processes. The practical importance of the research results lies in the applicability of the proposed Staking-ensemble

algorithm for solving the problems of information and analytical support of management decision-making when tracking the business processes of monitoring, controlling and forecasting the state of distributed academic objects at various levels of training, management and functioning.

Conclusion

To solve the analytical problems of academic statistics and to obtain more accurate results, a new approach is proposed that combines the several intellectual methods based on the creation of an ensemble of predictor models. To this end, a modified Staking-ensemble of intellectual methods for analyzing academic statistics has been developed, which allows the meta classifier to use the entire sample for learning and aggregates Bayesian algorithms, decision trees and neural networks.

To implement the experimental study of the Staking-ensemble algorithm of intelligent methods of data analysis, the indicators of academic statistics for forecasting the GPA transfer score and the employment of the graduate of the university were analyzed. The study was conducted on the basis of the data of academic statistics at D. Serikbayev EKTU for 2017-2020 on baccalaureate of the daytime form of education on the basis of secondary education.

References

[1] Cespón M. T., Lage J. M. D. Gamification, Online Learning and Motivation: A Quantitative and Qualitative Analysis in Higher Education //Contemporary Educational Technology. – 2022. – Т. 14. – №. 4. – С. ep381. https://doi.org/10.30935/cedtech/12297

[2] Larini M., Barthes A. Quantitative and statistical data in education: From data collection to data processing. – John Wiley & Sons, 2018

[3] Winkle-Wagner R., Lee-Johnson J., Gaskew A. (ed.). Critical theory and qualitative data analysis in education. – New York : Routledge, 2019

[4] Oharenko V., Kozachenko I. State Regulation Of The Education Sector Under The Conditions Of Decentralization //Baltic Journal of Economic Studies. – 2020. – Т. 6. – №. 3. – С. 99-106, doi: 10.30525/2256-0742/2020-6-3-99-106

[5] Romero C., Ventura S. Educational data mining and learning analytics: An updated survey //Wiley Interdisciplinary Reviews: Data Mining and Knowledge Discovery – 2020 – Т. 10 – №. 3 – С. e1355 doi: 10.1002/widm.1355

[6] Zamri N. E. et al. Amazon Employees Resources Access Data Extraction via Clonal Selection Algorithm and Logic Mining Approach //Entropy – 2020 – Т. 22 – №. 6 – С. 596, DOI: 10.3390/e22060596

[7] Z. Rakhmetullina, R. Mukhamedova, R. Mukasheva and E. Aitmukhanbetova, "Mathematical Model for Clinical Decision Support

System Using Genetic Algorithm," 2020 4th International Symposium on Multidisciplinary Studies and Innovative Technologies (ISMSIT), Istanbul, Turkey, 2020, pp. 1-5, doi: 10.1109/ISMSIT50672.2020.9255150

[8] Camacho D. et al. "The four dimensions of social network analysis: An overview of research methods, applications, and software tools" //Information Fusion. – 2020 – T. 63 – C. 88-120, DOI: 10.1016/j.inffus.2020.05.009

[9] L. Cai, R. Datta, J. Huang, S. Dong and M. Du, "Sleep Disorder Data Stream Classification Based on Classifiers Ensemble and Active Learning," 2019 IEEE International Conference on Bioinformatics and Biomedicine (BIBM), San Diego, CA, USA, 2019, pp. 1432-1435, doi: 10.1109/BIBM47256.2019.8983119

[10] F. Aziz, A. Lawi and E. Budiman, "Increasing Accuracy of Ensemble Logistics Regression Classifier by Estimating the Newton Raphson Parameter in Credit Scoring," 2019 5th International Conference on Computing Engineering and Design (ICCED), Singapore, 2019, pp. 1-4, doi: 10.1109/ICCED46541.2019.9161078

[11] K. Noh, J. Lim, S. Chung, G. Kim and H. Jeong, "Ensemble Classifier based on Decision-Fusion of Multiple Models for Speech Emotion Recognition," 2018 International Conference on Information and Communication Technology Convergence (ICTC), Jeju, Korea (South), 2018, pp. 1246-1248, doi: 10.1109/ICTC.2018.8539502

[12] X. LI, T. SHI, P. LI and W. ZHOU, "Application of Bagging Ensemble Classifier based on Genetic Algorithm in the Text Classification of Railway Fault Hazards," 2019 2nd International Conference on Artificial Intelligence and Big Data (ICAIBD), Chengdu, China, 2019, pp. 286-290, doi: 10.1109/ICAIBD.2019.8836988

[13] S. Guo, H. He and X. Huang, "A Multi-Stage Self-Adaptive Classifier Ensemble Model With Application in Credit Scoring," in IEEE Access, Vol. 7, pp. 78549-78559, 2019, doi: 10.1109/ACCESS.2019.2922676

[14] S. P. Paramesh, C. Ramya and K. S. Shreedhara, "Classifying the Unstructured IT Service Desk Tickets Using Ensemble of Classifiers," 2018 3rd International Conference on Computational Systems and Information Technology for Sustainable Solutions (CSITSS), Bengaluru, India, 2018, pp. 221-227, doi: 10.1109/CSITSS.2018.8768734

[15] N. A. Nguyen-Thi, Q. Pham-Nhu, S. Luong-Ngoc and N. Vu-Thanh, "Using noise filtering techniques to ensemble classifiers for credit scoring," 2019 International Conference on Technologies and Applications of Artificial Intelligence (TAAI), Kaohsiung, Taiwan, 2019, pp. 1-6, doi: 10.1109/TAAI48200.2019.8959831

[16] Uvalieva, I; Turganbayev, E; Tarifa, F. Development of information system for monitoring of objects of education on the basis of intelligent technology: a case study of Kazakhstan//15th International Conference on Sciences and Techniques of Automatic Control and Computer Engineering (STA) Hammamet, TUNISIA, 2014, 909-914 (ISBN:978-1-4799-5907-5)WOS:000392734600124

[17] Mohammadi A., Shaverizade A. Ensemble deep learning for aspect-based sentiment analysis //International Journal of Nonlinear Analysis and Applications – 2021 – T. 12 – C. 29-38, DOI: 10.22075/IJNAA.2021.4769

[18] Seni G., Elder J. F. Ensemble methods in data mining: improving accuracy through combining predictions //Synthesis lectures on data mining and knowledge discovery – 2010 – T. 2 – №. 1 – C. 1-126, doi: 10.2200/s00240ed1v01y200912dmk002

[19] Dimić G. et al. An approach to educational data mining model accuracy improvement using histogram discretization and combining classifiers into an ensemble //Smart Education and e-Learning 2019 – Springer, Singapore, 2019 – C. 267-280, DOI: 10.1007/978-981-13-8260-4_25

[20] Lin J. L. et al. An ensemble method for inverse reinforcement learning //Information Sciences – 2020 – T. 512 – C. 518-532, DOI: 10.1016/j.ins.2019.09.066

Parameter Estimation of Photovoltaic Model, Using Balancing Composite Motion Optimization

Nguyen Ngoc Son, Luu The Vinh

Faculty of Electronics Technology, Industrial University of Ho Chi Minh City, Ho Chi Minh City, Viet Nam
nguyenngocson@iuh.edu.vn; luuthevinh@iuh.edu.vn

Abstract: This paper investigates the dynamic parametric estimation of a solar cell system, by using balancing composite motions optimization (BCMO). The BCMO technique was first online published in 2019, the main idea is to balance composite motion properties of individuals in solution space, to equalize global and local searchability. To evaluate the performance of BCMO, experimental tests are carried out in photovoltaic cell parameters estimation of R.T.C.France which is collected under 1000 W/m^2 at 33^{o}C, by changing the population size of BCMO. And then, the performance of BCMO is compared with well-established parameters estimation methods in terms of convergence speed, computation time, and RMSE value. The results demonstrate that the proposed approach can be accurately estimated for photovoltaic model parameters.

Keywords: Balancing Composite Motions Optimization (BCMO); Photovoltaic Model; Parametric Estimation

1 Introduction

In order to cope with air pollution and climate change, renewable energy sources such as solar, wind, hydro and biomass energy are increasingly widely used and become mainstream worldwide. Among them, solar energy is one of the highest attention for generating electricity based on photovoltaic (PV) technology in recent years. To study the maximum power extracted from PV cells, characteristics including open-circuit voltage (V), short circuit current (I), and maximum power point (MPP) must be identified [1-3]. Many approaches have been proposed to model characteristics of PV cells used of the equivalent circuit models such as the single diode model (SDM) and double diode model (DDM) [4], and three diodes model (TDM) [5].

To solve the PV cell parameters extraction, deterministic and metaheuristics optimization techniques have been widely developed. With a deterministic method-

based approach, Paper [6] identified the five parameters of SDM of PV cells using a least-squares method. Paper [7] proposed a comparison of the Newton-Raphson method and the Levenberg–Marquardt algorithm in the PV cell parameters extraction. Paper [8] presented a Lambert W-function to extract seven parameters of DDM of the PV cell. However, these methods are easily trapped in local optima and sensitive to the initial condition.

On the contrary, the metaheuristics techniques are good at exploration and diversification to globally optimal solutions that do not need initial condition sensitivity and gradient information. These techniques have been applied to solve real-world problems recently such as analysis of geometry parameters variations for FinFET device based whale optimization algorithm (WOA) [9], optimizing of type-2 fuzzy controllers based slime mold algorithm [10], optimizing type-1 and type-2 fuzzy controllers based, grey wolf optimizer (GWO) [11], optimal production strategy using NSGA-II algorithm [12], cancer biomarkers identification using artificial bee colony based on dominance (ABCD) algorithm [13], deep reinforcement learning models with evolutionary algorithms [14], load forecasting based grasshopper optimization and neural network [15] and so on. To obtain the accuracy of PV cell parameters extraction, metaheuristics algorithms and variants were continuously proposed such as adaptive differential evolution (L-SHADE) algorithm [16], memetic differential evolution with Nelder-Mead simplex [17], JAYA and IJAYA [18], hybrid differential evolution with whale optimization algorithm (DE-WOA) [19], performance-guided Jaya algorithm (PGJAYA) [20], teaching-learning-based artificial bee colony (TLABC) [21], an advanced onlooker-ranking-based adaptive differential evolution (ORcr-IJADE) [22], adaptive Harris hawks optimization (AHHO) [23], comprehensive learning Rao-1 (CLRao-1) [24], random reselection particle swarm optimization (PSOCS) [25], radial movement optimization (RMO) [26], manta ray foraging optimization (MRFO) [27], improved gaining sharing knowledge (IGSK) algorithm [28], hybrid Jaya and DE algorithm (MJAYA) [29], salp swarm algorithm (SSA) [30], combining multi-task optimization and DE algorithm (SGDE) [31].

Recently, many new algorithms have been introduced such as Honey Badger Algorithm (HBA) [32], Artificial Gorilla Troops Optimizer (GTO) [33], Henry gas solubility optimization (HGSO) [34], Lévy flight distribution [35], Rao-1 [36] and logistic chaotic Rao-1 optimization algorithm (LCROA) [37]. Among them, Balancing Composite Motions Optimization (BCMO), which was first published online in 2019 [38], is via a probabilistic selection model that creates a movement mechanism of each individual to equal a global and local search in solution space. The purpose of this paper is to apply the BCMO algorithm for estimating the parameters of PV cells. To survey the effectiveness of BCMO, experimental tests are carried out in extracting parameters of SDM and DDM by changing the population size of BCMO. And then, BCMO is compared with other well-established parameters extraction methods such as JAYA [18], DE [19], MJAYA [29], SGDE [31], Rao-1, and LCROA [37].

The main contributions of this paper are given as follows:

- Investigate the influence of the population size - NP on the performance of the BCMO algorithm when estimating the PV cell parameters.
- The effectiveness of the BCMO algorithm is conducted by parameter extraction of R.T.C.France solar cell described in [31], which was collected under 1000 W/m^2 at 33^{o}C.
- Perform PV parameter estimation using the classical GA, DE, JAYA, and BCMO algorithms to analyze the convergence speed and computation time between these algorithms.
- Experiments are conducted to verify the superiority of the BCMO algorithm in comparison to other well-established parameters extraction methods such as JAYA [18], DE [19], MJAYA [29], SGDE [31], Rao-1, and LCROA [37]. The results prove that BCMO can be accurately identified and are highly competitive with other PV parameters extraction methods.

The rest of the paper is organized as follows. The mathematics of the solar cell and the optimization problem in modeling PV models is presented in Section 2. Section 3 introduces the BCMO technique and how to parameter extraction of the solar cell model. Section 4 shows the experimental results and analysis. Finally, the conclusions are presented in Section 5.

2 Problem Formulation

In general, there are two most commonly used in practice to describe the nonlinear features of the solar cell model, the single diode model (SDM) and the double diode model (DDM).

2.1 Single Diode Model

The equivalent circuit of a solar cell with a single diode includes a diode, a current source, a shunt resistor, and series resistance is illustrated in Fig. 1. In which, I_{PH} is a photogenerated current, I_{SD} is a reverse saturation current, n is a diode quality factor, R_S is a series resistance, and R_{SH} is shunt resistance.

According to Kirchhoff's current law, the output current I_L can be calculated as:

$$I_L = I_{PH} - (I_D + I_{SH}) \tag{1}$$

Where I_{PH} is the photogenerated current in a cell; I_D represents acquired by Shockley formula Eq. (2); I_{SH} is the shunt resistor current acquired by Eq. (3).

$$I_D = I_{SD}\left[\exp\left(\frac{q(V_L + R_S I_L)}{nkT}\right) - 1\right] \tag{2}$$

$$I_{SH} = \frac{V_L + R_S I_L}{R_{SH}} \tag{3}$$

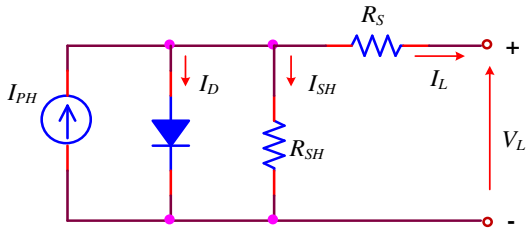

Figure 1
Equivalent circuit of SDM

In which, V_L mean for the output voltage. *n, k, q*, and *T* represent the diode ideality factor, the Boltzmann constant (1.3806503×10^{-23} J/K), the elementary charge (1.60217646×10^{-19} C), and the cell temperature in Kelvin. Hence, Eq. (1) can be rewritten as,

$$I_L = I_{PH} - \left\{I_{SD}\left[\exp\left(\frac{q(V_L + R_S I_L)}{nkT}\right) - 1\right] + \frac{V_L + R_S I_L}{R_{SH}}\right\} \tag{4}$$

It can be seen from Eq. (4) that there are five unknown parameters (i.e. $I_{PH}, I_{SD}, R_{SH}, R_S$ and n) that need to be extracted.

2.2 Double Diode Model

As shown in Fig. 2, the idea equivalent circuit model of a solar cell using a double diode model (DDM) consists of two diodes paralleled with both the shunt resistance and current source to shunt the photo-produced current source.

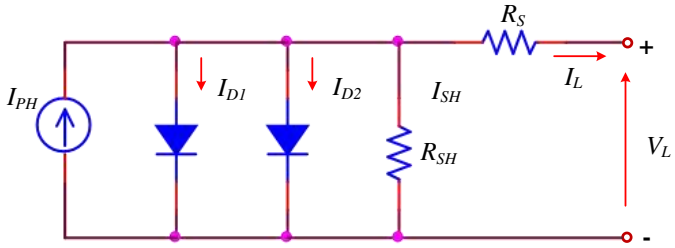

Figure 2
Equivalent circuit of DDM

According to Kirchhoff's current law, the output current is calculated as:

$$I_L = I_{PH} - (I_{D1} + I_{D2} + I_{SH}) \tag{5}$$

Moreover, currents I_{D1}, I_{D2} calculated by Shockley formula, therefore:

$$I_L = I_{PH} - \left\{ I_{SD1}\left[\exp\left(\frac{q(V_L + R_S I_L)}{n_1 kT} \right) - 1 \right] + I_{SD2}\left[\exp\left(\frac{q(V_L + R_S I_L)}{n_2 kT} \right) - 1 \right] + \frac{V_L + R_S I_L}{R_{SH}} \right\} \tag{6}$$

Where I_{D1} and n_1 are diffusion and diffusion ideality factors, respectively. I_{D2} and n_2 are saturation current and recombination diode ideality factors, respectively.

Obviously, there are seven unknown parameters (i.e. $[I_{PH}, I_{SD1}, I_{SD2}, R_S, R_{SH}, n_1, n_2]$) that need to be extracted.

2.3 Objective Function

The problem of PV cell parameters extraction can be solved by minimizing the root mean square error (RMSE) between the experimental data and simulated data which is defined as follows:

$$RMSE(\mathbf{x}) = \sqrt{\frac{1}{N}\sum_{i=1}^{N} f_i(V_L, I_L, \mathbf{x})^2} \tag{7}$$

Where I-V data (V_L, I_L) obtained from the experimental PV cell. *N* is the number of samples of the experimental data. **x** is the set of the extracted parameters.

In Eq. (7), for SDM model:

$$f_{SDM}(V_L, I_L, \mathbf{x}) = I_L - I_{PH} + I_{SD}\left[\exp\left(\frac{q(V_L + R_S I_L)}{nkT} \right) - 1 \right] + \frac{V_L + R_S I_L}{R_{SH}} \tag{8}$$

$$\mathbf{x} = [I_{PH}, I_{SD}, R_{SH}, R_S, n] \tag{9}$$

for DDM model:

$$\begin{aligned} f_{DDM}(V_L, I_L, \mathbf{x}) = I_L - I_{PH} &+ I_{SD1}\left[\exp\left(\frac{q(V_L + R_S I_L)}{n_1 kT} \right) - 1 \right] \\ &+ I_{SD2}\left[\exp\left(\frac{q(V_L + R_S I_L)}{n_2 kT} \right) - 1 \right] + \frac{V_L + R_S I_L}{R_{SH}} \end{aligned} \tag{10}$$

with $\mathbf{x} = [I_{PH}, I_{SD1}, I_{SD2}, R_S, R_{SH}, n_1, n_2]$ (11)

3 Balancing Composite Motions Optimization (BCMO) for Photovoltaic (PV) Parameter Estimation

3.1 BCMO Algorithm

The balancing composite motions optimization (BCMO) was first introduced in 2019 [38]. The BCMO algorithm includes the main phase as follows,

Initialization. Assume that it needs to minimize a *d* real-parameter function optimally. The population size (*NP*) of *d* real-parameter is defined. In the first generation, the population distribution is uniformly generated within the search space as follows:

$$\mathbf{x}_i = \mathbf{x}_i^{\min} + \mathbf{rand}(1,d)(\mathbf{x}_i^{\max} - \mathbf{x}_i^{\min}) \tag{12}$$

where $\mathbf{x}_i^{\min}, \mathbf{x}_i^{\max}$ are the min and max boundaries of the i^{th} individual, respectively. rand (1,d) is a uniformly distributed random number from [0,1]. Then, all individuals in population are ranked, based on the following sorting:

$$\mathbf{x} = \arg sort\left\{ f\left(\mathbf{x}\right)\right\} \tag{13}$$

In which, $f\left(\mathbf{x}\right)$ is the objective function values.

Determination of the instant global point and the best individual. We define an instant global optimum point $\mathbf{O_{in}}$ in the search space. The way to determine $\mathbf{O_{in}}$ in the t^{th} generation is as follows:

$$\mathbf{x}_{\text{o}_{\text{in}}}^t = \begin{cases} \mathbf{u}_1^t & if \quad f\left(\mathbf{u}_1^t\right) < f\left(\mathbf{x}_1^{t-1}\right) \\ \mathbf{x}_1^{t-1} & otherwise \end{cases} \tag{14}$$

Where, $\mathbf{x}_1^{t-1}$ is the best individual in the previous generation. A trial individual $\mathbf{u}_1^t$ is indicated by using the population of the previous generation as:

$$\mathbf{u}_1^t = \mathbf{u}_c + \mathbf{v}_{k_1/k_2}^t + \mathbf{v}_{k_2/1}^t \tag{15}$$

Where $\mathbf{u_c}$ is a center point of the search space [min$B$, max$B$] and can be expressed:

$$\mathbf{u}_c = \frac{\min B + \max B}{2} \tag{16}$$

$\mathbf{v}_{k_1/k_2}^t$ and $\mathbf{v}_{k_2/1}^t$ are the relative movement of the k_1^{th} individual concerning the k_2^{th} and the k_2^{th} individual to the previous best one. k_1 is randomly in a range [2, NP] and $k_2 < k_1$.

Composite motion of individuals in solution space. To balance the exploiting and exploring ability, the movement of the global search $\mathbf{v}_j$ is calculated as:

$$\mathbf{v}_j = \alpha_j \left(\mathbf{x}_{o_{in}} - \mathbf{x}_j \right) \tag{17}$$

Where α_j is the first-order derivative of the movement distance $\left(\mathbf{x}_{o_{in}} - \mathbf{x}_j \right)$ and is expressed as follows:

$$\alpha_j = L_{GS} \times \mathbf{dv}_j \tag{18}$$

Where L_{GS} is the global step size scaling the movement of the j[th] individual and dv_j is a direction vector. L_{GS} and dv_j are calculated based on a trial number TV_j which is generated uniformly from [0,1] as follows:

$$L_{GS} = \begin{cases} e^{-\frac{1}{d}\frac{j}{NP}r_j^2} & if \quad TV_j > 0.5 \\ e^{-\frac{1}{d}\left(1-\frac{j}{NP}\right)r_j^2} & otherwise \end{cases} \tag{19}$$

$$\mathbf{dv}_j = \begin{cases} rand\left(1,d\right) & if \quad TV_j > 0.5 \\ -rand\left(1,d\right) & otherwise \end{cases} \tag{20}$$

Where r_j is a distance from the j[th] individual to O_{in} and is determined as:

$$r_j = \left\| \mathbf{x}_{o_{in}} - \mathbf{x}_j \right\| \tag{21}$$

Similarly, $\mathbf{v}_j$, the relative movement $\mathbf{v}_{i/j}$ of the i[th] individual concerning the j[th] one can be calculated by $\mathbf{x}_i$ and $\mathbf{x}_j$ as:

$$\mathbf{v}_{i/j} = \alpha_{ij} \left(\mathbf{x}_j - \mathbf{x}_i \right) \tag{22}$$

Where α_{ij} is expressed as follows,

$$\alpha_{ij} = L_{LS} \times \mathbf{dv}_{ij} \tag{23}$$

L_{LS} can be fixed at 1 for balancing the local exploration and exploitation abilities of the i[th] individual. $\mathbf{dv}_{ij}$ is calculated as in Eq. (20).

The updated i[th] individual in the next generation is determined as follows:

$$\mathbf{x}_i^{t+1} = \mathbf{x}_i^t + \mathbf{v}_{i/j} + \mathbf{v}_j \tag{24}$$

3.2 Applied BCMO for Estimating the PV Parameters

BCMO is used to estimate the parameters of the PV model (five for the SDM and seven for the DDM) by minimizing the RMSE as shown in Fig. 3. The Pseudocode of the BCMO for PV parameters estimation is illustrated in Algorithm 1.

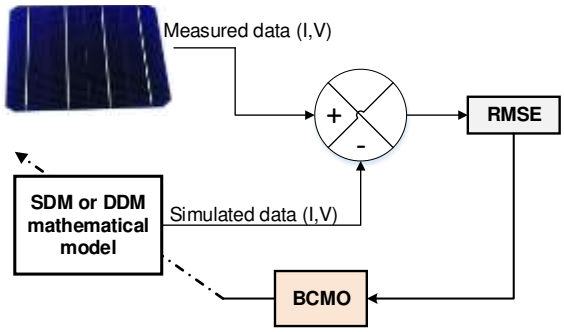

Figure 3
Block diagram of PV cell parameters estimation using BCMO algorithm

In which, *MinRMSE* is allowed error, *MaxIter* is the maximum number of generations. BCMO is a parameter-free optimization algorithm and the performance of BCMO only depends on the population size NP selected for each specific optimization problem.

Algorithm 1: The pseudo-code of BCMO used in parameter extraction

Generate the initial population
$\mathrm{x} = \left[I_{PH}, I_{SD}, R_S, R_{SH}, n\right]$ or $\mathrm{x} = \left[I_{PH}, I_{SD1}, I_{SD2}, R_S, R_{SH}, n_1, n_2\right]$
Evaluate the fitness of each individual in the population
Rank the population and find the best individual
while(*MinRMSE is attained or t* < *MaxIter*) **do**
    Generate a trial individual $\mathbf{u}_1^t$ by Eq. (15) and Eq. (16).
    Calculate $RMSE\left(\mathbf{u}_1^t\right)$
    Determine $\mathbf{x}_{o_{in}}^t$ by Eq. (14)
    $\mathbf{x}_1^t = \mathbf{x}_{o_{in}}^t$
    for i = 2 **to** *NP* **do**
        Calculate r_j by Eq. (21); $L_{LS} = 1$
        % Determine the global search of the i^th individual
        TV_j = *rand*[0, 1]
        if $TV_j > 0.5$
            $L_{GS} = e^{-\frac{1}{d}\frac{j}{NP}r_j^2}$

15: $\mathbf{dv}_j = rand(1,d)$; $\mathbf{dv}_{ij} = rand(1,d)$

16: **else**

17: $L_{GS} = e^{-\frac{1}{d}\left(1-\frac{j}{NP}\right)r_j^2}$

18: $\mathbf{dv}_j = -rand(1,d)$; $\mathbf{dv}_{ij} = -rand(1,d)$

19: **end**

20: $\alpha_j = L_{GS} \times \mathbf{dv}_j$

21: $\mathbf{v}_j = \alpha_j \left(\mathbf{x}_{o_{in}} - \mathbf{x}_j\right)$

22: *% Determine the local search of the i^{th} individual*

23: $\alpha_{ij} = L_{LS} \times \mathbf{dv}_{ij}$

24: $\mathbf{v}_{i/j} = \alpha_{ij} \left(\mathbf{x}_j - \mathbf{x}_i\right)$

25: $\mathbf{x}_i^{t+1} = \mathbf{x}_i^t + \mathbf{v}_{i/j} + \mathbf{v}_j$

26: **end for**

27: Rank the individuals

28: t = t + 1

29: **end while**

4 Results and Analysis

In order to prove the effectiveness of BCMO, it is used to extract parameters of two different PV cell models, i.e. single diode model (SDM) and double diode model (DDM) in comparison to other related studies. The benchmark I–V (current-voltage) data of PV cells was described in [39], which is collected on a 57 mm diameter commercial (R.T.C.France) PV cell under 1000 W/m^2 at 33 ºC. The lower and upper bounds of the PV cell parameters are shown in Table 1.

Table 1
Parameters range for SDM and DDM model

Parameter	Lower	Upper
$I_{PH}(A)$	0	1
$I_{SD}(\mu A)$	0	1
$R_S(\Omega)$	0	0.5
$R_{SH}(\Omega)$	0	100
n	1	2

Verification of the effectiveness of BCMO includes 2 steps, first, we evaluate the performance of the BCMO algorithm by changing the population size NP to estimate the PV cell parameters. And then, BCMO is compared with other well-established methods such as JAYA [18], DE [19], MJAYA [29], SGDE [31], Rao-1 algorithm, and logistic chaotic Rao-1 optimization algorithm (LCROA) [37]. The parameters of these methods are listed in Table 2. All methods are run from 30 to 50 independent times.

Table 2
Parameters setting of other related methods

Method	**Parameter setting**
JAYA [18]	NP = 20; *MaxIter = 50000; 30 runs*
DE [19]	The mutation scaling factor F and crossover rate Cr are uniformly distributed in (0.1,1) and (0,1); *MaxIter = 10000; 50 runs*
MJAYA [29]	Hybrid DE and JAYA; DE's parameters Cr = rand[0.7, 1.0]; F = rand[0.4, 1.0]; NP = 10*d (d = 5 with SDM and d = 7 with DDM).
SGDE [31]	NP = 150, LP = 20, |h|=60; MaxIter = 50000; 30 runs.
Rao-1, LCROA [37]	1000 iterations and 10 population; 30 runs.

4.1 Results on SDM Parameters Estimation

The results in terms of the best, worst, mean, STD (standard deviation) and the cost time computation for SDM are described in Table 3. The comparison convergence rates in changing NP of the BCMO algorithm are shown in Fig. 4. From Table 3 and Fig. 4, it can be seen that BCMO provides the least RMSE value (9.8602e-4) and BCMO will converge quickly about 3000 generations in the case of NP = 50*d. Where d is the number of parameters to be estimated for the SDM model (d = 5). When increasing the population size NP, the cost computation will be increased, on the contrary, the quality and convergence speed of PV parameters estimation achieve higher accuracy. Additionally, the I-V curve between the estimated data achieved by BCMO and experimental data for the SDM model in the case of NP =50*d is described in Fig. 5. Results prove that the parameters estimated by BCMO are of a high accuracy.

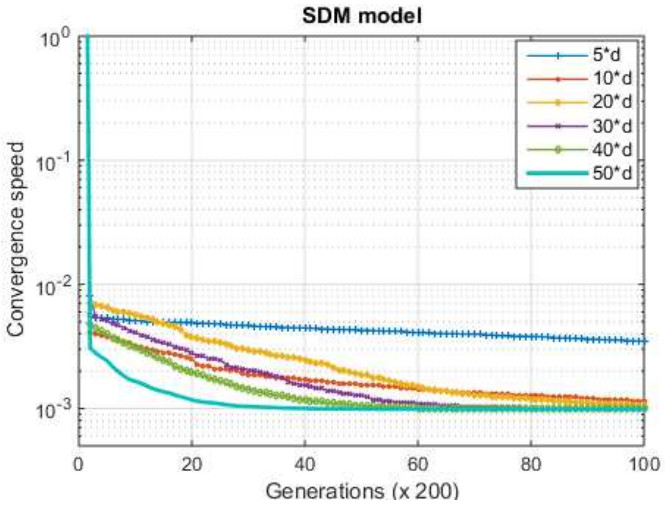

Figure 4

The convergence curve when changing NP for SDM

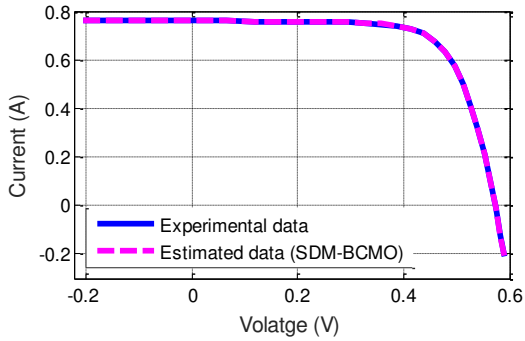

Figure 5

Comparison of the real data and the estimated data for SDM

Table 3

Comparisons of various NP extraction methods for SDM

NP	RMSE				
	Best	**Worst**	**Mean**	**Std.**	**Run(seconds)**
5*d (25)	0.0010	0.0089	0.0043	0.0028	333.8
10*d (50)	0.0011	0.0024	0.0015	5.33e-4	555.8
20*d (100)	9.87e-4	0.0011	0.0010	5.37e-5	864.6
30*d (150)	9.8613e-4	9.9509e-4	9.8722e-4	2.78e-6	1189.1
35*d (175)	9.8605e-4	9.9064e-4	9.8666e-4	1.43e-6	1341.0
50*d (250)	9.8602e-4	9.8603e-4	**9.8603e-4**	**3.08e-9**	**1835.1**

4.2 Results on DDM Parameters Estimation

Table 4 shows the performance of BCMO when changing NP for DDM parameter extraction in terms of the best, worst, mean, std. Fig. 6 describes the comparison of convergence rates in changing NP of the BCMO algorithm. From Table 4 and Fig. 6, it can be seen that BCMO provides the least RMSE value (9.8635e-4) and BCMO will converge quickly at about 1.500 generations in the case of NP = 50*d. Where d is the number of parameters to be estimated for the DDM model (d = 7). When changing NP from 20*d to 50*d, the performance of BCMO gives a nearly equal quality. Fig. 7 shows the I-V curve between the estimated data achieved by BCMO and experimental data for the DDM model in the case of NP =50*d.

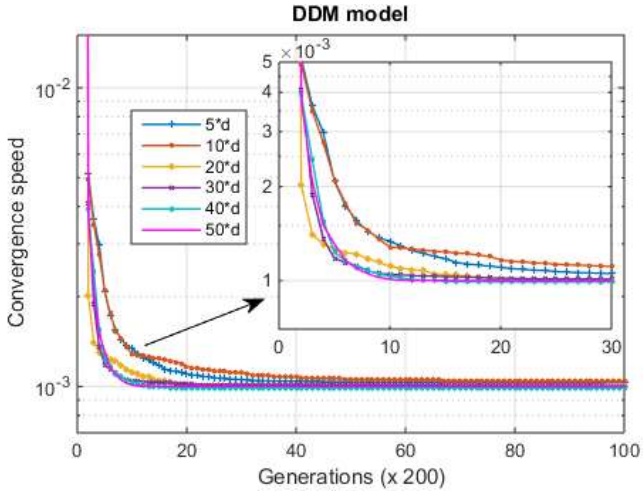

Figure 6

The convergence curve when changing NP for DDM

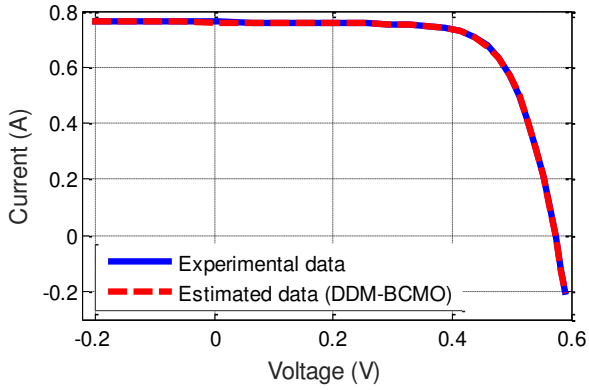

Figure 7

Comparison of the real data and the estimated data for DDM

Table 4
Comparisons of various NP extraction methods for DDM

NP	RMSE				
	Best	Worst	Mean	Std.	Run(seconds)
5*d (35)	9.8533e-4	0.0015	0.0011	1.69e-4	462.7
10*d (70)	9.8600e-4	0.0014	0.0011	1.47e-4	702.9
20*d (140)	9.8619e-4	0.0010	9.9563e-4	1.65e-5	1156.5
30*d (210)	9.8579e-4	0.0011	9.9776e-4	2.27e-5	1613.0
35*d (245)	9.8538e-4	0.0011	9.9755e-4	2.54e-5	1811.9
50*d (350)	9.8371e-4	9.8727e-4	**9.8635e-4**	**8.03e-7**	**2597.3**

4.3 Comparison with Other Techniques

For SDM, the RMSE value in terms of the best, mean, worst, and standard deviation (Std.) are shown in Table 5. The estimated parameters of the SDM model are described in Table 6.

Based on the results in Table 5 and Table 6, it can be proved that BCMO has better performance than those of classical JAYA, DE, and Rao-1. Details as, in term of average and standard deviation, JAYA, DE, Rao-1 and BCMO obtain (1.1617e-3, 1.88e-4), (1.0212e-3, 1.4469e-4), (9.912816e-4, 1.861748e-4) and (9.8603e-4, 3.08e-9), respectively. When compared with a modified classical algorithm, BCMO gives the same performance as MJAYA and SGDE and is better than LCROA. Moreover, the standard deviation of BCMO obtained 3.08e-9 proves that BCMO has robustness capabilities in PV cell parameters estimation.

Table 5
Comparisons of other well-established parameters extraction methods for SDM

Method	RMSE			
	Best	**Worst**	**Mean**	**Std.**
JAYA [18] 2017	9.8946e-4	1.4783E−3	1.1617E−3	1.88E−4
DE [19] 2018	9.860219e-4	1.810590e-3	1.0212e-3	1.4469e-4
MJAYA [29] 2020	9.860218e-4	9.860218e-4	9.860218e-4	1.99e-17
SGDE [31] 2020	9.860219e-4	9.860354e-4	9.86022e-4	2.47465e-9
Rao-1 [37] 2021	7.749435e-4	1.348222e-3	9.912816e-4	1.861748e-4
LCROA [37] 2021	7.730063e-4	1.348222e-3	1.272813e-2	4.054798e-2
BCMO (NP = 50*d)	9.8602e-4	9.8603e-4	9.8603e-4	3.08e-9

Table 6
Details estimated results of SDM

Parameters	$I_{PH}(A)$	$I_{SD}(\mu A)$	$R_S(\Omega)$	$R_{SH}(\Omega)$	n	**RMSE**
JAYA [18] 2017	0.7608	0.3281	0.0364	54.9298	1.4828	9.8946E−4
DE [19] 2018	0.76078	0.32302	0.03638	53.71852	1.48118	9.860219e-4
MJAYA [29] 2020	0.7608	0.3230	0.0364	53.7185	1.4812	9.860219e-4
SGDE [31] 2020	0.76078	0.32302	0.03638	53.71853	1.48118	9.860219e-4
LCROA [37] 2021	0.76079	0.31068	1.51690	0.03655	52.88979	7.730063
BCMO (NP = 50*d)	0.76078	0.3230	0.0364	53.7185	1.4812	9.8602e-4

For DDM, Table 7 gives the comparison of BCMO with other well-established parameters extraction methods in terms of the best, mean, worst, and Std. The estimated optimal parameters of the DDM model are described in Table 8.

Table 7
Comparisons of other well-established methods for DDM

Method	**RMSE**			
	Best	Worst	Mean	Std.
JAYA [18] 2017	9.8934e-4	1.1767e-3	1.4793e-3	1.93e-4
DE [19] 2018	9.829363e-4	2.009408e-3	1.068617e-3	2.233253e-4
MJAYA [29] 2020	9.824848e-4	9.860218e-4	9.8260e-4	6.46e-7
SGDE [31] 2020	9.84413e-4	9.86022e-4	9.85774e-4	4.01504e-7
Rao-1 [37] 2021	7.60703e-4	1.66267e-3	1.05394e-3	2.65619e-4
LCROA [37] 2021	7.49007e-4	6.61635e-2	1.41491e-2	2.18517e-2
BCMO (NP = 50*d)	9.8371e-4	9.8727e-4	9.8635e-4	8.03e-7

Table 8
Details estimated results of DDM

Parameters	$I_{PH}(A)$	$I_{SD1}(\mu A)$	$R_S(\Omega)$	$R_{SH}(\Omega)$	n_1	$I_{SD2}(\mu A)$	n_2	RMSE
JAYA [18]	0.7607	0.00608	0.0364	52.6575	1.8436	0.3151	1.4788	9.893e-4
DE [19]	0.76078	0.49922	0.0366	54.8509	1.9979	0.2559	1.4615	9.829e-4
MJAYA [29]	0.7608	0.22597	0.0367	55.4854	1.4510	0.7494	2.000	9.825e-4
SGDE [31]	0.76079	0.2807	0.0365	54.3667	1.4697	0.2499	1.9323	9.844e-4
LCROA [37]	0.7608	0.14582	0.0372	54.8589	1.4554	0.7351	1.8937	1.415e-2
BCMO (NP = 50*d)	0.7608	0.20588	0.0364	53.9364	1.4786	0.7494	2.000	9.837e-4

Based on results in Table 7 and Table 8, it can be seen that BCMO gets the smallest RMSE value in terms of the average and standard deviation has a better performance compared to those of JAYA, DE, Rao-1, and LCROA. When compared with a modified classical algorithm, BCMO gives slightly worse than MJAYA and SGDE but not significantly.

4.4 Discussions of Convergence and Computation Time

In this part, we perform PV parameter estimation using the original GA, DE, JAYA, and BCMO algorithms to analyze the convergence speed and computation time between these algorithms. In which, the mutation scaling factor F and crossover rate Cr for DE are uniformly distributed in (0.1,1) and (0,1) [19]. BCMO and JAYA are parameter-free optimization algorithms. The crossover and mutation factors of GA are selected by trial and error method and are equal to 0.9 and 0.01, respectively. The simulations were performed by Matlab version 2014b on an Intel Core i3 computer with a clock rate of 2.53 GHz and 2.00 GB of RAM. All methods are run 30 independent times and MaxIter = 20000 generations.

The convergence rate of the original GA, JAYA, DE, and BCMO algorithms is shown in Fig. 8. For SDM model estimation, it can be seen that BCMO has a slightly worse convergence rate than JAYA and DE algorithms. For DDM model estimation, BCMO has a competitive convergence rate with the DE algorithm and a faster convergence rate than JAYA and GA algorithms. This proves that BCMO has good exploration ability and is highly competitive with other methods.

From the results described in Table 9 and Table 10, it can be seen that BCMO needs a longer computation time when compared with those of GA, DE, and JAYA algorithms. Specifically, for SDM model estimation, the average computation time of BCMO is 555.8 seconds, about 5 times compared to the JAYA in the case of NP = 50. When BCMO achieves the best accuracy results with NP = 250, the average time of BCMO is 1835.1 seconds, about 15 times compared to the JAYA.

Table 9
Comparisons of various NP extraction methods for SDM

NP	Methods	RMSE				
		Best	**Worst**	**Mean**	**Std.**	**Run (seconds)**
50	GA	0.0483	0.1901	0.1417	0.0541	104.2
	JAYA	9.8602 e-4	9.8602 e-4	9.8602 e-4	1.3525e-12	120.8
	DE	**9.8602e-4**	**9.8602e-4**	**9.8602e-4**	**1.0114e-12**	**152.4**
	BCMO-50	0.0011	0.0024	0.0015	5.33e-4	555.8
250	BCMO-250	9.8602e-4	9.8603e-4	9.8603e-4	3.08e-9	1835.1

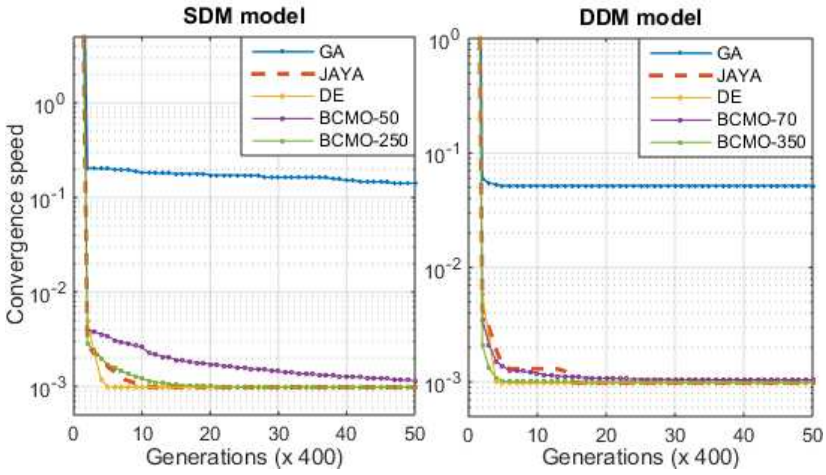

Figure 8
The convergence curve of the original GA, JAYA, DE, BCMO algorithms

Table 10
Comparisons of various NP extraction methods for DDM

NP	Methods	RMSE				
		Best	Worst	Mean	Std.	Run (seconds)
70	GA	0.05192	0.13003	0.07718	0.0328	149.3
	JAYA	9.8248e-4	0.0012	0.0010	8.0306e-5	141.8
	DE	**9.8248e-4**	**9.8602e-4**	**9.8366e-4**	**1.7258e-6**	**186.9**
	BCMO	9.8600e-4	0.0014	0.0011	1.47e-4	702.9
350	BCMO	9.8371e-4	9.8727e-4	9.8635e-4	8.03e-7	2597.3

In summary, the above discussions indicate that BCMO can be accurately identified and are highly competitive convergence rate with other PV parameters extraction methods. But the computational cost of BCMO has longer than other algorithms such as GA, DE, and JAYA algorithms.

Conclusions

In this paper, BCMO has been applied to estimate PV cell parameters. The experimental results on benchmark test PV cell models, i.e., a single diode model and a double diode model in terms of the convergence speed, computation time, and the RMSE value are analyzed. First, we survey the impact of a population size NP on the quality of the BCMO algorithm. And then, the estimated performance of the BCMO algorithm is compared with other algorithms including classical algorithms and variants. The experimental results strongly proved that BCMO performs significantly better convergence speed and RMSE value than the classical JAYA [18], DE [19], Rao-1 [37] and is highly competitive with some

modified algorithms published in 2020-2021 such as MJAYA [29], SGDE [31], and LCROA [37]. For computation time criteria, BCMO has longer than the classical GA, DE, and JAYA algorithms. In summary, BCMO can be used as a promising method for the parameter estimation problem in energy systems. In future work, we will perform further enhance the BCMO algorithm and apply it for real-time model-based fault diagnosis of the PV system.

Acknowledgment

This research is supported by Industrial University of Ho Chi Minh City (IUH) under grant number 79/HĐ-ĐHCN.

Data link

https://drive.google.com/drive/folders/1KgYhhKGiSLPe9zIJXArJFjmewXD_MRf7?usp=sharing

References

[1] A. Mellit, G. M. Tina, and S. A. Kalogirou, "Fault detection and diagnosis methods for photovoltaic systems: A review," *Renew. Sustain. Energy Rev.*, Vol. 91, pp. 1-17, 2018

[2] J. Jurasz, F. A. Canales, A. Kies, M. Guezgouz, and A. Beluco, "A review on the complementarity of renewable energy sources: Concept, metrics, application and future research directions," *Sol. Energy*, Vol. 195, pp. 703-724, 2020

[3] N. M. Ali and N. H. Rafat, "Modeling and simulation of nanorods photovoltaic solar cells: A review," *Renew. Sustain. Energy Rev.*, Vol. 68, pp. 212-220, 2017

[4] D. S. H. Chan and J. C. H. Phang, "Analytical methods for the extraction of solar-cell single-and double-diode model parameters from IV characteristics," *IEEE Trans. Electron Devices*, Vol. 34, No. 2, pp. 286-293, 1987

[5] M. H. Qais, H. M. Hasanien, and S. Alghuwainem, "Parameters extraction of three-diode photovoltaic model using computation and Harris Hawks optimization," *Energy*, Vol. 195, p. 117040, 2020

[6] F. J. Toledo, J. M. Blanes, and V. Galiano, "Two-step linear least-squares method for photovoltaic single-diode model parameters extraction," *IEEE Trans. Ind. Electron.*, Vol. 65, No. 8, pp. 6301-6308, 2018

[7] J. Appelbaum and A. Peled, "Parameters extraction of solar cells–A comparative examination of three methods," *Sol. Energy Mater. Sol. Cells*, Vol. 122, pp. 164-173, 2014

[8] X. Gao, Y. Cui, J. Hu, G. Xu, and Y. Yu, "Lambert W-function based exact representation for double diode model of solar cells: Comparison on fitness and parameter extraction," *Energy Convers. Manag.*, Vol. 127, pp. 443-460, 2016

[9] G. Kaur, S. S. Gill, and M. Rattan, "Whale optimization algorithm for performance improvement of silicon-on-insulator FinFETs," *Int. J. Artif. Intell.*, Vol. 18, No. 1, pp. 63-81, 2020

[10] R.-E. Precup, R.-C. David, R.-C. Roman, A.-I. Szedlak-Stinean, and E. M. Petriu, "Optimal tuning of interval type-2 fuzzy controllers for nonlinear servo systems using Slime Mould Algorithm," *Int. J. Syst. Sci.*, pp. 1-16, 2021

[11] C.-A. Bojan-Dragos, R.-E. Precup, S. Preitl, R.-C. Roman, E.-L. Hedrea, and A.-I. Szedlak-Stinean, "GWO-Based Optimal Tuning of Type-1 and Type-2 Fuzzy Controllers for Electromagnetic Actuated Clutch Systems," *IFAC-PapersOnLine*, Vol. 54, No. 4, pp. 189-194, 2021

[12] J. Čabala and J. Jadlovský, "Choosing the Optimal Production Strategy by Multi-Objective Optimization Methods," *Acta Polytech. Hungarica*, Vol. 17, No. 5, 2020

[13] V. Coleto-Alcudia and M. A. Vega-Rodríguez, "A multi-objective optimization approach for the identification of cancer biomarkers from RNA-seq data," *Expert Syst. Appl.*, p. 116480, 2022

[14] Y. Shao *et al.*, "Multi-objective neural evolutionary algorithm for combinatorial optimization problems," *IEEE Trans. Neural Networks Learn. Syst.*, 2021

[15] M. Talaat, M. A. Farahat, N. Mansour, and A. Y. Hatata, "Load forecasting based on grasshopper optimization and a multilayer feed-forward neural network using regressive approach," *Energy*, Vol. 196, p. 117087, 2020

[16] P. P. Biswas, P. N. Suganthan, G. Wu, and G. A. J. Amaratunga, "Parameter estimation of solar cells using datasheet information with the application of an adaptive differential evolution algorithm," *Renew. energy*, Vol. 132, pp. 425-438, 2019

[17] S. Li, W. Gong, X. Yan, C. Hu, D. Bai, and L. Wang, "Parameter estimation of photovoltaic models with memetic adaptive differential evolution," *Sol. Energy*, Vol. 190, pp. 465-474, 2019

[18] K. Yu, J. J. Liang, B. Y. Qu, X. Chen, and H. Wang, "Parameters identification of photovoltaic models using an improved JAYA optimization algorithm," *Energy Convers. Manag.*, Vol. 150, pp. 742-753, 2017

[19] G. Xiong, J. Zhang, X. Yuan, D. Shi, Y. He, and G. Yao, "Parameter extraction of solar photovoltaic models by means of a hybrid differential evolution with whale optimization algorithm," *Sol. Energy*, Vol. 176, pp. 742-761, 2018

[20] K. Yu, B. Qu, C. Yue, S. Ge, X. Chen, and J. Liang, "A performance-guided JAYA algorithm for parameters identification of photovoltaic cell and module," *Appl. Energy*, Vol. 237, pp. 241-257, 2019

[21] X. Chen, B. Xu, C. Mei, Y. Ding, and K. Li, "Teaching–learning–based artificial bee colony for solar photovoltaic parameter estimation," *Appl. Energy*, Vol. 212, pp. 1578-1588, 2018

[22] N. Muangkote, K. Sunat, S. Chiewchanwattana, and S. Kaiwinit, "An advanced onlooker-ranking-based adaptive differential evolution to extract the parameters of solar cell models," *Renew. Energy*, Vol. 134, pp. 1129-1147, 2019

[23] S. Song, P. Wang, A. A. Heidari, X. Zhao, and H. Chen, "Adaptive Harris hawks optimization with persistent trigonometric differences for photovoltaic model parameter extraction," *Eng. Appl. Artif. Intell.*, Vol. 109, p. 104608, 2022

[24] A. Farah, A. Belazi, F. Benabdallah, A. Almalaq, M. Chtourou, and M. A. Abido, "Parameter extraction of photovoltaic models using a comprehensive learning Rao-1 algorithm," *Energy Convers. Manag.*, Vol. 252, p. 115057, 2022

[25] Y. Fan, P. Wang, A. A. Heidari, H. Chen, and M. Mafarja, "Random reselection particle swarm optimization for optimal design of solar photovoltaic modules," *Energy*, Vol. 239, p. 121865, 2022

[26] B. S. S. G. Pardhu and V. R. Kota, "Radial movement optimization based parameter extraction of double diode model of solar photovoltaic cell," *Sol. Energy*, Vol. 213, pp. 312-327, 2021

[27] E. H. Houssein, G. N. Zaki, A. A. Z. Diab, and E. M. G. Younis, "An efficient Manta Ray Foraging Optimization algorithm for parameter extraction of three-diode photovoltaic model," *Comput. Electr. Eng.*, Vol. 94, p. 107304, 2021

[28] K. M. Sallam, M. A. Hossain, R. K. Chakrabortty, and M. J. Ryan, "An improved gaining-sharing knowledge algorithm for parameter extraction of photovoltaic models," *Energy Convers. Manag.*, Vol. 237, p. 114030, 2021

[29] T. V. Luu and N. S. Nguyen, "Parameters extraction of solar cells using modified JAYA algorithm," *Optik (Stuttg).*, Vol. 203, p. 164034, 2020

[30] R. Ben Messaoud, "Extraction of uncertain parameters of single and double diode model of a photovoltaic panel using Salp Swarm algorithm," *Measurement*, Vol. 154, p. 107446, 2020

[31] J. Liang *et al.*, "Evolutionary multi-task optimization for parameters extraction of photovoltaic models," *Energy Convers. Manag.*, Vol. 207, p. 112509, 2020

[32] F. A. Hashim, E. H. Houssein, K. Hussain, M. S. Mabrouk, and W. Al-Atabany, "Honey Badger Algorithm: New metaheuristic algorithm for solving optimization problems," *Math. Comput. Simul.*, Vol. 192, pp. 84-110, 2022

[33] B. Abdollahzadeh, F. Soleimanian Gharehchopogh, and S. Mirjalili, "Artificial gorilla troops optimizer: A new nature-inspired metaheuristic algorithm for global optimization problems," *Int. J. Intell. Syst.*, Vol. 36, No. 10, pp. 5887-5958, 2021

[34] F. A. Hashim, E. H. Houssein, M. S. Mabrouk, W. Al-Atabany, and S. Mirjalili, "Henry gas solubility optimization: A novel physics-based algorithm," *Futur. Gener. Comput. Syst.*, Vol. 101, pp. 646-667, 2019

[35] E. H. Houssein, M. R. Saad, F. A. Hashim, H. Shaban, and M. Hassaballah, "Lévy flight distribution: A new metaheuristic algorithm for solving engineering optimization problems," *Eng. Appl. Artif. Intell.*, Vol. 94, p. 103731, 2020

[36] R. Rao, "Rao algorithms: Three metaphor-less simple algorithms for solving optimization problems," *Int. J. Ind. Eng. Comput.*, Vol. 11, No. 1, pp. 107-130, 2020

[37] B. Lekouaghet, A. Boukabou, and C. Boubakir, "Estimation of the photovoltaic cells/modules parameters using an improved Rao-based chaotic optimization technique," *Energy Convers. Manag.*, Vol. 229, p. 113722, 2021

[38] T. Le-Duc, Q.-H. Nguyen, and H. Nguyen-Xuan, "Balancing composite motion optimization," *Inf. Sci. (Ny).*, Vol. 520, pp. 250-270, 2020

[39] T. Easwarakhanthan, J. Bottin, I. Bouhouch, and C. Boutrit, "Nonlinear minimization algorithm for determining the solar cell parameters with microcomputers," *Int. J. Sol. energy*, Vol. 4, No. 1, pp. 1-12, 1986

Adaptation Strategies for Human-Machine Interactions in Dialect Specific Environment

György Szaszák and Piero Pierucci

Telepathy Labs GmBH, Militärstrasse. 36, 8004 Zürich Switzerland
E-mail: gyorgy.szaszak@telepathy.ai, piero.pierucci@telepathy.ai

Abstract: Offering human machine interfaces capable of handling cultural variation in speech is an exciting topic in cognitive info-communication. From a machine learning point-of-view, this paper examines Automatic Speech Recognition (ASR) with respect to transcribing interactions occurring in a language environment where a particular dialect of a pluricentric language is spoken. Conservative retraining, transfer learning, multi-task training, matrix factorization, i-vector based techniques as well as adversarial and teacher-student training are all considered suitable approaches for the adaptation of deep neural acoustic models in ASR. Facing a problem of adaptation for accented speech, which method should be preferred? Comparing these techniques is often complicated, as different experiments are carried out on diverse datasets and within various frameworks. It is also worthwhile analysing possible combination of such techniques within complex systems. The objective of this work is to systematically compare and analyse a number of domain adaptation techniques for ASR using the same framework, in order to allow for a fair comparison on adapting US English acoustic models for particular accents. Our results indicate that, when properly hyperparametrized and carefully regularized, the easiest approaches, requiring less complexity and reduced computational power, can perform equally well as the more complex ones.

Keywords: human-machine interaction; speech recognition; adaptation; dialect; conservative training

1 Introduction

In human-machine infocommunication [1, 2] Automatic Speech Recognition Systems (ASR) are often used to convert speech into text. Just like in most machine learning tasks, where data scarcity is not a hindering factor, the deep learning paradigm has infused ASR technology in the past 5-6 years, leading to formerly unseen low error rates, through neural hybrid or all neural (end-to-end) models [6, 7]. However, when shifting away from the former state-of-the-art Gaussian Mixture Model (GMM) approach in acoustic modelling, some capabilities and elegant engineering solutions [4, 5] were lost, which impact

personalization and social convenience of ASR in a negative way. More precisely, with GMM based acoustic models, adaptation of the acoustic models was a very easy and effective task [3, 4], which moreover, did not require much data in case of Maximum Likelihood Linear Regression (MLLR) based model refinement. The MLLR adaptation made it possible to customize ASR for interactions taking place in specific social and language environments, therefore covering various speech styles and language varieties spoken in different communities.

With the neural network approach in acoustic modelling, no simple adaptation method is available, as the parameters of the acoustic model do not reflect direct spectral (or cepstral) phoneme mapping any more. This is a problem since variation in pronunciation [3, 4, 5, 8, 9] within the same language constitutes a so-called domain mismatch as the acoustic model cannot cope well with data points which are different from the ones seen during the training. Given that, ASR for interactions occurring in an unfamiliar social or language environment lead to a considerable increase in Word Error Rates (WER). This motivated starting up a number of research activities targeting acoustic adaptation of neural acoustic models, which resulted in a multitude of techniques being proposed one after the other. In the following section, we overview some of these, but we also point out that we observe a general tendency for these techniques to became more and more complex, making questionable whether the obtained small performance improvement is worth the large effort required by the adaptation approach. Another problem consists in the large variety of experimental conditions, which makes a comparison close to impossible when various datasets are used for training and benchmarking, where often this experimental condition variety actually reflects different levels of mismatches related to socio-cultural environment.

Unlike GMM acoustic models, which can be adapted by using some minutes of data, neural hybrid acoustic models usually require much more adaptation data to obtain a measurable performance improvement. This is understandable if one considers the relative data scarcity versus the number of parameters of the acoustic model. Training or retraining with low amount of data can lead to catastrophic forgetting or overfitting [10, 11], which means that the model may become corrupted and therefore incapable of generalizing in order to handle unseen cases. To avoid this, some adaptation approaches can apply a slightly different logic to minimize the risks of overfitting: either selecting a subset of the parameters to be updated by freezing all other network parameters (as part of a very conservative retraining with high emphasis on low learning rates) or adopting a more impactful, “aggressive” regularization.

As acoustic model adaptation is unavoidable for model customization for language varieties spoken in different socio-cultural entities, in this paper we are going to review and evaluate several adaptation techniques for ASR with neural acoustic model [12, 13, 14, 15, 16, 17, 18, 19, 20, 21].

Those entities use the same language in human-machine communication, but with slightly different acoustic and linguistic configurations. Our goal is to compare a number of adaptation paradigms within the same framework for the same task to get a clearer picture of their capabilities. As we already discussed, the multitude of baselines and benchmarking datasets makes this comparison close to impossible, despite the rich scientific literature on the acoustic model adaptation subject. Our approach will also allow us to analyse how specific paradigms and training techniques interact – especially those having a regularizing effect and looking at the available amount of adaptation data, both crucial for adaptation and whether the benefits they yield are additive to some extent (that is whether their combination leads to more improvement). We will use a standard English ASR acoustic model trained with the Kaldi toolkit [22] and adapt it for Indian English to demonstrate the results. We also compare adaptation for varieties being less different from the US baseline, including the UK, Canadian, Australian and specific US accents. Please note that the Indian accent itself is not uniform and could be further divided based on geographical consideration, but our datasets did not allow for such a fine grade evaluation in this work.

2 Adaptation Paradigms

Considering adaptation of neural acoustic models, ideas were initially driven by trying to adopt the Maximum Likelihood Linear Regression (MLLR) adaptation framework to non-neural Gaussian Mixture Model (GMM) based acoustic models for ASR. Imposing similar linear or non-linear transformations on one or more network layers [12, 13] was proposed in the so-called Learning of Hidden Unit Contributions (LHUC) model [14]. When LHUC transformation is applied to bottom-wise layers of the neural model, a normalizing effect is produced which makes the model domain invariant, as bottom-wise layers are thought to perform mostly the feature extraction part of the processing. If we use LHUC in the upper-wise (topmost) layers prior to the softmax, we adapt the model in the classical sense, as top layers act as classifiers [15] especially in networks with convolutional alike bottom layers and feed-forward (or eventually recurrent) top layers such as Time Delay Neural Networks (TDNN) [23].

A similar reasoning leads to another adaptation technique based on transfer learning [15], optionally coupled with multi-task training. The idea here is to transfer a feature extractor trained on a large out-of-domain dataset, and train only the classifier from scratch on an in-domain dataset. This approach, referred to as transfer learning hereafter, reduces the number of parameters to be trained and hence allows for using less data keeping the risk of overfitting under control. As basic speech features tend to be less language dependent, usually the bottom layers are transferred, and the top layers are removed or re-initialized (trained

from scratch). Multi-task training [16] is a technique often used in such transfer learning setups, as it allows for an intrinsic normalization of the features, producing less domain dependent bottom layers. A drawback of multitask training is that it takes longer to train, but the most disturbing constraint is that the in-domain adaptation data is required already for the training, which moreover has to be abundant enough to avoid heavy imbalance between the datasets associated with the multiple tasks.

Another popular method exploits matrix factorization from linear algebra in order to adapt some neural model's weight matrices. Factorizing the weight matrix can be regarded as equivalent to adding a linear bottleneck layer between the two specific layers [24]. As the dimension of this bottleneck layer can be configured in a wide range, adaptation is highly scalable and hence allows to adjust the number of parameters to be adapted to the amount of the available data. Some works use factorized neural models by default for acoustic modelling, which has been shown to slightly improve overall performance in [24]. Another often used factorization approach is called Low Rank Plus Diagonal (LRPD) decomposition [17].

Embedding alike vectors, better known as i-vectors, x-vectors [18, 25] or d-vectors [19], can also help in acoustic model adaptation. Hereafter we will use the term i-vector, but thereby referring to other similar embedding vectors such as x- or d-vectors. We can demonstrate their usage if we think like adding a bias in the first hidden layer of the network through the i-vectors [26]. Even if they are tipically used to describe speaker characteristics, they can also be used to capture domain specific variation. Please note that once i-vectors are used in the acoustic model (which is often the case), these intrinsically may already capture part of the variation resulting from domain variance. Eventually, i-vectors can be piped into lightweight auxiliary networks which perform an attention alike rescaling or add bias to the respective parameters in the acoustic model network [17], similar to the LHUC paradigm [14].

Adversarial learning can also be considered for training domain invariant models [20]. Its advantage that it supports unsupervised adaptation. However, as high amount of data is required for various accents during training, it should be regarded as a training method for obtaining invariant models, but the framework cannot be applied to classical adaptation scenarios with small amount of in-domain data. In [27] the authors claim that within the Kaldi ASR toolkit, no benefit was observed in terms of ASR performance when considering adversarial training techniques. The reason for this may be that such methods [20] may be beneficial with very high amount of training data.

Last, but not least, the teacher-student paradigm has also been demonstrated to be leveraged by the Kaldi toolkit for acoustic model training in [21]. Despite being an interesting approach, teacher-student learning requires a parallel corpus for in domain and out of domain data, which is a criterion hard to fulfil in practice, as far as ASR is considered.

3 Material and Methods

3.1 Baseline

For this work we have chosen widely used open-source tools and open-source data to allow for reproducibility of the results. The ASR was trained with the Kaldi toolkit [22], following the Librispeech [28] TDNN [24] standard `1c' recipe on 960 hours of `cleaned' data. For decoding, we simply adopted the open source `tgsmall' grammar, associated with Librispeech data and widely used for benchmarking ASR trained on the Librispeech recipe. We did not consider the adaptation of the language models, but focused exclusively on the acoustic models, which we think have to cope with higher variance in case dialect adaptation is required for human-ASR interactions.

Adding i-vectors to the input was part of our baseline, and it is also part of the default Kaldi Librispeech recipe. This means that part of the variation related to the accent mismatch may therefore be captured by i-vectors, even if the i-vector extractor is trained on only source domain (e.g. Librispeech) data.

3.2 Accented Data

We use the Mozilla Common Voice speech corpus [29] for providing adaptation data in the target domain. In the Common Voice corpus for English, 15 varieties of English are represented, out of which the variants labelled as Australian, Canadian, British (England) and US datasets contain at least 8 hours of good quality transcribed data. For each of these 5 varieties, we created c.a. 1.5 hours test sets to be discarded from training for adaptation.

3.3 Regularization

Regularization and conservative training are very important when performing model adaptation, as we usually work with a low amount of in-domain data, and by typically at least two orders of magnitude difference in dataset sizes (i.e. adapting a baseline trained on 1000 hours with 10 hours of in-domain data). Whereas regularization usually operates by controlling the cost function and preventing sudden changes, the learning rate can also be directly reduced to ensure new data does not modify model parameters in an excessive manner. The learning rate can be specified to be different for each layer and each epoch. This means that bottom most layers can be updated extremely carefully whereas letting topmost layers learn by a slightly higher rate. This coincides with the assumption that bottom layers tend to perform feature extraction, and classification is obtained in the top layers. Reducing the learning rate as iterations follow each other is also an effective and easy way of keeping the training conservative.

A very often used regularization technique in the field of model adaptation is the Kullback-Leibler Divergence (KLD) based regularization [30]. One of its advantages is that KLD can be carried out without any modification in the core training algorithms, but simply by rescaling the targets themselves [30], provided that the objective allows for this (i.e., with an objective based on frame based cross entropy). To achieve this with a cross-entropy minimization objective (or maximizing negative cross entropy), a new target probability distribution has to be created which can be obtained as a linear combination of the original target distribution $\hat{p}$ and the distribution computed via forced alignment with the adaptation data p. So in the objective

$$D_{KL} = \frac{1}{N}\sum_{t=0}^{N-1}\sum_{y\in C}\hat{p}(y|x_t)\log\left(p(y|x_t)\right) \tag{1}$$

dealing with N samples and C senones for the estimated distribution p at time frame t, the target distribution $\hat{p}$ is computed from the original target $\hat{p}_0$ and the estimate of the source model:

$$\hat{p}(y|x_t) = (1-\alpha)\hat{p_0}(y \mid x_t) + \alpha p(y \mid x_t), \tag{2}$$

where α is the regularization coefficient. The term senone may need a brief explanation: a senone is an abstract entity to be modelled that can be linked to the tied state of a traditional triphone model, i.e., the leaves of the decision tree used to represent context in ASR acoustic models.

However, in recent acoustic model training recipes the frame based cross-entropy objective has been replaced by the so-called chain objective. Scaling the targets is unfortunately not feasible for a chain objective (or would be so complex to make it that it cannot be tolerated even during training), but we still have the opportunity to use KLD regularization as part of the regularization in place already: the chain objective D_{chain} may be itself regularized by interpolating it with the cross entropy based framewise objective D_{fCE} (this is even supported by Kaldi through the *output-xent* output layer):

$$D_{chain+fCE} = (1-\beta)D_{chain} + \beta D_{fCE} \tag{3}$$

By extending the objective to

$$D_{chain+fCE+KL} = (1-\beta)D_{chain} + \beta D_{KL} \tag{4}$$

we can observe a frame based regularizing term. Technically such regularization is carried out by preserving a copy of the original model (the source model) and use it in parallel to the newly trained branch of network.

4 Analysed Adaptation Approaches

4.1 Vanilla Retraining

Retraining is probably the simplest way of adapting a model. For retraining, we use target domain data in the same manner we use the source domain data for training the source model, with the exception that retraining has to be more conservative. The topology of the source model is not adapted, which means that the senone representation reflects knowledge extracted essentially from the source domain data. This has advantages and disadvantages: the pro side is that we can preserve a robust tree estimate which would be hard to achieve on the low amount of target domain data; the negative side however, is that the tree may be mismatched if context dependency in the target domain differs too much from the source domain. Unfortunately, this is an often case, to reduce the negative effects, the number of senones can be reduced so that we use a broader model that has higher chance to match the target dialect better. What is the optimal number of senones, however, has to be determined experimentally on a development set.

To prevent overfitting, the primary interest is to use low learning rates, which we will set layerwise so that we let the top layers learning more. The secondary way to regularize retraining consists in increasing the weights α and β in the regularization terms of the objective $D_{chain+fCE+KL}$, as explained in subsection 3.3. In the supervised adaptation scheme, alignments for the adaptation data can be generated with the source model, but the source model can also be used to decode the target data in the first step and use the so-obtained lattices as soft alignments for the retraining phase. Using lattices fits perfectly into the chain training of TDNN acoustic models with the Lattice Free Maximum Mutual Information (LF-MMI) objective, as numerator lattices are directly available from the decoder.

4.2 Transfer Learning

The transfer learning approach is also based on retraining, but the model structure is not preserved in this case [15]. As the SoftMax output layer represents the phone context dependency tree, this means that both have to be trained from scratch, based on target domain data. At least the last hidden layer of the source model has also to be removed, as the number of output nodes will be likely different compared to the source model. These layers are newly initialized, and their parameters are learned from scratch by training the modified model on target domain data. The context dependency tree is obtained as resulting from training a GMM based acoustic model on the target domain data. The same GMM can then be used to generate alignments for supervised adaptation. Compared to simple retraining, the advantage is that the output is tuned according to the target domain statistics. The drawback is that this tuning has to be carried out on relatively low

amount of data in case of adaptation, which is a risk factor of getting a somewhat mismatched senone layout. Using unsupervised adaptation gets mostly out of the scope as well, as for training the small target domain GMM model transcriptions are desirable, but even if transcription is automated with the source domain decoder, using a lattice is not as straightforward as with the unchanged topology in simple retraining.

4.3 Factorization

As outlined earlier, factorization-based adaptation approaches offer an alternative for adaptation scenarios with very low amount of target domain data available [17, 24]. In this work we use the Singular Value Decomposition (SVD) algorithm and decompose the weight matrix W between two particular layers as follows:

$$W_{m \times n} = U_{m \times k} S_{k \times k} V_{k \times n}. \tag{5}$$

Factorization goes hand-by-hand with modifying the network structure, but this is a non-invasive action compared to the reinitialization of the complete top layers required for the transfer learning approach. With SVD, the output senone layout is not changed. Usually a single bottleneck is created (or an existing bottleneck is used) in the neural acoustic model. The dimensions of the bottleneck allow for a fine control over the number of parameters to be retrained. Comparing SVD to simple retraining, we select or create a small subset of latent network parameters and freeze all other (meaning a zero-learning rate).

The advantages of the factorization approach include the scalability and aptitude to work with low amount of data, whereas its drawbacks can be summarized as limiting the adaptation to a small part of the parameters which allows for only slight shifts in model outputs. Both supervised and unsupervised adaptation schemes can be suitable as the output layer is not affected by the adaptation.

5 Research Hypotheses

One of our goals in this work is to compare different acoustic model adaptation approaches for ASR. As we discussed in the introduction, several approaches in several flavours have been proposed for acoustic model adaptation, but most of them were evaluated within specific setups and special conditions, making a fair comparison intractable. Therefore, we will use a common baseline setup and the same environment for all experiments, with the main research questions condensed around which approach could be suitable given an hour or some ten hours of adaptation (target) data. Our research questions and null hypotheses are as follows:

- Can factorization-based approaches outperform vanilla retraining in the case if very low amount of target data is available for adaptation? – We hypothesize that vanilla retraining is better as factorization introduces loss through the used bottleneck (H1).
- Can transfer learning outperform vanilla retraining in the case if higher amount of adaptation data is available? Our hypothesis is that after reaching a threshold transfer learning yields better results since it has a better matching output layout (H2).
- Can we leverage KLD regularization for better convergence in the case if we combine it with cross entropy-based regularization for chain models? We hypothesize that KLD regularization improves the convergence (H3).

6 Experiments

6.1 Configurations

We perform the source model adaptation with the 3 different strategies by gradually adding more target data and by also gradually performing more and more training epochs with dynamically decreasing learning rate. We test the ASR performance in terms of Word Error Rate (WER) on the held-out test set.

We use and adopt the Kaldi Librispeech recipe for all kinds of adaptation experiment. Alignments on the target data are generated with the Librispeech `tri6b-cleaned' model (the same used for training the source acoustic model TDNN) for supervised adaptation. In case of unsupervised adaptation, we use the default offline Librispeech Kaldi decoder with its default settings (for the 1c recipe as of October 2018) and the 'tgsmall' language model. We did not perform second pass rescoring for the obtained lattices. For the individual approaches we use the following configurations:

- for transfer learning, we train the GMM acoustic model and its associated phone context decision tree on the target data and we reduce the target number of tree leaves from 7k to 1.8k. (No further fine tuning for the number of leaves was investigated depending on the amount of the target data.)
- for factorization, we create the bottleneck after the last TDNN layer and before the 'prefinal' layer with 256 dimensions, and initialize it following [17] (S is initialized as an identity matrix). In the recent Kaldi recipes with factorized TDNN architecture (F-TDNN), we can simply add a linear layer initialized as an identity matrix for this purpose.
- for vanilla retraining we tune α and β in the range of [0,1], letting them to sum to 1 in each case.

6.2 Number of Iterations

Plotting WER from epoch to epoch for a vanilla retraining illustrates in Fig. 1 as the model is being shifted toward the target domain: we observe reducing WER on target evaluation data and increasing WER on source domain test data. Most of the performance gain is obtained within the first three iterations (1 iteration contains 1.5 M chain examples in the used setup).

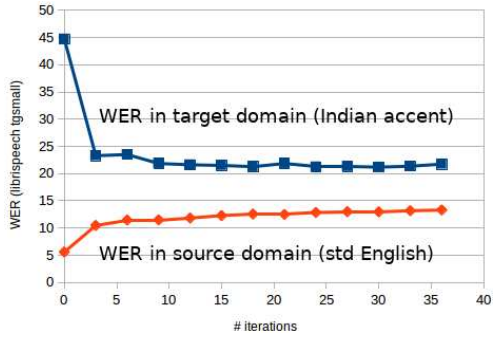

Figure 1
Illustration of the adaptation process with simple retraining (WER in %) using 10 hours of Indian English adaptation data

Final reduction on WER in the target domain is as high as 50% relative, although the basis is also high, given the Indian accent is far from the US English one. It is not worth running more than 18 iterations with this setup using 10 hours of Indian accent data and 1.5 M frames per iteration (note, this depends both on minibatch size and the amount of available adaptation data), as there is no more performance gain, but models may overfit, i.e., the WER seen with source data keeps worsening. In parallel, robustness of the AM is likely to become worse.

6.3 Amount of Data

Taking again the example of Indian English adaptation of the US English source model, Figs. 2a-c show convergence seen on eval data for all the 3 adaptation scenarios and gradually adding data of 1k, 2k, 5k and 10k utterances, corresponding roughly to 1 hour, 2 hours, 5 hours and 10 hours of target domain data, respectively. We can observe, that – according to reasonable expectations – the more data we use, the higher WER reduction we obtain; and that the more data we have, also the more iterations we have to run during the retraining phase.

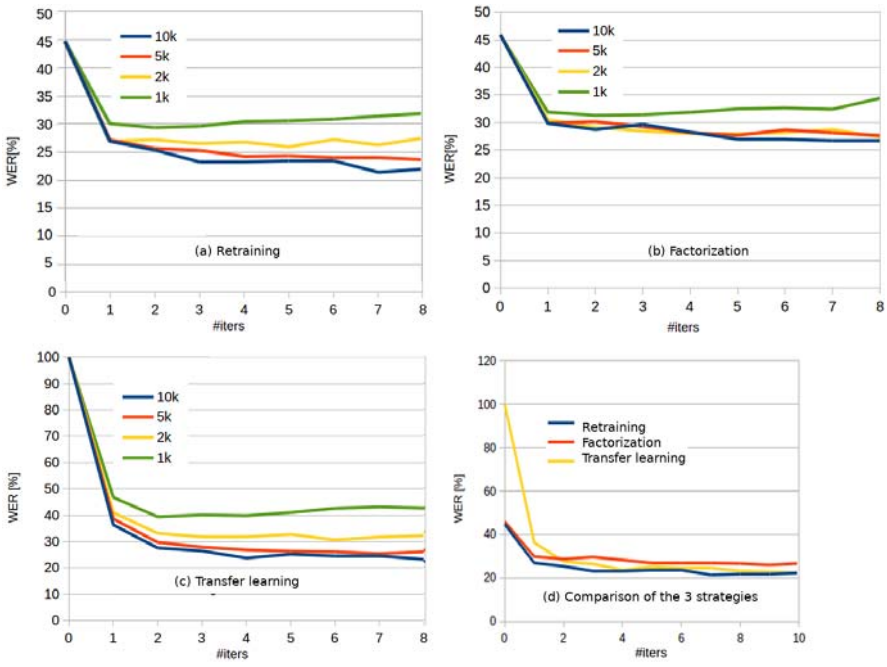

Figure 2

Illustration of the adaptation process with the 3 strategies: (a) simple retraining (upper left), (b) factorization (upper right) and (c) transfer learning (bottom). Pane (d) shows the comparison of the 3 methods (on 10 hours of Indian accented English).

Fig. 2b shows the factorization adaptation outcome, where we see a performance gain saturating at 2 hours of adaptation data and adding further data does not result in additional WER improvement. This can be explained partly by the fixed bottleneck size at 256 nodes irrespective of data quantity, but as both other strategies overperformed the factorization approach already by smaller amount of data, we did not find it worthwhile to increase bottleneck dimensionality. This also means that albeit the available amount of data is usually considered a key parameter when choosing the adaptation strategy, i.e., factorization alike approaches are reported to have the advantage of scalability [17] and work well with low amount of target data, we still found vanilla retraining outperforming it by using equal amount of data. This corresponds to confirming our H1 (by 5% confidence). Even with datasets containing only 15 and 30 minutes of speech and despite scaling the bottleneck size down to 128, we were not able to demonstrate such difference between the approaches. Using i-vectors in the baseline system may interplay in this result, but as i-vectors are regarded to be state-of-the-art, we found it pointless from a practical perspective to experiment with discarding them.

6.4 Effect of Top Layout Adaptation

By using all the 10 hours of Indian development data we compared the convergence of the 3 strategies in Fig. 2d. Still the vanilla retraining approach is the best performing one. We can therefore conclude that for the used 10 hours of data, the advantages of a better fitting output layer cannot counteract the benefit of having a somewhat mismatched output layer, which was trained on more data even it is out-of-domain data. Looking at Table 1 we observe however, that for other dialects associated with more training data, adapting the top layout can yield a better model than the one obtained with vanilla retraining, as is shown in the case of English spoken in England. On British English with 31 hours of adaptation data, transfer learning performs better. The case of US English may seem contradictory to this finding, as with even higher amount of 59 hours of adaptation data we again observe vanilla retraining yielding a better model, but we resolve this contradiction with the following arguments: the source model is trained on the Librispeech dataset, which contains dominantly US English utterances. The domain mismatch therefore does not arise from different variants of the same language, but rather from a mismatch in the acoustic conditions of the speech data used for adaptation, taken from the US English samples of the Mozilla Common Voice database. We argue that as dialect mismatch should be minimal between the two corpora, the worse performance of the adjusted topology model can rather be attributed to the poorer modelling capabilities of the context dependency decision tree, which, trained on less data can provide a poor representation for the particular dialect.

Table 1

WER reduction obtained with different supervised adaptation strategies

	AUS	CDN	ENG	IND	USA
Amount of adaptation data (hours)	8	8	31	10	59
Baseline WER	25.3	13.3	19.9	44.8	24.5
WER reduction vanilla retraining	**35.2**	**20.3**	31.7	**52.1**	**46.9**
WER reduction top layer reinitialization	28.9	12.0	**35.2**	50.3	44.1
WER reduction factorization	-	-	-	42.0	-

The difference in the relative WER improvement with the transfer learning and the retraining strategies is significant in the case of the ENG variety (by 5% confidence level), so our H2 hypothesis is confirmed. However, the threshold point for the amount of data when reinitialization of the top layer becomes beneficial does not only depend on the number of hours of the target data: it may hence be worth considering on a case-by-case basis that transfer learning requires an additional precursory step to architect the output layout by training a GMM on the adaptation data.

6.5 Learning Rate and Regularization

We applied a factor of *0.05..0.5* to the default learning rates worked out by the Kaldi TDNN trainer. On 10 hours of adaptation data we consistently experienced that the learning rate factors between 0.1 and 0.15 work the best. Letting the learning rate be higher (up to 0.5) we observed a consistent increase in WER after adaptation leading to by 5-6% less relative improvement in WER.

We were experimenting with applying KL regularization as part of the cross-entropy regularization. Although the difference between using simply the $D_{chain+fCE}$ objective or the $D_{chain+fCE+KL}$ objective is not large, we experienced smoother convergence and slightly better performance with $D_{chain+fCE+KL}$, the difference remaining however below significance (by 5% confidence, we obtained the best results with $\alpha=0.3$ and $\beta=0.6$). We hence had to reject our H3. Using KL-regularization is reportedly beneficial when training with cross-entropy objective [30, 31]. Using this approach for regularizing chain training was hence not significantly better; we had the impression that in part regularizing with cross-entropy (without KL) is already effective enough, and in part that the backstitch training [28] has a similar regularizing effect than has adding KL-regularization. We did not carry out targeted experiments to do further research on these, however.

7 Unsupervised Adaptation

In several cases there may be no available gold transcription for the utterances which nevertheless could be valuable for acoustic (or language) model adaptation. By providing an unsupervised adaptation scheme, systems can make a step toward self-learning. Obviously, for training, a transcription has to be provided in any case. In the unsupervised case, this transcription is obtained by decoding with the existing baseline model. The source model may also be a specific model which needs further adaptation (incremental adaptation).

For unsupervised adaptation, the quality of transcriptions is never good enough, otherwise the adaptation would not be required. Therefore, a mechanism allowing for either predicting the accuracy (or confidence) of the transcripts, or soft target training to represent multiple hypotheses can be very useful to carry out the adaptation on reliable data.

7.1 Predicting Confidence

The ASR itself is able to produce confidence in a normalized range associated with words in the decoded lattice. These confidences result from the acoustic and the language model scores, hence are less favourable for acoustic model

adaptation, because if the grammar used for decoding is poorly fitting, confidences get heavily biased. Analysing some recordings along with their confidence lattices has revealed that the predicting power of the confidence scores for telling whether a word is correctly recognized is too low for a meaningful exploitation in our task. Indeed, providing confidence is known to be a hard task, no standalone feature is known with strong predicting power, therefore, an ensemble of weak classifiers was considered an alternative: TranscRater [32] is a freely available toolkit building upon an abundant feature set to predict WER, and the prediction is independent from ASR confidence and does not require reference (supervision) for inference. The input features rely on four main categories: speech signal (MFCC plausibility), lexicon (how difficult is to transcribe a given word), language model (several can be used, even different from the one used for decoding, word likelihoods and perplexities are extracted) and part-of-speech (to estimate whether the observed syntax makes sense). As said, there is no confidence score used from the ASR, but TranscRater has to be trained prior to using it, which however requires a supervised subset, or at least a correct (high precision) value for the WER. This is obviously a considerable drawback.

While evaluating TranscRater capabilities for our task, we found a very weak correlation between the actual and predicted WER on our development sets, therefore, we dropped using it. We were also experimenting with predicting the M-measure [33], which evaluates acoustic consistence and plausibility and therefore it can be a promising candidate to prepare acoustic model adaptation, as it considers only the acoustic aspects of data. In a similar framework to M-measure, it is also possible to use acoustic model posteriors for WER prediction (or provide a score for the goodness of the transcript), which completely eliminates the dependence on the HCLG (and hence language model). Without representing here, the exact formulae, the idea behind M-measure is to capture posterior divergence of the acoustic model for several time spans and compute the mean of them. Divergence is computed as the symmetric Kullback-Leibler distance between posterior distributions yielded by the acoustic model for a certain time. Intuitively, this term penalizes smooth distributions (where there is no outstanding posterior probability associated with a certain senone), and also penalizes inconsistency over time, i.e. a recurrent senone should be consistently represented at the posterior level, which could minimize the KLD and hence M-measure, too. M measure was found to yield better estimates than ASR confidence or TranscRater, but still below a fair correlation between the M-measure and the WER.

7.2 Soft Targets with Lattice Supervision

An alternative to predicting confidence (reliability of transcripts) is to provide a soft transcript, which allows for multiple hypotheses. A lattice is an ideal choice instead of a hard transcript. Using a lattice moreover matches perfectly with

discriminative training strategies and given the computation load reduction resulting from applying a lattice free denominator, the numerator can be allowed to remain more complex.

We prepared experiments by using standard decoder settings (in terms of beam and other respective parameters) with the Librispeech TDNN baseline and the 'tgmed' language model. The first task is augmenting the data: a speed and volume perturbation-based augmentation can be used, followed by extraction of high resolution (hires) features. Thereafter, the decoder can be run by preserving the produced lattices for the numerator in TDNN discriminative training.

Adaptation results are summarized in Table 2. Results suggest that the closer the accent is to the standard one, the less amount of data is required, and that the more target data we have, the more powerful becomes creating a new layout (last hidden layer, SoftMax and output based on target domain state tying tree).

Table 2
WER reduction obtained with unsupervised adaptation

	AUS	CDN	ENG	IND	USA
Amount of adaptation data (hours)	8	8	31	10	59
Baseline WER	25.3	13.3	19.9	44.8	24.5
WER reduction vanilla retraining	**16.4**	11.3	**15.4**	33.3	**16.2**
WER reduction top layer reinitialization	**16.4**	**11.7**	13.3	**34.1**	15.4

Compared to the supervised case, the obtained WER reduction is lower, but still over 10% in all cases. Changing the output layout was slightly better performing than vanilla retraining, probably because training a new context dependency tree was better fitting to automatic transcripts (lattices) containing errors. As a rule of thumb, we may suggest using a new context dependency tree and adjusted model topology for unsupervised adaptation, or stay with vanilla retraining when adaptation data is in the range of 10 or a few tens of hours.

Conclusions

In this paper we have addressed dialect adaptation of the ASR acoustic models. We compared vanilla retraining without network topology changes to two alternatives involving topology changes: factorization between hidden layers and creating new senone layout by preserving lower network structure with transfer learning. We found that even with low amount of adaptation data available, factorization alike approaches underperformed vanilla retraining. Regarding transfer learning with changing the top layout, we obtained better results than with vanilla retraining if adaptation data was abundant. Adding cross-entropy based Kullback Leibler regularization did not improve significantly the WER after adaptation, as other regularizing component and techniques – using cross-entropy and backstitch – are likely to have a similar effect. Our overall conclusion can be summarized as follows: instead going for sophisticated approaches, the more

traditional solutions work also well by much lower complexity and requiring less effort.

References

[1] P. Baranyi and A. Csapo, Cognitive infocommunications: coginfocom, in 2010 11th International Symposium on Computational Intelligence and Informatics (CINTI) IEEE, 2010, pp. 141-146

[2] A. Csapo and P. Baranyi, An adaptive tuning model for cognitive info-communication channels, in 2011 IEEE 9th Int. Symposium on Applied Machine Intelligence and Informatics (SAMI) IEEE, 2011, pp. 231-236

[3] L. Czap and L. Zhao, Phonetic aspects of Chinese Hhaanxi Xi'an dialect, in 2017 8th IEEE International Conference on Cognitive Infocommunications (CogInfoCom) IEEE, 2017, pp. 000 051-000 056

[4] G. Szaszák and P. N. Garner, Evaluating intra-and crosslingual adaptation for non-native speech recognition in a bilingual environment, in 2013 IEEE 4th International Conference on Cognitive Infocommunications (CogInfoCom) IEEE, 2013, pp. 357-362

[5] J. Galić, B. Popović, and D. Š. Pavlović, Whispered speech recognition using hidden markov models and support vector machines, Acta Politechnica Hungarica, Vol. 15, No. 5, 2018

[6] A. López-Zorrilla, M. de Velasco Vázquez, S. Cenceschi, and M. I. Torres, Corrective Focus Detection in Italian Speech Using Neural Networks, Acta Polytechnica Hungarica, Vol. 15, No. 5, 2018

[7] Y. Kiryu, A. Ito, and M. Kanazawa, Recognition Technique of Confidential Words Using Neural Networksin Cognitive Infocommunications, Acta Polytechnica Hungarica, Vol. 16, No. 2, pp. 129-143, 2019

[8] I. Poggi, F. DErrico, and L. Vincze, Uncertain Words, Uncertain Texts. Perception and Effects of Uncertainty in Biomedical Communication, Acta Polytechnica Hungarica, Vol. 16, No. 2, 2019

[9] M. Rusko and M. Finke, Using speech analysis in voice communication: A new approach to improve air traffic management security, in 2016 7th IEEE International Conference on Cognitive Infocommunications (CogInfoCom) IEEE, 2016, pp. 000 181-000 186

[10] I. J. Goodfellow, M. Mirza, D. Xiao, A. Courville, and Y. Bengio, An empirical investigation of catastrophic forgetting in gradient-based neural networks, arXiv preprint arXiv:1312.6211, 2013

[11] D. M. Hawkins, The problem of overfitting, Journal of chemical information and computer sciences, Vol. 44, No. 1, pp. 1-12, 2004

[12] J. Neto, L. Almeida, M. Hochberg, C. Martins, L. Nunes, S. Renals, and T. Robinson, Speaker-adaptation for hybrid HMM-ANN continuous speech

recognition system, in 4th Conference on Speech Communication and Technology, 1995

[13] R. Gemello, F. Mana, S. Scanzio, P. Laface, and R. De Mori, Linear hidden transformations for adaptation of hybrid ANN/HMM models, Speech Communication, Vol. 49, No. 10-11, pp. 827-835, 2007

[14] P. Swietojanski, J. Li, and S. Renals, Learning hidden unit contributions for unsupervised acoustic model adaptation, IEEE/ACM Trans. on Audio, Speech and Lang. Proc., Vol. 24, No. 8, pp. 1450-1463, 2016

[15] P. Ghahremani, V. Manohar, H. Hadian, D. Povey, and S. Khudanpur, Investigation of transfer learning for ASR using LF-MMI trained neural networks, in Automatic Speech Recognition and Understanding Workshop (ASRU) 2017 IEEE. IEEE, 2017, pp. 279-286

[16] S. Parveen and P. Green, Multitask learning in connectionist robust asr using recurrent neural networks, in Eighth European Conference on Speech Communication and Technology, 2003

[17] Y. Zhao, J. Li, and Y. Gong, Low-rank plus diagonal adaptation for deep neural networks, in Acoustics, Speech and Signal Processing (ICASSP), 2016 IEEE International Conference on. IEEE, 2016, pp. 5005-5009

[18] G. Saon, H. Soltau, D. Nahamoo, and M. Picheny, Speaker adaptation of neural network acoustic models using i-vectors, in ASRU, 2013, pp. 55-59

[19] R. Doddipatla, N. Braunschweiler, and R. Maia, Speaker Adaptation in DNN-Based Speech Synthesis Using d-Vectors, in INTERSPEECH, 2017, pp. 3404-3408

[20] Tripathi, A. Mohan, S. Anand, and M. Singh, Adversarial learning of raw speech features for domain invariant speech recognition, in Acoustics, Speech and Signal Processing (ICASSP) 2018 IEEE International Conference on. IEEE, 2018

[21] V. Manohar, P. Ghahremani, D. Povey, and S. Khudanpur, A Teacher-Student Learning Approach for Unsupervised Domain Adaptation of Sequence-Trained ASR Models, in 2018 IEEE Spoken Language Technology Workshop (SLT) IEEE, 2018, pp. 250-257

[22] D. Povey, A. Ghoshal, G. Boulianne, L. Burget, O. Glembek, N. Goel, M. Hannemann, P. Motlicek, Y. Qian, P. Schwarz et al., The Kaldi speech recognition toolkit, in IEEE 2011 workshop on automatic speech recognition and understanding, no. EPFL-CONF-192584. IEEE Signal Processing Society, 2011

[23] V. Peddinti, D. Povey, and S. Khudanpur, A time delay neural network architecture for efficient modeling of long temporal contexts, in Sixteenth Annual Conference of the International Speech Communication Association, 2015

[24] D. Povey, G. Cheng, Y. Wang, K. Li, H. Xu, M. Yarmohammadi, and S. Khudanpur, Semi-Orthogonal Low-Rank Matrix Factorization for Deep Neural Networks, in Interspeech 2018, 2018, pp. 3743-3747

[25] D. Snyder, D. Garcia-Romero, G. Sell, D. Povey, and S. Khudanpur, X-vectors: Robust DNN embeddings for speaker recognition, in 2018 IEEE International Conference on Acoustics, Speech and Signal Processing (ICASSP) IEEE, 2018, pp. 5329-5333

[26] D. Yu and L. Deng, Adaptation of deep neural networks, in Automatic Speech Recognition. Springer, 2015, pp. 193-215

[27] Y. Wang, V. Peddinti, H. Xu, X. Zhang, D. Povey, and S. Khudanpur, Backstitch: Counteracting finite-sample bias via negative steps, In: Interspeech 2017, pp. 1631-1635

[28] V. Panayotov, G. Chen, D. Povey, and S. Khudanpur, "Librispeech: an ASR corpus based on public domain audio books," in Acoustics, Speech and Signal Processing (ICASSP) 2015 IEEE International Conference on. IEEE, 2015, pp. 5206-5210

[29] The Mozilla Common Voice corpus, https://voice.mozilla.org/, 2017

[30] D. Yu, K. Yao, H. Su, G. Li, and F. Seide, KL-divergence regularized deep neural network adaptation for improved large vocabulary speech recognition, in 2013 IEEE International Conference on Acoustics, Speech and Signal Processing. IEEE, 2013, pp. 7893-7897

[31] D. Falavigna, M. Matassoni, S. Jalalvand, M. Negri, and M. Turchi, DNN adaptation by automatic quality estimation of ASR hypotheses, Computer Speech & Language, Vol. 46, pp. 585-604, 2017

[32] S. Jalalvand, M. Negri, M. Turchi, J. G. de Souza, D. Falavigna and M. R. Qwaider, Transcrater: a tool for automatic speech recognition quality

[33] B. T. Meyer, S. H. Mallidi, H. Kayser and H. Hermansky, *Predicting error rates for unknown data in automatic speech recognition*. 2017 IEEE International Conference on Acoustics, Speech and Signal Processing (ICASSP) IEEE, 2017

Handwriting and Drawing Features for Detecting Personality Traits: An Analysis on Big Five Sub-dimensions*

Anna Esposito[1], Terry Amorese[1], Michele Buonanno[1], Marialucia Cuciniello[1], Antonietta M. Esposito[2], Marcos Faundez-Zanuy[3], Laurence Likforman-Sulem[4], Maria Teresa Riviello[1], Carmine Spagnuolo[5], Alda Troncone[1], and Gennaro Cordasco[1]

[1]Department of Psichology, University of Campania "L. Vanvitelli", Viale Ellittico, 31 - 81100 Caserta, and IIASS, Italy
Email: anna.esposito@unicampania.it, terry.amorese@unicampania.it michele.buonanno@studenti.unicampania.it, marialucia.cuciniello@unicampania.it, mariateresa.riviello@unicampania.it, alda.troncone@unicampania.it, gennaro.cordasco@unicampania.it

National Institute of Geophysics and Volcanology (INGV/OV), Via Diocleziano, 328, 80125 Napoli, Italy; Email: antonietta.esposito@ingv.it

[3]Escola Superior Politecnica, TecnoCampus Mataro-Maresme Mataro, Carrer d'Ernest Lluch, 32, 08302 Mataró, Barcelona, Spain
Email: faundez@tecnocampus.cat

[4]Télécom ParisTech, Université Paris-Saclay, 19 Place Marguerite Perey, 91120 Palaiseau, France; Email: likforman@telecom-paristech.fr

[5]Department of Computer Science, University of Salerno, Via Giovanni Paolo II, 132 - 84084 Fisciano (SA), Italy; Email: cspagnuolo@unisa.it

Abstract: Handwriting and Drawing are functional tasks involving physical and cognitive processes. Recently they have been investigated for detecting cognitive and motor disorders. In this work, handwriting/drawing features are investigated for identifying connections with personality traits. For this purpose, an experiment comprising seven handwriting/drawing tasks has been administrated to 78 young adults (mean age=24.6 ± 2.4 years) equally balanced by gender. Handwriting and Drawing activities - both on and close to the paper – had been recorded online through a digitizing tablet able to measure handwriting and drawing features such as pressure, speed, dimension, and inclination of

* A preliminary version of this paper was presented at the 10th IEEE International Conference on Cognitive Infocommunication (CogInfoCom 2019), [4]

each pen-stroke on the paper. Participants were asked to fill the Big Five Personality Questionnaire (BFQ) and according to the scores obtained for each of the 5 dimensions and 10 Big Five sub-dimensions, were partitioned into three categories: low, typical, and high. To evaluate whether the recorded handwriting/drawing features are connected with personality traits ANOVA repeated measures have been performed with gender and group category (low, typical, and high) as between and the listed handwriting/drawing features as within factors. The analyses show significant differences among low, typical and, high BFQ scores for the main Big Five dimensions and the ten Big Five sub-dimensions, indicating that personality traits can be revealed by a quantitative analysis of the proposed handwriting/drawing features.

Keywords: Personality traits; Big Five; Handwriting and drawing tasks; Graphology

1 Introduction

The act of writing and drawing by hand is the result of a complex interaction of physical and mental processes involving several cognitive, kinesthetic, and perceptual-motor skills. Indeed, handwritten texts convey considerable information on how some areas of the human brain are working [24]. Neurology, for example, utilizes writing and drawing tasks as a noninvasive method for diagnosing and monitoring of disorders such as Alzheimer's and Parkinson's disease, and developmental impairments among others [10, 12, 25].

Handwriting and drawing are a physical way for human of expressing themselves, and therefore creative processes involving conscious and unconscious factors among self's motivations, emotions, mood, and temperament [22]. Thus, handwriting and drawing analyses may allow identifying both neurological psychological individual's characteristics.

Personality may be among these characteristics [13]. Personality is related to a pattern of relatively unique and individual's traits giving consistency and individuality to a person's behavior [5]. It includes thoughts, emotions, and attitudes, both innate and learned, influencing an individual's "interactions with, and adaptations to, the intrapsychic, physical, and social environments" [16]. Indeed, that topic is increasingly attracting researchers, as detecting individual's personality is ca way to predict individual behaviors and preferences [9] across different application's contexts from health care [8] to marketing [23].

Personal individual traits are commonly measured by validated questionnaires made up of items aimed to envisage respondents' attitudes and conducts.

The most used questionnaire to identify individual's personality traits is the "Big Five Questionnaire" (BFQ) [3, 19]. Such a questionnaire is based on the empirically "Five Factors Model" [6], representing the personality in terms of five dimensions, each consisting of two sub-dimensions, (see details in Section 2.2).

The Big Five Model has been exploited for different purposes, form preventive medicine [11] to recruitment [1].

The oldest and widespread method to identify and understand personality through handwriting analysis is graphology [14]. Graphology provides some hints for assessing individuals' personality by evaluating strokes, patterns and pressure applied while writing. Unfortunately, graphology is based on subjective non-standardized evaluations carried out by graphologists requiring be very costly and time-consuming analyses. On the other hand, modern drawing devices like graphics tablets and digital pens or web whiteboards can gather data to allow quantitative (objective) handwriting and drawing analyses. Gathered data consist of timing information associated with pen position (on a 2D space), pen inclination (two angles with respect to the paper) and pen state (drawing a stroke on the paper or in-air between two strokes). In this paper, we define a stroke as a continuous line drawn using the same pen state (on paper or in-air). Some devices enable to measure also the pressure applied on the paper. Such data has been effectively exploited for impairment detection and personality traits assessment [17, 18, 21] as well as for the detection of mood and emotional states [2].

The present study investigates the link between handwriting/drawing features and personality traits as measured by the "Big Five" questionnaire. A preliminary analysis of these data has been reported in [4], where it has been shown that the Big Five main dimensions describing personality can be significantly detected through the following set of computable handwriting features:

a) the time and number of strokes required to perform a handwriting/drawing task;
b) the pressure applied on the paper;
c) the space occupied by the strokes;
d) the inclination of handwriting strokes.

The results reported in the present study differs from those reported and discussed in [4] since it provides a deeper investigation assessing the capability of the above-mentioned features to characterize the 10 Big Five sub-dimensions.

2 Handwriting Analysis for the Detection of Personal Traits

2.1 Handwriting/Drawing Digital Analysis

Thanks to the recent development of new technological tools (digital scanners, touch screens, digital pens, and graphics tablets), handwriting analysis can be performed on a computerized platform. Computerized online handwriting/drawing analysis provides two main advantages: a) data collection of several invisible features, such as pen pressure, pen tilt, in air movements; b) data collection of timings, which can be exploited to dynamically analyze the entire handwriting/drawing process instead of a single static set of on a paper strokes representing the final handwriting/drawing task. These online measures had revealed themselves very useful to detect (through appropriately defined handwriting/drawing tasks) diseases, like dementia and /or brain stroke risk factors [15, 20, 22].

In this work, handwriting/drawing analysis was performed using the INTUOS WACOM Series 4 digital tablet and the Intuos Inkpen writing device. The tablet captures digitally signals describing the Inkpen movements performed by the subjects while writing/drawing an A4 plain paper placed on the tablet screen.

During each handwriting/drawing activity, the following data are acquired continuously at intervals of approximately 8 milliseconds (125 Hz):

1) Time in milliseconds;
2) Pen tip x-position;
3) Pen tip y-position;
4) Pen status (*in air*, coded as 0 or *on paper*, coded as 1);
5) Azimuth angle of the pen with respect to the plane of the writing surface;
6) Altitude angle of the pen with respect to the plane of the writing surface;
7) Pressure applied on the writing surface (only when the status is *on paper*).

Each acquisition is stored as one line in a text file; a comma separates the seven acquired values.

2.2 Personal Traits: The Big Five and Sub-Dimensions

Big Five questionnaire (BFQ) has identified five basic dimensions for character description and evaluation. Each of them considers two sub-dimensions. These dimensions do not represent specific theoretical views, but are derived from the analysis of natural language terms that people use to describe themselves and

others. Each sub-dimension is evaluated using 12 items, of which 6 are positive and 6 are negative, in order to control the desirability bias, i.e. "the tendency of research subjects to give socially desirable responses instead of choosing responses that are reflective of their true feelings" [7].

BFQ comprises also a Lie Scale (L) designed to evaluate subjects' propensity to provide false information. The scale L is composed of 12 items and involves ideal behaviors in society. Overall, BFQ comprises 132 items, each of which is answered through 5 point a Likert scale (1 = "very false for me" to 5 = "very true for me").

The Big Five main dimensions and the two sub-dimensions associated to each of them are described as follows:

1) *Openness to Experience*: refers to the ability and tendency of people to explore and create new experiences, showing curiosity, imagination, creativity, appreciation of art and out-of-the-box ideas. The two sub-dimensions are *Intellect* and *Openness*. Intellect reflects the tendency to participate in abstract and intellectual information, while Openness reflects the tendency to participate in aesthetic and sensory information (perception and imagination).

On this scale, people score according to a dichotomy: inventive/curious (higher score) and consistent/cautious (lower score).

2) *Conscientiousness*: refers to a person who is careful, thoughtful, responsible, organized, hardworking, accomplished, and persevering. The secondary dimensions of consciousness are *Industriousness* and *Orderliness*. *Industriousness* refers to the ability to engage in continuous, goal-oriented endeavors, which is related to productivity and professional ethics, while Orderliness refers to the tendency of arrangement, organization, and systemization, which is related to qualities such as cleanliness and diligence.

On this scale, people score according to a dichotomy: efficient/organized (higher scores) vs. easy-going/careless (lower scores)

3) *Extroversion*: refers to people who express positive emotions easily, are sociable, gregarious, decisive, talkative, and active. The two sub-dimensions are *Enthusiasm* and *Assertiveness*. Enthusiasm means friendliness, sociability, and a tendency to experience positive influences, while Assertiveness reflects a tendency toward agency, driving force, and social dominance

On this scale, people score according to a dichotomy: outgoing/energetic (higher scores) vs. solitary/reserved (lower scores).

4) *Agreeableness*: refers to a person who tends to be compassionate, trusting and helpful, flexible and tolerant. The sub-dimensions of agreeableness are *Compassion* and *Politeness*. Compassion refers to the tendency to care for others emotionally, while Politeness refers to the tendency to show good manners, observe social norms, and avoid aggression.

On this scale, people score according to a dichotomy: friendly/compassionate (higher scores) vs. alleging/detached (lower scores).

5) *Neuroticism*: Refers to people who lack stability and control of their emotions and are easily emotional, anxious, depressed, angry, worried, and insecure. The sub-dimensions of neuroticism are *Withdrawal* and *Volatility*. Withdrawal refers to the susceptibility to negative inward influences (inhibition), while Volatility refers to emotional instability, difficulty in controlling emotional impulses, and sensitivity to negative outward influences (disinhibition).

On this scale, people score according to a dichotomy: sensitive/nervous (higher scores) vs. secure/confident (lower scores).

3 The Design of the Experiment

To investigate the link among handwriting/drawing features and personality traits, in terms of Big Five and sub-dimensions, an experimental protocol has been devised. The protocol consisted in administering both the Big Five questionnaire and a series of handwriting and drawing tasks, through the above-mentioned digital tablet. Participants were properly informed about the protocol and signed informed consent before being enrolled in the experiment.

3.1 Subjects

A total of 78 participants (40 men and 38 women, mean age: 24.6, SD: 2.4) were recruited among the students of the University of Campania "Luigi Vanvitelli" in Caserta (southern Italy). They were first asked to fill in the Big Five questionnaire and then to perform the seven handwriting/drawing tasks described in Figure 1.

For each of the Big Five main dimensions and sub-dimensions, participants were divided into the group categories, “low”, “typical” and “high”, based on the BFQ scores obtained. In particular, subjects with BFQ scores less than 46 were classified as "low", those with a BFQ scores between 46 and 54 were classified as "typical" and those with BFQ scores greater than 54 were classified as "high".

Tables 1 and 2 show the distribution of participants according to the gender (FEMALE: F and MALE: M) and the three categories (LOW, TYPICAL and HIGH) defined above, for each Big Five (Table 1) and each sub-dimension (Table 2).

Table 1
Big Five main dimension and associated subjects' distributions with respect to their gender and group category (high, typical and low)

	High		Typical		Low	
	F	M	F	M	F	M
Extraversion	17	16	13	17	8	7
Agreeableness	12	18	8	14	18	8
Conscientiousness	16	16	5	14	7	10
Neuroticism	7	14	18	15	13	11
Openness to Experience	16	27	14	9	8	4

Table 2
Big Five sub-dimension and associated subject's distribution with respect to their gender and group category (high, typical and low)

		High		Typical		Low	
		F	M	F	M	F	M
Extraversion	Enthusiasm	16	17	14	12	8	11
	Assertiveness	17	19	15	12	6	9
Agreeableness	Compassion	16	16	15	15	7	9
	Politeness	11	16	11	14	16	10
Conscientiousness	Industriousness	20	18	15	13	3	9
	Orderliness	14	16	17	13	7	11
Neuroticism	Withdrawal	9	14	17	14	12	12
	Volatility	7	14	14	12	17	14
Openness to Experience	Intellect	20	27	12	7	6	6
	Openness	17	25	8	9	13	6

3.2 Tasks and Features

The handwriting/drawing tasks, performed by each subject were and acquired through the tablet were the following:

• Pentagons drawing;

• House drawing);

•*Four Italian words written in capital letters* (BIODEGRADABILE (biodegradable), FLIPSTRIM (flipstrim), SMINUZZAVANO (collapse), CHIUNQUE (anyone));

• *A series of loops with the left hand*;

• *A series of loops with the right hand*;

• *A clock drawing task* (with the hours and clock hands);

• The following *phonetically complete Italian sentence to be written in cursive letters*: I pazzi chiedono fiori viola, acqua da bere, tempo per sognare (crazy people are looking for purple flowers, drinking water, and time to dream).

Figure 1 illustrates the seven tasks as requested to each participant.

From the set of dynamic features recorded by the tablet and described in Section 2.1, it is possible to compute more features such as pen acceleration, velocity, instantaneous trajectory angle, instantaneous displacement, time characteristics, and ductus-based characteristics. In addition, in this article, we use the method defined in [2] to classify the strokes into three categories:

- **down strokes**, when the pen touches the surface. They are recorded with state 1 (since we are using an Inkpen, they appear on the paper and provide feedback to the subjects);
- **up strokes**, when the pen is close but does not touch the surface. They do not appear on the paper, but since the pen is close to the surface they are recorded with state 0 by the digital tablet;
- **idle strokes**, when the pen is far from the surface. The tablet does not recognize them, but they are still recognizable using time stamps.

In this paper, the following 17 handwriting/ drawing features are considered, grouped into five categories:

Pressure features, computed by measuring the pressure applied by the pen on the tablet surface during a specific task (only down strokes are considered):

1) P_{min}, minimum pressure recorded during a specific task;
2) P_{max}, maximum pressure recorded during a specific task;
3) P_{avg}, average pressure recorded during a specific task;
4) P_{sd}, standard deviation of pressures recorded during a specific task;

5) P_{10}, 10^{th} percentile. Assuming assume that the recorded pressures are sorted in ascending order, the 10^{th} percentile is the value that divides the data so 10% is below it;
6) P_{90}, 90^{th} percentile;

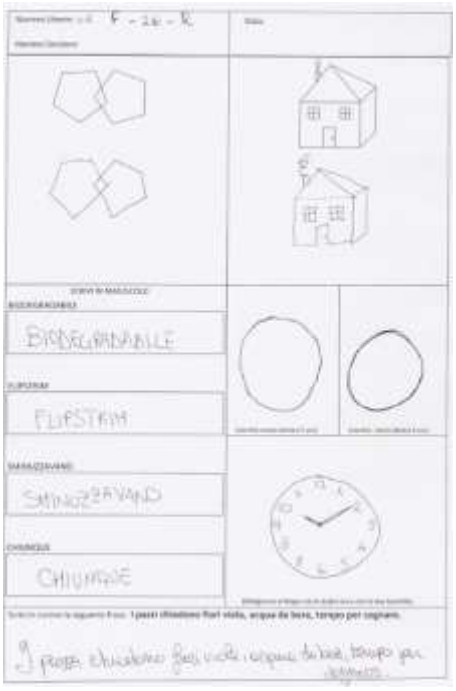

Figure 1
The seven handwriting/drawing tasks as they have been proposed to each participant

Ductus features, based on the number of strokes, in each pen status, performed during the task:

7) N_{up}, number of up strokes (the strokes that do not appear on the paper, but have been performed close to the surface);
8) N_{down}, number of down strokes (the strokes that appear on the paper);
9) N_{idle}, number of idle strokes (the number of times the pen is moved away from the paper/tablet, during a task).

Time features, based on the time spent, in each pen status, during the task:

10) T_{up}, time spent on up strokes;
11) T_{down}, time spend on down strokes;
12) T_{idle}, time spent in the idle status;
13) T_{total}, total time elapsed for the task ($T_{total} = T_{up} + T_{down} + T_{idle}$).

Space features, based on the area used by the strokes:

14) S_{bb}, sum of spaces used by on paper strokes. For each stroke, we compute the smallest axis aligned box containing the stroke and sum its area;
15) S_{avg}, average Euclidean distance between consecutive down strokes;
16) S_{total}, sum of the Euclidean distance between consecutive down strokes.

Inclination features, based on the inclination of strokes:

17) I_{avg}, average inclination of down strokes.

3.2 Results on the Main Big Five Dimension

Table 3 below provides a summary of the significant results observed for the main Big Five dimensions and discussed in detail in [4].

In this work, we provide a more detailed description and a deeper analysis of each Big Five sub-dimension. To this end, several repeated measures analysis of variance (ANOVAs) have been performed for each feature (divided into 5 categories), each task, and each Big Five sub-dimensions. It is worth mentioning that a single repeated measures analysis of variance was performed on the Inclination category, because it contains a single feature. The Bonferroni post-hoc test was performed with a significance equal to $\alpha = .05$.

Table 3
For each dimension, the table provides the task and the corresponding handwriting/drawing features for which it has been observed a significant difference among groups

Big Five Dimension	Task	Features
Extraversion	Loops with the left hand	T_{down}, T_{total}
	Loops with the right hand	T_{down}, T_{total}
Agreeableness	Clock drawing	N_{idle}
	House drawing	T_{total}, N_{up}, N_{down}, N_{idle}
	Writing in cursive letters	S_{bb}, N_{up}, N_{down}, N_{idle} s
	Pentagons drawing	N_{up}, N_{down}, N_{idle}
Conscientiousness	Loops with the right hand	T_{down}, T_{total}
	Pentagons drawing	N_{up}, N_{down}, N_{idle}
	House drawing	N_{up}, N_{down}, N_{idle}
	Clock drawing	N_{up}, N_{down}, N_{idle}
Openness to Experience	Writing in capital letters	P_{max}, P_{sd}, P_{10}, P_{90}, N_{up}, N_{down}, N_{idle}, S_{bb}, S_{avg}
	Loops with the left hand	T_{down}, T_{total}
	Loops with the right hand	T_{down}, T_{total}
	Writing in cursive letters	N_{up}, N_{down}, N_{idle}
Neuroticism	House drawing	S_{bb}, S_{avg}, S_{total},

4 Results

In the following, we provide the significant results obtained, grouped by features categories. A summary of these results is also provided in the following Table 4.

4.1 Pressure Features

- **Extraversion -> Assertiveness:**

a) Task 5: A series of loops with the right hand. There are significant differences between the three Assertiveness group categories [$F(2,72)<3.636$; $p=0.031$]. Bonferroni post-hoc tests showed a significant difference ($p=0.030$) between the score of participants in the *typical* group ($M=559.830$; $SD=18.995$) and the score of participants in the *low* group ($M=473.367$; $SD=25.849$). In particular, this difference is due to the scores of the following features:

   - P_{max}: The score of the *low* group ($M=786.13$; $SD=161.43$) is significantly different ($p=0.047$) with respect to the score of the *typical* group ($M=887.74$; $SD=121.03$);
   - P_{avg}: The score of the *low* group ($M=645.08$; $SD=189.84$) is significantly different ($p=0.026$) with respect to the score of the *typical* group ($M=768.85$; $SD=141.13$);
   - P_{90}: The score of the *low* group ($M=732.47$; $SD=174.15$) is significantly different ($p=0.033$) with respect to the score of the *typical* group ($M=849.56$; $SD=135.68$).

4.2 Ductus Features

- **Agreeableness -> Politeness:**

a) Task 6: A clock drawing task. There are significant differences between the three Politeness group categories [$F(2,72)<4.435$; $p=0.015$]. Bonferroni post-hoc tests showed a significant difference ($p=0.004$) between the score of participants in the *low* group ($M=21.37$; $SD=1.63$) and the score of participants in the *high* group ($M=28.16$; $SD=1.59$). In particular, this difference is due to the scores of the following features:

   - N_{up}: The score of the *high* group ($M=28.99$; $SD=1.26$) is significantly different ($p=0.043$) with respect to the score of the *low* group ($M=24.41$; $SD=1.30$) and significantly different ($p=0.014$) with respect to the score of the *typical* group ($M=23.67$; $SD=1.30$);
   - N_{down}: The score of the *high* group ($M=29.63$; $SD=1.28$) is significantly different ($p=0.043$) with respect to the score of the *low* group ($M=25.01$; $SD=1.32$) and significantly different ($p=0.014$) with respect to the score of the *typical* group ($M=24.24$; $SD=1.32$);

- N_{idle}: The score of the *low* group (M=14.68; SD=3.16) is significantly different (p=0.041) with respect to the score of the *high* group (M=25.84; SD=3.07) and significantly different (p=0.016) with respect to the score of the *typical* group (M=27.56; SD=3.16).

4.3 Time Features

- **Extraversion -> Enthusiasm:**

a) Task 5: A series of loops with the right hand. There are significant differences between the three Enthusiasm group categories [F(2,72)<3.831; p=0.026]. Bonferroni post-hoc tests showed a significant difference (p=0.023) between the score of participants in the *low* group (M=3655.22; SD=264.46) and the score of participants in the *high* group (M=4909.44; SD=273.20). In particular, this difference is due to the scores of the following features:

- T_{down}: The score of the *low* group (M=6970.42; SD=3614.54) is significantly different (p=0.006) with respect to the score of the *high* group (M=9773.61; SD=2638.94);
- T_{total}: The score of the *low* group (M=7314.53; SD=3811.99) is significantly different (p=0.022) with respect to the score of the *high* group (M=9793.00; SD=2653.03).

- **Agreeableness -> Compassion:**

a) Task 3: Four Italian words in capital letters. There are significant differences between the three Compassion group categories [F(2,72)<4.800; p=0.011]. Bonferroni post-hoc tests showed a significant difference (p=0.009) between the score of participants in the *low* group (M=19350.45; SD=1057.52) and the score of participants in the *typical* group (M=15329.87; SD=766.24). In particular, this difference is due to the scores of the following features:

- T_{up}: The score of the *low* group (M=16458.50; SD=6911.05) is significantly different (p=0.044) with respect to the score of the *typical* group (M=12625.13; SD=4025.33);
- T_{idle}: The score of the *low* group (M=5986.37; SD=6388.06) is significantly different (p=0.036) with respect to the score of the *typical* group (M=3406.73; SD=1734.23);
- T_{total}: The score of the *low* group (M=39417.57; SD=14216.22) is significantly different (p=0.009) with respect to the score of the *typical* group (M=28166.33; SD=4273.03).

- **Agreeableness -> Politeness:**

a) Task 4: A series of loops with the left hand. There are significant differences between the three Politeness group categories [$F(2,72)<4.392$; $p=0.016$]. Bonferroni post-hoc tests showed a significant difference ($p=0.022$) between the score of participants in the *low* group ($M=4113.86$; $SD=400.60$) and the score of participants in the *high* group ($M=5680.64$; $SD=389.23$). In particular, this difference is due to the scores of the following features:

   - T_{down}: The score of the *low* group ($M=7681.88$; $SD=3855.59$) is significantly different ($p=0.020$) with respect to the score of the *high* group ($M=10282.04$; $SD=3306.64$) and significantly different ($p=0.023$) with respect to the score of the *typical* group ($M=10513.24$; $SD=3901.02$);
   - T_{total}: The score of the *low* group ($M=8102.42$; $SD=4063.94$) is significantly different ($p=0.019$) with respect to the score of the *high* group ($M=11120.26$; $SD=3895.06$).

- Task 5: A series of loops with the left hand. There are significant differences between the three Politeness group categories [$F(2,72)<5.972$; $p=0.004$]. Bonferroni post-hoc tests showed a significant difference ($p=0.009$) between the score of participants in the *low* group ($M=3637.38$; $SD=302.70$) and the score of participants in the *typical* group ($M=5005.07$; $SD=302.55$). In particular, this difference is due to the scores of the following features:
   - T_{down}: The score of the *low* group ($M=7099.92$; $SD=3712.54$) is significantly different ($p=0.012$) with respect to the score of the *high* group ($M=9302.37$; $SD=2690.20$) and significantly different ($p=0.003$) with respect to the score of the *typical* group ($M=9876.94$; $SD=2651.90$);
   - T_{total}: The score of the *low* group ($M=7320.81$; $SD=3842.68$) is significantly different ($p=0.022$) with respect to the score of the *high* group ($M=9326.07$; $SD=2711.47$) and significantly different ($p=0.006$) with respect to the score of the *typical* group ($M=9907.84$; $SD=2625.55$).

- Task 6: A clock drawing task. There are significant differences between the three Politeness group categories [$F(2,72)<3,879$; $p=0.025$]. Bonferroni post-hoc tests showed a significant difference ($p=0.005$) between the score of participants in the *low* group ($M=13782.99$; $SD=1500.79$) and the score of participants in the *high* group ($M=19468.68$; $SD=1458.21$). In particular, this difference is due to the scores of the following features:
   - T_{up}: The score of the *low* group ($M=11498.73$; $SD=4468.06$) is significantly different ($p=0.026$) with respect to the score of the *high* group ($M=16926.52$; $SD=7929.66$);
   - T_{total}: The score of the *low* group ($M=26440.96$; $SD=11594.21$) is significantly different ($p=0.025$) to the score of the *high* group ($M=39754.11$; $SD=20125.58$).

- **Conscientiousness -> Orderliness:**

a) Task 3: Four Italian words in capital letters. There are significant differences between the three Orderliness group categories [$F(2,72)<4.117$; $p=0.020$]. Bonferroni post-hoc tests showed: i) a significant difference ($p=0.028$) between the score of participants in the *low* group ($M=19118.55$; $SD=1026.73$) and the score of participants in the *high* group ($M=15860.77$; $SD=777.14$); ii) a significant difference ($p=0.016$) between the score of participants in the *low* group ($M=19118.55$; $SD=1026.73$) and the score of participants in the *typical* group ($M=15696.32$; $SD=782.40$). In particular, this difference is due to the scores of the following feature:

  - T_{total}: The score of the *low* group ($M=38550.22$; $SD=12719.49$) is significantly different ($p=0.041$) with respect to the score of the *high* group ($M=31792.77$; $SD=5250.42$) and significantly different ($p=0.030$) with respect to the score of the *typical* group ($M=31267.60$; $SD=7741.35$).

- **Conscientiousness -> Industriousness:**

a) Task 3: Four Italian words in capital letters. There are significant differences between the three Industriousness group categories [$F(2,72)<4.117$; $p=0.020$]. Bonferroni post-hoc tests showed: i) a significant difference ($p=0.017$) between the score of participants in the *low* group ($M=21077.16$; $SD=1379.89$) and the score of participants in the *high* group ($M=15874.71$; $SD=672.47$); ii) a significant difference ($p=0.046$) between the score of participants in the *low* group ($M=21077.16$; $SD=1379.89$) and the score of participants in the *typical* group ($M=16287.81$; $SD=784.32$). In particular, this difference is due to the scores of the following features:

  - T_{idle}: The score of the *low* group ($M=6587.75$; $SD=7220.71$) is significantly different ($p=0.001$) with respect to the score of the *high* group ($M=3838.71$; $SD=2372.66$) and significantly different ($p=0.002$) with respect to the score of the *typical* group ($M=3873.04$; $SD=2163.73$);
  - T_{total}: The score of the *low* group ($M=39513.25$; $SD=12697.87$) is significantly different ($p=0.003$) with respect to the score of the *high* group ($M=31671.74$; $SD=6010.51$) and significantly different ($p=0.011$) with respect to the score of the *typical* group ($M=32429.64$; $SD=9190.34$).

b) Task 4: A series of loops with the left hand. There are significant differences between the three Industriousness group categories [$F(2,72)<7.475$; $p=0.001$]. Bonferroni post-hoc tests showed a significant difference ($p=0.006$) between the score of participants in the *low* group ($M=2737.72$; $SD=650.66$) and the score of participants in the *high* group ($M=5531.10$; $SD=317.09$). In particular, this difference is due to the scores of the following features:

- T_{down}: The score of the *low* group (M=6753.92; SD=4022.90) is significantly different (p=0.001) with respect to the score of the *high* group (M=10393.47; SD=3585.75) and significantly different (p=0.014) with respect to the score of the *typical* group (M=9434.86; SD=3724.66);
- T_{total}: The score of the *low* group (M=6905.50; SD=4168.29) is significantly different (p=0.001) with respect to the score of the *high* group (M=11080.37; SD=4061.33) and significantly different (p=0.016) with respect to the score of the *typical* group (M=9796.93; SD=3741.61).

c) Task 5: A series of loops with the right hand. There are significant differences between the three Industriousness group categories [$F(2,72)<11.041$; $p<<0.001$]. Bonferroni post-hoc tests showed: i) a significant difference (p=0.001) between the score of participants in the *low* group (M=2344.45; SD=471.93) and the score of participants in the *high* group (M=4805.04; SD=229.99); ii) a significant difference (p=0.013) between the score of participants in the *low* group (M=2344.45; SD=471.93) and the score of participants in the *typical* group (M=4447.34; SD=268.24). In particular, this difference is due to the scores of the following features:

- T_{down}: The score of the *low* group (M=5973.17; SD=3301.74) is significantly different ($p<<0.001$) with respect to the score of the *high* group (M=9655.47; SD=2954.48) and significantly different (p=0.001) with respect to the score of the *typical* group (M=8717.04; SD=3016.30);
- T_{total}: The score of the *low* group (M=6039.42; SD=3340.61) is significantly different ($p<<0.001$) with respect to the score of the *high* group (M=9672.32; SD=2966.07) and significantly different (p=0.001) with respect to the score of the *typical* group (M=8922.14; SD=3053.51).

- **Openness to Experience -> Intellect:**

a) Task 4: A series of loops with the left hand. There are significant differences between the three Intellect group categories [$F(2,72)<6.114$; p=0.004]. Bonferroni post-hoc tests showed: i) a significant difference (p=0.004) between the score of participants in the *low* group (M=3148.16; SD=572.72) and the score of participants in the *high* group (M=5335.02; SD=292.65); ii) a significant difference (p=0.010) between the score of participants in the *low* group (M=3148.16; SD=572.72) and the score of participants in the *typical* group (M=5322.08; SD=471.78). In particular, this difference is due to the scores of the following features:

- T_{down}: The score of the *low* group (M=5878.83; SD=3311.66) is significantly different (p=0.002) with respect to the score of the *high* group (M=9932.30; SD=3304.53) and significantly different (p=0.002) with respect to the score of the *typical* group (M=10674.26; SD=4307.50);

- T_{total}: The score of the *low* group (M=6296.33; SD=3675.26) is significantly different (p=0.003) with respect to the score of the *high* group (M=10608.87; SD=3774.48) and significantly different (p=0.014) with respect to the score of the *typical* group (M=10740.05; SD=4368.18).

b) Task 5: A series of loops with the right hand. There are significant differences between the three Intellect group categories [F(2,72)<8,627;p<<0.001]. Bonferroni post-hoc tests showed: i) a significant difference (p=0.001) between the score of participants in the *low* group (M=2846.81; SD=424.14) and the score of participants in the *high* group (M=4802.80; SD=216.73); ii) a significant difference (p=0.004) between the score of participants in the *low* group (M=2846.81; SD=424.14) and the score of participants in the *typical* group (M=4647.25; SD=349.39). In particular, this difference is due to the scores of the following features:

- T_{down}: The score of the *low* group (M=5627.92; SD=3181.35) is significantly different (p<<0.001) with respect to the score of the *high* group (M=9305.30; SD=2862.221) and significantly different (p=0.004) with respect to the score of the *typical* group (M=9356.79; SD=3211.24);
- T_{total}: The score of the *low* group (M=5694.17; SD=3229.410) is significantly different (p<<0.001) with respect to the score of the *high* group (M=9441.11; SD=2872.27) and significantly different (p=0.005) with respect to the score of the *typical* group (M=9356.79; SD=3211.24).

4.4 Space Features

- **Agreeableness -> Politeness:**

a) Task 5: A series of loops with the right hand. There are significant differences between the three Politeness group categories [F(2,72)<3.557; p=0.034]. Bonferroni post-hoc tests showed a significant difference (p=0.030) between the score of participants in the *low* group (M=3913.62; SD=657.32) and the score of participants in the *typical* group (M=6344.11; SD=656.99). In particular, this difference is due to the scores of the following feature:

- S_{bb}: The score of the *low* group (M=11832.27; SD=7476.26) is significantly different (p=0.027) to the score of the *typical* group (M=19218.80; SD=11845.08).

- **Conscientiousness -> Orderliness:**

a) Task 3: Four Italian words in capital letters. There are significant differences between the three Orderliness group categories [F(2,72)<6.183; p=0.003]. Bonferroni post-hoc tests showed a significant difference (p=0.003) between the score of participants in the *low* group (M=112500.147; SD=5463.13) and

the score of participants in the *high* group (M=88811.80; SD=4135.11). In particular, this difference is due to the scores of the following features:

- S_{bb}: The score of the *low* group (M=255313.83; SD=64520.85) is significantly different (p=0.003) to the score of the *high* group (M=201763.87; SD=56429.60);
- S_{total}: The score of the *low* group (M=79326.67; SD=19118.84) is significantly different (p=0.009) to the score of the *high* group (M=63650.60; SD=14186.71);
- S_{avg}: The score of the *high* group (M=1062.40; SD=216.63) is significantly different (p=0.018) with respect to the score of the *low* group (M=1262.17; SD=244.79) and significantly different (p=0.015) with respect to the score of the *typical* group (M=1244.37; SD=260.77).

Table 4

For each Big Five sub-dimension, the table provides the dimension, the task and the corresponding features for which it has been observed a significant difference among groups

Big Five Sub-dimension	**Big Five Dimension**	**Task**	**Features**
Enthusiasm	Extraversion	Loops with right hand	T_{down}, T_{total}
Assertiveness	Extraversion	Loops with right hand	P_{max}, P_{avg}, P_{90}
Compassion	Agreeableness	Writing in capital letters	T_{up}, T_{idle}, T_{total}
Politeness	Agreeableness	Clock drawing	N_{up}, N_{down}, N_{idle}, T_{up}, T_{total}
	Agreeableness	Loops with left hand	T_{down}, T_{total}
	Agreeableness	Loops with right hand	T_{down}, T_{total}, S_{bb}
Industriousness	Conscientiousness	Writing in capital letters	T_{idle}, T_{total}
	Conscientiousness	Loops with left hand	T_{down}, T_{total}
	Conscientiousness	Loops with right hand	T_{down}, T_{total}
Orderliness	Conscientiousness	Writing in capital letters	T_{total}, S_{bb}, S_{total}, S_{avg}
Volatility	Neuroticism	Copy of a house drawing	I_{avg}
	Neuroticism	Clock drawing	I_{avg}
Intellect	Openness to Experience	Loops with left hand	T_{down}, T_{total}
	Openness to Experience	Loops with right hand	T_{down}, T_{total}

4.5 Inclination Feature

Being the Inclination category composed of a single feature (I_{avg}), a single repeated measurement ANOVA was performed considering the results of all the tasks.

- **Neuroticism -> Volatility:**

There are significant differences between the three Volatility group categories [F(2,71)<5,047; p=0.009]. Bonferroni post-hoc tests showed a significant difference (p=0.003) between the score of participants in the *low* group (M=1.75; SD=0.009) and the score of participants in the *typical* group (M=2.20; SD=0.10). In particular, this difference is due to the scores in the following tasks:

- Task 2: A copy of a house drawing. The score of the *low* group (M=3.48; SD=1.75) is significantly different (p=0.020) to the score of the *typical* group (M=4.95; SD=2.61);
- Task 6: A clock drawing task. The score of the *low* group (M=1.12; SD=0.56) is significantly different (p=0.011) to the score of the *high* group (M=1.92; SD=1.45).

Conclusion

The results of the proposed statistical analyses show that online handwriting and drawing features collected through appropriately defined tasks can be used to distinguish among different personality dimensions and sub-dimensions of the Big Five Questionnaire. With more details, the analysis carried out in this paper and in [4] shows that the considered features discriminate among 4 out of the 5 Big Five dimensions and 8 out of the 10 Big-Five sub-dimensions. Table 4synthesizes the features for which significant differences are observed allowing categorizing participants with different personalities. A comparison among tasks shows that although all the envisaged tasks have proven to be useful, the simpler ones (such as loops or writing in capital letters) are more informative about subject's personalities. Finally, comparing the different types of features, it can be observed that timing ductus and pressure features are the more promising and may deserve deeper investigation.

Acknowledgement

The research leading to these results has been funded by the EU Horizon 2020 Research and Innovation Program under funding agreements N. 769872 (EMPATHIC) and N. 823907 (MENHIR). Partial support comes also from the Italian project SIROBOTICS, funded by MIUR, PNR 2015-2020, DD 1735 13/07/2017 and the Italian project ANDROIDS, Università della Campania "Luigi Vanvitelli" programma V:ALERE 2019, DR 906, 04/10/2019, n. 157264.

References

[1] J. Camps, J. Stouten, and M. Euwema: The Relation Between Supervisors' Big Five Personality Traits and Employees' Experiences of Abusive Supervision. In Frontiers in Psychology, 7, pp. 1-11, 2016

[2] G. Cordasco, F. Scibelli, M. Faundez-Zanuy, L. Likforman-Sulem, and A. Esposito: Handwriting and Drawing Features for Detecting Negative Mood. In WIRN 2017: Quantifying and Processing Biomedical and Behavioral Signals, Smart Innovation, Systems and Technologies, Vol. 103, pp. 73-86, 2017

[3] C. G. De Young, L. C. Quilty, and J. B. Peterson: Between facets and domains: 10 aspects of the Big Five. In Journal of Personality and Social Psychology, 93 (5), pp. 880-896, 2007

[4] A. Esposito, T. Amorese, M. Buonanno, M. Cuciniello A. M. Esposito, M. Faundez-Zanuy, L. Likforman-Sulem, M. T. Riviello, A. Troncone and G. Cordasco: Handwriting and Drawing Features for Detecting Personality Traits. In IEEE 10th International Conference on Cognitive Infocommunications, 2019

[5] J. Feist and G. J. Feist: Theories of personality, Boston: McGraw-Hill, 2009

[6] L. R. Goldberg: Personality structure: emergence of the five factors model. In Annual Review of Psychology, 41, pp. 417-440, 1990

[7] P. Grimm: Social desirability bias. Wiley international encyclopedia of marketing. https://doi.org/10.1002/9781444316568.wiem02057, 2010

[8] A. Hajek, J. O. Bock, and H. H. Knig: The role of personality in health care use: Results of a population-based longitudinal study in Germany. In PloS one, 12(7), 2017

[9] D. Hassabis, R. N. Spreng, A. A. Rusu, C. A. Robbins, R. A. Mar, D. L. Schacter: Imagine all the people: how the brain creates and uses personality models to predict behavior. Cerebral cortex, 24(8), (2014)

[10] D. Impedovo, G. Pirlo: Dynamic Handwriting Analysis for the Assessment of Neurodegenerative Diseases: A Pattern Recognition Perspective. In IEEE Reviews in Biomedical Engineering, 12, pp. 209-220, 2019

[11] S. Israel, T. E. Moffitt, D. W. Belsky, R. J. Hancox, R. Poulton, B. Roberts, W. Murray Thomson, A. Caspi: Translating personality psychology to help personalize preventive medicine for young adult patients. In J. Pers. Soc. Psychol., 106, pp. 484-498, 2014

[12] K. H. James, R. J. Jao, V. Berninger: The development of multileveled writing systems of the brain: Brain lessons for writing instruction. In MacArthur, C. A., Graham, S., Fitzgerald, J. (Eds.), Handbook of writing research 2nd ed., pp. 116-129, 2016

[13] P. M. Joshi, A. Agarwal, A. Dhavale, R. Suryavanshi, S. Kodolikar: Handwriting Analysis for Detection of Personality Traits using Machine Learning Approach. In International Journal of Computer Applications 130, pp. 40-45, 2015

[14] S. Kedar, V. Nair and S. Kulkarni: Personality Identification through Handwriting Analysis: A Review. In International Journal of Advanced Research in Computer Science and Software Engineering, 5(1), 2015

[15] H. Kim: The clockme system: Computer-assisted screening tool for dementia. Ph.D. dissertation, College Computing, Georgia Inst. Technol., 2013

[16] R. R. Larsen and D. M. Buss: Personality Psychology: Domains of Knowledge About Human Nature, 3rd edition, McGraw-Hill Inc. 2008

[17] T. Li-Ping Tang: Detecting honest people's lies in handwriting. In Journal of Business Ethics, 106(4), pp-389-400, 2012

[18] L. Likforman-Sulem, A. Esposito, M. Faundez-Zanuy, S. Clmenon, and G. Cordasco: Emothaw: A novel database for emotional state recognition from handwriting and drawing. In IEEE Transactions on Human-Machine Systems, 2016

[19] R. R. McCrae and O. P. John: An Introduction to the Five-Factor Model and Its Applications. In Journal of Personality, 60(2), pp. 175-215, 1992

[20] C. O'Reilly and R. Plamondon: Design of a neuromuscular disorders diagnostic system using human movement analysis. In 11th International Conference on Information Science, Signal Processing and their Applications, ISSPA 2012, pp. 787-792, 2012

[21] R. Plamondon and S. N. Srihari: On-line and off-line handwriting recognition: A comprehensive survey. In IEEE Trans. Pattern Anal. Mach. Intell, 22(1), pp. 63-84, 2000

[22] R. Plamondon, C. O'Reilly, and C. Ouellet-Plamondo: Strokes against stroke - strokes for strides. In Pattern Recognition, 47(3) pp. 929-944, 2014

[23] J. Rawat and B. Mann: Role of consumer personality and involvement in understanding customer experience. In Innovative Marketing, 12(3), pp. 19-33, 2016

[24] M. Schiegg, D. Thorpe: Historical Analyses of Disordered Handwriting: Perspectives on Early 20th-Century Material from a German Psychiatric Hospital. Written Communication, 34(1), pp. 30-53, 2017

[25] L. Trojano, G. Gainotti: Drawing Disorders in Alzheimer's Disease and Other Forms of Dementia. Journal of Alzheimer's disease, JAD, 53(1), pp. 31-52, 2016

Aluminium-Rubber Composite - Experimental and Numerical Analysis of Perforation Process at Ambient and High Temperatures

M. Klosak[a*], A. Bendarma[a,b], T. Jankowiak[b], S. Bahi[c], A. Rusinek[c]

[a] Universiapolis, Technical University of Agadir, Laboratory for Sustainable Innovation and Applied Research, Bab Al Madina, BP 8143, Qr Tilila, 80000 Agadir, Morocco; E-mail: klosak@e-polytechnique.ma, b.amine@e-polytechnique.ma

[b] Poznan University of Technology, Institute of Structural Analysis, Piotrowo 5, 60-965, Poznan, Poland; E-mail: tomasz.jankowiak@put.poznan.pl

[c] University of Lorraine, Laboratory of Microstructure Studies and Mechanics of Materials LEM3, 7 Rue Félix Savart, 57070 Metz, France; E-mail: mohamed-slim.bahi@univ-lorraine.fr, alexis.rusinek@univ-lorraine.fr

Abstract: In this work, the impact resistance of an aluminium–rubber sandwich composite plate under impact loading is investigated using experimental and numerical approaches. The experimental tests were carried out using a perforation gas gun for a wide range of impact velocities from 40 m/s to 120 m/s and for two different temperatures 20°C and 150°C. Based on experimental results, the failure mode, initial/residual velocity curves and the ballistic limit velocities of aluminium under different temperatures were analysed. The effect of rubber reinforcement layer thickness in the aluminium sandwich was also evaluated. It was found that the composite plate with 9 mm of rubber provides higher performance in terms of energy absorption than that of 3 mm thick, which is demonstrated by approximately 10% reduction in the ballistic limit. In contrast, an increase in temperature considerably reduces these ballistic performances. It was also found that petaling is a typical failure mode in the perforation process. The rubber has an effect on the failure pattern of both aluminum plates. In addition, a thermomechanical model using a finite element method was developed to simulate the response of the aluminum–rubber composite plate under a high energy rate loading condition. The numerical results show a good agreement in relation to the experimental results in terms of failure mechanism, number of petals and energy absorption.

Keywords: aluminium-rubber sandwich panel; pneumatic gas gun; high strain rates

1 Introduction

For many years, the perforation capability of armor plates made of aluminum alloys has been studied due to their good formability, low-density, and high impact performance. The recent studies have been proposed in order to investigate the ballistic performance of aluminum plates under impact of projectile through experimental and numerical approaches [1-5]. Alavi Nia and Hoseini [6] compared ballistic resistance performance of monolithic, in-contact layered and spaced layered aluminum plates. They found that under the same total target thickness, the monolithic target behaved in the most optimal way, followed by an in-contact layered target and a spaced layered target. Moreover, with a specially designed drop weight tower, low velocity impact behavior of AA 2024-T3 aluminum at -60° C was investigated by Martínez et al. [7]. It was observed that the target absorbed a larger impact energy with decreasing temperature, and the improved protection performance at low temperature came from temperature sensitivity of the material.

In order to investigate perforation behavior of materials at elevated temperatures, Rusinek et al. [8] proposed a heating chamber coupled with a ballistic impact device. With the thermal chamber, Klosak et al. [9] studied perforation behaviour of brass alloy plates under temperatures ranging from 20° C to 260° C. Results showed that the energy absorption capacity decreased with increasing temperature: the absorbed energy changed from 31.2 J at room temperature to 20.9 J at 260° C. Bin et al. [10], studied the deformation behaviour of 304 austenite stainless steel under dynamic loading from -165° C to 260° C. It was shown that the ballistic limit velocity V_B is sensitive to the testing temperature. It increases slightly from 93 m/s at 200° C to 103 m/s at -20° C and then remains constant at still lower temperatures. The material shows better energy absorption capacity at low temperatures. The improved ballistic resistance performance at low temperatures comes from not only temperature sensitivity of the material but also its Strain-Induced Martensitic Transformation (SIMT) effect.

In the last decades, many researchers have focused on performance improvement of structural protections against impact threats [11-13] by including a hyperelastic material as a shock absorber. These different studies concluded that the use of hyperelastic reinforcement in composite structures decreases the damage due to blast load and penetration of projectile with higher dissipation of kinetic energy under impact loadings.

One of the widely used materials exploited as a shock absorber reinforcement is the natural rubber, which is characterized by a higher impact resistance, high level of damping properties and flexibility, and an excellent puncture and tear resistance [14-20]. In fact, a proper composite structure should keep a balance between strength and ductility which are opposite material features.

The purpose of this study, therefore, is to study the effect of temperature on perforation behaviour of the sandwich structure aluminium-rubber using a gas gun setup. First, the effect of rubber thickness on the energy of absorption, reaction force is presented at room temperature. The initial temperature effect on the ballistic performance is discussed for tests carried out under room temperature and at 150° C. The experimental setup helps measure the initial velocity and residual velocity curves of the material in order to determine the Ipson and Recht model coefficients [21]. The failure pattern, initial and residual velocity curves and absorbed energy of the reinforced structure at two different temperatures were compared to numerical model results and then discussed.

2 Experimental Set-up

The dynamic study was carried out using a pneumatic gas gun, whose scheme and photo are presented in Fig. 1. A wide range of impact velocities from 40 m/s to 120 m/s has been covered during the perforation tests.

The projectile with a conical shape is launched through a tube using a pneumatic gas gun. At the end of the gun barrel, two laser sensors are mounted to measure the initial velocity of the projectile V_0. This can later be obtained by dividing the distance Δd between two sensors by the time $\Delta t = t1 - t2$, needed for the projectile to cover the distance between them. Based on the same measurement method, the residual velocity V_R is measured after the perforation process. The impact velocity V_0 of the projectile is controlled by changing the initial gas gun pressure P_0.

The apparatus is equipped with a thermal chamber in which a specimen is heated. This system which deals with impact loading at elevated temperatures is still not very common in experimental practice, the standard gas gun is usually not coupled with a heating tool. The usual approach is to carry out perforation tests at room temperature and to extrapolate results using numerical simulations at higher temperatures by applying the defined constitutive relation. A detailed description of the thermal chamber is given in [8, 9] and will not be discussed here, the extended experimental analysis using this set-up can be found in [8-10, 22-27].

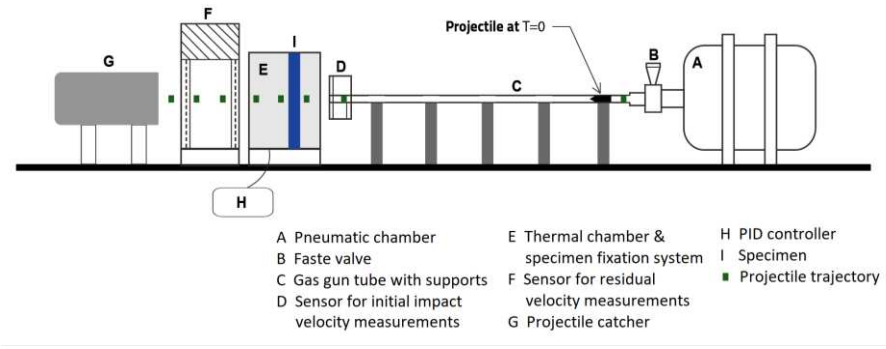

a)

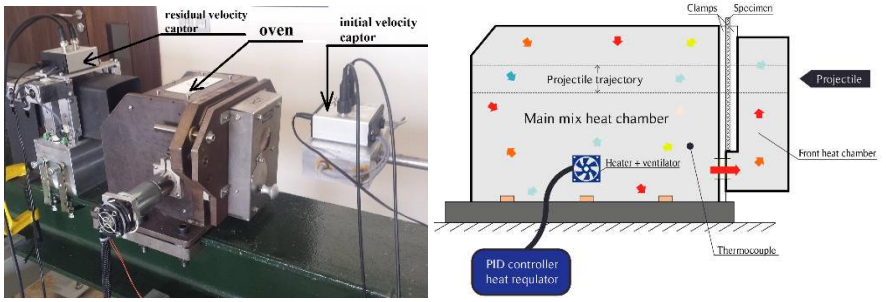

b)

Figure 1

Apparatus for high temperature perforation testing: (a) general view of the ballistic impact device (photo and scheme), (b) thermal chamber (photo and schematic view) [9]

For the measurement of the perforation force, the ballistic impact device is equipped with four piezoelectric sensors fixed on the four corners of the rigid target holder, Fig. 2. A single sensor can undertake a maximum of 20 kN, which makes up a 4-sensor set-up maximum equal to 80 kN.

During the perforation process, part of the kinetic energy of the projectile is absorbed by the sandwich structure. Once the initial V_0 and the residual V_R velocities of the projectile are determined, the energy absorbed by the structure $W_{\text{structure}}$ can be calculated as follows:

$$W_{\text{structure}} = ½\, M_p\, (V_0^2 - V_R^2) \tag{1}$$

where M_p is the mass of the projectile. A part of the kinetic energy, Eq. 1, is transferred to the structure during the process of impact or perforation.

As discussed in [10], the energy lost due to the elastic deformation of the sandwich structure, friction between the projectile and the target as well as that transferred to the ejected debris can be neglected. Then, the energy balance absorbed by the structure can be described as follows:

$$W_{\text{structure}} = W_{pb} + W_{ps} + W_p + W_c \tag{2}$$

where W_{pb} is the plastic bending energy of the sandwich structure, W_{ps} is the plastic stretching energy of the target, W_p is the plastic bending energy of the petals and W_c is the energy dissipation during crack formation and propagation processes.

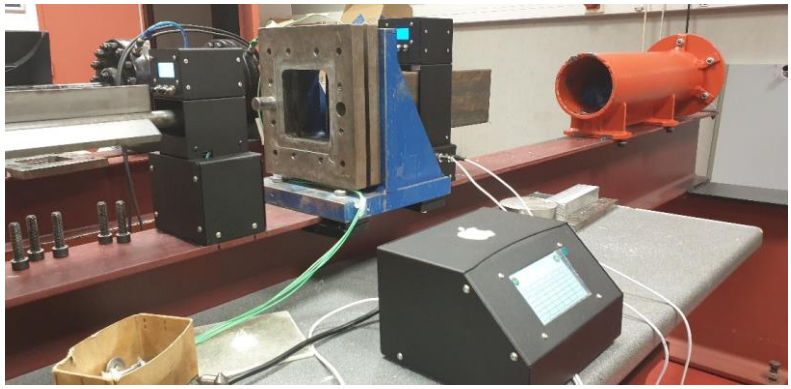

Figure 2
Ballistic impact device equipped with compressive force measurement sensors

The plate-projectile configuration is presented in Fig. 3. The cylindrical projectile with a conical nose has a 72° conical edge, 11.5 mm in diameter and 35 mm in length; its weight is 28 g. The plate specimens are 130 mm x 130 mm and are fully clamped along their perimeter by two rigid metallic rigs, placed in both sides of the plates. The aluminium specimens are made of the alloy with the following chemical composition: Al 99,40% and Fe 0.6%, the material can be considered pure aluminium. Their thickness is 1.0 mm, whereas the rubber element is 3 mm thick. Three configurations of the aluminium-rubber composite were studied and

they are presented in Fig. 4. It is to be noted that no glue was applied between metallic plates and rubber. The 9 mm rubber specimen was composed of three identical pieces of rubber put together with no gluing, either.

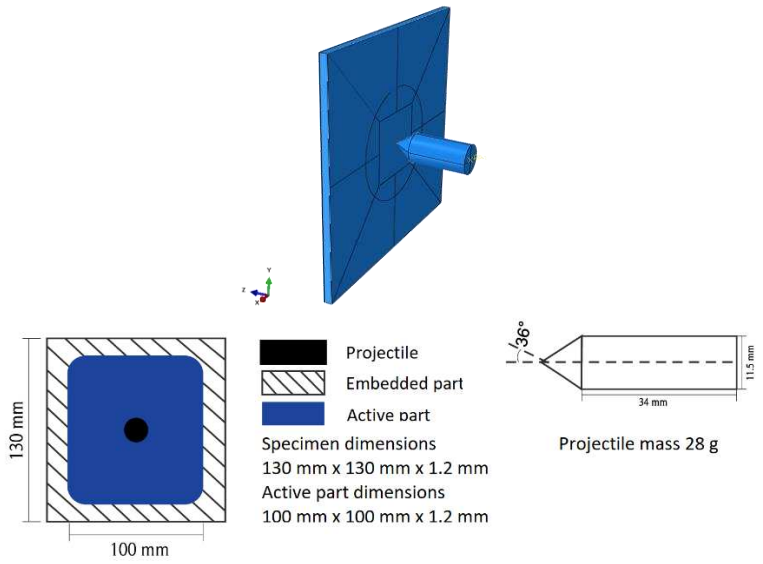

Figure 3

Configuration of plate and cylindrical projectile with a conical nose for the laboratory experiments

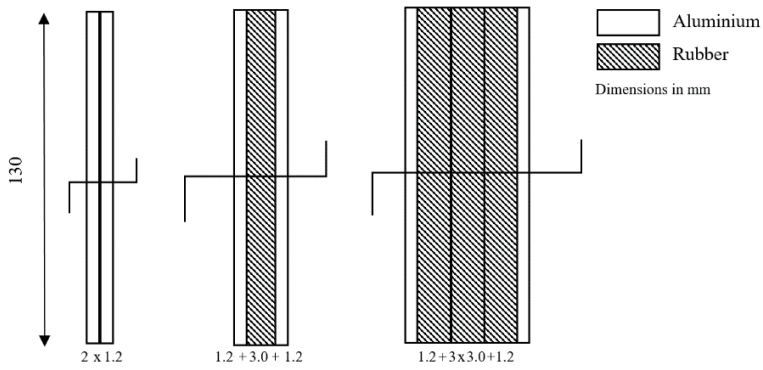

Figure 4

Three configurations of the analysed composite (dimensions in mm), a) no rubber sheet (aluminium plates only), b) aluminium + 1 rubber sheet (3 mm), c) aluminium + 3 rubber sheets (9 mm); no glue beteween sheets

3 Perforation Testing and Ballistic Properties Definition

Perforation tests were carried out with the protocol widely used in literature taking into account the interesting analyses found in [28-32] in which the petaling as a typical failure mode in perforation of the metal plates by a conical projectile is highlighted. The experimental results are collected in Table 1. For each test the laser sensors enabled calculation of the initial and residual velocities. The initial temperatures considered were T_0=293 K, 353 K, 423 K. The determined ballistic limits are presented later in the next section for a comparison with numerical simulations.

The typical petaling is observed in metal plates, although its shape is different for each aluminium plate, which can be seen in Fig. 5. The outer plate develops shapely petals whose observed number is 3 to 4, whereas the inner plate has rather a rugged form with 5-8 irregular petals. The rubber part is torn along one or two lines, experiencing large deformations during the projectile pass, but as the material is hyperelastic, only a small permanent deformation occurs in the vicinity of the perforation.

As may be defined from Table 1, the rubber has an effect on the ballistic limit. The estimated ballistic value increased from 76 m/s to 93 m/s (+22%) for room temperature and from 63 m/s to 74 m/s (+17%) at T_0=423 K when 9 mm rubber layer was added to the sandwich specimen. It confirms that a rubber plate acts as an efficient shock absorber. As the mechanical performances of rubber are by far worse than those of aluminium, this effect can be described as considerable.

Figure 5

Aluminum-rubber composite, from the left: outer aluminium plate, rubber, inner aluminium plate (the inner plate is impacted first by projectile); testing initial conditions: V_0=121.47 m/s, T_0=353 K

Table 1
Experimental data

Aluminium plates only (2x1.0 mm)											
Press. (bars)	**Test No**	**T_0 [K]**	**V_0 (m/s)**	**t (ms)**	**V_R (m/s)**	**Press. (bars)**	**Test No**	**T_0 [K]**	**V_0 (m/s)**	**t (ms)**	**V_R (m/s)**
2.5	31*	293	71.84	0.000	0.00	2.0	41A	423	65.10	4.240	11.79
3.0	32	293	77.88	1.600	31.25	2.5	41	423	73.53	1.320	37.88
4.0	33	293	90.58	0.860	58.14	3.0	42	423	80.91	0.940	53.19
5.0	34	293	100.40	0.700	71.43	4.0	43	423	91.91	0.660	75.76
7.5	35	293	120.77	0.510	98.04	5.0	44	423	100.89	0.560	89.29
						7.5	45	423	120.12	0.470	106.38
Ballistic limit estimation **76 m/s** * projectile stuck						Ballistic limit estimation **63 m/s**					
Aluminium plates + 3 mm rubber											
Press. (bars)	**Test No**	**T_0 [K]**	**V_0 (m/s)**	**t (ms)**	**V_R (m/s)**	**Press. (bars)**	**Test No**	**T_0 [K]**	**V_0 (m/s)**	**t (ms)**	**V_R (m/s)**
3.0	46	293	78.84	0.000	0.00	2.0	56A	423	65.27	0.000	0.00
3.5	47	293	85.62	1.680	29.76	2.5	56	423	72.05	1.860	26.88
4.0	48	293	90.25	1.200	41.67	3.0	57	423	78.37	1.116	44.80
5.0	49	293	100.00	0.780	64.10	4.0	58	423	90.25	0.810	61.73
7.5	50	293	120.77	0.570	87.72	5.0	59	423	100.00	0.670	74.63
						7.5	60	423	120.19	0.490	102.04
Ballistic limit estimation 82 m/s						Ballistic limit estimation 69 m/s					
Aluminium plates + 9 mm rubber											
Press. (bars)	**Test No**	**T_0 [K]**	**V_0 (m/s)**	**t (ms)**	**V_R (m/s)**	**Press. (bars)**	**Test No**	**T_0 [K]**	**V_0 (m/s)**	**t (ms)**	**V_R (m/s)**
2.5	61*	293	-	-	-	2.5	71A	423	71.60	0.000	0.00
3.0	62*	293	-	-	-	2.8	71	423	76.22	1.620	30.86
4.0	63	293	89.60	Project. stuck	0.00	3.5	72	423	86.51	0.960	52.08
4.6	63A	293	96.60	1.440	34.72	4.0	73	423	90.58	0.870	57.47
5.0	64	293	100.00	1.140	43.86	5.0	74	423	101.04	0.720	69.44
7.5	65	293	118.28	0.700	71.43	7.5	75	423	121.36	0.540	92.59
Ballistic limit estimation 93 m/s * no records						Ballistic limit estimation 74 m/s					

The estimation of the energy bulk dissipated during the perforation process is presented in Fig. 6. The values of the energy dissipated did not reveal any visible trend, they change as a function of the initial temperature of the experiment.

It is important to propose a reliable numerical model in order to reproduce experimental results and extend the analysis to the domain not covered by experiment. The estimation of the local temperatures and strain rates encountered during the perforation process will be given using a FE model.

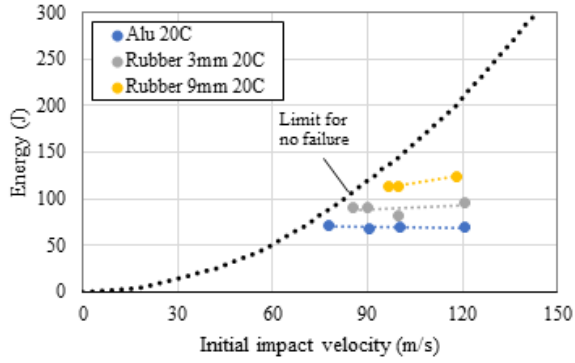

a)

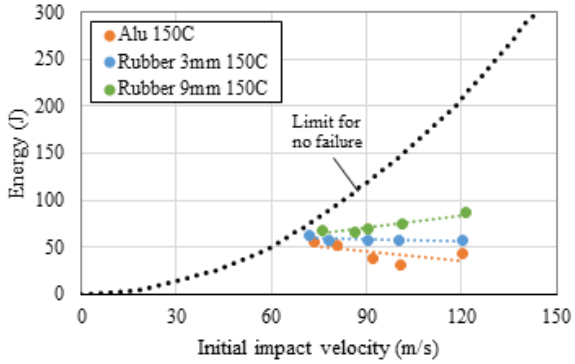

b)

Figure 6

Experimental results of energy absorbed by the specimen as a function of the initial impact velocity V_0 for different specimen configurations and temperatures (T_0=293 K/20˚C and T_0=423 K/150˚C); "limit for no failure" denotes a transition between perforation and non-perforation zones

4 Numerical Thermomechanical Model for Perforation

4.1 Initial and Boundary Conditions

Numerical calculations were performed using Abaqus/Explicit program dedicated for high rates of deformations in line with the practice used in previous works [33-34]. In all calculations, the aluminium-rubber composite and projectile were modelled as presented in Fig. 7. Aluminum plates were modelled as shell finite elements and the rubber as solid finite elements.

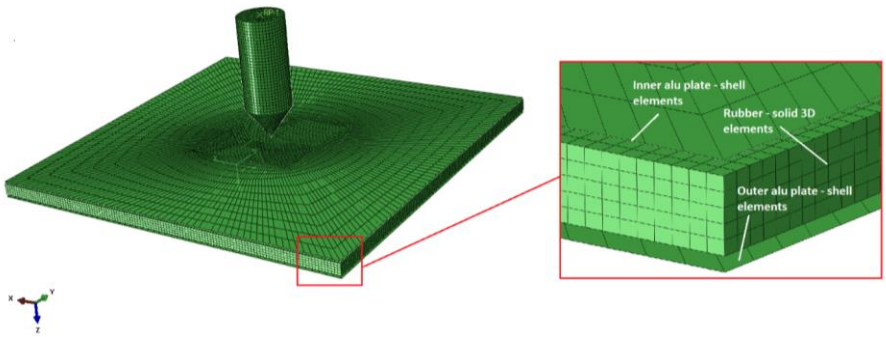

Figure 7
FE model of aluminium plates and rubber

During computer calculations the aluminium-rubber composites were fixed along the four sides of the specimen in order to model the boundary conditions used in the laboratory tests (full fixation).

The mesh size sensitivity were checked in the simulations. The failure patterns and the value of the residual velocity were compared for different meshes. Thanks to this analysis, the optimal mesh is used then in all further simulations of the perforation process. The following number of elements was used:

- for discretization of the specimen: fine mesh in the middle: 3570 nodes, 3450 elements type Shell S4R; remaining part: 2611 nodes, 2598 elements type Shell S4R; both parts of the specimen were tied in the analysis, the refined mesh part has a form of a circle 5 cm in diameter in the region of contact between the two acting bodies,
- for discretization of the rubber component:

  3 mm thickness case: 95256 nodes, 78125 elements type Solid (C3D8R, 5 elements along the thickness, average element dimensions is $8x10^{-5}$ mm x $8x10^{-5}$ mm x $8x10^{-5}$ mm),
- 9 mm thickness case: 254016 nodes, 234375 elements type Solid 185(8) (C3D8R. 15 elements along the thickness, average element dimensions is $8x10^{-5}$ mm x $8x10^{-5}$ mm x $8x10^{-5}$ mm),
- for discretization of the projectile: 10842 nodes, 9648 elements.

The friction between the projectile and the plate is an important parameter as discussed in [22, 35-37], it was assumed as constant and equal to 0.3 to reflect the friction observed between the bodies. The general contact was used together considering interior contact surfaces created during failure or erosion of the mesh related to the material. The friction rubber-metal is defined using the friction coefficient equal to 0.4.

The analysis was assumed as adiabatic. The adiabatic heat effect is defined using the heat equation without conductivity (k=0) and assuming a Quiney-Taylor coefficient as constant and equal to 0.9. The material parameters used are a specific heat C_p=900 J/kgK and a density ρ=2700 kg/m^3. The range of the initial temperatures T_0 reflect the experiment range, i.e., 293 K-423 K.

4.2 Material Modelling

The Johnson-Cook [38] constitutive hardening relation is used to describe the dynamic material behaviour of the aluminium plate:

$$\overline{\sigma}\left(\overline{\varepsilon}_{pl}, \dot{\overline{\varepsilon}}_{pl}, T\right) = \left(A + B\overline{\varepsilon}_{pl}{}^{n}\right)\left(1 + C ln\frac{\dot{\overline{\varepsilon}}_{pl}}{\dot{\varepsilon}_0}\right)\left[1 - \left(\frac{T-T_0}{T_m-T_0}\right)^m\right] \tag{3}$$

where A is the yield stress, B and n are the strain hardening exponent, C is the strain rate sensitivity coefficient, $\dot{\varepsilon}_0$ is strain rate reference value and m is the temperature sensitivity parameter. The last bracket in Eq. 3, describes the thermal softening of the material and reduces the limit of the Mises equivalent stress $\overline{\sigma}$ from the reference temperature T_0 to zero at melting temperature T_m.

The constants of Johnson-Cook constitutive model adopted for numerical simulations are given in Table 2. The basic constants A, B and n were deducted from our own testing results, whereas the temperature and strain rate effect were adopted from [22].

Table 2
Constants of Johnson-Cook model

A (MPa)	B (MPa)	n (-)	C (-)	m (-)	T_0 (K)	T_m (K)	$\dot{\varepsilon}_0$ (-)
104	90	0.40	0.01	1.8	293.15	933	1.0

Concerning the failure criterion, the equivalent plastic strain at failure $\varepsilon_{pl}^{f}(T)$ as a function of temperature was adopted, this damage initiation value changes linearly from 1.22 at T=293 K to 0.7 at T=603 K. The use of this simplified criterion was reported with success in [22, 24, 26, 37]. The parametrical analysis of the effective failure criterion consisted of observing the failure modes (petaling) and fitting the numerical ballistic curves to the experimental ones. The failure criterion applied in simulations eliminates the elements in which the critical value of the equivalent plastic strain ε_{pl}^{f} is reached.

The deformations of the middle layer of the perforated composite slabs are modelled by coupling the hyperelasticity with rate-dependent plasticity together with damage and failure of the material. The temperature softening is also considered since it affects the rubber behaviour [39]. From mathematical point of view, the model is using the multiplicative split of deformation gradient into elastic and plastic parts according to:

$$F = F_e \cdot F_p, \tag{4}$$

where F_e is the elastic part of the deformation gradient and it represents the hyperplastic behaviour and F_p is the plastic part of the deformation gradient (permanent). The incompressible isotropic hardening Mises plasticity with associated flow rule is used in the model together with hyperelasticity. In the current analysis the Marlow model is assumed [40]. The strain rates effect is included only in the plastic part of deformation. In the current analysis, the rate independent behaviour was assumed. The damage and failure is also imposed on the plastic part of the deformation gradient. In this analysis, the temperature sensitivity was additionally added to both the hyperelastic and plastic part of the deformations. The important fact is that the hyperalastic model should be defined by nominal stress versus nominal strain curve. Abaqus automatically identifies the parameters of the selected optimal model (Marlow model selected). The plasticity is defined by the true stress vs. true plastic strain curve. The constant value of 1.25 of the initiation damage plastic strain was assumed. The evolution of the damage was defined by the displacement at failure (0.01 mm). The energetic strain softening regularisation was used as it was for aluminium, 50% maximum degradation was allowed before the final failure at which the finite element was deleted from the mesh. The definition of the rubber is presented in Fig. 8 and Table 3.

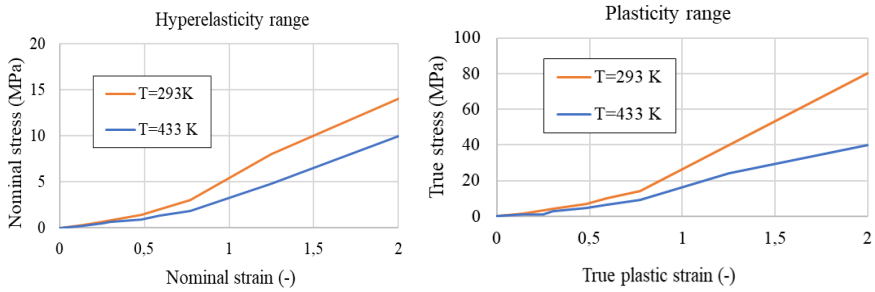

Figure 8

Rubber modelling – stress-strain curves for hypelastic and plastic ranges at different temperatures

Table 3
Rubber modelling – Abaqus command used for material definition

*Hyperelastic, Marlow, Poisson=0.5 *Uniaxial Test Data	*Plastic
*Damage Initiation, criterion=DUCTILE 1.25 *Damage Evolution, type=DISPLACEMENT 0.01 *Density 9.6e-10	

5 Results and Discussions

Numerical results are presented in Fig. 9. The model successfully reproduced the experimental behaviour presented in Fig. 5. Very similar petaling forms are given. In case of the internal plate (Fig. 9b), an extended form is produced with walls partially perpendicular to the specimen plane. The petaling is in a rather rugged form. Some 5-8 non-shaped petals are reported. Another form is observed in the outer specimen – 3-4 typical petals as usually seen in aluminium only studies [21, 41].

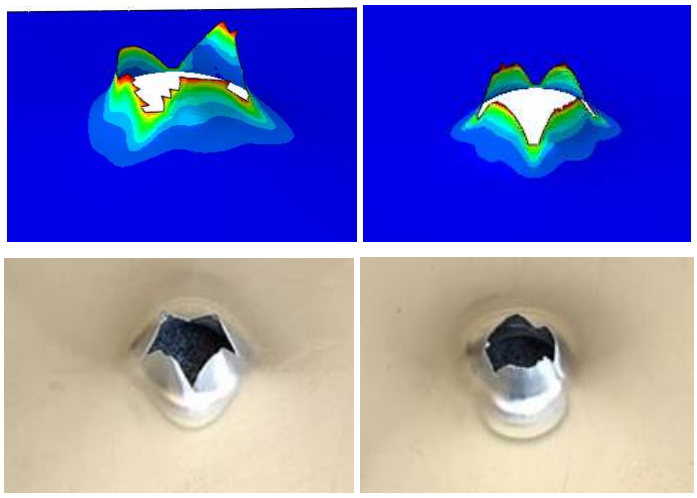

a) b)

Figure 9
View of the perforation forms in metal specimens – numerical simulation vs. experiment, a) inner plate (impacted first), b) outer plate

The numerical simulations permitted to estimate the mean temperature increase during the adiabatic heating in petals: configuration 1 (aluminium only) - $\Delta T = 66$ K, configurations 2 and 3 (aluminium-rubber composite) - $\Delta T = 54$ K. The mean strain rates values in petals developed during impact were the following: configuration 1 (aluminium only) - $\dot{\varepsilon} = 9.1 \cdot 10^3$ 1/s, configurations 2 and 3 (aluminium-rubber composite) - $\dot{\varepsilon} = 5.4 \cdot 10^3$ 1/s. No temperature increase was measured in rubber. In both cases, i.e., in numerical calculations and experimental tests, the same characteristic petals in the region of perforation are observed, which confirms the accuracy of the constitutive law and failure criterion used.

Figure 10 presents comparison of the material response obtained from analytical, experimental and numerical studies. The results presented in the form of the initial impact velocity V_0 vs. residual velocity V_R have shown the numerical values overlap with the experimental ones. The numerical findings are close to Ipson-Recht analytical approach [21] and experiments. The Ipson-Recht coefficient κ was slightly changing across the analysis as shown in Table 4.

Table 4

The Ipson-Recht coefficient κ

□	Configuration 1: 2 aluminium plates	Configuration 2: aluminium-3 mm rubber-aluminum	Configuration 3: aluminium-9 mm rubber-aluminum
T_0=293 K	2.0	1.75	2.2
T_0=423 K	2.5	2.2	2.0

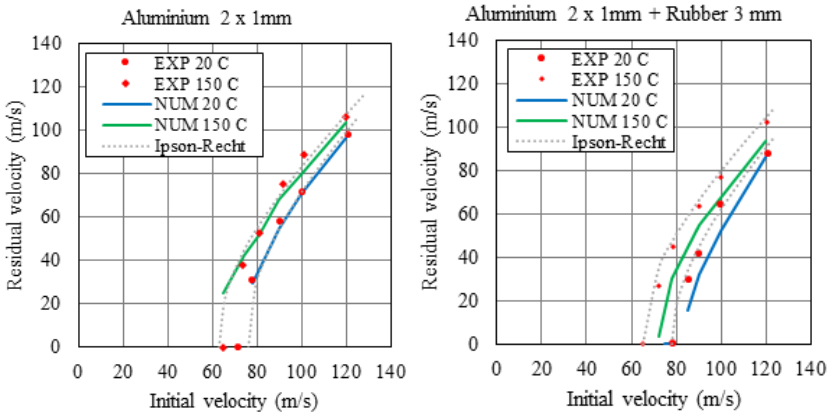

a) b)

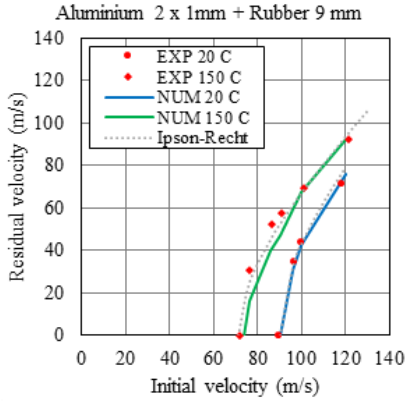

c)

Figure 10
Initial impact velocity V_0 vs. residual velocity V_R – analytical vs. experimental vs. numerical results, a) config. 1, T_0=273 K/423 K, b) config. 2, T_0=273 K/=423 K, c) config. 3, T_0=273 K/423 K

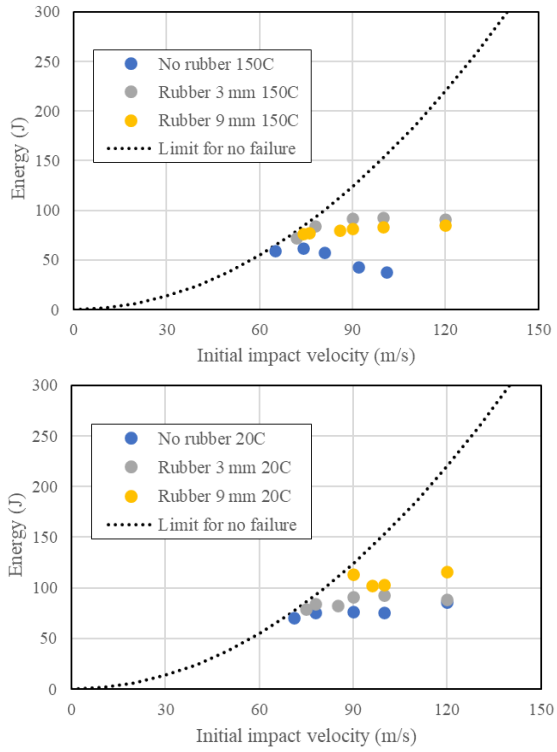

Figure 11
Numerical simulations results of energy absorbed by the specimen as a function of the initial impact velocity V_0 for different specimen configurations and temperatures (T_0=293 K/20˚C and T_0=423 K/150˚C); “limit for no failure” denotes a transition between perforation and non-perforation zones

In Figure 11 numerical simulations results of energy absorbed by the specimen as a function of the initial impact velocity V_0 can be found. The values are given for two different temperatures (T_0=293 K and T_0=423 K) and for all specimens configurations. Close similarities of results are found when compared with Figure 6 where the energy values are given for the same test conditions but in real experiment.

The experimental records concerning the reaction force is given in Fig. 12. The preliminary tests were performed at one temperature of 293 K and one initial impact velocity V_0~90 m/s. The aim of that extra study consisted of checking the effect of the sandwich configuration on the force exerted during perforation. The general observation was that the reaction force diminished with the rubber thickness increase. As discussed in [42], the value of the experimentally determined reaction force may be obscured by the inertia of the system that impacts the measurements. A complex numerical model would be then required for better reaction force estimation. Different approaches to estimate reaction forces may be used in the numeric model: summing up nodal values in fixation points, using the acceleration history of the projectile or by building up a complex FE model including heavy metal support and 3D sensor geometries.

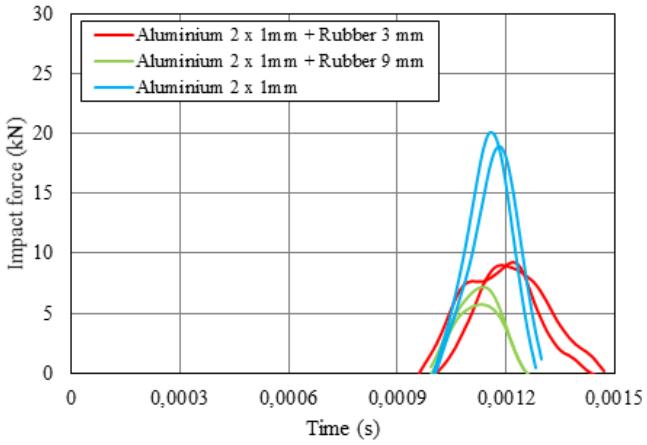

Figure 12

Reaction force measured during experiment for 3 composite configurations (ambient temperature, V_0~90 m/s)

Conclusions

The paper presents results of experimental tests and numerical simulations by FE method carried out on the aluminium-rubber composite. The composite specimens were tested under perforation regime within a wide range of impact velocities V_0 and initial temperatures T_0. The aim of the study was to analyze different configurations of the composite, especially in terms of the thickness of the rubber component. The increase of the rubber layer increased the ballistic limit.

Conversely, the temperature diminished the ballistic properties of the rubber composite: it lowered the ballistic limit as both aluminium and rubber softened. The maximum analysed temperature (T=423 K) is close to the melting point of rubber (T_m~453 K) and its impact on the ballistic resistance at these temperature conditions was observed both in experiment and simulations. An interesting observation concerned the measurements of the reaction force: the increasing of the rubber thickness resulted in decreasing of the reaction force.

The implemented Johnson-Cook constitutive relation in the FE analysis combined with the proposed effective failure criterion allowed reproduction of experimental findings in terms of the ballistic limit and failure modes. The model allowed us to estimate the local maxima of the adiabatic temperature increase (ΔT = 54-66 K) and local maxima of strain rate recorded during perforation ($\dot{\varepsilon}$ = 5.4-9.1·10^3 1/s).

The typical failure mode of the aluminium plates was observed during the tests with the same number of 3 or 4 petals in the outer plate and 5-8 petals in the inner one. A good correlation between the results calculated by FEM method and those obtained from experiments is observed. The shape of petaling was different for internal and external aluminium plates. Concerning the rubber, one or two cracks remained after the projectile passage, but with no plastic deformation of the material, which reflected the hyperelastic nature of the material.

Acknowledgments

The support of Richard Bernier from University of Lorraine, Laboratory of Microstructure Studies and Mechanics of Materials LEM3 during the perforation tests in Metz is highly acknowledged.

References

[1] G. Tiwari, M. Iqbal, P. Gupta, Energy absorption characteristics of thin aluminium plate against hemispherical nosed projectile impact, Thin-Walled Struct. 126 (2018) 246-257

[2] Z. Rosenberg, R. Kositski, E. Dekel, On the perforation of aluminum plates by 7.62 mm APM2 projectiles, Int. J. Impact Eng. 97 (2016) 79-86

[3] M. Iqbal, S. Khan, R. Ansari, N. Gupta, Experimental and numerical studies of double-nosed projectile impact on aluminum plates, Int. J. Impact Eng. 54 (2013) 232-245

[4] M. Rodriguez-Millan, D. Garcia-Gonzalez, A. Rusinek, F. Abed, A. Arias, Perforation mechanics of 2024 aluminium protective plates subjected to impact by different nose shapes of projectiles, Thin-Walled Struct. 123 (2018) 1-10

[5] K. Senthil, M. Iqbal, B. Arindam, R. Mittal, N. Gupta, Ballistic resistance of 2024 aluminium plates against hemispherical, sphere and blunt nose projectiles, Thin- Walled Struct. 126 (2018) 94-105. [6] K. Ackland, C.

Anderson, T. D. Ngo, Deformation of polyurea-coated steel plates under localised blast loading, Int. J. Impact Eng. 51 (2013) 13-22

[6] Alavi Nia A, Hoseini GR. Experimental study of perforation of multi-layered targets by hemispherical-nosed projectiles. Materials & Design 2011;32:1057-65

[7] Rodríguez-Martínez JA, Rusinek A, Arias A. Thermo-viscoplastic behaviour of 2024-T3 aluminium sheets subjected to low velocity perforation at different temperatures. Thin-Walled Structures 2011;49:819-32

[8] Rusinek A, Bernier R, Boumbimba RM, Klosak M, Jankowiak T, Voyiadjis GZ. New devices to capture the temperature effect under dynamic compression and impact perforation of polymers, application to PMMA. Polymer Testing 2018;65:1-9

[9] Klosak M, Rusinek A, Bendarma A, Jankowiak T, Lodygowski T, Klosak M, et al. Experimental study of brass properties through perforation tests using a thermal chamber for elevated temperatures. Latin American Journal of Solids and Structures 2018;15

[10] Jia, B., Rusinek, A., Bahi, S., Pesci, R., Bendarma, A. Perforation Behavior of 304 Stainless Steel Plates at Various Temperatures, Journal of Dynamic Behavior of Materials, 2019, 5(4), pp. 416-431

[11] K. Ackland, C. Anderson, T. D. Ngo, Deformation of polyurea-coated steel plates under localised blast loading, Int. J. Impact Eng. 51 (2013) 13-22

[12] R. Gamache, C. Giller, G. Montella, D. Fragiadakis, C. Roland, Elastomer-metal laminate armor, Mater. Des. 111 (2016) 362-368

[13] I. Mohagheghian, G. J. McShane, W. Stronge, Quasi-static and impact perforation of polymer-metal bi-layer plates by a blunt indenter, Thin-Walled Struct. 117 (2017) 35-48

[14] Y. Dong, Y. Ke, Z. Zheng, H. Yang, X. Yao, Effect of stress relaxation on sealing performance of the fabric rubber seal, Compos. Sci. Technol. 151 (2017) 291-301

[15] H. Yang, X.-F. Yao, Y.-C. Ke, Y.-j. Ma, Y.-H. Liu, Constitutive behaviors and mechanical characterizations of fabric reinforced rubber composites, Compos. Struct. 152 (2016) 117-123

[16] H. Yang, X.-F. Yao, H. Yan, Y.-n. Yuan, Y.-F. Dong, Y.-H. Liu, Anisotropic hyper- viscoelastic behaviors of fabric reinforced rubber composites, Compos. Struct. 187 (2018) 116-121

[17] A. Khodadadi, G. Liaghat, H. Ahmadi, A. R. Bahramian, O. Razmkhah, Impact response of Kevlar/rubber composite, Compos. Sci. Technol. 184 (2019) 107880

[18] P. Zhang, X. Kong, Z. Wang, C. Zheng, H. Liu, G. Shi, J. P. Dear, W. Wu, High velocity projectile impact of a composite rubber/aluminium fluid-filled container, International Journal of Lightweight Materials and Manufacture 4 (2021) 1-8

[19] D. Rajkumar, V. Mahesh, S. Joladarashi, S. M. Kulkarni, Parametric study on impact behaviour of sisal and cenosphere reinforced natural rubber-based hybrid composites: FE approach, Materials Today: Proceedings, vol. 46 (17), 8767-8771, 2021

[20] Z. Huanga, L. Suia, F. Wanga, S. Dub, Y. Zhoua, J. Ye, Dynamic compressive behavior of a novel ultra-lightweight cement composite incorporated with rubber powder, Composite Structures 244 (2020) 112300

[21] R. F. Recht and T. W.Ipson, Ballistic perforation dynamics, Journal of Applied Mechanics, 30, 3, pp. 384-390, 1963

[22] A. Bendarma, T. Jankowiak, T. Łodygowski, A. Rusinek and M. Klosak, Experimental and numerical analysis of the aluminum alloy AW5005 behaviour subjected to tension and perforation under dynamic loading, Journal of Theoretical and Applied Mechanics, 55, 4, pp. 1219-1233, 2016

[23] M. Klosak, T. Jankowiak, A. Rusinek, A. Bendarma, P. W. Sielicki and T. Lodygowski, Mechanical Properties of Brass under Impact and Perforation Tests for a Wide Range of Temperatures: Experimental and Numerical Approach, Materials, 13, 24, 5821, 2020

[24] A. Bendarma, T. Jankowiak, A. Rusinek, T. Lodygowski, M. Klosak, Perforation Tests of Aluminum Alloy Specimens for a Wide Range of Temperatures Using High-Performance Thermal Chamber-Experimental and Numerical Analysis, In IOP Conference Series: Materials Science and Engineering, IOP Publishing, 491, 1, 012027, 2019

[25] A. Bendarma, H. Gourgue, T. Jankowiak, A. Rusinek, S. Kardellass, M. Klosak, Perforation tests of composite structure specimens at wide range of temperatures and strain rates-experimental analysis, Materials Today: Proceedings, 24, 7-10, 2020

[26] A. Bendarma, A. Rusinek, T. Jankowiak, T. Lodygowski, B. Jia, Experimental analysis of the aluminum alloy sheet subjected to impact and perforation process, Materials Today: Proceedings, 36, 88-93 2021.[

[27] D. Garcia-Gonzalez, A. Rusinek, A. Bendarma, R. Bernier, M. Klosak, S. Bahi, Material and structural behaviour of PMMA from low temperatures to over the glass transition: Quasi-static and dynamic loading, Polymer Testing, 81, 106263, 2020

[28] T. Jankowiak, A. Rusinek, K.M. Kpenyigba and R. Pesci, Ballistic behaviour of steel sheet subjected to impact and perforation, Steel and Composite Structures, 16, 6, pp. 595-609, 2014

[29] A. Rusinek, J. A. Rodrıguez-Martınez, R. Zaera, J. R. Klepaczko, A. Arias and C. Sauvelet, Experimental and numerical study on the perforation process of mild steel sheets subjected to perpendicular impact by hemispherical projectiles, International Journal of Impact Engineering, 36, 4, pp. 565-587, 2009

[30] T. Børvik, O, S. Hopperstad, M. Langseth and K. A. Malo, Effect of target thickness in blunt projectile penetration of Weldox 460 E steel plates, International Journal of Impact Engineering, 28, 4, pp. 413-464, 2003

[31] B. Landkof and W. Goldsmith, Petaling of thin metallic plates during penetration by cylindro-conical projectiles, International Journal of Solids and Structures, 21, 3, pp. 245–266, 1985

[32] K. M. Kpenyigba, T. Jankowiak, A. Rusinek and R. Pesci, Influence of projectile shape on dynamic behaviour of steel sheet subjected to impact and perforation, Thin-Walled Structures, 65, pp. 93-104, 2013

[33] T. Jankowiak, A. Rusinek and P. Wood, A numerical analysis of the dynamic behaviour of sheet steel perforated by a conical projectile under ballistic conditions, Finite Elements in Analysis and Design, 65, pp. 39-49, 2013

[34] A. Arias, J. A. Rodríguez-Martínez and A. Rusinek, Numerical simulations of impact behaviour of thin steel plates subjected to cylindrical, conical and hemispherical non-deformable projectiles, Engineering Fracture Mechanics, 75, pp. 1635-1656, 2008

[35] A. Massaq, A. Rusinek, M. Klosak, F. Abed and M. El Mansori, A study of friction between composite-steel surfaces at high impact velocities, Tribology International, 102, pp. 38-43, 2016

[36] Z. Rosenberg and Y. Vayig, On the friction effect in the perforation of metallic plates by rigid projectiles, International Journal of Impact Engineering, 149, 103794, 2021

[37] A. Bendarma, T. Jankowiak, A. Rusinek, T. Lodygowski, B. Jia, M. H. Miguélez, M. Klosak, Dynamic Behavior of Aluminum Alloy Aw 5005 Undergoing Interfacial Friction and Specimen Configuration in Split Hopkinson Pressure Bar System at High Strain Rates and Temperatures. Materials, 13(20), 4614, 2020

[38] G. R. Johnson and W. H. Cook, A constitutive model and data for metals subjected to large strains, high strain rates and high temperatures, in Proceedings of the 7th International Symposium on Ballistics, 21, pp. 541-547, 1983

[39] G. Weber, L. Anand, Finite Deformation Constitutive Equations and Time Integration Procedure for Isotropic Hyperelastic-Viscoplastic Solids, Computer Methods in Applied Mechanics and Engineering, 79, 173-202, 1990

[40] A. Aidy, M. Hosseini, B. B. Sahari, A Review of Constitutive Models for Rubber-Like Materials, American Journal of Engineering and Applied Sciences, 3 (1), 232-239, 2010

[41] W. Mocko, J. Janiszewski, J. Radziejewska and M. Grazka, Analysis of deformation history and damage initiation for 6082-T6 aluminium alloy loaded at classic and symmetric Taylor impact test conditions, International Journal of Impact Engineering, 75, pp. 203-213, 2015

[42] W. Z. Zhong, A. Mbarek, A. Rusinek, R. Bernier, T. Jankowiak and G. Sutter, Development of an experimental set-up for dynamic force measurements during impact and perforation, coupling to numerical simulations, International Journal of Impact Engineering, 91, pp. 102-114, 2016

Properties of NBR and CR Hyperelastic Materials in a Wide Range of Both Positive and Negative Temperatures

Marcin Konarzewski[1], Michał Stankiewicz[1], Robert Panowicz[1], Marcin Sarzyński[2], Marcin Wieczorek[1]

[1]Faculty of Mechanical Engineering, Military University of Technology, Sylwestra Kaliskiego Street 2, 00-908, Warsaw, Poland; marcin.konarzewski@wat.edu.pl (M.K.), michal.stankiewicz@wat.edu.pl (M.S.), robert.panowicz@wat.edu.pl (R.P.), marcin.wieczorek@wat.edu.pl (M.W.)

[2]Faculty of Mechatronics and Aeronautics, Military University of Technology, Sylwestra Kaliskiego Street 2, 00-908, Warsaw, Poland; marcin.sarzynski@wat.edu.pl (M.Sz.)

Abstract: Hyperelastic materials are widely used in many industries. Their use requires thorough knowledge of their strength parameters over a wide temperature range. However, determination of the parameters of hyperelastic materials is still a challenge. Therefore, the paper presents research methodology allowing determination of the properties of hyperelastic materials in a wide range of stretch and temperatures (from +50°C to -25°C) on the example of NBR (nitrile butadiene rubber) and CR (chloroprene rubber) elastomers. On the basis of physical premises, a hyperelastic constitutive model was also modified through introducing an explicit dependence of strain energy on temperature, allowing an accurate reflection of the properties of the tested materials. The material parameters of the adopted strain energy functions for the NBR and CR were determined with R2 not less than 0.999.

Keywords: elastomers; polymers; uniaxial tension; temperature effects; failure

1 Introduction

Nowadays, hyperelastic materials are as often used in industry as other, more traditional materials. Particularly the automotive industry shows its great interest in this type of materials. In addition to their main application, i.e., for car tires, elastomers are used as vehicle suspension components, engine vibration dampers, and sealing in various types of connections. Hyperelastic materials are also used in other industries, including civil engineering, aviation or also biomechanics.

Due to such a wide spectrum of a usage of hyperelastic materials, it is crucial to precisely determine their mechanical properties. Hyperelastic materials, similarly as other elastomers in general, are polymers in which polymer chains are joined by intermolecular bonds. It should be noted that due to their internal structure, those materials properties, such as tensile strength, stiffness or stress, change depending on the temperature [1-3]. This relationship was not noticed at the beginning, therefore, their parameters were initially determined only in an ambient temperature. In a later period of the experimental studies this influence taken into account, however, mainly in the range of positive temperatures [4-9]. It could be assumed that as the temperature increases, much larger displacements and elongation of the sample are obtained. However, in the case of hyperelastic materials, at elevated temperatures, there occurs a rapid degradation of polymer chains as well as their weakening and breaking. For this reason, higher elongation values are obtained for negative temperatures [10]. This phenomenon only occurs to a certain limit called the brittleness temperature [11]. Thus, testing properties of this type of materials over a wide temperature range is crucial.

There is a whole range of hyperelastic materials differing significantly in their mechanical properties and, thus, their usage [12]. The presented article focuses on two commonly used materials, namely, NBR (nitrile butadiene rubber) and CR (chloroprene rubber) rubbers. NBR, which is a copolymer of acrylonitrile and butadiene, is characterised by an excellent resistance to a wide range of oils of mineral, animal and vegetable origin as well as to fuels and other chemicals [13]. It is an elastic material with a high tensile strength and a low compression deformation [14]. For this reason, it is frequently used in the automotive or aviation industry, to produce seals (for both hydraulic and pneumatic installations), vibration damping elements and self-sealing fuel tanks. This material owes its oil-resistant properties to the presence of nitrile: the greater the proportion of nitrile, the better the resistance to chemicals while reducing the flexibility [15]. A theoretical range of the operating temperature is between -40°C and 110°C [16].

CR is a synthetic material created in the process of polymerisation of chloroprene [17]. This material is characterised by high resistance to weather conditions, ozone and even to weak acids. Due to high chemical stability, it is relatively well resistant to aging [18]. It shows some resistance to oils and fuels, however, not as strong as NBR rubber does. Due to its properties, it is widely used for production of gaskets for joints exposed to environmental and corrosive factors. However, the most common use is the production of all kinds of wetsuits since CR provides very good insulation form the cold. In the case of CR, the maximum operating temperature is about 80°C.

While analysing available literature on the subject, it can be concluded that a relatively small number of publications concern the testing of material properties of rubber materials at both positive and negative temperatures [19]. For example, in work [20], the authors analyse butadiene rubber filled with carbon black, subjected to dynamic loading at three temperatures: -40, 20 and 70°C. Based on the results

obtained from experimental studies the authors proposed a new constitutive model for finite rubber viscoelasticity. In paper [21] the results of tests on the dependence of temperature on mechanical properties of the reinforced rubber are presented. In this paper, the range from -20 to 100°C was considered and cylindrical samples were tested. Two thermocouples were used to control the sample temperature during the tests: one was attached to the external surface of the sample, the other was placed in a hole drilled in the centre of the sample. It was found that the temperature equilibrium was obtained after about 20 minutes from placing the sample in the temperature chamber. The research showed that both the elastic and the rate dependent properties depend on the temperature: the elastic behaviour is determined by entropy elasticity, whereas the viscous behaviour by a non-linear temperature dependent viscosity. In [22], the authors analysed silicone elastomer filled with silica. Uniaxial tension and shear tests were performed in a wide range of temperatures (from -55 to 70°C). Similarly to other works, the dependence of the temperature on the material properties was confirmed.

The basic experimental test, not only in the case of hyperelastic materials, is the tensile test [10, 23-25]. In the case of elastomers, due to significant deformations that they undergo, measuring mechanical parameters is a more difficult issue than in the case of traditional materials. The use of traditional extensometers in this case is significantly limited, therefore, it is necessary to utilise specialized extensometers for high elongations [25] or optical and digital image correlation (DIC) methods [26, 27]. The DIC method assumes the use of a series of markers, placed on the tested sample, whose position change during the test is recorded by an optical device (e.g., video camera). The recorded images are compared with each other and the desired parameters are determined on this basis. The use of each of the abovementioned methods has some advantages as well as limitations. The extensometers need to be placed near the sample since in the case of tests with use of a small-scale temperature chamber their use can be difficult due to low space. In addition, their operating temperature is in the range of -40°C to 80°C, due to the properties of the material from which the measuring element is made (usually in the form of a long tape, attached to the tested sample). The use of DIC methods requires special preparation of the surface of the tested samples by applying the measuring points or a layer of paint, in such a way that they are clearly visible in the camera lens throughout the test. Testing in sub-zero temperatures also requires proper preparation of the observation field to prevent frost build-up.

Hyperelastic materials are used in a wide range of temperatures, both positive and negative. In the literature it is possible to find descriptions and results of studies on the impact of positive temperatures on the properties of such materials, however, in the case of the negative temperatures there are much less publications on this subject. In addition, the number of constitutive models describing the behaviour of hyperelastic materials with regard to the thermal load is relatively small.

The main aim of presented article is to show the impact of a wide range of temperatures on the properties of CR and NBR materials. The selected temperature

range corresponds to the typical operating conditions of such materials. In addition, numerical models are currently used in many research areas, so an attempt was made to modify the constitutive model of hyperelastic materials by a part describing the effect of the thermal load.

2 Materials and Methods

2.1 Speciment Preparation

As it was mentioned earlier, two materials commonly used in the industry were selected for the research: NBR and CR. The test materials were delivered in the form of premade 300x300 mm and 2 mm thick sheets. The composition of tested materials is presented in the Table 1. The dimensions of the samples were determined on the basis of the PN-ISO 37:2007 standard concerning determination of the tensile properties of rubber (Fig. 1). The water jet cutting technique was used to prepare the test samples presented in Fig. 2.

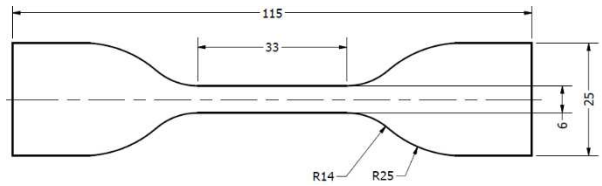

Figure 1
Dimensions of the test samples according to the PN-ISO 37:2007 standard

Table 1
Composition of tested hyper elastic materials (phr - weight parts per 100 parts of rubber)

Component [phr]	**CR**	**NBR**
Chloroprene rubber (Denka S-40)	100	-
Acrylonitrile-butadiene rubber (Ker N-29)	-	100
Carbon black (N-550)	45	50
Crosslinking complex (sulfur, ZnO, et al.)	-	13,6
Crosslinking complex (MgO, ZnO, et al.)	14,6	-
Softener (ADO or AN-68*)	10	15
Hardness Shore A (at 21°C)	65	62

White paint markers were applied on every sample in the measuring part. It was necessary to determine the deformations of the samples during the tensile test using a motion tracking method.

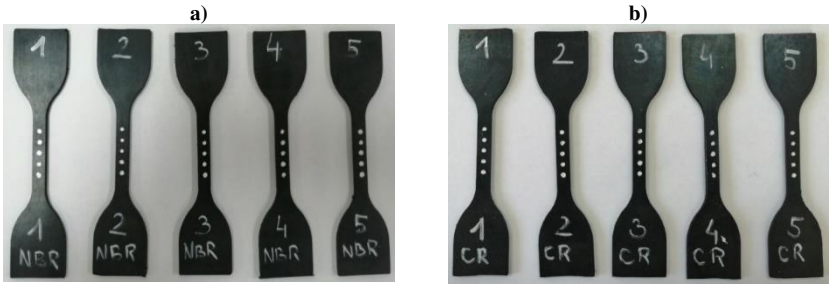

Figure 2
Test samples: (a) NBR; (b) CR

2.2 Tensile Test Method

The test was carried out on the MTS Criterion Model 45 electromechanical universal test system (Fig. 3). The maximum displacement range was ± 500 mm and the maximum piston speed was 750 mm/min. During the test, LED lighting (Fig. 4a) was used to increase the brightness and quality of the recordings.

Tests in negative and positive temperatures were carried out using the ThermCraft temperature chamber, installed on the MTS test system, which allows conducting the test at temperatures from -150°C to 320°. To reduce the temperature in the chamber below the ambient temperature, liquid nitrogen fed from a Dewar cryogenic storage was used (Fig. 3).

The test system automatically recorded the loading force and the position of the traverse in time with 50 Hz frequency. The tests were performed by applying displacement-controlled loading. The speed of the traverse was equal to 50 mm/min and a strain rate during the test was constant and equal to $3.3 \cdot 10^{-2}$ 1/s. The forces recorded by the test system along with the displacements determined using the motion tracking method allowed for determination of strain and stress curves for all considered samples.

The tensile tests were carried out on the basis of the PN-ISO 37:2007 standard. According to the standard the tests are performed with use of the dog bone samples at a constant strain rate. The test samples can be formed directly at the manufacturer or cut out from the premade sheets. Tensile stress is calculated as the force related to the initial cross-section area of the gage length of the tested sample. Tensile strength is defined as the maximum recorder tensile stress and elongation at break as the gage length deformation at break. The effect of transverse deformations of the sample during the test is not taken into account.

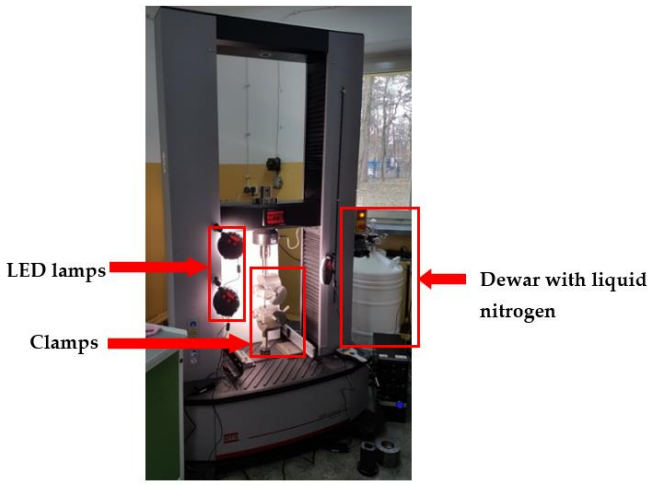

Figure 3
MTS Criterion Model 45 universal test system

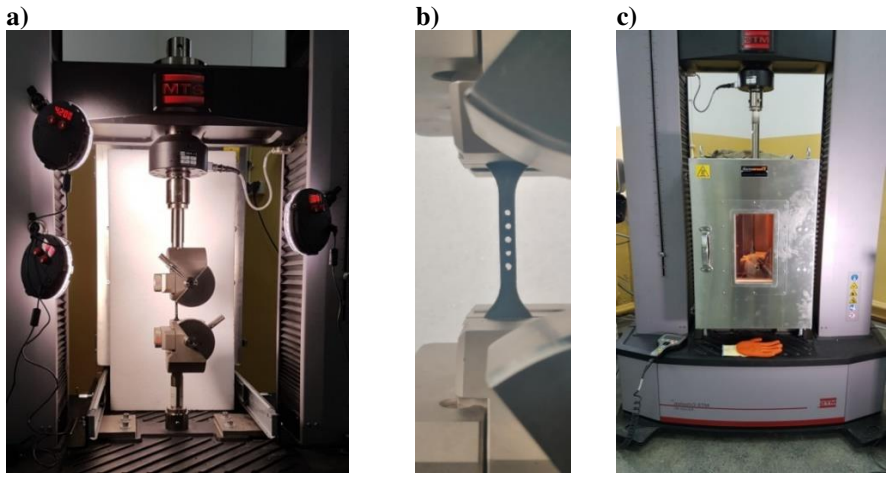

Figure 4
Sample installed in the test system clamps:
(a) general view; (b) close-up of a sample; (c) temperature chamber

The samples were tested in the following temperature range: -25°C, 0°C, 25°C, 50°C. After mounting the samples in the clamps of the testing system and closing the climate chamber, about 10 minutes were allowed to settle and normalize the temperature inside the chamber. Measurements of the temperature inside the chamber were performed by using the two K type thermocouples: one placed in the working field of the chamber and the other fixed between two layers of the tested material (two pieces of the test material were applied to each other and a

thermocouple was placed between them). The tests were carried out when the control system was showing a constant, set temperature. According to the chamber specification it allows temperature stabilization in the range of ±1°C, and the permissible K type thermocouple error is ±1.5°C.

At the ambient temperature 5 samples of every material were tested, while in other temperatures it was 3 samples.

The motion tracking method was used to determine the deformation of the samples during the tensile tests. Each test was recorded using a high resolution (1920x1080 px) camera with a speed of 25 frames/second. The recorded movies were imported into the TEMA software and then subjected to the image analysis. Figure 5a presents a sample with markers used as measuring points (Fig. 5b). During the image analysis process three points were tracked by the software and a change of their coordinates in time was recorded. The example of the motion tracking process for the sample during the tensile test is presented in Fig. 5c. It can be observed that markers are stretching along with the sample; however the measuring points are located in the centre of the markers during the whole test procedure. Based on the obtained data, the strains of the samples were calculated.

a)

b)

c)

Figure 5
Method of strain determination measurement: (a) sample with visible markers; (b) measurement points; (c) sample during the analysis process

3 Results

As it was mentioned earlier the tensile test was performed on the NBR and CR materials. In Figure 6, the samples destroyed during the tests at the ambient temperature are presented.

Figure 6
Test samples: (a) NBR; (b) CR

The stresses, determined with the use of the motion tracking method, for all 5 samples of both tested materials at the ambient temperature are presented in Fig. 7. It can be observed that all the curves are located in relatively narrow range. The standard deviation of extension for CR is only 0.1 and 0.17 for NBR. On this basis, it was found that at the remaining temperatures only 3 samples made from each material will be tested.

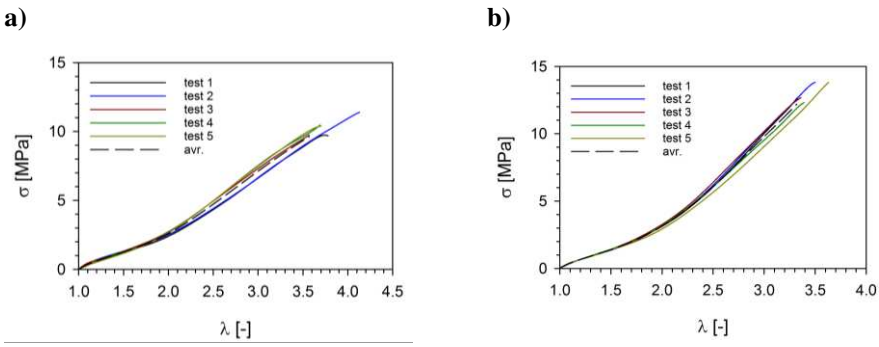

Figure 7
Stress-extension curves for tests at the ambient temperature: (a) NBR ; (b) CR

The averaged curves of stress-extension rate for tests performed in the considered range of temperatures are presented in Fig. 8.

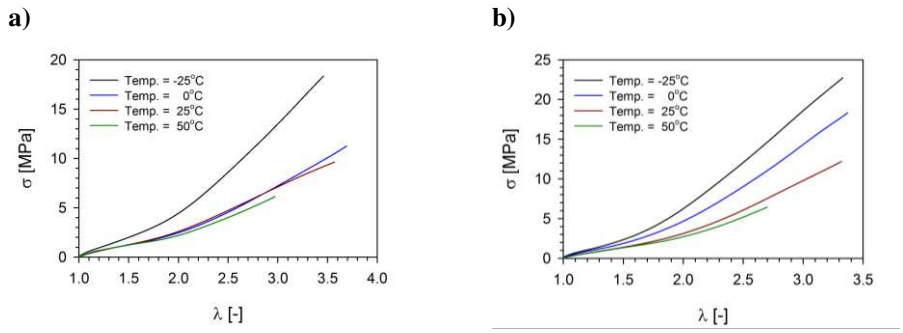

Figure 8

Stress-extension curves for a wide range of temperatures: (a) NBR; (b) CR

Analysing the above graphs, it can be observed that the curves for the NBR material for temperatures in the range from 0 to 50°C are very similar. Up to extension $\lambda=2$ the curves practically coincide. When $\lambda>2$ a change in the slope of the curve representing tests at 50°C can be observed, whereas the curves for 0 and 25°C continue to coincide until they are finally separated at $\lambda=3$. Such behaviour means that NBR is characterised by similar stiffness in this temperature range. The difference in the maximum stresses, and thus in the strength, results from the degradation process of the polymer chains in the material. This process occurs faster as the thermal load of the sample increases, therefore, the lowest strain value (6 MPa) was obtained at 50°C.

At -25°C there is a significant change in the stiffness and strength of the NBR material. The maximum stress was 19 MPa, which is almost a twofold increase compared to the stress at 0°C (10 MPa). The maximum extension λ was about 3.4, similarly to the values obtained from temperature of 0□C. It resulted from to the fact that in these cases the sample was not fractured due to a limited movement range of the test system traverse caused by the size limitation of the used temperature chamber.

In the case of the CR material it can be observed that only the curves for ambient and 50°C temperatures coincide to the value of the extension of about 1.8. In other cases the distribution of the stress-extension curves is even and a difference in the maximum stress is about 6 MPa. For the ambient temperature, the maximum obtained stress was 12 MPa, for 0°C it was about 18 MPa, while the maximum value of 23 MPa was obtained for a temperature of -25°C. Therefore, there is no rapid change in the stiffness after exceeding a certain critical temperature.

The influence of the temperature on both NBR and CR samples stretching process is also presented in Fig. 9. It shows a relationship between the stress and the temperature for selected extension values. In the case of the NBR (Fig. 9a), a change

in the temperature influence occurs at 0°C, whereas in the case of the CR (Fig. 9b) at 25°C. Above these values the temperature has a significantly smaller effect on the stress of the deformed material.

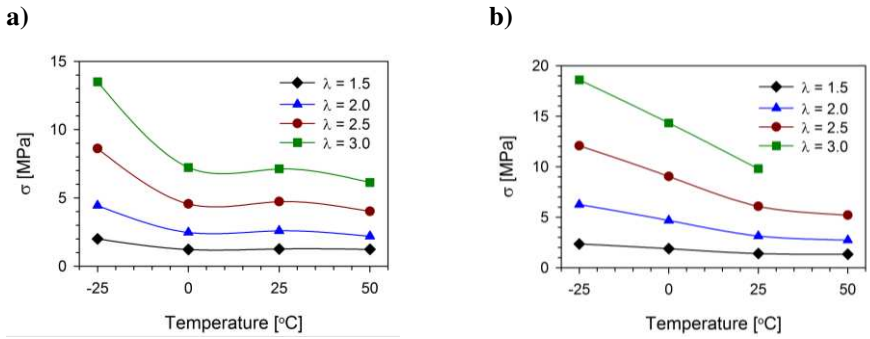

Figure 9
Stress-temperature curve for different values of extension (a) NBR; (b) CR

Such effects is also seen in Fig. 10. Stress-extension curves for 0°C and 25°C temperatures in the case of the NBR practically coincide. However, in the case of the CR material a significant influence of the temperature can be observed. It should be noted that despite, such a different impact of the temperature in both cases, the maximum deformation increases with a decrease in temperature.

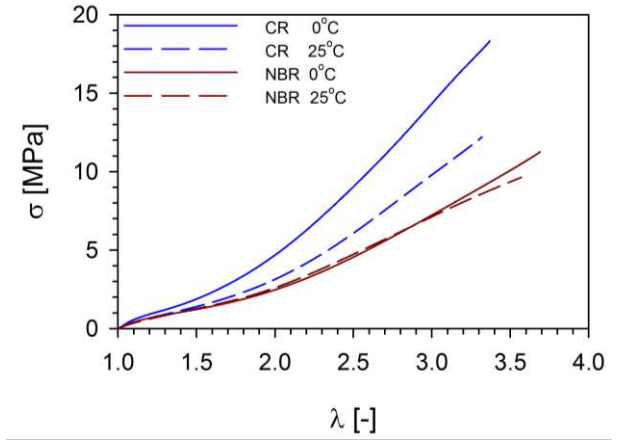

Figure 10
Stress-extension curves for selected temperatures

3 Hyperelastic Constitutive Models

The behaviour of hyperelastic material is usually described by means of the Cauchy stress tensor [28]:

$$\tilde{\sigma} = 2\frac{\tilde{B}}{\sqrt{I_3}}\frac{\partial W}{\partial \tilde{B}} = 2\frac{\tilde{B}}{\sqrt{I_3}}\left(\frac{\partial W}{\partial I_1}\frac{\partial I_1}{\partial \tilde{B}} + \frac{\partial W}{\partial I_2}\frac{\partial I_2}{\partial \tilde{B}} + \frac{\partial W}{\partial I_3}\frac{\partial I_3}{\partial \tilde{B}}\right)\tilde{\sigma} = 2\frac{\tilde{B}}{\sqrt{I_3}}\frac{\partial W}{\partial \tilde{B}} = 2\frac{\tilde{B}}{\sqrt{I_3}}\left(\frac{\partial W}{\partial I_1}\frac{\partial I_1}{\partial \tilde{B}} + \frac{\partial W}{\partial I_2}\frac{\partial I_2}{\partial \tilde{B}} + \frac{\partial W}{\partial I_3}\frac{\partial I_3}{\partial \tilde{B}}\right) \quad (1)$$

$$I_1 = tr\tilde{B} \quad (2)$$

$$I_2 = \frac{1}{2}\left[I_1^2 - tr\left(\tilde{B}^2\right)\right] \quad (3)$$

$$I_3 = det\tilde{B} \quad (4)$$

where: $\tilde{B}$ is the left Cauchy – Green tensor, I_i (i = 1, 2, 3) are strain invariants, W is strain energy function dependent on strain invariants $W(I_1, I_2, I_3)$.

Derivatives of strain energy functions occurring on the right side of equation (1) can be described by the following relationships:

$$\frac{\partial I_1}{\partial \tilde{B}} = \tilde{I} \quad (5)$$

$$\frac{\partial I_2}{\partial \tilde{B}} = I_1\tilde{I} - \tilde{B} \quad (6)$$

$$\frac{\partial I_3}{\partial \tilde{B}} = I_2\tilde{I} - I_1\tilde{B} + \tilde{B}^2 \quad (7)$$

For incompressible material, what is conventional assumption for hyperelastic materials, taking into account (5) - (7) the Cauchy stress tensor (1) takes the form:

$$\tilde{\sigma} = -p\tilde{I} + 2\left(\frac{\partial W}{\partial I_1} + I_1\frac{\partial W}{\partial I_2}\right)\tilde{B} - 2\frac{\partial W}{\partial I_2}\tilde{B}^2 \quad (8)$$

where p is pressure.

The assumption of rubber incompressibility also limits the number of variables on which strain energy functions depends (I_3 = 1, to $W(I_1, I_2)$).

Strain energy functions should allow reflecting the behaviour of hyperelastic material including dependence on symmetry, thermodynamic, energetic and entropic considerations in the whole range of extension variability. Functions should also meet certain conditions [29]:

1. Energy vanishes in the undeformed configuration:

$$W|_{I_1=3} = 0 \quad (9)$$

2. strain energy functions and stress tends to infinity at very large deformation:

$$\lim_{\lambda_i \to 0} W = +\infty, \lim_{\lambda_i \to 0} \frac{\partial W}{\partial \lambda_i} = -\infty, \tag{10}$$

$$\lim_{\lambda_i \to +\infty} W = +\infty, \lim_{\lambda_i \to +\infty} \frac{\partial W}{\partial \lambda_i} = +\infty, \tag{11}$$

3. stress is equal to zero in the undeformed configuration and strain energy functions achieves minimum

$$\left.\frac{\partial W}{\partial \lambda_i}\right|_{\lambda_1=\lambda_2=\lambda_3=1} = 0, \left.\frac{\partial^2 W}{\partial \lambda_i^2}\right|_{\lambda_1=\lambda_2=\lambda_3=1} > 0, \; det\left[H_{ij}\right] > 0, \tag{12}$$

where: H_{ij} is Hessian matrix and i, j =1, 2, 3

Numerous articles are devoted to the problems associated with the definition of strain energy functions. Those articles present phenomenological approach [30-33], theoretical approach using statistical mechanics of molecular chains network [34, 35] or a mixed approach.

Based on the kinetic theory of elasticity developed by Wall [36], Treloar defined the simplest form of strain energy functions commonly known as neo-Hookean model [37]:

$$W = \frac{\mu}{2}(I_1 - 3) \tag{13}$$

where: m is shear modulus.

The value of the shear modulus is related to the temperature and chain density dependence:

$$\mu = nkT \tag{14}$$

where: *k* is Boltzmann constant, *T* is temperature, *n* is chain density.

This relationship shows that strain energy functions *W* are dependent on temperature. In [37] Xu Li and others used a model for thermal deformation to show that m can be described with a good approximation as the square function of temperature:

$$\mu = \mu_0 \left[1 + C_{T1}\frac{\Delta T}{T_0} + C_{T2}\left(\frac{\Delta T}{T_0}\right)^2\right] \tag{15}$$

where: T_0 is a reference temperature, DT = T - T_0, , T is a temperature at which the experiments were carried out, m_0 is shear modulus at T_0 temperature, C_{T1}, C_{T2} are materials constants.

Arruda and Boyce [34, 35], using phenomenological approach, developed a model with other material constants dependent on temperature assuming their linear temperature dependence. They also showed that the adopted model successfully reflects the behaviour of tire rubbers even at relatively high temperatures and under a moderate finite deformation.

Using the above-described approach, an explicit dependence of the strain energy function on temperature was introduced to the equation [38]:

$$W = A\{exp[m_A(I_1 - 3)] - 1\} + B\{exp[m_B(I_2 - 3)] - 1\} \tag{16}$$

which after modification took the form of:

$$W = \left[A_0 + A_{T1}\frac{\Delta T}{T_0} + A_{T2}\left(\frac{\Delta T}{T_0}\right)^2\right]\{exp[m_A(I_1 - 3)] - 1\} + \left[B_0 + B_{T1}\frac{\Delta T}{T_0} + B_{T2}\left(\frac{\Delta T}{T_0}\right)^2\right]\{exp[m_B(I_2 - 3)] - 1\} \tag{17}$$

The modified equation (17) as well as equation (16) meet conditions 1-3 described before.

Equation (17) was chosen with a trial-and-error method using the review work [37] thus R^2 and RMSE in the case of tested materials reach the largest and smallest value, respectively in the whole range of temperatures considered with the smallest number of material parameters.

Based on the experimental tests the determination of the material parameters is carried out by minimizing the functional:

$$g = min\left[\sum_i^k \left(y_{\exp i} - y_{num\,i}\right)^2\right] \tag{18}$$

where: $y_{exp\,i}$ – i-th measured experimental quantity, $y_{num\,i}$ – i-th calculated function value, k – number of measuring points.

Process of minimizing the functional is accomplished using a non-linear least squares method [39] and in particular using the Levenberg–Marquardt (LM) method [40-42].

In accordance with the methodology presented in [33], initially the parameters A_0, B_0, m_{A0} and m_{B0} were determined by analysing the reference temperature T_0 = 25 C. Then, using the experimental results for temperatures different from the reference temperature, other material constants were determined (A_{T1}, A_{T2}, B_{T1}, B_{T2}) using the LM algorithm and Matlab software. In the case of both tested materials the last term of equation (17) dependent on the invariant I_2 is almost a linear function of the temperature. Therefore, B_{T2} = 0 was adopted. The obtained material parameters are presented in Table 2. In each considered case R^2 was greater than 0.999, while the RMSE was less than 0.1.

Table 2

Determined material parameters

	A_0	A_{T1}	A_{T2}	m_A	B_0	B_{T1}	m_B	R^2	RMSE
NBR	0.353	-0.963	4.221	0.03112	0.2804	1.675	-3.928	0.9997	0.03
CR	0.3917	-1.228	6.782	0.06884	0.2886	0.9735	-4.134	0.999	0.1

The comparison of the experimental results with the results of the calculations for the reference temperature is presented in Fig. 11. The obtained parameters allow for a good mapping of the behaviour of the tested materials in the entire range of temperatures and deformations. The accuracy of the approximation decreases at the negative temperatures at which the rubber properties change significantly.

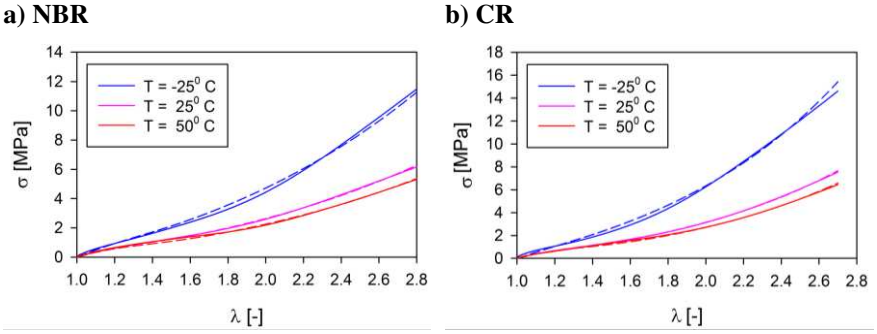

Figure 11

Comparison of the experiment (solid line) and numerical (dashed line) stress-extension curves: (a) NBR; (b) CR

Conclusions

The article presents the results of the research on the NBR and CR hyperelastic materials. Static tensile tests were carried out in the wide range of temperatures (-25, 0, 25, 50°C) using a temperature chamber. The motion tracking technique was used to determine the deformation of the samples. Analysing the obtained results it can be concluded that:

- the strain-extension curves for the NBR are similar in the range of 0-50°C. No change in the NBR stiffness was observed in this temperature range contrary to the temperature of -25°C at which strength and stiffness increased significantly;
- the maximum achieved stress for the NBR material was 19 MPa (for temperature -25°C), while the lowest value of 6 MPa was obtained at 50°C with extension λ=3;
- the stress-extension curves for the CR material for the ambient temperature and 50°C coincide up to the value of the extension of 1.8. For other temperatures the distribution of the curves is even;
- the maximum stress of 23 MPa was obtained for the temperature of -25°C temperature, whereas for the 50°C a value of the stress was about 6 MPa;
- at temperature of 50°C there is a significant reduction in strength for both the tested hyperelastic materials.
- the CR in the considered temperature range is characterised by a greater strength than the NBR, while maintaining the same extension as the NBR.

On the basis of the experimental data the hyperelastic constitutive model was also modified by introducing an explicit dependence of strain energy on the temperature, allowing to accurately reflect the properties of the tested materials. The material parameters of the adopted strain energy functions for the NBR and CR were determined with R^2 not less than 0.999.

The results presented in the article do not exhaust the hyper elastic materials issue. Further research is needed in order to accurately determine the properties and behaviour of such materials in various loading conditions and temperatures. Examples of such tests can be tensile tests at temperatures below -25°C in order to determine the brittleness temperature, compression tests in the range of high strain rates with simultaneous thermal load or biaxial tensile tests.

Acknowledgement

This research was funded under the Project of the Ministry of National Defense of the Republic of Poland Program - Research Grant (GBMON/13-999/2018/WAT) and the article was written as part of the implementation of the university research grant No 22-750 of Military University of Technology.

References

[1] Li, X.; Dong, Y.; Li, Z.; Xia, Y. EXPERIMENTAL STUDY ON THE TEMPERATURE DEPENDENCE OF HYPERELASTIC BEHAVIOR OF TIRE RUBBERS UNDER MODERATE FINITE DEFORMATION. *Rubber Chem. Technol.* **2011**, *84*, 215-228, doi:10.5254/1.3577534

[2] Treloar, L. R. G. *The physics of rubber elasticity*; Oxford classic texts in the physical sciences; 3rd ed.; Clarendon Press ; Oxford University Press: Oxford : New York, 2005; ISBN 978-0-19-857027-1

[3] Smith, T. L. Dependence of the ultimate properties of a GR-S rubber on strain rate and temperature. *J. Polym. Sci.* **1958**, *32*, 99-113, doi:10.1002/pol.1958.1203212409

[4] Bell, C. L. M.; Stinson, D.; Thomas, A. G. Measurement of Tensile Strength of Natural Rubber Vulcanizates at Elevated Temperature. *Rubber Chem. Technol.* **1982**, *55*, 66-75, doi:10.5254/1.3535876

[5] Thomas, A. G.; Whittle, J. M. Tensile Rupture of Rubber. *Rubber Chem. Technol.* **1970**, *43*, 222-228, doi:10.5254/1.3547249

[6] Hussein, M. Effects of strain rate and temperature on the mechanical behavior of carbon black reinforced elastomers based on butyl rubber and high molecular weight polyethylene. *Results Phys.* **2018**, *9*, 511-517, doi:10.1016/j.rinp.2018.02.043

[7] Ovalle Rodas, C.; Zaïri, F.; Naït-Abdelaziz, M.; Charrier, P. Temperature and filler effects on the relaxed response of filled rubbers: Experimental observations on a carbon-filled SBR and constitutive modeling. *Int. J. Solids Struct.* **2015**, *58*, 309-321, doi:10.1016/j.ijsolstr.2014.11.001

[8] Zhang, W.; Gong, X.; Xuan, S.; Jiang, W. Temperature-Dependent Mechanical Properties and Model of Magnetorheological Elastomers. *Ind. Eng. Chem. Res.* **2011**, *50*, 6704-6712, doi:10.1021/ie200386x

[9] Chu, H.; Hong, Y.; Chen, Q.; Wang, R. Establishment of rubber thermo-viscoelastic constitutive model and analysis of temperature field. *IOP Conf. Ser. Mater. Sci. Eng.* **2019**, *531*, 012042, doi:10.1088/1757-899x/531/1/012042

[10] Stevenson, A. The influence of low-temperature crystallization on the tensile elastic modulus of natural rubber. *J. Polym. Sci. Polym. Phys. Ed.* **1983**, *21*, 553-572, doi:10.1002/pol.1983.180210406

[11] D20 Committee Test Method for Brittleness Temperature of Plastics and Elastomers by Impact; ASTM International

[12] Barlow, C.; Jayasuriya, S. K.; Tan, C. S. *The world rubber industry*; Routledge: London ; New York, 1994; ISBN 978-0-415-02369-6

[13] Huang, Y.; Li, Y.; Zhao, H.; Wen, H. Research on constitutive models of hydrogenated nitrile butadiene rubber for packer at different temperatures. *J. Mech. Sci. Technol.* **2020**, *34*, 155-164, doi:10.1007/s12206-019-1217-x

[14] *ASM metals reference book*; Bauccio, M., American Society for Metals, Eds.; 3rd ed.; ASM International: Materials Park, Ohio, 1993; ISBN 978-0-87170-478-8

[15] *Rubber nano blends: preparation, characterization and applications*; Markovic, G., Visakh P. M., V. P., Eds.; Springer: Cham, 2017; ISBN 978-3-319-48720-5

[16] Hickman, J. A. *Polymeric seals and sealing technology*; Rapra review reports; Rapra Technology Ltd: Shawbury, Shrewsbury, 1997; ISBN 978-1-85957-096-8

[17] Chandrasekaran, C. Raw Materials for Rubber Lining Compounds. In *Anticorrosive Rubber Lining*; Chandrasekaran, C., Ed.; William Andrew Publishing, 2017; pp. 77-86 ISBN 978-0-323-44371-5

[18] Kanny, K.; Mohan, T. P. Rubber nanocomposites with nanoclay as the filler. In *Progress in Rubber Nanocomposites*; Thomas, S., Maria, H. J., Eds.; Woodhead Publishing, 2017; pp. 153-177 ISBN 978-0-08-100409-8

[19] Raut, P.; Swanson, N.; Kulkarni, A.; Pugh, C.; Jana, S. C. Exploiting arene-perfluoroarene interactions for dispersion of carbon black in rubber compounds. Polymer 2018, 148, 247-258, doi:10.1016/j.polymer.2018.06.025

[20] Delattre, A.; Lejeunes, S.; Lacroix, F.; Méo, S. On the dynamical behavior of filled rubbers at different temperatures: Experimental characterization and constitutive modeling. *Int. J. Solids Struct.* **2016**, *90*, 178-193, doi:10.1016/j.ijsolstr.2016.03.010

[21] Lion, A. On the large deformation behaviour of reinforced rubber at different temperatures. *J. Mech. Phys. Solids* **1997**, *45*, 1805-1834, doi:10.1016/S0022-5096(97)00028-8

[22] Martinez, J. M.; Boukamel, A.; Méo, S.; Lejeunes, S. Statistical approach for a hyper-visco-plastic model for filled rubber: Experimental characterization and numerical modeling. *Eur. J. Mech. - ASolids* **2011**, *30*, 1028-1039, doi:10.1016/j.euromechsol.2011.06.013

[23] Mullins, L. Effect of Stretching on the Properties of Rubber. *Rubber Chem. Technol.* **1948**, *21*, 281-300, doi:10.5254/1.3546914

[24] Chanliau-Blanot, M. T.; Nardin, M.; Donnet, J. B.; Papirer, E.; Roche, G.; Laurenson, P.; Rossignol, G. Temperature dependence of the mechanical properties of EPDM rubber-polyethylene blends filled with aluminium hydrate particles. *J. Mater. Sci.* **1989**, *24*, 649-657, doi:10.1007/BF01107456

[25] RP, B. Physical Testing of Rubber. *Phys. Test. Rubber* **2006**, 1-387, doi:10.1007/0-387-29012-5

[26] Pascual-Francisco, J. B.; Farfan-Cabrera, L. I.; Susarrey-Huerta, O. Characterization of tension set behavior of a silicone rubber at different loads and temperatures via digital image correlation. *Polym. Test.* **2020**, *81*, 106226, doi:10.1016/j.polymertesting.2019.106226

[27] Zhang, R. Elastic Parameters Measurement of Rubber by Digital Image Correlation. *Appl. Mech. Mater.* **2014**, *444-445*, 1532-1535, doi:10.4028/www.scientific.net/AMM.444-445.1532

[28] Large elastic deformations of isotropic materials VII. Experiments on the deformation of rubber. *Philos. Trans. R. Soc. Lond. Ser. Math. Phys. Sci.* **1951**, *243*, 251-288, doi:10.1098/rsta.1951.0004

[29] Darijani, H.; Naghdabadi, R.; Kargarnovin, M. H. Hyperelastic materials modelling using a strain measure consistent with the strain energy postulates. *Proc. Inst. Mech. Eng. Part C J. Mech. Eng. Sci.* **2010**, *224*, 591-602, doi:10.1243/09544062JMES1590

[30] Mooney, M. A Theory of Large Elastic Deformation. *J. Appl. Phys.* **1940**, *11*, 582-592, doi:10.1063/1.1712836

[31] Rivlin, R. S.; Rideal, E. K. Large elastic deformations of isotropic materials IV. further developments of the general theory. *Philos. Trans. R. Soc. Lond. Ser. Math. Phys. Sci.* **1948**, *241*, 379-397, doi:10.1098/rsta.1948.0024

[32] Rivlin, R. S.; Saunders, D. W. Large Elastic Deformations of Isotropic Materials. VII. Experiments on the Deformation of Rubber. *Philos. Trans. R. Soc. Lond. Ser. Math. Phys. Sci.* **1951**, *243*, 251-288

[33] Yeoh, O. H. Characterization of Elastic Properties of Carbon-Black-Filled Rubber Vulcanizates. *Rubber Chem. Technol.* **1990**, *63*, 792-805, doi:10.5254/1.353828

[34] Arruda, E. M.; Boyce, M. C. A three-dimensional constitutive model for the large stretch behavior of rubber elastic materials. *J. Mech. Phys. Solids* **1993**, *41*, 389-412, doi:10.1016/0022-5096(93)90013-6

[35] Boyce, M. C.; Arruda, E. M. Constitutive Models of Rubber Elasticity: A Review. *Rubber Chem. Technol.* **2000**, *73*, 504-523, doi:10.5254/1.3547602

[36] Treloar, L. R. G. The elasticity of a network of long-chain molecules—II. *Trans Faraday Soc* **1943**, *39*, 241-246, doi:10.1039/TF9433900241

[37] Li, X.; Dong, Y.; Li, Z.; Xia, Y. Experimental study on the temperature dependence of hyperelastic behavior of tire rubbers under moderate finite deformation. *Rubber Chem. Technol.* **2011**, *84*, 215-228, doi:10.5254/1.3577534

[38] Mansouri, M. R.; Darijani, H. Constitutive modeling of isotropic hyperelastic materials in an exponential framework using a self-contained approach. *Int. J. Solids Struct.* **2014**, *51*, 4316-4326, doi:10.1016/j.ijsolstr.2014.08.018

[39] Kelley, C. T. *Iterative methods for optimization*; Frontiers in applied mathematics; SIAM: Philadelphia, 1999; ISBN 978-0-89871-433-3

[40] Levenberg, K. A method for the solution of certain non-linear problems in least squares. *Q. Appl. Math.* **1944**, *2*, 164-168, doi:10.1090/qam/10666

[41] Marquardt, D. W. An Algorithm for Least-Squares Estimation of Nonlinear Parameters. *J. Soc. Ind. Appl. Math.* **1963**, *11*, 431-441, doi:10.1137/0111030

[42] Kanzow, C.; Yamashita, N.; Fukushima, M. Levenberg–Marquardt methods with strong local convergence properties for solving nonlinear equations with convex constraints. *J. Comput. Appl. Math.* **2004**, *172*, 375-397, doi:10.1016/j.cam.2004.02.013

Holistic Online Learning, in a Post COVID-19 World

Kevin M. Jackson, Márta Konczosné Szombathelyi

Doctoral School of Regional and Business Administration Sciences, Szechenyi Istvan University, Egyetem tér 1, 9026 Győr, Hungary;
kevin.jackson@sze.hu, kszm@sze.hu

Abstract: In August of 2020, the United Nations reported that the COVID-19 pandemic had affected 1.6 billion learners, in more than 190 countries and on all continents [1]. The closing of schools and other learning spaces impacted an astonishing 94% of the world's student population. These sudden school closures, at all levels, had the immediate and unprecedented effect of triggering a mass migration to emergency remote teaching. While mass vaccinations have enabled educational institutions to reopen and students to return to classrooms in the Fall of 2021, the educational disruption caused by the COVID-19 pandemic is far from over. Higher education must now permanently transition from reductionist, emergency remote learning systems to permanent, holistic online learning platforms. In order to better understand this transition, an online survey was delivered to diverse groups of international students attending Corvinus University and ESSCA School of Management, at the beginning and end of the Spring 2021 semester. The analysis of this survey, strongly indicates that the home and social environments of University, had a significant impact on the student's learning aptitudes.

Keywords: higher education; COVID-19; emergency online learning; learning experience; sentiment analysis

1 Introduction

According to the UNESCO Institute of Statistics, there were 32.6 million students enrolled in higher education in 1970. In 2000, this number rose to 99.9 million students. Despite headwinds such as a declining youth population and lower fertility rates, the UIS estimates that the enrollment in high education could potentially be 377.4 million students (2030), 471.4 million by 2035, and 594.1 million by 2040 [2]. Even if one halves each of these forecasts, these numbers and growth rates are staggering.

The growth of online learning before the COVID-19 pandemic, can be characterized by four phases: 1990s (Internet propelled distance education), 2000-2007 (increasing use of Learning Management Systems – LMS), 2008-2012 (growth of

Massive Open Online Courses – MOOCs), and beyond where online enrollments in higher education outpaced traditional higher education enrollments [3]. Since the first phase back in 1990, international organizations, such as UNESCO, the World Bank, and the European Commission, have all argued that online education has the unique opportunity to cost effectively reach rural and disadvantaged areas of the world). Considering the tremendous growth of online that has occurred during the past few years, educators continuously face the significant challenge of ensuring that the quality of online education keeps pace with the quantity of users [4].

During these four phases, the effectiveness of traditional vs. online learning has been vigorously debated and conclusions vary. In the past decade, there have been a few notable randomized trials studying the effects of online instruction on student learning. One such study involved a large introductory microeconomics course at a major research university where students were randomly selected to watch either live lectures or the same lectures in a traditional educational setting [5]. The results indicate that live-only teaching was moderately more effective than online teaching, although this effectiveness was more significant for Hispanic students, male students, and lower achieving students. In another well-known randomized trial, students at six public universities were given either a hybrid "blended" format (one hour of face time instruction per week) or a traditional format (three hours of face-to face instruction). The results of this study showed that the students learning in the hybrid mode had learning outcomes that were approximately the same as those who attended traditional classes and at a significantly reduced cost. One of the key conclusions of this study was that properly designed online learning programs have the potential to achieve at least equal outcomes as traditional learning [6]. Lastly, a randomized trial involving 1,519 students across four semesters revealed that the students who completed purely online course had learning outcomes that were inferior to those attending live classes [7]. In any case, it must be understood that delivering effective online learning is very complex and the result of careful planning and an evolving design fueled by significant feedback from teachers and students.

The COVID-19 pandemic forced a mass migration to emergency remote learning (ERT) where the primary objective of educators was to get all students online as quickly as possible [8-16]. This rapid transition lies in contrast to how many effective online platforms were previously built using careful design, planning, and significant student feedback [17]. While the shock of rapid online migration has somewhat diminished, the challenge of delivering online education that is comparable with live classroom teaching has not. We now live in a world where online teaching is no longer an option, but rather a necessity [18]. Educators must now understand and properly respond to the fact that dismantling of the physical and social environments of universities will have a permanent impact on the mental and physical well-being of their [19].

A higher education, comparative study was conducted during the COVID-19 pandemic regarding the online learning perceptions of 559 students from South

Africa, Wales, and Hungary [20]. As one might expect, the results of this study show that there were significant differences in how students experienced online learning. The underlying causes behind these differences were related to how well a particular country responded to the pandemic and the level of support and resources given to students. The home environments of these students, therefore, played a critical role in shaping online learning perceptions. In another international study conducted during the COVID-19 pandemic involving 1,047 participants, the results revealed that the psychosocial strain was significantly increased during periods of home confinement [21]. A larger study done the in the U.S. involved 30,725 undergraduate students and 15,346 graduate students showed that the prevalence of major depressive disorders was two times higher in 2020 compared to 2019 and anxiety disorders were 1.5 times higher than in 2019 [22]. Finally, a sample of 30,383 students from 62 countries revealed that negative impact of the COVID-19 pandemic, particularly for the most vulnerable student groups [23].

As these research studies indicate, university students from all over the world have been harmed and damaged by the effects of the COVID-19 pandemic. This harm and damage grew as the shared facilities and face to face communities were dismantled [19]. Educators find themselves in the position to not only reflect on what has transpired since March of 2020, but to also use this experience to create online learning platforms that do far more than just "go online" [24]. Universities around the world can longer deny the fact that online learning has already become a permanent part of education at all levels. Success in future, therefore, will lie in the recognition that holistic online learning must replace emergency remote teaching (ERT) practices [25].

This paper studies the critical importance of home and social environments on university students' learning experiences during the COVID-19 pandemic and poses the following research questions:

RQ_1: What was the level of home and social disruption for university and graduate students during the Fall 2020 semester?

RQ_2: How did home and social disruption for university and graduate students progress during the Spring 2021 semester?

RQ_3: How did emergency remote learning impact the quality of education in the Spring 2021 semester?

The rest of the paper will be organized as follows: Section 2 introduces the materials and methods used, Section 3 presents and discusses the results, Section 4 justifies the results, Section 5 draws conclusions and summarizes the research as well as outlines possible future research options.

2 Materials and Methods

2.1 Demographics of Participants

A total of 212 students from Corvinus University (103 students) and the ESSCA School of Management (109 students) were surveyed at the beginning of the Spring 2021 semester (Figures 1, 2 and 3).

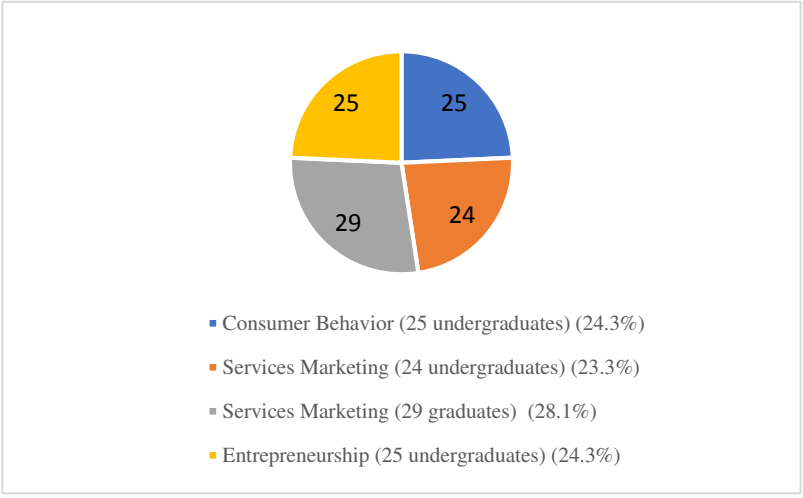

Figure 1
Students' majors surveyed at Corvinus University, N=103

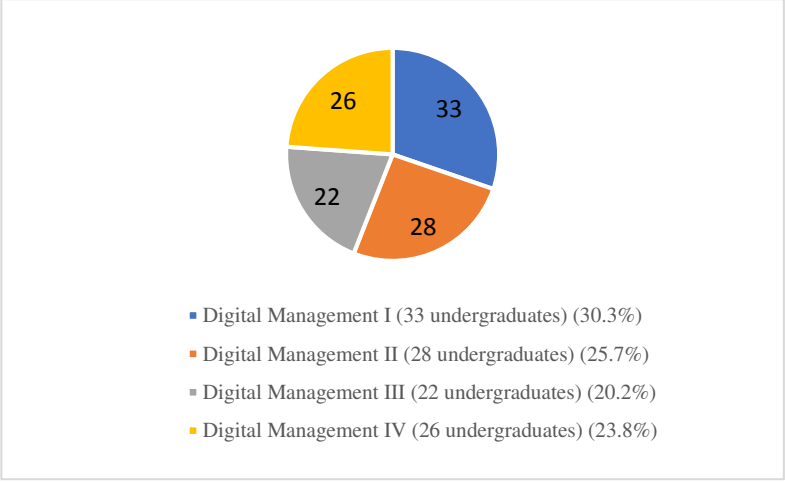

Figure 2
Students' majors surveyed at ESSCA School of Management, N=109

Figure 3
Students' Academic Disciplines (Corvinus University and the ESSCA School of Management), N=212

The survey given at the beginning of the Spring 2021 semester (BOS) measured the student remote learning sentiment from the Fall 2020 and Spring 2020 semesters. The end of the Spring 2021 semester survey (EOS) was primarily focused on the changes in student remote learning sentiment that occurred during this semester. All the following classes were taught entirely in English and online using Microsoft Teams.

There were 109 students who responded to the BOS survey that included 45 males (41.3%) and 64 females (58.7%). The average age was 21.5 years (standard deviation = 2.2) (Figure 4).

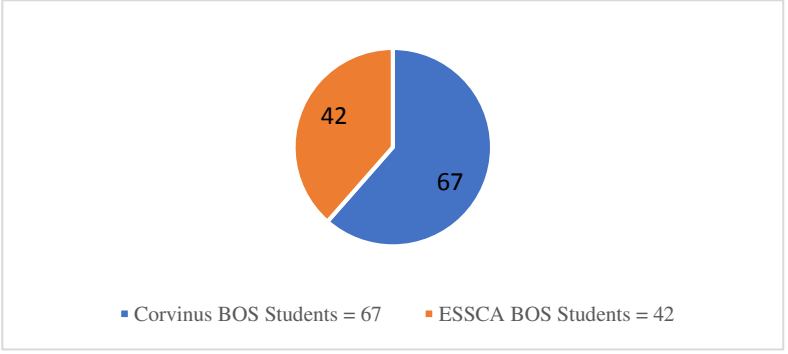

Figure 4
BOS Corvinus vs. ESSCA students, N=109

There were 129 students who participated in the EOS survey that included 53 males (41%) and 76 females (58.9%). The average age was 21.8 years of age (standard deviation = 2.2) (Figure 5).

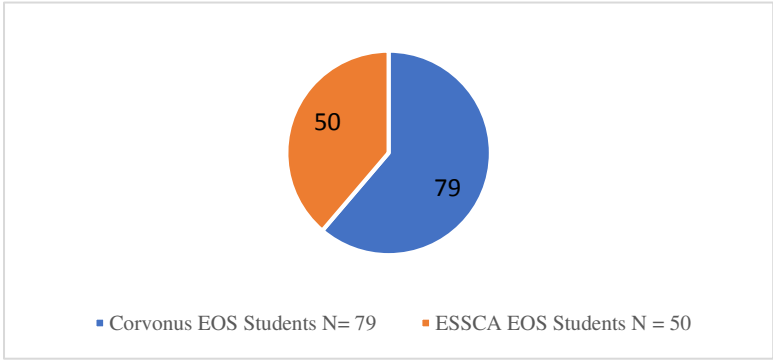

Figure 5
EOS Corvinus vs. ESSCA students, N=129

The sample size of the EOS Average Age is only 87 students, which only includes the students who took both the BOS and EOS surveys. The data, however, shows that there not a significant difference between the average age of the students in BOS vs. EOS.

The students participating in the BOS and EOS surveys were from 29 different countries. The highest concentrations of students came from the following countries: France (52), Germany (12), Hungary (6), Azerbaijan (5), Romania (4), China (3), Ireland (3) (Figure 6).

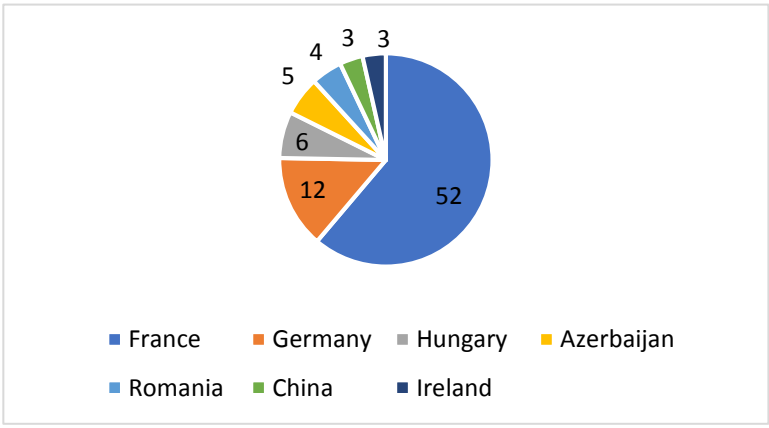

Figure 6
The highest concentrations of students came from the following seven countries, N=85

2.2 Internet and Technical Issues

When considering that a total of 83 students completed both the BOS and EOS surveys, we can conclude that there was a relatively low number of students who experienced poor Internet conditions throughout the Spring 2021 semester. Using a chi square test ($\chi 2 = 0.98607$ and $p = 0.3207$), the data shows that Internet problems were not a consistent problem for these students and that students who reported a problem in the beginning of the semester did not also report problem at the end of the semester. It can be concluded that poor Internet was a not big problem amongst this sample during the Spring 2021 semester and therefore, did not affect student remote learning sentiment.

Applying a Spearman's rank correlation between the student Internet BOS sentiment and student BOS remote learning sentiment (0.066, $p = 0.501$, $n= 109$) again shows that Internet problems did not weigh heavily on students' sentiments toward remote learning. In a similar fashion, the Spearman's rank correlation between student Internet EOS sentiment and student EOS remote learning sentiment (-0.077, $p = 0.389$, $n = 129$) yields a similar result.

2.3 Confirmation of Dimensions

As it was previously mentioned, due to the COVID-19 pandemic, all the students who participated in the BOS Spring 2021 survey had at least some experience with online learning during the Fall 2020 and Spring 2020 and semesters. While this drastic and sudden shift to online learning has clearly had significant impact on university education, it has also pushed educators to discover and embrace the benefits of using online tools. This purpose f this research is to shed light on how universities need to adapt to a world that has permanently changed in just two years. PCA analysis was used to recognize the patterns related to student sentiments from the Fall 2020 and Spring 2020 semesters and the ones that occurred during the Spring 2021 semester.

The initial parallel analysis revealed the following three dimensions that displayed significant loadings. Two of these dimensions ("Home Environment" and "Social Sentiment") were immediately recognizable and display a clear connection between BOS and EOS. The third dimension includes a mix of student responses that were not consistent from BOS to EOS and offered weaker and inconsistent data. For example, many loadings appeared in either BOS or EOS, but not both. In other circumstances, the values themselves were not significant enough to offer insight and had higher variances. After eliminating this dimension and using only two dimensions, the loadings became stronger and more significant. These two dimensions are labeled as "Home Environment" and "Social Sentiment" (Table 1).

3 Results

3.1 Home Environment Dimension BOS vs. EOS

When analyzing the home environment loadings from the BOS and EOS, the shift to remote learning clearly had a significant impact on the students participating in these surveys. A strong negative value (-0.687) was observed for the statement "I like working at my own pace" at the BOS, which indicates many students were missing the organization and structure provided by traditional teaching and found the task of organizing the pace of their learning to be difficult. While this loading in the EOS dropped to (-0.532), it can still be concluded that many students found organizing the pace of their own learning to be a challenge even after another semester of remote learning experience. A moderate, negative value of (-0.519) (was observed in the BOS regarding how much students like to set their own daily schedules. This value became even more negative (-0.579) at the EOS. Both values indicate that many students still value the organization and structure offered by live classrooms and physical school campuses and view organizing their own schedules negatively. When students were asked about their struggles in keeping up with a daily routine, we observed a moderate, positive loading (0.504) in the BOS, but a much stronger one (0.669) in the EOS. Overall, many students struggled with organizing their daily schedules and learning activities at the beginning and end of the Spring 2021 semester. These difficulties created a negative impact on the university students' remote learning environments and are ones not adequately addressed by emergency remote teaching.

A strong, positive value of (0.782) was observed in the BOS regarding how easily students become distracted at home when compared to the classroom. This value dropped significantly in the EOS to (0.539). These values tell us that students were able to better adapt to remote learning during the Spring 2021 semester and find ways to reduce or become more tolerant of distractions while learning from home. This may also indicate a higher self-efficacy (an ability targeted in my Fall 2021 research). At the BOS, a moderate, negative value of (-0.630) was observed showing that students reject the idea that distractions at school are significant. At the EOS, we curiously do not see a loading in this dimension, although we do observe a moderate, positive value (0.688) for how students feel they are not learning as much remotely as in the classroom and a strong, negative value (-0.734) for the statement that students are learning more remotely than in the classroom.

A strong, positive value of (0.754) was observed in the BOS regarding how motivated students are to complete their assignments. At the EOS, this value dropped to (0.641). While these students' abilities to motivate themselves may have improved marginally during the Spring 2021 semester, the end results still show that staying motivated while learning remotely was still an issue and one that must be recognized and addressed by educational institutions seeking to create holistic online learning platforms. The negative, moderate value of (-0.657) in the BOS

further reinforces that many students saw remote learning as inferior to traditional classrooms in terms of their education. At the EOS, this value strengthened to (-0.734) further underscoring that many students became wearier of remote learning and the quality of education that it delivered as the Spring 2021 semester progressed (Table 1).

Table 1
BOS vs. EOS Home Environment Sentiment (Applied rotation method is oblimin.)

Survey Questions	BOS Home Environment	EOS Home Environment
I like working at my own pace	-0.687	-0.532
I miss my friends		
I am more easily distracted at home than in the classroom	0.782	0.539
I like setting my own daily schedule for schoolwork	-0.519	-0.579
I miss my teachers		
I have difficulty staying motivated to complete my assignments	0.754	0.614
I miss participating in sports		
I feel I am learning more than I do in school	-0.657	-0.734
It is easier to focus without the distractions of school	-0.630	0
I feel that I'm not learning as much as I would in the classroom	0.543	0.688
I struggle to keep up with a daily routine	0.504	0.669
I miss the social environment at school		

3.2 Social Dimension

In the BOS, there was a moderately strong value of (0.560) for students who missed their friends. Not surprisingly, this value became much stronger (0.763) at the EOS as lockdown fatigue became greater and the time away from friends became more significant. This makes sense as the participants in these surveys are foreign exchange students predominantly living away from friends and family. It is also interesting that while a strong value for missing friends was observed, the analysis showed a low EOS value of (-0.467) for "I miss the social environment at school." This most likely indicates that the survey participants separated their friends from the social environment of the school, which was heavily disrupted due to COVID-19.

A moderate, positive value of (0.535) is observed in the BOS regarding how much students miss contact with their teachers. At the EOS, this value strengthened to (0.641) indicating that student weariness with lockdowns and remote learning

became more acute over time and this result is consistent with data from the home environment dimension. At the BOS, there is a moderate, positive value of (0.451) regarding how much students miss participating in sports. This value became more significant (0.701) at the EOS as the length of the lockdown became greater and the weather became warmer. This upward trend indicates that lockdowns are detrimental to the lives of students and close off needed outlet areas. A strong, positive value of (0.703) is observed at the BOS, and value weakened to (0.466) at the EOS. One explanation for this weakening value is that students became more accustomed to remote learning and found new ways to socialize. Another explanation is that many students were able to go home before the end of the Spring 2021 semester and this lifted their spirits (Table 2).

Table 2

BOS vs. EOS Social Sentiment (Applied rotation method is oblimin.)

Survey Questions	BOS Social Sentiment	EOS Social Sentiment
I like working at my own pace		
I miss my friends	0.560	0.763
I am more easily distracted at home than in the classroom		
I like setting my own daily schedule for schoolwork		
I miss my teachers	0.535	0.641
I have difficulty staying motivated to complete my assignments		
I miss participating in sports	0.451	0.701
I feel I am learning more than I do in school		
It is easier to focus without the distractions of school		
I feel that I'm not learning as much as I would in the classroom		
I struggle to keep up with a daily routine		
I miss the social environment at school	0.703	0.466

3.2.1 Remote Learning Sentiment (Before) vs. Home Environment Sentiment (Before)

Sample size = 108

A p-value of <.001 and a Pearson correlation (r) of -0.483 indicates a strong negative correlation between how students felt about remote learning at the beginning of the semester and how they felt about their home environments at the beginning of the Spring 2021 semester. The students who experienced more problems with their home environment at the BOS were also the ones who were less satisfied with remote learning. The students who had less problems with their home environment were more satisfied with remote learning.

3.2.2 Remote Learning Sentiment (Before) vs. Home Environment Sentiment (After)

Sample size = 82

A p-value of <.001 and a Pearson correlation (r) of -0.509 indicates that strong negative correlation between how students felt about remote learning at the beginning of the semester and how they felt about their home environments at the EOS. The students who displayed a more positive remote sentiment were the ones who experienced less problems with their home environments at the EOS. The students who had a negative remote learning sentiment were the ones who experienced lots of problems with their home environments at the EOS.

3.2.3 Remote Learning Sentiment (After) vs. Home Environment Sentiment (After)

Sample size = 124

A p-value of <.001 and a Pearson correlation (r) of -0.322 indicates a moderate, negative correlation between how students felt about remote learning at the end of the Spring 2021 semester and how they felt about their home environments at the end of this semester. The correlation is weaker than in the previous examples, but nonetheless still indicates that a student with a low remote learning sentiment most likely also experienced problems in their home.

4 Discussion

RQ_1 What was the impact on the home and social environments for university and graduate students at the beginning and end of the Spring 2021 semester?

For the home environment at the BOS, there were strong, positive loadings for the negative impact of distractions at home and the difficulty of staying motivated to complete assignments. The students did not see the ability to work at their own pace as a positive more moderate loadings were observed for students who expressed difficulties with setting their own daily schedules and maintaining their daily routines. In the BOS, students who experienced problems with their home environments were also the ones who were less satisfied with remote learning. Similarly, the students who had less problems with their home environment viewed remote learning more favorably. Overall, students at the BOS rejected the statement that they were learning more remotely than they were in the classroom.

At the BOS, there were moderate loadings for missing friends, teachers, and participating in sports. A more significant positive loading was observed for missing the social environment at school. It was clear that students at the BOS did not feel the impact on their social environment and were nostalgic about the social scene from their home universities from the Fall 2020 semester.

RQ2: How did home and social disruption for university and graduate students progress during the Spring 2021 semester?

The loadings for daily routines and setting daily schedules were higher in the EOS suggesting that these continued to be problems for many students throughout the semester. The data also shows that the students who a negative remote learning sentiment in the BOS, were the ones who also experienced problems with their home environments in the EOS. A more moderate loading was also observed connecting those who have negative remote learning sentiment to those who have a poor home environment sentiment in the EOS. Strong loadings were also observed for students how did not feel they were learning as much as they otherwise would in the classroom.

For the social environment impact at the EOS, a much stronger loading was observed for missing friends, teachers, and participating in sports. These stronger loadings clearly reflect the fatigue students felt during the semester and the isolation caused by COVID-19 lockdowns. The loadings for missing the social environment at school was significantly lower and could be caused by students returning home for the summer.

RQ3: How did emergency remote learning impact the quality of education in the Spring 2021 semester?

Emergency remote teaching (ERT) was a necessary step made by educational institutions to keep education working during a global pandemic. The main goal was to get everyone online as quickly as possible where attention was focused on the platform being used and technical and Internet related issues. Microsoft Teams was used by all 212 students in this study, and it is a developed, multi-functional educational platform. Despite this capability, however, it did little or even nothing to alleviate the problems identified by this research. Home and social environments are key components to the learning experiences of university students and are ones not addressed by emergency remote teaching [26].

Schools are designed to create the optimal learning environments for students and some certainly achieve this better than others. During remote learning, the school's lose control of the physical environment and assume that the students will create adequate home environments for themselves. The home environment goes way beyond an adequate Internet connection or personal computer, and a bad one can significantly and negatively affect a student's learning experience. Bad home environment can include elements like distracting noises, poor heating and/o cooling, too many people living in one space, bad furniture, inadequate lighting, thin walls, and many other factors. If the home environment can affect student learning experiences during remote learning, then schools need to transcend beyond emergency remote teaching and ensure students at least know what a suitable home environment is.

Having a good home environment, however, is not enough to ensure that a student will learn effectively from home. As the loadings from the research indicate, students struggled to set their daily schedules, create effective routines, and organize their own studies. The loss of contact with the school creates various responsibilities that students are not used to undertaking. A student who is lacking in organizational skills can struggle with keeping up with online studies even though that student did well in a live classroom.

The social environment is another aspect that is critical to successful student learning experiences and not addressed by emergency remote learning. As it was previously mentioned, the prevalence of major depressive disorders was two times higher in 2020 compared to 2019 and anxiety disorders were 1.5 times higher than in 2019 [22]. Universities cannot also assume that the well-being of students is constant and healthy when there is so much evidence to the contrary.

Conclusions and Future Work

The rise of online learning is not a new phenomenon, but the rise of emergency remote teaching (ERT) is. The COVID-19 pandemic has permanently changed education at all levels, and it is time for educational institutions to transition to the "new normal." Online education is no longer a consideration, but rather an imperative. While many are quick to point out, however, all the benefits of online learning, such as convenience and cost, it also has some serious side effects that must be addressed. Holistic online learning is a way to view students as more than icons on a dashboard and to understand that the loss or reduction of a school environment has consequences.

To better understand the factors contributing to the well-being of university students and how universities can implement holistic online learning, we are conducting a follow up survey at the beginning and end of the Fall 2021 semester, with a diverse group of International Students.

References

[1] United Nations, "Policy Brief: Education during COVID-19 and beyond", https://www.un.org/development/desa/dspd/wp-content/uploads/sites/22/2020/08/sg_policy_brief_covid-19_and_education_august_2020.pdf, 2020

[2] A. J. Calderon, "Massification of higher education revisited", Melbourne, Australia: RMIT University

[3] C. Dziuban, A. G. Picciano, C. R. Graham and D. M. Patsy, "Conducting research in online and blended learning environments: New pedagogical frontiers", 2015, New York: Routledge. https://doi.org/10.4324/9781315814605

[4] T. Joyce, S. Crockett, D. Jaeger, O. Altindag, S. and D. O'Connell, "Does classroom time matter?", Economics of Education Review, Volume 46, pp. 64-77, 2015, https://doi.org/10.1016/j.econedurev.2015.02.007

[5] D. N. Figlio, M. Rush and Y, Lu, "Is it live or is it internet? Experimental estimates of the effects of online instruction on student learning", Journal of Labor Economics, Vol. 31, No. 4, pp. 763-784, 2013

[6] C. Bowen and L. Nygren, "Interactive learning online at public universities: evidence from a six-campus randomized trial,", Journal of Policy Analysis and Management, Vol. 33, No. 1, pp. 94-111, 2013

[7] W. T. Alpert, K A. Couch and O. R. Harmon, "A randomized assessment of online learning," American Economic Review, Vol. 106, No. 5, pp. 378-82, 2016, doi: 10.1257/aer.p20161057

[8] K. Nagy, B. Orosz, Z. Szűts, Z. Balogh, M. Martin, S. Koprda; R. Pintér and Gy. Molnár, "Responses to the challenges of fast digital conversion,in the light of international research results - A comparative look at virtual spaces," Acta Polytechnica Hungarica, Vol. 18, No. 1, pp. 175-192, 2021

[9] P. Baranyi and Á. Csapó, "Definition and synergies of cognitive infocommunications," Acta Polytechnica Hungarica, Vol. 9, No. 1, pp. 67-83, 2012

[10] M. Konczosné Szombathelyi, P. Waldbuesser and R. Tench, "Digital age: Information and communication technologies, tools and trends for communication management," 6th IEEE Conference on Cognitive Infocommunications (CogInfoCom) Proceedings, pp. 229-234, 2015

[11] Gy. Molnár, J. Cserkó and Z. Balogh, "Visual, experiential assessment methods in the teaching process,". in J. Nikodem, R. Klempous (eds.) 12th IEEE International Conference on Cognitive Infocommunications (CogInfoCom) Proceedings, pp. 1091-1094, 2021

[12] Gy. Molnár, Z. Balogh and Zs. Námesztovszki, "The possibilities of using augmented reality (AR) in education through interactive applications," in J. Nikodem, R. Klempous (eds.) 12th IEEE International Conference on Cognitive Infocommunications (CogInfoCom) Proceedings, pp. 997-1000, 2021

[13] Z. Balogh, Gy. Molnár, K. Nagy, B. Orosz and Z. Szűts, "A digitális kompetencia és a digitális kultúra társadalomra és oktatásra gyakorolt hatásai, jellemzői, kihívásai," [The effects, characteristics and challenges of digital competence and digital culture on society and education] Civil Szemle, Vol. 17, No. 2, pp. 69-88, 2021

[14] B. Lampert, A. Pongrácz, J. Sipos, A. Vehrer and I. Horvath, "MaxWhere VR-learning improves effectiveness over clasiccal tools of e-learning," Acta Polytechnica Hungarica, Vol. 15, No. 3, pp. 125-147, 2018

[15] I. Horváth and M. Konczosné Szombathelyi, "3D VR as a platform of interaction in blended learning. in J. Nikodem, R. Klempous (eds.) 12th IEEE International Conference on Cognitive Infocommunications (CogInfoCom) Proceedings, pp. 167-172, 2021

[16] M. Konczosné Szombathelyi, I. Horváth and K. Jackson, "Understanding and interpretation of the terminology of 'blended learning." in J. Nikodem, R. Klempous (eds.) 12th IEEE International Conference on Cognitive Infocommunications (CogInfoCom) Proceedings, pp. 311-314, 2021

[17] C. B. Hodges, S. Moore, B. Lockee, T. Trust and M. A. Bond, "The difference between emergency remote teaching and online learning", Educause Review, https://er.educause.edu/articles/2020/3/the-difference-between-emergency-remote-teaching-and-online-learning

[18] S. Dhawan, "Online Learning: A panacea in the time of COVID-19 Crisis", Journal of Educational Technology Systems, Vol. 49, No. 1, pp. 5-22, 2020, https://doi.org/10.1177/0047239520934018

[19] R. Raaper and C. Brown, "The Covid-19 pandemic and the dissolution of the university campus: implications for student support practice", Journal of Professional Capital and Community, Vol. 5, No. 3/4, pp. 343-349, 2020, https://doi.org/10.1108/JPCC-06-2020-0032

[20] D. J. Cranfield, A. Tick, I. M. Venter, R. Blignaut and K. Renaud, "Higher education students' perceptions of online learning during COVID-19 - a comparative study", Education Sciences, Vol. 11, No. 8, p. 403, 2021, https://doi.org/10.3390/educsci11080403

[21] A. Ammar, H. Chtourou, O. Boukhris, K. Trabelsi, L. Masmoudi, M. Brach, B. Bouaziz, E. Bentlage, D. How, M. Ahmed, P. Mueller, N. Mueller, H. Hsouna, A. Aloui, O. Hammouda, L. Paineiras-Domingos, A. Braakman-Jansen, C. Wrede, S. Bastoni, C. S. Pernambuco, L. Mataruna, M. Taheri, K. Irandoust, A. Khacharem, N. L. Bragazzi, J. Strahler, J. A. Washif, A. Andreeva, S. C. Khoshnami, E. Samara, V. Zisi, P. Sankar, W. N. Ahmed, M. Romdhani, J. Delhey, S. J. Bailey, N. T. Bott, F. Gargouri, L. Chaari, H. Batatia, G. M. Ali, O. Abdelkarim, M. Jarraya, K. E. Abed, N. Souissi, L. V. Gemert-Pijnen, B. L. Riemann, W. Moalla, J. Gómez-Raja, M. Epstein, R. Sanderman, S. Schulz, A. Jerg, R. Al-Horani, T. Mansi, M. Jmail, F. Barbosa, F. Ferreira-Santos, B. Šimunič, R. Pišot, A. Pišot, A. Gaggioli, P. Zmijewski, C. Apfelbacher, J. Steinacker, H. B. Saad, J. M. Glenn, K. Chamari, T. Driss and A. Hoekelmann, A., "COVID-19 home confinement negatively impacts social participation and life satisfaction: a worldwide multicenter study," International Journal of Environmental Research and Public Health, Vol. 17, No. 17, 2020, 6237, doi: 10.3390/ijerph17176237, PMID: 32867287; PMCID: PMC7503681

[22] I. Chirikov, K. M. Soria, B. Horgos and D. Jones-White, "Undergraduate and graduate students' mental health during the COVID-19 pandemic", UC

Berkeley: Center for Studies in Higher Education, 2020, Retrieved from https://escholarship.org/uc/item/80k5d5hw

[23] A. Aristovnik, D. Keržič, D. Ravšelj, N. Tomaževič and L. Umek, "Impacts of the COVID-19 pandemic on life of higher education students: a global perspective", Sustainability, Vol. 12, No. 20, 2020, 8438, doi.org/10.3390/su12208438

[24] R. Watermeyer, T. Crick, C. Knight and J. Goodall, "COVID-19 and digital disruption in UK universities: afflictions and affordances of emergency online migration", Higher Education, Vol. 81, pp. 623-641, 2021, https://doi.org/10.1007/s10734-020-00561-y

[25] M. Browning, L. R. Larson, I. Sharaievska, A. Rigolon, O. McAnirlin, L. Mullenbach, S. Cloutier, M. Tue, Vu, J. Thomsen, N. Reigner, E. Covelli Metcalf, A. D'Antonio, M. Helbich, N. G. Bratman and H. A. Olvera, "Psychological impacts from COVID-19 among university students: Risk factors across seven states in the United States", PLoS ONE, Vol. 16, No. 1, 2021, e0245327, https://doi.org/10.1371/journal.pone.0245327

[26] C. Arnou, G. Cornelis, P. Heymans, S. Howard, G. Leemans, J. Tondeur, J. Vaesen, M. Van Den Driessche, M. Valcke and J. Elen, "COVID-19 and educational spaces: Creating a powerful and social inclusive learning environment at home", New York: Springer, 2020

Appendixes

Beginning of the Semester (BOS) and End of the Semester (EOS) Surveys

BOS Survey

Q1 – "What is your name?"
Q2 – "What is your age?"
Q3 – "What is your home city and country?"
Q4 – "What is your home university?"
Q5 – "Which of the following best describes the focus of your academic studies?"

- Finance and Accounting
- Communications
- Business and Management
- Engineering
- Computer Science
- Other

Q6 – "How do you feel about remote learning?"

- Very Unhappy
- Unhappy
- Somewhat Happy
- Somewhat Happy
- Happy
- Very Happy

Q7 – "What are the top three things you like about online learning?" (Free Answer)
Q8 – "What are the biggest challenges of online learning?" (Free Answer)
Q9 – "After spending a lot of time learning online, please answer how strongly you agree or disagree with the following?"

- B_MS01 "I like working at my own pace."
- B_MS02 "I am getting more sleep."
- B_MS03 "I miss my friends."
- B_MS04 "I am more easily distracted at home than in the classroom."
- B_MS05 "I like setting my own daily schedule for schoolwork"
- B_MS06 "I miss my teachers."
- B_MS07 "I have difficulty staying motivated to complete my assignments."
- B_MS08 "I am less stressed about my schoolwork."
- B_MS09 "I miss participating in sports."
- B_MS010 "I feel I am learning more than I do in school."
- B_MS011 "It is easier to focus without the distractions of school."
- B_MS012 "It's hard to keep school and home separate - I can't escape!"
- B_MS013 "I sometimes have difficulty understanding online assignments."
- B_MS014 "It's nice to have a break from the stress of the school environment."
- B_MS015 "I miss participating in extracurricular activities."
- B_MS016 "I feel that I'm not learning as much as I would in the classroom."
- B_MS017 "I struggle to keep up with a daily routine."
- B_MS018 "Teachers are assigning too much homework for now."

Q10 – "Do you have a reliable internet connection at home to take part in remote learning and complete your assignments without interference or delay?" (Y/N)
Q11 – "Do you have access to a computer that is adequate for your needs, allowing you to take part in remote learning and complete your school assignments?" (Y/N)
Q12 – "In your home university, which of the following learning attributes apply to your previous online experience?"

- Live online lectures
- Pre-recorded online lectures
- Online group activities and presentations
- Interactive online learning games
- Personalized and individual feedback with professors
- Online multiple-choice testing
- Individual essay testing
- Other

Q13 – "What learning method is the one you have experienced the most during your university experience thus far?"

- Traditional Online Learning – Classroom centric
- Only online learning

- Hybrid learning: a combination of traditional and online
- Other

Q14 – "What learning method do you feel is the most effective for your education?"

- Traditional Online Learning – Classroom centric
- Only online learning
- Hybrid learning: a combination of traditional and online
- Other

Q15 – "Please tell us how you would improve university education experience in the future." (Free Answer)

EOS Survey

Q1 – "What is your name?"
Q2 – "What is your home university?"
Q3 – "Do you have a reliable internet connection at home to take part in remote learning and complete your assignments without interference or delay?" (Y/N)
Q4 – "Do you have access to a computer that is adequate for your needs, allowing you to take part in remote learning and complete your school assignments?" (Y/N)
Q5 – "After spending a lot of time learning online, please answer how strongly you agree or disagree with the following?"

- E_MS01 "I like working at my own pace."
- E_MS02 "I am getting more sleep."
- E_MS03 "I miss my friends."
- E_MS04 "I am more easily distracted at home than in the classroom."
- E_MS05 "I like setting my own daily schedule for schoolwork."
- E_MS06 "I miss my teachers."
- E_MS07 "I have difficulty staying motivated to complete my assignments."
- E_MS08 "I am less stressed about my schoolwork."
- E_MS09 "I miss participating in sports."
- E_MS010 "I feel I am learning more than I do in school."
- E_MS011 "It is easier to focus without the distractions of school."
- E_MS012 "It's hard to keep school and home separate - I can't escape!"
- E_MS013 "I sometimes have difficulty understanding online assignments."
- E_MS014 "It's nice to have a break from the stress of the school environment."
- E_MS015 "I miss participating in extracurricular activities."
- E_MS016 "I feel that I'm not learning as much as I would in the classroom."
- E_MS017 "I struggle to keep up with a daily routine."
- E_MS018 "I miss the social environment at school."

Q6 – "Reflecting back on this course, what are the top three things you like about your online learning experience?" (Free Answer)
Q7 – "Reflecting back on this course, what were the biggest challenges of your online learning experience?" (Free Answer)

Q8 – "Reflecting back on this course, did the usage of Voice Over lectures, managed on your time, help you to better understand course materials when using distance learning?"

- Not at all
- A little bit
- Does not add or detract
- Adds some value
- Adds a lot of value

Q9 – "Reflecting back on this course, did the usage of the virtual group activities (sharing resources, ideas) enhance distance learning?"

- No value
- Little value
- Does not add or detract
- Adds some value
- Adds a lot of value

Q10 – "Reflecting back on this course, did the usage of Kahoot games enhance your distance learning experience?"

- No value added
- Adds little value
- Does not add or detract
- Adds some value
- Adds a lot of value

Q11 – "Reflecting back on this course, did the usage of invited judges for final presentations add value to your online learning experience?"

- Not at all
- Somewhat
- Neutral
- Adds value
- Adds a lot of value
- No judge was used

Q12 – "Based on your experience in this class, how are you currently feeling about remote learning? "
A score of 1 is "not at all satisfied" and a score of 10 is "completely satisfied." Drag the bar from left to right to find your score.

Q13 – "What learning method do you feel is the most effective for your education?"

- Traditional Online Learning – Classroom centric
- Only online learning
- Hybrid learning: a combination of traditional and online
- Other

Q14 – "Why did you select this learning method? Please describe the top three reasons for your selection." (Free Answer)

Q15 – "Now that you have done entire semesters both in class and online, please select all of the statements below that you agree with."

- Traditional in-class learning is outdated

- Traditional in-class learning is important for developing social skills
- Traditional in-class learning is long and boring
- Traditional in-class learning can never be replaced by online learning
- Traditional in-class learning is effective, but class times need to be shorter
- Traditional in-class learning really depends on the subject
- Traditional in-class learning really depends on the instructor
- Traditional in-class learning is more motivational
- Traditional in-class learning better facilitates collaboration
- Traditional in-class learning involves too much travel time

Q16 – "We are grateful to receive your honest input. Please provide any additional suggestions regarding how university education should be improved." (Free Answer)

Towards the Control of Multistability, in a PWM-Driven DC Motor Drive by Short Forcing

Oleksiy Kuznyetsov[1,2]

[1]Department of Electromechanics and Electronics, Hetman Petro Sahaidachnyi National Army Academy, 32 Heroiv Maidanu Str., 79026, Lviv, Ukraine

[2]Institute of Power Engineering and Control Systems, Lviv Polytechnic National University, 12 S. Bandera Str., 79000, Lviv, Ukraine
oleksii.o.kuznietsov@lpnu.ua

Abstract: PWM-driven feedback systems are known for demonstrating the multistable behavior within the stability margins of a nominal operating mode. With the transition of the system to the stable coexisting mode, the ripples of the variables increase and the overall efficiency deteriorates; therefore, it is an undesired behavior. We study the possibility of controlling multistability on the model of a chopper-fed DC drive. The proposed control takes the form of short forcing, temporarily moving the margins between the basins of attraction of the coexisting modes and thus driving the system to the nominal mode of operation. We also propose a universal control strategy, combining different types of short forcing, that are applied in a repeated manner with different settings. The latter control strategy overcomes unpredictability of the system's behavior caused by the fractal basin boundaries, and also, by external disturbances or noise.

Keywords: DC drive; multistability; basin of attraction; control of multistability

1 Introduction

Pulse width modulation (PWM) is a common solution for high-efficiency voltage regulation. In technical systems, it is implemented with the use of different topologies of power converters [1]. Accompanied with a microprocessor or a microcontroller unit [2] [3], it provides the possibility to implement complicated control strategies [4], in particular, for electric drives and servo systems; these are fuzzy-logic-based control [5], neuro-fuzzy-based control [6], model predictive control [7], reinforcement-learning-based control [8], *etc*.

The synthesis of the control strategy and parameter tuning, besides the task of providing the desirable static and dynamic indices, has to deal with the stability issues. With the assumption that the system's behavior is approximated as a linear system, we obtain the advantage of a well-developed synthesis and stability theory

for linear systems [2]. Alternatively, optimization algorithms are applied to tune classical linear controllers [9] or nonlinear controllers are synthesized to ensure robustness of the system [10].

However, with the inclusion of switching power converters, the system obtains the special type of nonlinearity—the switching one. Thus, if a simple electric circuit is combined of a resistor, a capacitor, and an inductor it is mathematically well represented by a simple linear time-invariant dynamical system. However, if the considered circuit is fed by a PWM-driven converter with a voltage or current feedback, the system becomes piecewise-linear leading to different nonlinear phenomena [11].

These phenomena have obtained a well-elaborated theory and were experimentally observed [11]. Electric drive systems fed from power electronic converters inhere their features [12]. In the current work, we focus on one of these features, *multistability*—the coexistence of several stable modes of operation for the same set of parameters. Multistability itself is a general feature of many physical systems of different nature and is observed both theoretically and experimentally [13] [14]. Each of the coexisting stable modes has its own *basin of attraction*—the set of initial states from which the trajectory of the system is attracted to the particular mode. Under noise or external disturbances, the transition between the coexisting states can occur—what is known as *tipping* [15] [16]. Those phenomena corresponding to multistability are also observed in switching power converters [17-19].

In PWM-controlled systems, the nominal operating mode is characterized by the lowest ripples of the system variables; therefore, the operation in any other coexisting mode is characterized by lower efficiency and should be avoided. It is worth noting that synthesis and tuning techniques take into account the nominal operating mode, neglecting the possible coexisting modes; however, they can have harmful effects on the system's behavior [20] [21].

What is utilized as a case study for our current work, a chopper-fed DC drive (Fig. 1a) under the parameters as given in Appendix, is known for demonstrating multistability [22] (see also [23]). Previously, we have depicted phenomena related to tipping in the considered system [24] [25]. What is sufficient for our study, it is demonstrated in [24] that the nominal mode is the most robust-to-noise among the coexisting ones for several sets of parameters.

Controlling multistability itself is of interest to scientific community [26]. The solutions can be classified into two categories: (i) the system is driven to a desired regime by some perturbation [27-29] and (ii) the undesired regime is annihilated under implementing some control [30-35].

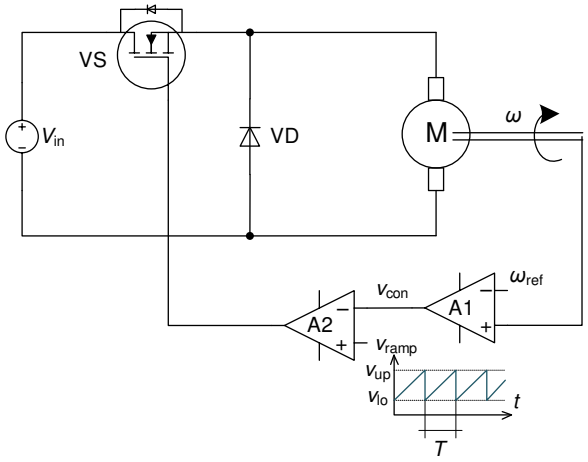

Figure 1
Circuit diagram of a chopper-fed DC drive, after [12]

It is obvious that the best solution is the second one ensuring the monostability operation of the system. However, several control techniques require the knowledge of the system dynamics, such as the linear augmentation technique [32], while others are based on the use of periodic modulation [30] [31] and are simple in implementation and tuning. On the other hand, adding additional control loops is in many cases undesirable as far as it complicates the tuning of the controller to achieve the control tasks (*e.g.* speed of operation, overshoot, *etc.*). In contradiction to those techniques, in the current work, we elaborate the first solution as being simpler for implementation. In general, the perturbation can be implemented in the form of constant periodic action [28], temporal feedback [29], or short pulses [27].

In a PWM-driven system, the perturbation can be applied in the form of slight changes of the switching function. The idea has been theoretically proven for extending the stability margins of the nominal regime [36] [37] (however, it requires constant control).

In the current work, our idea is that the same short disturbing action as in [37] has been developed specifically for the switching power converters (but with the different purpose and implemented as a constant action) slightly varies the margins of the basins of attraction of the coexisting modes. Hence, being shortly applied, as it has been proposed in [27] for a laser system, the control in the form of short perturbations can drive system to the nominal regime. Thus, the proposed control strategy uses short forcing only to force the system to return to the desired nominal mode of operation if a multistable system tips to the undesired mode and is only applied if the coexisting mode is detected. Therefore, the objective of the study is to obtain an advantage of the simple for implementation controller that can guarantee the nominal operation of the system.

2 Mathematical Model of a DC Drive

2.1 Mathematical Model in Continuous Time

The system under analysis is a permanent magnet DC motor fed from a chopper in the form of buck converter with the speed feedback loop and PWM-2 control (Fig. 1a).

The state of the switch VS is dictated by the relation between the values of a control signal v_{con} and a carrier (ramp) signal v_{ramp}. Thus, if $v_{\text{con}} < v_{\text{ramp}}$, the switch is on, and the system is depicted by the equation

$$\frac{d}{dt}\begin{bmatrix}\omega(t)\\ i(t)\end{bmatrix} = \begin{bmatrix}-\frac{B}{J} & \frac{K_T}{J}\\ -\frac{K_E}{L} & -\frac{R}{L}\end{bmatrix}\begin{bmatrix}\omega(t)\\ i(t)\end{bmatrix} + \begin{bmatrix}-\frac{T_L}{J}\\ \frac{V_{\text{in}}}{L}\end{bmatrix} \tag{1a}$$

while if $v_{\text{con}} \geq v_{\text{ramp}}$, the switch is off, and

$$\frac{d}{dt}\begin{bmatrix}\omega(t)\\ i(t)\end{bmatrix} = \begin{bmatrix}-\frac{B}{J} & \frac{K_T}{J}\\ -\frac{K_E}{L} & -\frac{R}{L}\end{bmatrix}\begin{bmatrix}\omega(t)\\ i(t)\end{bmatrix} + \begin{bmatrix}-\frac{T_L}{J}\\ 0\end{bmatrix} \tag{1b}$$

where the notation is explained in the Appendix. Given

$$\mathbf{A} = \begin{bmatrix}-B/J & K_T/J\\ -K_E/L & -R/L\end{bmatrix},\ \mathbf{x} = \begin{bmatrix}\omega(t)\\ i(t)\end{bmatrix},\ \mathbf{E}_{\text{off}} = \begin{bmatrix}-T_L/J\\ 0\end{bmatrix},\ \mathbf{E}_{\text{on}} = \begin{bmatrix}-T_L/J\\ V_{\text{in}}/L\end{bmatrix}$$

the system is represented by the state-space equation dependent on the state of the switch VS:

$$\dot{\mathbf{x}} = \mathbf{A}\mathbf{x} + \mathbf{E}_k \tag{2}$$

where $\mathbf{E}_k$, $k = \{\text{on}, \text{off}\}$ is the product $\mathbf{Bu}$ from the standard state-space representation, is the subscript representing the state of the switch VS.

For the sawtooth carrier signal with the ramp period T:

$$v_{\text{ramp}}(t) = v_{\text{lo}} + \left(v_{\text{up}} - v_{\text{lo}}\right)\left(\frac{t}{T} \bmod 1\right) \tag{3}$$

where v_{lo} and v_{up} are lower and upper levels of the sawtooth signal (Fig. 1). With a proportional speed controller, the control signal v_{con} is:

$$v_{\text{con}}(t) = g(\omega(t) - \omega_{\text{ref}}) \tag{4}$$

where g is a feedback gain, $\omega(t)$ is instantaneous speed, and ω_{ref} is the reference speed.

2.2 Derivation of Discrete-Time Mapping

For the purposes of analyzing the periodic steady state of the system, and since the behavior of the system is governed by the clock cycle T, it is natural to obtain a discrete-time model in the form of "stroboscopic" mapping $\mathbf{x}_{n+1} = P(\mathbf{x}_n)$ synchronized with the period T (as it has been explained in [11]), where $\mathbf{x}_n = \mathbf{x}(t_0)$, and $\mathbf{x}_{n+1} = \mathbf{x}(t_0 + T)$, where the evolution of the system between periodic instances is governed by the continuous-time model, here, (1-4). The model (1-4) was implemented in the Matlab environment utilizing the `ode45` solver with the built-in event detection.

3 Periodic Steady State of the System

With the derived discrete-time stroboscopic mapping, an arbitrary nT-periodic steady state is reduced to a period-n mode of the stroboscopic map. In particular, the nominal period-1 mode of the stroboscopic map (nT-periodic mode of the system, its period is equal to the clock cycle T) corresponds to a fixed point of a stroboscopic map, $2T$-periodic, to period-2 mode, *etc*.

The previous publications [22] [23] have demonstrated the coexistence of several stable regimes for the same parameters of the considered system (the parameters are given in the Appendix). The time-domain and state-space representation of the coexisting modes are demonstrated in Fig. 2 and Fig. 3, respectively. In Fig. 2 and Fig. 3, the corresponding discrete-time cycles (sampling of the continuous-time model) are marked with circles.

Comparing the three coexisting stable modes (Figs. 2 and 3), it is obvious that higher-periodic modes are situated in the same area of the state space, however, they are characterized by the higher ripples of the state variables. Therefore, from the practitioner's point of view, they correspond to undesirable lower-efficiency modes and should be avoided. On the other hand, the ripples can be measured and used to evaluate whether the system operates in its nominal mode or not.

Previously [23], we have analyzed the evolution of the coexisting regimes as the feedback gain g varies by means of the bifurcation diagrams. Afterwards, we have analyzed the behavior of the system for several gain values corresponding to several coexistence scenarios (those depicted in Fig. 4, period-1 and chaotic mode for g = 1.195, period-1, -3 and -4 for g = 2, and period-1 and period-6, for g = 2.2) [24]. What was also observed in [24] is that the nominal period-1 regime for all analyzed cases $g = \{1.195; 2; 2.2\}$ is the most robust to noise and external disturbances. Below, we also utilize the studies of the basins of attraction of the coexisting periodic modes to understand that kind of behavior of the regimes.

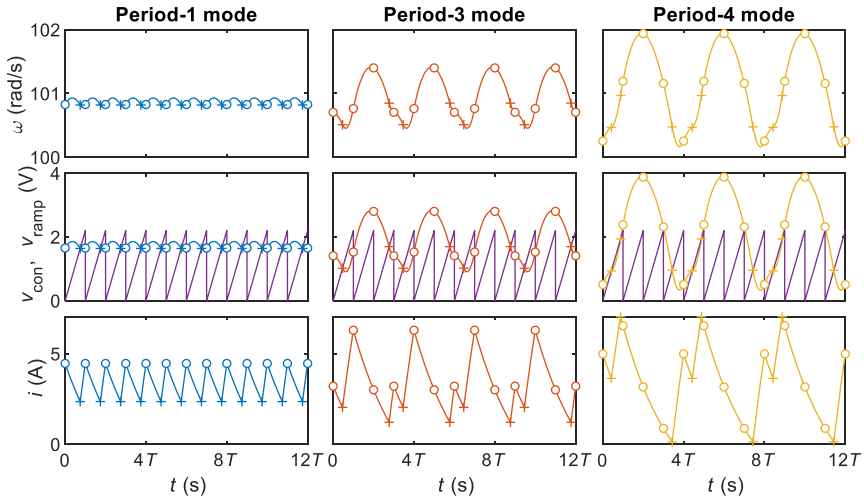

Figure 2
Trajectories of the coexisting period-1, -3 and -4 modes in the time domain, after [23]

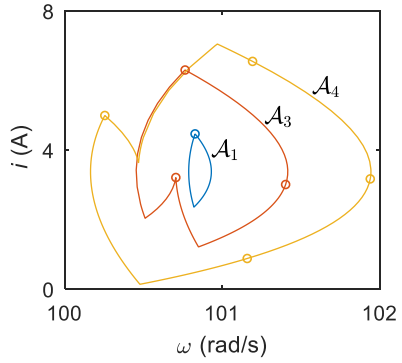

Figure 3
Trajectories $\mathcal{A}_i$ of the coexisting period-i modes, $i = \{1; 3; 4\}$, in the state-space, after [23]

4 Basins of Attraction of the Coexisting Regimes

Proceeding to studying multistability in the considered system, we analyze the basins of attraction for several values of gain g (corresponding to the values denoted in Fig. 3). The basins of attraction are depicted in Fig. 5 for the grid 500×500 of initial conditions, where $\mathcal{B}_i$ stands for the basin of attraction of the period-i mode (and χ is used for chaotic mode).

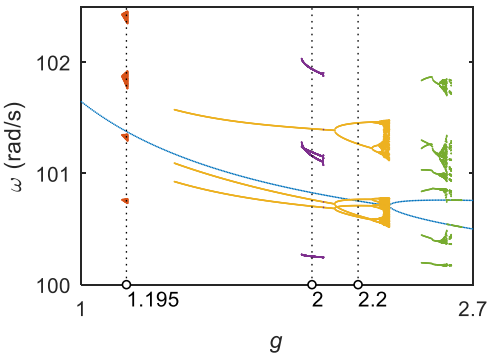

Figure 4
Several cases of coexisting stable modes at the bifurcation diagram of the speed ω taking feedback gain g as a parameter

The general feature is that for all analyzed cases in Fig. 4, we observe the complex interwoven structure of the basins, resulting in the practical unpredictability of the behavior. However, we summarize the basins have one thing common—the basins of the nominal period-1 mode near the point of its steady-state operation has the largest distance to the basin margin. That is demonstrated in Fig. 5 (the blow-up of the marked area in Fig. 4) for the case $g = 2$, the same can be observed in other cases. The basins of the coexisting states can be characterized by the commensurate distance to the margin (as $\mathcal{B}_3$ for $g = 2$ and $\mathcal{B}_6$ for $g = 2.2$) or lower (as $\mathcal{B}_\chi$ for $g = 1.195$ and $\mathcal{B}_4$ for $g = 2$). That determines the robustness of a mode to external action. In Fig. 5, red circle stands for period-1 mode, blue for period-3, and yellow for period-4.

5 Control of Multistability by Short Forcing

Between the periodic instances, the switch changes its state if the switching function $h(\mathbf{x}, t) = 0$ is satisfied. For the analyzed system, as it has been explained in the Modelling Section 2.1, $h(\mathbf{x}, t) = v_{\text{con}}(t) - v_{\text{ramp}}(t) = 0$ and therefore it is defined after (3) and (4) as follows:

$$h(\mathbf{x}, t) = g(\omega(t) - \omega_{\text{ref}}) - \left(v_{\text{lo}} + \left(v_{\text{up}} - v_{\text{lo}}\right)t^*\right) \tag{5}$$

where for ease of representation we use $t^* = t \bmod T$ as the time from the beginning of the examined period. The block diagram of the PWM signal generation corresponding to (5) is depicted in Fig. 7.

The three considered control strategies rely on slightly changing the switching function (5). The same idea is applied in [36] [37] with the other purpose of extending the stability margins of the nominal regime by stabilizing the period-1 mode becoming unstable.

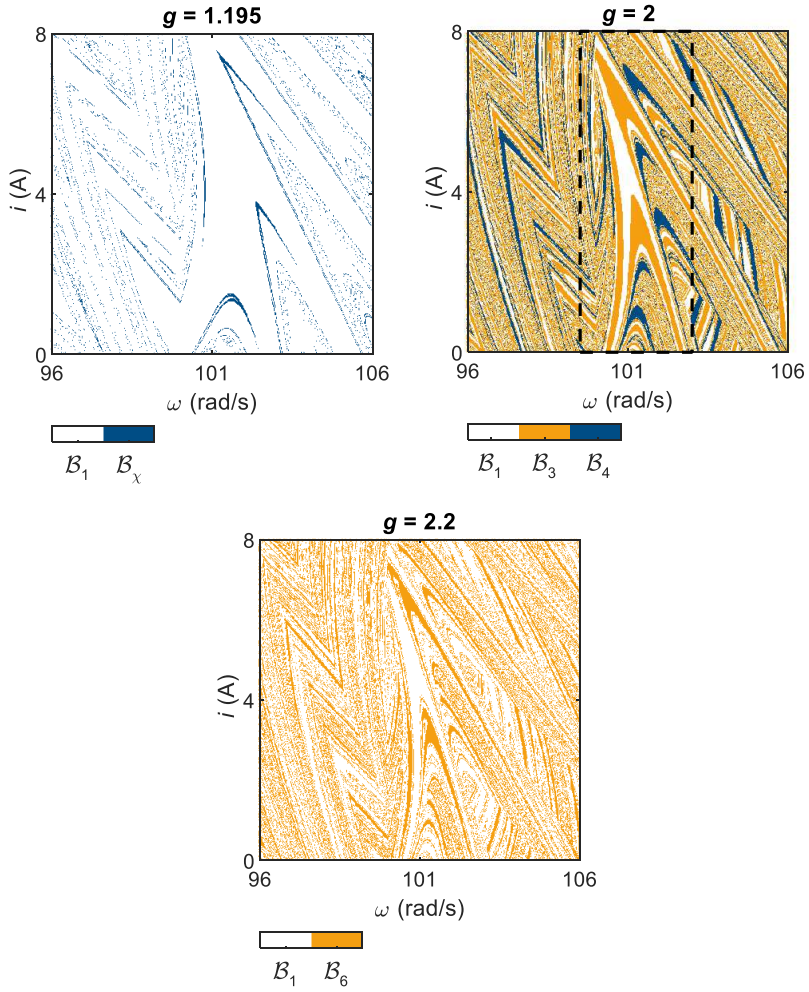

Figure 5

Basins of attraction $\mathcal{B}_i$ of coexisting stable states for several values of gain g corresponding to Fig. 4

Respectively, in our work, we consider that slight changes of the switching function slightly move the margins of the basins of the coexisting regimes, therefore, it can result in the tipping between the coexisting modes. As to our knowledge, the technique has never been applied to control the tipping between the coexisting modes. Below, we propose several strategies of modifying the switching function and analyze the system's behavior under those actions.

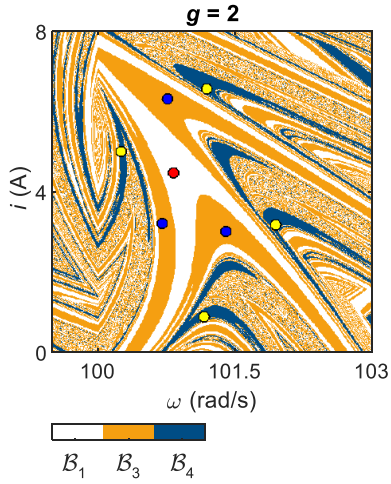

Figure 6
Blow-up of the marked region of the basins of attraction in Fig. 5 with the corresponding sampled periodic modes

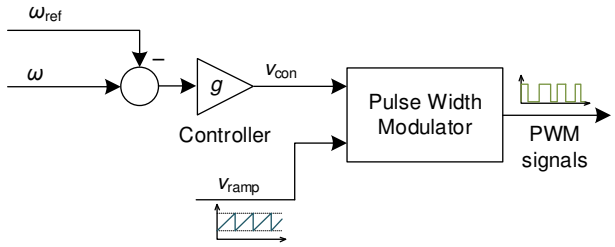

Figure 7
Block diagram of the PWM signals generation corresponding to the switching function $h(\mathbf{x}, t)$, (5)

In Figs. 9-11, the corresponding control strategies are applied within the shaded area, refer to the captions for explanation. In the figures below, circles stand for samples (discrete-time model), while crosses for switching.

5.1 Strategy 1: Utilizing an Additional Sinusoidal Perturbation of the Reference Signal

The first strategy is based on slight sinusoidal changes of the reference signal ω_{ref}:

$$h_1(\mathbf{x}, t) = g\left(\omega(t) - \omega_{\text{ref}}\left(1 - a \sin\frac{2\pi t^*}{T}\right)\right) - \left(v_{\text{lo}} + \left(v_{\text{up}} - v_{\text{lo}}\right)t^*\right) \tag{6}$$

where a is an adjustment coefficient for the strategy (6) as well as for those discussed below. For the purposes of the current study, its value is not under discussion, as far as we aim to analyze the general behavior under the proposed

control. In the study, the value is taken as $a = 10^{-3}$. The PWM signal generation block diagram corresponding to the strategy (6) is demonstrated in Fig. 8a (the control is enabled if the function $k_1(t)$ is ON).

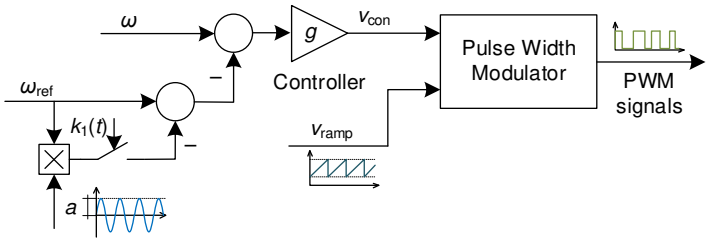

(a)

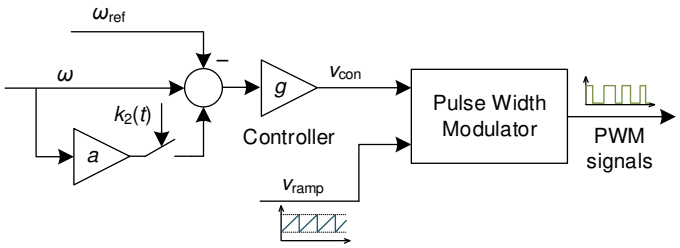

(b)

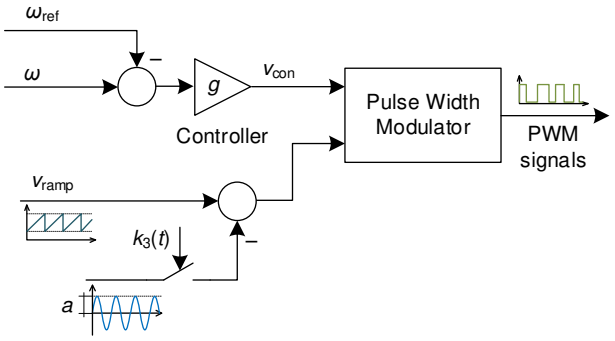

(c)

Figure 8

Block diagrams of the PWM signals generation corresponding to the switching functions $h_1(\mathbf{x}, t)$, equation (6) (a), $h_2(\mathbf{x}, t)$, equation (7) (b), and $h_3(\mathbf{x}, t)$, equation (8) (c)

5.2 Strategy 2: Adding a Signal Proportional to a State Variable

The second possible control strategy (Fig. 8b, enabled by $k_2(t)$) corresponds to the addition of the signal proportional to $\omega(t)$:

$$h_2(\mathbf{x},t) = g\big((1+a)\omega(t) - \omega_{\text{ref}}\big) - \big(v_{\text{lo}} + \big(v_{\text{up}} - v_{\text{lo}}\big)t^*\big) \tag{7}$$

5.3 Strategy 3: Utilizing an Additional Sinusoidal Perturbation of the Carrier Signal

And the third strategy (Fig. 8c, enabled by $k_3(t)$) utilizes sinusoidal perturbation applied to the carrier ramp signal:

$$h_3(\mathbf{x},t) = g(\omega(t) - \omega_{\text{ref}}) - \left(v_{\text{lo}} + \big(v_{\text{up}} - v_{\text{lo}}\big)t^* - a\sin\frac{2\pi t^*}{T}\right) \tag{8}$$

5.4 Discussion and Proposal of a Combined Control Strategy

Let us analyze the observations depicted in Figs. 7-9, where the results of applying different control strategies to the system operating in the coexisting modes are demonstrated.

First, we should keep in mind that the proposed control strategies are related to slight changes of basin margins; therefore, they cause controlled tipping from one mode to another one. However, some other perturbations being applied simultaneously (*e.g.*, noise), can cause changes to the direction of tipping.

Second, in the proposed solution, there is no such control strategy that, being applied to the system, causes tipping *exactly* to the desired mode; even if simulation demonstrates that behavior for some parameter set, there is no guarantee the same occurs under real-world conditions with inevitable noise and parameter variation (therefore, due to the complex structure of basin boundaries, see Fig. 5, the tipping in a real application becomes absolutely unpredictable).

Third, for the selected value of a, there is no transition from the nominal period-1 regime to some other; however, there is no guarantee that it will not occur under real-world conditions.

With the above mentioned considerations, our proposal is to apply a combined control strategy including the following. The control should be applied if the system operates in the undesired coexisting stable mode in the steady state; if the control action results in tipping to the undesired mode, the control should be applied again. As it has already been mentioned, the detection of the undesired mode can be applied in the form of detecting the increased ripples of variables.

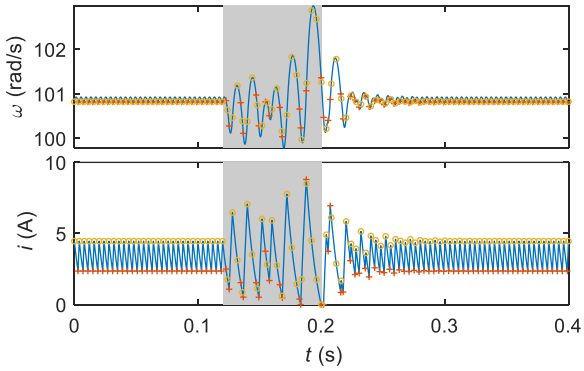

(a) from period-1 mode

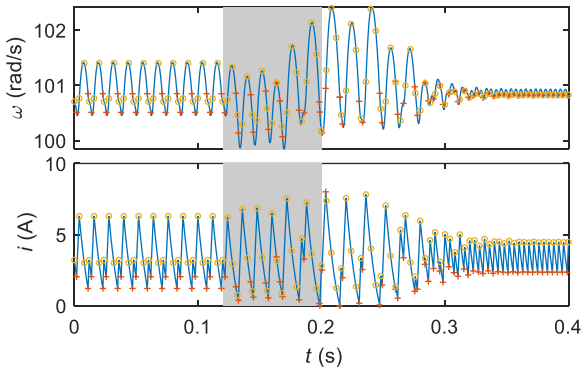

(b) from period-3 mode

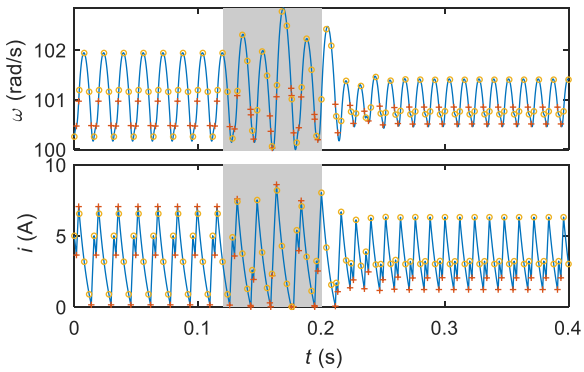

(c) from period-4 mode

Figure 9
Transitions from the coexisting modes corresponding to implemented Strategy 1—for utilizing an additional sinusoidal perturbation of the reference signal

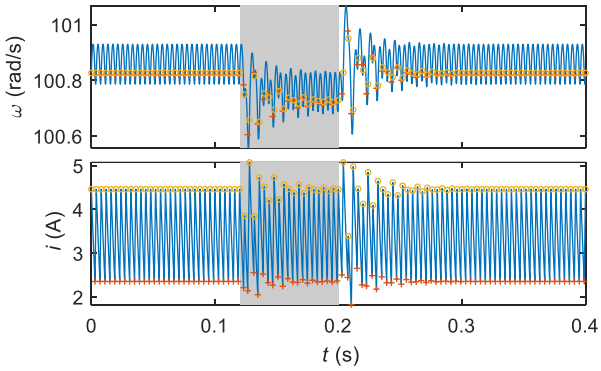

(a) from period-1 mode

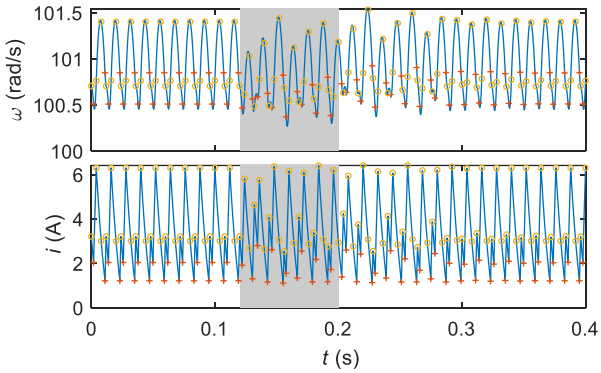

(b) from period-3 mode

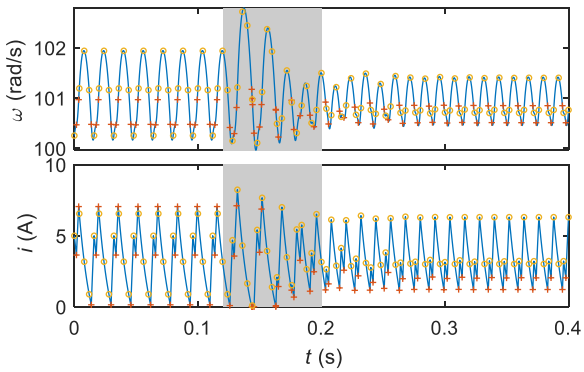

(c) from period-4 mode

Figure 10
Transitions from the coexisting modes corresponding to the implemented Strategy 2—for adding a signal proportional to a state variable

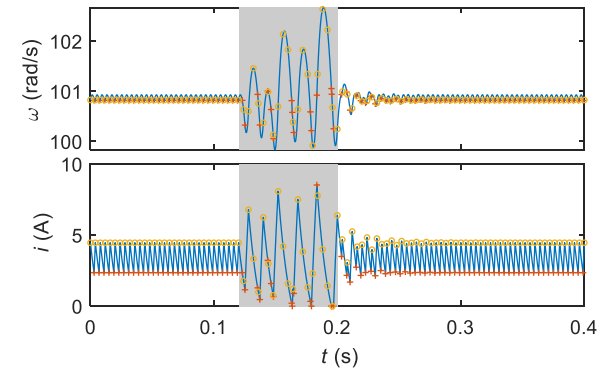

(a) from period-1 mode

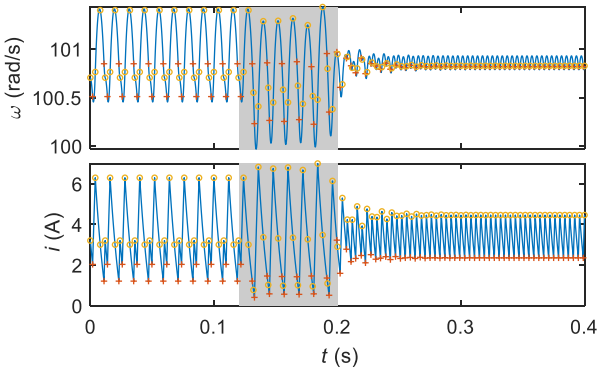

(b) from period-3 mode

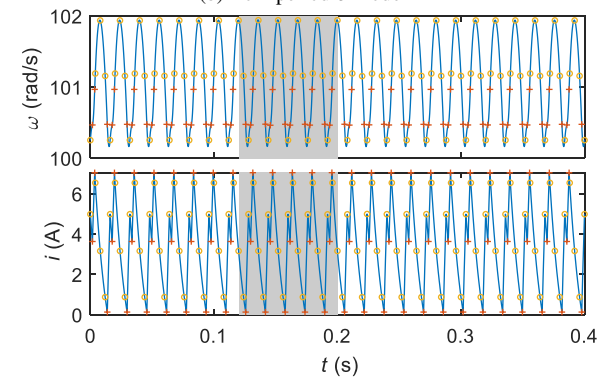

(c) from period-4 mode

Figure 11

Transitions from the coexisting modes corresponding to the implemented Strategy 3—for utilizing an additional sinusoidal perturbation of the carrier signal

The next consideration is that we should apply different control strategies alternately to avoid the situation demonstrated in Fig. 11c, where applying the

control action causes no transition to another mode (and even no noticeable transients).

Now, let us summarize the observations and formulate the requirements for the combined control. Thus, there is no universal control strategy that inevitably drives the system to the nominal period-1 mode (in general, we should assume that no tuning of the control strategies (6)–(8), selecting the modulation coefficient a and a forcing duration t, guarantee to obtain a universal controller). Then, the universal combined control strategy should contain several different forcing types repeated cyclically until the nominal mode is achieved. The example algorithm is depicted by the flowchart in Fig. 12. It corresponds to the application of the three depicted control strategies (6-8) repeatedly, that case is used for the simulations in Fig. 13. However, it is worth noting that in general, the base of forcing types can be widened by using different coefficient a and t values.

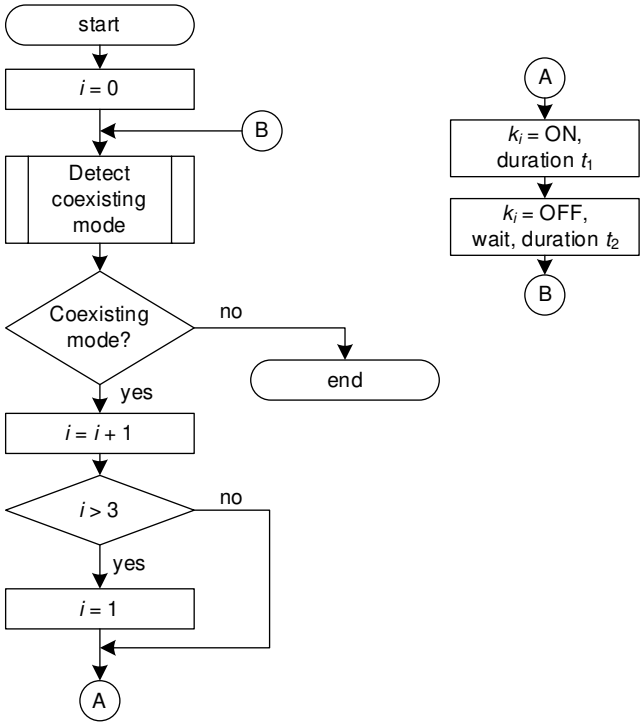

Figure 12
Flowchart of the concept of a combined control strategy

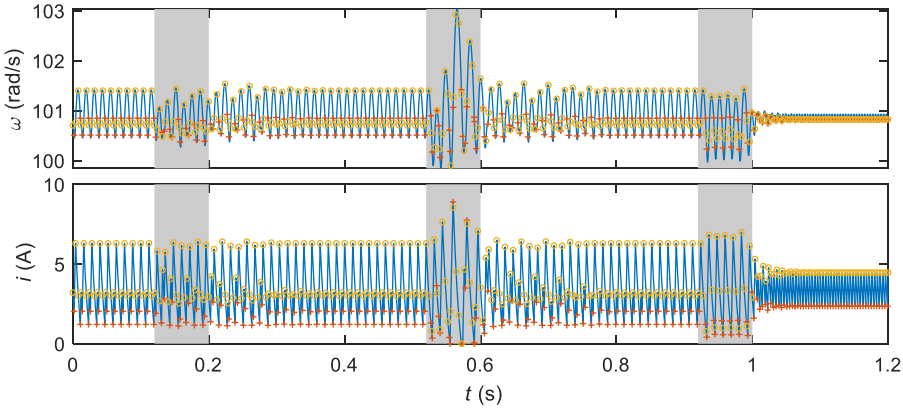

(a) from period-3 mode

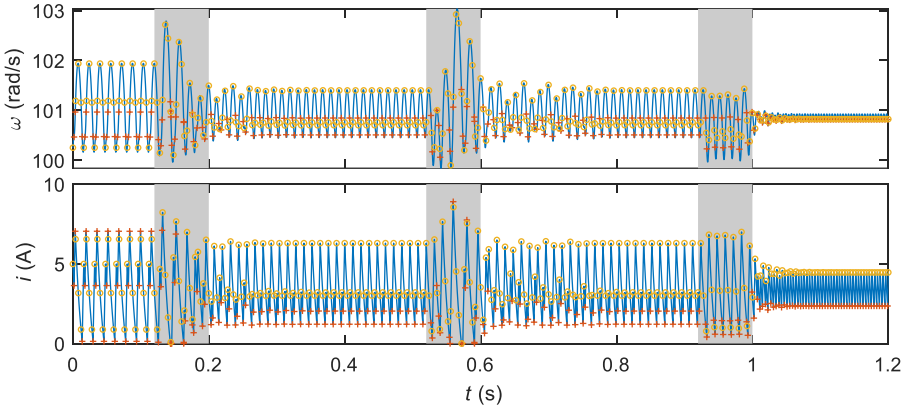

(b) from period-4 mode

Figure 13
Example of application of a combined control strategy (Strategy 2 → Strategy 1 → Strategy 3)

Conclusions

As it is known, in a PWM-controlled feedback system, different nonlinear behaviors can be observed, including multistability—the coexistence of several stable periodic modes for the same set of parameters; particularly, within the stability margins of the nominal operating mode it is an undesired behavior. In a coexisting mode, the overall system's efficiency deteriorates and that determines the requirement to have the possibility of controlling multistability, *i.e.* to guarantee the nominal operating mode.

In the example of a chopper-fed DC drive, we study the possibility of controlling multistability by short forcing. That is applied in the form of short, slight changes of the PWM switching function, slightly moving the margins between the basins of the coexisting mode resulting in a tipping between the coexisting modes. Several control strategies could be proposed with different disturbing actions applied.

To obtain a universal control algorithm, we propose a control strategy that combines different types of short forcings, that are applied in a repeated manner. That also guarantees that the system is driven, after several iterations, to its nominal mode even if it is subjected to any external disturbances (*e.g.* noise) thus overcoming the unpredictability of the system's behavior caused by the fractal boundaries of the basin of attraction.

Appendix: Parameters of the DC Drive [22]

Ramp voltage: Lower level $v_{\mathrm{lo}} = 0$ V, upper level $v_{\mathrm{up}} = 2.2$ V, period $T = 4$ ms

DC motor and load: Armature resistance $R = 3.5\ \Omega$, armature inductance $L = 36$ mH, back-EMF constant $K_E = 0.1356$ V·s, torque constant $K_T = 0.1324$ N·m/A, viscous damping $B = 0.000564$ N·m·s, load inertia $J = 0.000971$ N·m·s^2, load torque $T_{\mathrm{L}} = 0.39$ N·m

Control system: Input voltage $V_{\mathrm{in}} = 100$ V, feedback gain $g = 2$, reference speed $\omega_{\mathrm{ref}} = 100$ rad/s

References

[1] B. K. Bose, *Power Electronics and Motor Drive Advances and Trends*. MA, Burlington: Elsevier, 2006

[2] C. A. Iordache, M. Bodea, "Analysis and design of a high efficiency current mode buck converter with I^{2}C controlled output voltage," *Roman. J. Inform. Sci. Technol.*, Vol. 23, No. 2, pp. 188-203, 2020

[3] T. S. Kumar and R. N. Banavar, "Observer based control of a brushed DC motor at very low speeds over controller area network: An application in astronomical telescopes," in *2017 11th Asian Control Conf. (ASCC)*, Dec. 2017, pp. 1449-1453, doi: 10.1109/ASCC.2017.8287386

[4] D. A. Barkas, G. C. Ioannidis, C. S. Psomopoulos, S. D. Kaminaris, and G. A. Vokas, "Brushed DC Motor Drives for Industrial and Automobile Applications with Emphasis on Control Techniques: A Comprehensive Review," *Electronics*, Vol. 9, No. 6, Art. No. 887, May 2020, doi: 10.3390/electronics9060887

[5] R.-E. Precup *et al.*, "Generic two-degree-of-freedom linear and fuzzy controllers for integral processes," *J. Franklin Inst.*, Vol. 346, No. 10, pp. 980-1003, 2009, doi: 10.1016/j.jfranklin.2009.03.006

[6] Y. Paranchuk, P. Evdokimov, and O. Kuznyetsov, "Electromechanical positioning system with a neuro-fuzzy corrector," *Przegl. Elektrotechn.*, Vol. 96, No. 9, 2020, doi: 10.15199/48.2020.09.11

[7] A. Reda, A. Bouzid, J. Vásárhelyi, "Model predictive control for automated vehicle steering," *Acta Polytechn. Hungar.*, Vol. 17, No. 7, pp. 163-182, 2020, doi: 10.12700/APH.17.7.2020.7.9

[8] I. A. Zamfirache, R.-E. Precup, R.-C. Roman, E. M. Petriu, "Reinforcement Learning-based control using Q-learning and gravitational search algorithm with experimental validation on a nonlinear servo system," *Inform Sci.*, Vol. 583, pp. 99-120, 2022, doi: 10.1016/j.ins.2021.10.070

[9] R.-C. Roman *et al.*, "Iterative Feedback Tuning Algorithm for Tower Crane Systems," *Procedia Comp. Sci.*, Vol. 199, pp. 157-165, 2021, doi: 10.1016/j.procs.2022.01.020

[10] R.-E. Precup, S. Preitl, "PI-Fuzzy controllers for integral plants to ensure robust stability," *Inform. Sci.*, Vol. 177, No. 20, pp. 4410-4429, 2007, doi: 10.1016/j.ins.2007.05.005

[11] S. Banerjee and G. C. Verghese, Eds., *Nonlinear Phenomena in Power Electronics: Bifurcations, Chaos, Control, and Applications*. Wiley-IEEE Press, 2001

[12] K. T. Chau and W. Zheng, *Chaos in Electric Drive Systems: Analysis, Control and Application*. Wiley-IEEE Press, mar 2011

[13] U. Feudel, "Complex dynamics in multistable systems," *Int. J. Bifurc. Chaos*, Vol. 18, No. 6, pp. 1607-1626, 2008, doi: 10.1142/ S0218127408021233

[14] A. N. Pisarchik, A. E. Hramov, *Multistability in Physical and Living Systems: Characterization and Applications*. Springer, 2022

[15] U. Feudel, A. N. Pisarchik, and K. Showalter, "Multistability and tipping: From mathematics and physics to climate and brain—Minireview and preface to the focus issue," *Chaos*, Vol. 28, No. 3, Art. No. 033501, mar 2018, doi: 10.1063/1.5027718

[16] G. Ambika, J. Kurths, "Tipping in complex systems: theory, methods and applications," *Eur. Phys. J. Spec. Top*., Vol. 230, pp. 3177-3179, 2021, doi: 10.1140/epjs/s11734-021-00281-z

[17] Z. T. Zhusubaliyev and E. Mosekilde, "Multistability and hidden attractors in a multilevel DC/DC converter," *Math. Computers Simulation*, Vol. 109, pp. 32-45, 2015, doi: 10.1016/j.matcom.2014.08.001

[18] A. el Aroudi, J. Huang, M. S. Al-Numay, and Z. Li, "On the Coexistence of Multiple Limit Cycles in H-Bridge Wireless Power Transfer Systems With Zero Current Switching Control," *IEEE Trans. Circ. Syst. I: Reg. Papers*, Vol. 67, No. 5, pp. 1729-1739, May 2020, doi: 10.1109/TCSI.2019.2960575

[19] L. Benadero, E. Ponce, A. el Aroudi, and L. Martinez-Salamero, "Analysis of coexisting solutions and control of their bifurcations in a parallel LC resonant inverter," in *Proc. IEEE Int. Symp. Circ. Syst.*, May 2017, pp. 1-4, doi: 10.1109/ISCAS.2017.8050512

[20] M. A. Kiseleva, N. V. Kuznetsov, and G. A. Leonov, "Hidden attractors in electromechanical systems with and without equilibria," *IFAC-*

PapersOnLine, Vol. 49, No. 14, pp. 51-55, Jan. 2016, doi: 10.1016/J.IFACOL.2016.07.975

[21] H. Kim, S. H. Lee, J. Davidsen, and S. W. Son, "Multistability and variations in basin of attraction in power-grid systems," *New J. Phys.*, Vol. 20, No. 11, p. 113006, 2018, doi: 10.1088/1367-2630/aae8eb

[22] N. Okafor, "Analysis and Control of Nonlinear Phenomena in Electrical Drives," Ph.D. dissertation, Newcastle University, Newcastle, UK, 2012

[23] O. O. Kuznyetsov, "Calculation of stable and unstable periodic orbits in a chopper-fed DC drive," *Math. Modeling Comput.*, Vol. 8, No. 1, pp. 43-57, 2021, doi: 10.23939/mmc2021.01.043

[24] O. Kuznyetsov and Y. Paranchuk, "Remarks on the behavior of a multistable DC drive in the presence of noise," *2021 IEEE 12th Int. Conf. Electron. Inf. Technol. (ELIT)*, Lviv, Ukraine, 2021, pp. 175-180, doi: 10.1109/ELIT53502.2021.9501090

[25] O. Kuznyetsov and Y. Paranchuk, "Phenomena related to noise-induced and disturbance-induced tipping in a multistable DC drive," *IEEE EUROCON 2021 - 19th Int. Conf. Smart Technol.*, Lviv, Ukraine, 2021, pp. 408-413, doi: 10.1109/EUROCON52738.2021.9535584

[26] A. N. Pisarchik and U. Feudel, "Control of multistability," *Phys. Rep.*, Vol. 540, No. 4, North-Holland, pp. 167-218, Jul. 30, 2014, doi: 10.1016/j.physrep.2014.02.007

[27] B. K. Goswami and A. N. Pisarchik, "Controlling multistability by small periodic perturbation," *Int. J. Bifurc. Chaos*, Vol. 18, No. 06, pp. 1645-1673, Jun. 2008, doi: 10.1142/S0218127408021257

[28] F. Hegedűs, W. Lauterborn, U. Parlitz, and R. Mettin, "Non-feedback technique to directly control multistability in nonlinear oscillators by dual-frequency driving," *Nonlin. Dyn.*, Vol. 94, No. 1, 2018, pp. 273-293, doi: 10.1007/s11071-018-4358-z

[29] K. Yadav, A. Prasad, and M. D. Shrimali, "Control of coexisting attractors via temporal feedback," Phys. Lett., Sect. A: Gen., Atomic Solid State Phys., Vol. 382, pp. 2127-2132, aug 2018, doi: 10.1016/ j.physleta.2018.05.041

[30] R. Sevilla-Escoboza, A. N. Pisarchik, R. Jaimes-Reátegui, and G. Huerta-Cuellar, "Selective monostability in multi-stable systems," *Proc. Royal Soc. A: Math., Phys. Eng. Sci.*, 2015, doi: 10.1098/rspa.2015.0005

[31] R. Sevilla-Escoboza et al., "Error-feedback control of multistability," *J. Franklin Inst.*, Vol. 354, No. 16, pp. 7346-7358, Nov. 2017, doi: 10.1016/j.jfranklin.2017.08.052

[32] Z. T. Njitacke et al., "Control of Coexisting Attractors with Preselection of the Survived Attractor in Multistable Chua's System: A Case Study," *Complexity*, Vol. 2020, pp. 1-16, Sep. 2020, doi: 10.1155/2020/5191085

[33] A. el Aroudi, L. Benadero, E. Ponce, C. Olalla, F. Torres, and L. Martinez-Salamero, "Suppression of Undesired Attractors in a Self-Oscillating H-Bridge Parallel Resonant Converters under Zero Current Switching Control," *IEEE Trans. Circ. Syst. II: Expr. Briefs*, Vol. 66, No. 4, pp. 692-696, Apr. 2019, doi: 10.1109/TCSII.2018.2880139

[34] Z. Zhang, J. Páez Chávez, J. Sieber, and Y. Liu, "Controlling grazing-induced multistability in a piecewise-smooth impacting system via the time-delayed feedback control," *Nonlin. Dyn.*, May 2021, doi: 10.1007/s11071-021-06511-2

[35] J. A. Taborda and F. Angulo, "Computing and controlling basins of attraction in multistability scenarios," *Math. Probl. Eng.*, Vol. 2015, pp. 1-13, 2015, doi: 10.1155/2015/313154

[36] D. Giaouris, A. Elbkosh, S. Banerjee, B. Zahawi and V. Pickert, "Control of switching circuits using complete-cycle solution matrices," *2006 IEEE Int. Conf. Ind. Technol.*, 2006, pp. 1960-1965, doi: 10.1109/ICIT.2006.372582

[37] D. Giaouris, S. Banerjee, B. Zahawi and V. Pickert, "Control of Fast Scale Bifurcations in Power-Factor Correction Converters," in *IEEE Trans. Circ. Syst. II: Expr. Briefs*, Vol. 54, No. 9, pp. 805-809, Sept. 2007, doi: 10.1109/TCSII.2007.900350

Development of Available IoT Data Collection Devices to Evaluate Basic Emotions

Zoltán Balogh [1], Kristián Fodor [1], Martin Magdin [1], Jan Francisti [1], Štefan Koprda [1], Attila Kővári [2,3,4,5]

[1] Department of Informatics, Faculty of Natural Sciences and Informatics, Constantine the Philosopher University in Nitra
Tr. Andreja Hlinku 1, 979 01 Nitra, Slovakia

{zbalogh, kristian.fodor, mmagdin, jfrancisti, skoprda}@ukf.sk

[2] Institute of Engineering, University of Dunaujváros, Táncsics M. u. 1/a, 2400 Dunaujváros, Hungary, kovari@uniduna.hu

[3] Alba Regia Technical Faculty, Óbuda University, Budai út 45, 8000 Székesfehérvár, Hungary, kovari.attila@amk.uni-obuda.hu

[4] GAMF Faculty of Engineering and Computer Science, John von Neumann University, Izsáki u. 10, 6000 Kecskemét, Hungary
kovari.attila@gamf.uni-neumann.hu

[5] Eszterházy Károly Catholic University, Institute of Digital Technology, Faculty of Informatics, Eszterházy tér 1, 3300 Eger, Hungary
kovari.attila@uni-eszterhazy.hu

*Abstract: For most users, everyday objects are connected to the Internet, using their computational capabilities to form a whole entity, called the **IoT** (Internet of Things). This article deals with the creation of an available IoT device, with which we will be able to classify the emotional states of the user. Using existing technical solutions and methods that use approaches based on the application of sensors while maintaining their non-invasiveness, we have created such a device. In the analysis of the current state, we describe the possibilities of classifying human emotions, existing classification methods and how the measured data are related to human emotions. Next, we describe the methods used to analyze the collected human physiological signals. We propose a complex system for measuring physiological human signals and subsequent recognition of emotional states. We describe the composition of the proposed system, as well as the specific hardware and software used. At the end, we focus on the functionality and testing of the proposed system. Finally, we perform several measurements, where we evaluate their results and the reliability of the proposed system.*

Keywords: Internet of Things; emotions; data; sensors; heart rate; facial recognition

1 Introduction

Emotion recognition can serve as a scientific foundation for tracking emotional well-being and detecting the physiological and mental diseases linked to emotions. Emotions are conveyed in a variety of ways, including psychological behavior and physiological changes. Humans have no conscious control over these physiological changes. Thus, physiological signals can more objectively reflect participants' genuine feelings [1].

The Internet of Things (IoT) is a new Internet revolution and a developing research topic. The Internet of Things is always changing. A variety of methodologies and concepts from related technologies such as cloud computing, the internet of the future, big data [2], robotics, and semantic technologies [3] [4] are used to assess further possibilities. The Internet of Things (IoT) has a lot of potential in healthcare. Sensors that can measure and monitor a variety of medical characteristics in the human body can be used [5]. For example automatic recognition of emotions is usually performed by measuring various parameters of the human body or electrical impulses in the nervous system and analyzing their changes [6].

The Internet of Things is evolving at a rapid pace and remains the latest and most popular concept in the world of information technology. The Internet of Things can also be seen as a global network that enables communication between people, people and things all around the world, and gives each object a unique identity [7]. The concept of the Internet of Things, created by Ashton in 1999, has attracted and continues to attract a wealth of research and industrial interest [8]. The IoT ecosystem platform can in principle be divided into three layers, namely the sensor layer (for data generation), the communication layer (for connection and data transmission) and the layer of management (for data collection, storage, modification and management) [9]. Thanks to advances in the Internet of Things, it is possible to monitor the environment as well as users and their behavior at a very detailed level, reflecting their individual preferences [10]. Skin conductance (SC), heart rate variability (HRV), skin temperature (SKT), peripheral plethysmography (PPG), and other commercial monitoring equipment have been created to read human bio-signals [11]. One of the most crucial aspects of one's own personal health care is health monitoring. It is critical for gathering information about the user's circumstance. Fitness trackers, smart fitness bands, and portable ECG sensors are examples of health care monitoring devices. Companies can make better decisions when identifying a user's poor health because this data is constantly collected. Complex systems can now be implemented on small devices thanks to the Internet of Things [12]. We can only examine and calculate this data for our own needs with the help of a smartphone or a computer [13]. Sensors have shrunk in size, enabling for the creation of a wide range of wearable devices [14].

The article deals with the development of a compact device and the implementation of an effective health monitoring system based on IoT. The suggested system monitors critical human health metrics such as heart rate combined with face detection with the ability to wirelessly communicate the collected data to a database over Wi-Fi. A web application or a mobile application can be used to access the received data at any time.

2 Related Work

An integral part of these tasks are our smartbands and smartphones, which allow us to make life easier by controlling devices and storing important information, while displaying information about their status in real time on other devices [15]. Each device has its own UID with which it can recognize and transmit data over the network without requiring interaction between the user and the computer [16]. Smart devices based on wireless communication, through which information is sent from sensors, have been designed for ubiquitous monitoring of health and activity [17]. Smart devices can be used to monitor activities, health, sports and fitness [18]. Because there are many of these functions, it is impossible to capture a unique signal that can provide a good compressed system for variable analysis [19]. Cheng et al. designed smart clothing based on cloud and IoT technology for next generation healthcare systems [20]. This study presented a proposal for a practical mechanism based on computational technology for the analysis of emotions using predictive models in controllable interactions. The results showed that the use of components to collect physiological data and obtaining the results of analyzes of the patient's emotional state provided by cloud, machine intelligence and wearable devices can significantly improve the quality of experiences and services for users [21] [22]. A perfect emotion recognition system [23] would need a huge number of sensors and would still evaluate data inaccurately. It is due to the complexity of expressing these emotions, at the same time people themselves are unique in expression, gesticulation and facial expressions. The research used audio and video recordings as experimental materials to collect ECG electrocardiogram signals, pulse signals, skin temperature, and skin conductivity signals for emotion recognition research, and the results showed that the rate of emotion recognition decreased significantly with increasing emotion types [24]. GSR signals, heart rate and temperature were used to recognize emotional states [25].

2.1 Emotional States and Facial Recognition

The study of human emotions and their proper determination has been a research area in psychology since the time of Charles Darwin. However, from the perspective of computer science, it is a relatively new area of inquiry that has been

jointly developed since about the 1960s. The merging of computer science and psychology in the context of determining emotional states is primarily related to the design of the first algorithm that provided face recognition [26]. However, the first functional fully automatic system is considered to be the one made by Kanade in 1973 [27].

In the context of linking the research fields of psychology and computer science, over the following decades, a number of different studies have confirmed the link between evoked emotional states and their characteristic expressions in the human face [28-33]. From the perspective of psychology, a number of different models have been defined that allow us to classify emotional states [34] [35], but two in particular have been most prominent and are currently the most dominant: Ekman's classification [36] and the Russell Circumplex model [37].

Ekman's classification is a model that is mainly applied in the context of direct observation of an individual's face (e.g., using a webcam). In the field of computer vision research, different methods are used in the context of Ekman classification for different phases of the recognition process. In particular, the most common method for the detection phase is the use of the Viola-Jones algorithm [38-41].

However, classifying the emotional state only from the face of the observed individual has several shortcomings. Ekman's model is very strict; it does not consider the so-called dynamic multimodal behavioral patterns in the individual under study. On the contrary, Russell's model assumes that, under certain conditions, there may be overlapping of some features that could clearly classify a given type of emotion (e.g., happiness and surprise, fear and sadness...). Therefore, several authors state that in order to be able to classify an emotional state unambiguously, it is necessary to consider other factors as well. Such factors are, for example, changes in physiological processes [42] [43].

2.2 Emotional States and Physiological Functions

Human emotions can be identified by facial expression, speech, behavior or physiological signals. However, the first three methods of recognizing emotions are subjective. For example, study subjects may intentionally conceal their true feelings, which may be inconsistent with their performance. In contrast, recognizing emotions using physiological functions is more reliable and objective.

Wearable sensors and various modules along with microcontrollers and microcomputers can be used to collect physiological features that we can use for the classification of emotional states. Collected signals can be:

- Galvanic skin resistance (Galvanic Skin Resistance - GSR)
- Electrocardiography (EKG)
- Heart rate (Heart Rate - HR)

- Electromyography (EMG)
- Body temperature

Galvanic Skin Resistance

There are specific sweat glands that cause a change in skin conductance and lead to GSR. These sweat glands, located in the palms and soles, respond to psychological stimulation rather than changes in body temperature [44] between GSR and arousal is a linear correlation [45] and reflects emotional reactions as well as cognitive activity [46].

Electrocardiograms (ECG)

They measure the electrical activity of the heart. Heart rate can be calculated from ECG [47] and it reflects emotional activity and is used to distinguish emotions (positive and negative).

Body Temperature

Normal body temperature (normothermia, euthermia) is a typical temperature range found in humans. The normal human body temperature range is usually listed between 36.5 and 37°C (97.7 – 98.6°F). Human body temperature varies. It depends on gender, age, level of physical activity, state of health, in which part of the body the measurement is performed, state of consciousness and emotions. Body temperature is maintained within a normal range by thermoregulation, in which temperature regulation is initiated by the central nervous system [48].

3 Materials and Methods

The aim of the article is to design and create a system for identifying and classifying the emotional state of the user using available IoT devices and to create a system for monitoring basic vital functions while maintaining non-invasiveness. Our goal is to create a system that can measure and process human physiological signals and use them to display results in the user interface. The system will also be able to determine from the acquired image from the connected camera focused on the user's face, what emotion is the user feeling based on an API cloud solution, in which it is not necessary for the microcomputer to perform complex calculations in neural networks.

Recent studies have shown that physiological signals contribute to the recognition of emotions. In an article by Wiem and Lachari [49], the authors focus on the classification of affective states into two defined classes in the arousal / valence model using peripheral physiological signals. To this end, they examined the multimodal MAHNOB-HCI database, which contains the body reactions of 24 participants to 20 affective videos. After pre-processing the data and extracting the

functions, the emotions were classified using the Support Vector Machine (SVM) technique. The classification level was implemented on Raspberry Pi III model B using Python.

In the proposed approach, Wiem and Lachiri [49] used the recent Raspberry Pi III model. In addition, it allows machines to identify and recognize emotional states of affective interaction with humans. In addition, various ports, Bluetooth and Wi-Fi modules make it easy to interact with vulnerable people and children with autism who have physiologically wearable sensors.

They used the latest multimodal MAHNOB-HCI database for evaluation, which is freely available to researchers. After a preprocess phase followed by element extraction, they implemented a classification step on a Raspberry Pi III model B (ARMv8-A, 1 GB SDRAM). They divided emotion into two defined classes in the arousal and valence dimension, which are most commonly used in related works. Two classes are considered, which are "high" and "low" in arousal, "negative" and "positive" in valence.

3.1 Recognition of Human Emotions Based on Facial Images

The importance of facial expressions in determining a person's emotions cannot be overstated. It was discovered that just a little amount of research has gone towards recognizing emotions in real time using photos. Suchitra, Suja, and Tripathi offer a method for identifying emotions in real time from a face in a paper. They employ three phases to detect a face in the suggested technique [50]:

- Haar cascade
- Extraction of elements using the active shape model (ASM)
- The Adaboost classifier, to classify five emotions (anger, disgust, happiness, neutrality and surprise).

In a social services context where emotion recognition is important, the Raspberry Pi II is mounted to a mobile robot that can dynamically recognize emotions in real time.

A camera captures the real-time input image, which is then supplied as input to the emotion recognition software. The Raspberry Pi II runs emotion recognition software, which generates a list of categorized emotions as an output. On the monitor, the detected emotion is presented (Figure 1). The proposed approach is very valuable for society in a variety of applications where emotion recognition is important.

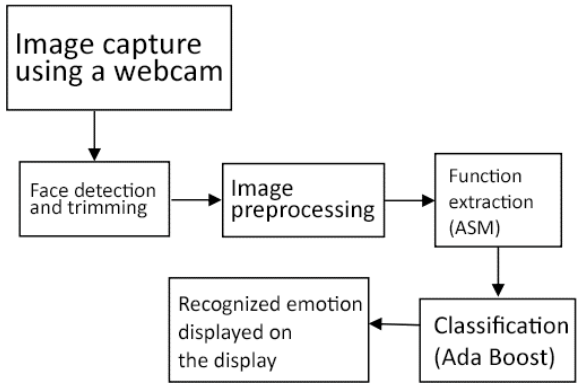

Figure 1
Illustrated wiring diagram (own figure)

3.2 Specification of the System

The measuring device consists of a Raspberry Pi microcomputer, an Arduino Uno microcontroller a MLX90640 thermal camera, a NoIR camera V2, a GSR sensor and Fitbit Sense fitness tracker. The thermal camera and the NoIR camera are connected to the Raspberry Pi, while the GSR sensor is connected to the Arduino Uno. The architecture of the proposed system can be seen in the figure (Figure 2).

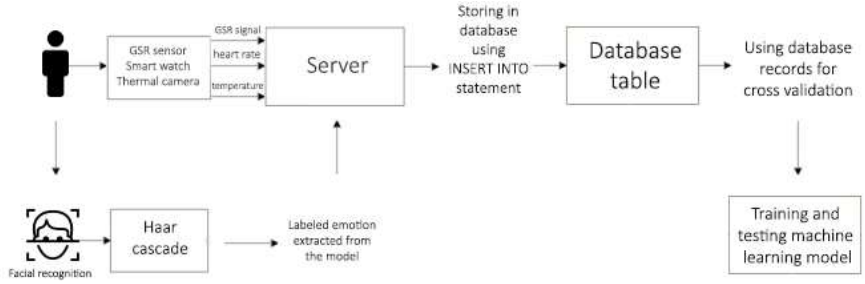

Figure 2
Proposed system architecture of the created system (own figure)

3.3 Classifying Human Emotions

Recognizing emotions by using facial recognition features can be done by using A. Balaji's [51] library. To recognize basic emotions, the program also adopts Ekman's [52] classification commonly known as "The Big Six." Happiness, sadness, fear, surprise, anger, and disgust were among the emotions, and they are still the most widely acknowledged contenders for basic emotions among emotion

theorists [53]. In the event that the model is unable to detect any of the six basic emotional states, a seventh emotional state – a neutral state – is added to the classification. In order to use the model, it requires the following dependencies to be installed on the Raspberry Pi:

- Python version 3 (we used Python 3.6)
- OpenCV (Computer Vision)
- Tensorflow

35887 images of faces from the Facial Expression Recognition 2013 (FER-2013) dataset were used to train the machine learning model [54]. This dataset contains 48x48 grayscale photos that have been labeled with the emotion expressed. The figure depicts a random sample (Figure 3).

Figure 3

FER-2013 dataset image samples [55]

The model detects faces in each frame of the camera stream using the haar cascade method. Paul Viola and Michael Jones suggested an effective object recognition approach employing a cascade classifier based on Haar features in their 2001 paper "Rapid Object Detection with a Boosted Cascade of Simple Features" [56]. A cascade function is trained from several photos in this method, which is based on machine learning (positive and negative). As seen in the Figure 4, the classified emotion is overlayed on the camera stream.

Figure 4

The overlayed emotion on the camera stream (own figure)

3.4 Created User Interface for the Web Server

To display the measured values, as well as the results and historical records, it was necessary to create a web application that will access the MariaDB database and display data from it in a user-friendly environment. The web server will run online on a hosting as well as the database.

The entire user interface consists of several pages; on which we have added several components to better understand the data. All of the components have their own use. To create the user interface, we have used Laravel, which is a free, open-source Symfony-based PHP web framework that allows developers to create web applications that follow the model–view–controller (MVC) architectural paradigm. We have used DataTables to display the data in the database for the user. DataTables is a jQuery plugin, which offers a large number of configurations to improve the ergonomics of viewing the data, especially when the data is large.

DateTime	Heart Rate
12/18/2021, 19:47:56	64
12/18/2021, 19:47:57	63
12/18/2021, 19:47:58	63
12/18/2021, 19:47:59	63
12/18/2021, 19:48:00	63

Figure 5
The data displayed in DataTables in the user interface (own figure)

The data in our user interface can be seen in the figure (Figure 5). By using the LavaCharts library, we can also visualize the data (Figure 6).

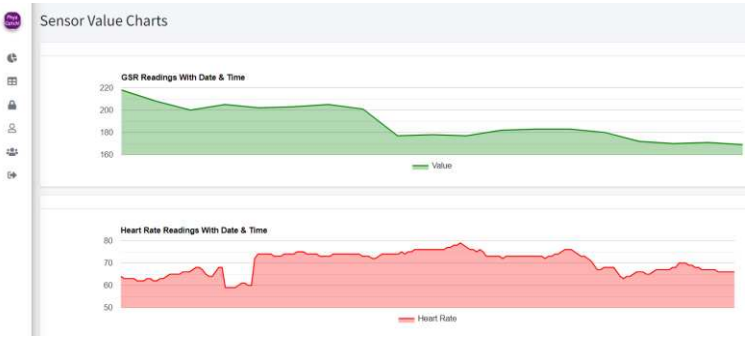

Figure 6
The data visualized in the user interface (own figure)

4 Results and Discussion

With the created system, an experiment can be carried out to gather physiological functions from users in real-time, while the video feed from the camera attached to the Raspberry Pi will be use in a classification algorithm, which will be able to classify basic emotional states based on the facial expressions of the user. The layout of the sensors can be seen in the figure (Figure 7).

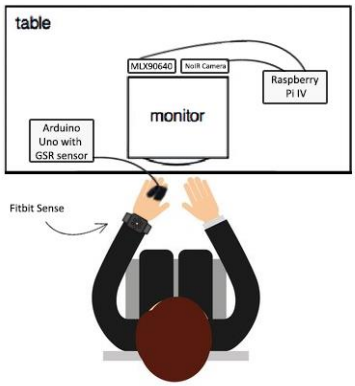

Figure 7
The layout of the sensors during the experiment (own figure)

During the experiment, we can show emotional movie clips to elicit emotions, which is a highly popular and effective method. Schaefer et. al. conducted a research, where they asked fifty film experts to name specific films that can elicit basic emotions. These film clips were then tested on 364 participants and a database of movies was created, which can be used in the context of emotional recognition [57].

In the experiment, the only invasive device is using is the GSR sensor, where the electrodes are attached to the finger of the user, however, in the future, it will be possible to measure glavanic skin response non-invasively as an electrodermal activity (EDA) ring is already being developed [58].

The main idea is to automatically gather physiological functions in real-time, while the sensor data is also sent to a database without any user input. At the same time, a facial recognition software is used to classify the emotions based on the facial expressions of the user. After a dataset is created, the measured physiological functions can be paired with the classified emotions based on the facial recognition software. In some cases, a delay in emotional stimulus must be calculated.

When studying the dataset, this strategy can also assist us in gaining indisciplinary knowledge:

- We can determine how much the measured physiological data reduced or increased for each user when they were experiencing specific emotions.
- We can determine how long the participants were in a neutral state and how long each emotion lasted during the experiment.
- We would not only be able to classify, but also predict emotional states. If we can assess physiological functions in real time and see changes in physiological functions that are typical of a certain emotional state, we may predict that the user will soon be in that emotional state. For example, if the GSR, HR, and body temperature levels gradually increase, the user is likely to experience fear or rage.

The dataset can later be used as an input to a machine learning algorithm, where the measured physiological functions would be the features and the emotion classified by the facial recognition tool will be the target attribute. The machine learning model will then try to predict the emotional state of the users only by using new measurements of physiological functions without using the facial recognition software.

Before using the created solutions on a larger number of participants in the academic environment, an alpha test has been carried out on five participants to test the created device. The physiological functions of User 1 is displayed in the following section. The user was monitored while he was browsing videos on social media.

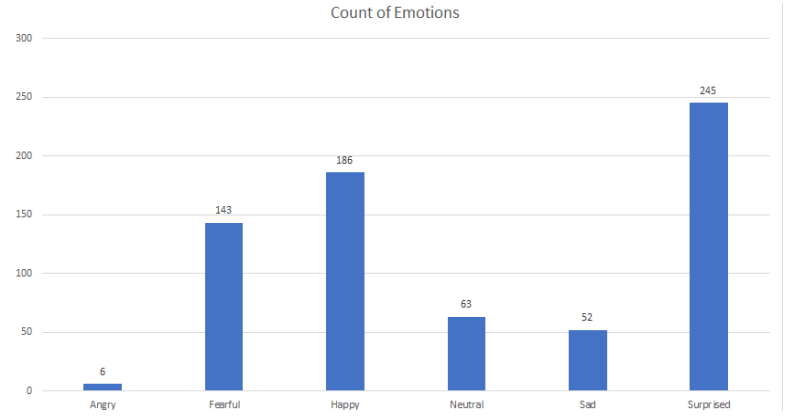

Figure 8
The count of emotions while the user was monitored (own figure)

According to the Figure 8, mostly he was surprised by the videos and the facial recognition software recognized the emotion of anger only six times. The user was not in the emotional state of disgust during the experiment.

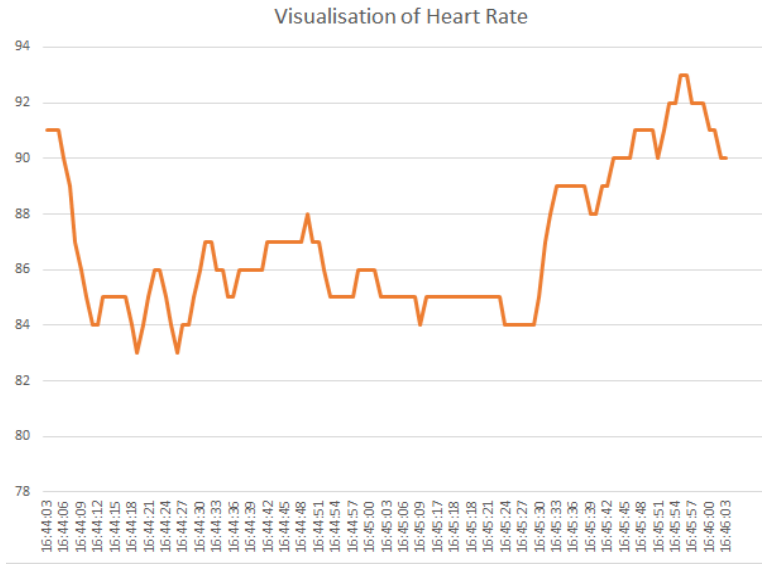

Figure 9
The visualisation of heart rate while the user was monitored (own figure)

The Figure 9 visualises the heart rate of the user during a short period time (2 minutes), while the user was being monitored.

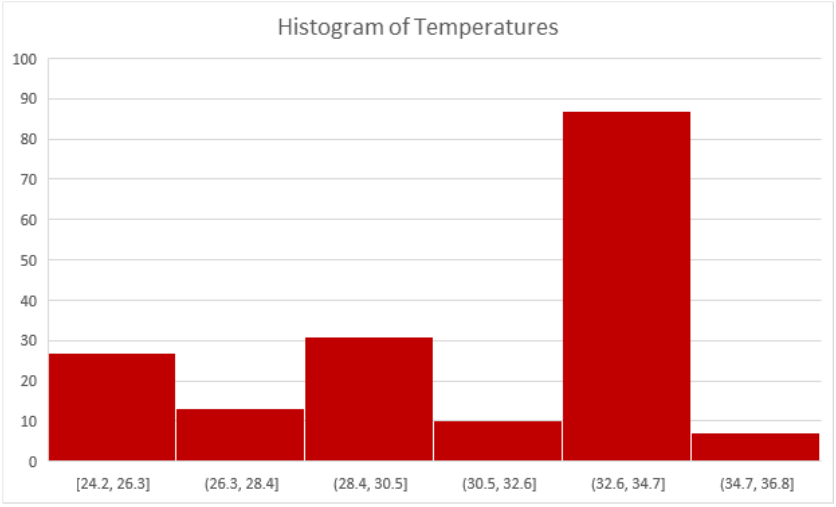

Figure 10
The visualisation of body temperature while the user was monitored (own figure)

Figure 10 shows the distribution of the surface temperature measurements of user 1's face. The temperature of the user's forehead was mostly between the values of

32.6 and 34.7Cº. Extremely low values can be explained by the fact, that the user was moving during the experiment and the center point of the camera wasn´t detecting the user's forehead.

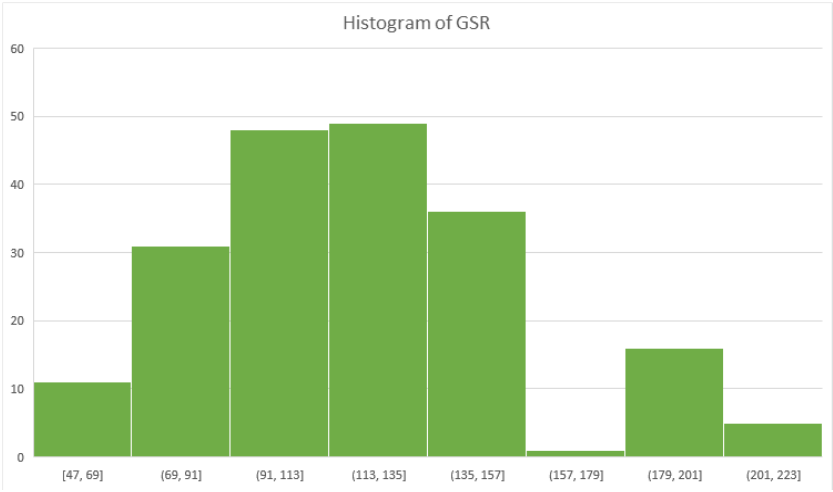

Figure 11
The visualisation of GSR while the user was monitored (own figure)

The user´s skin resistance is visualised in the Figure 11. Most measured values were between 113 and 135 ohms.

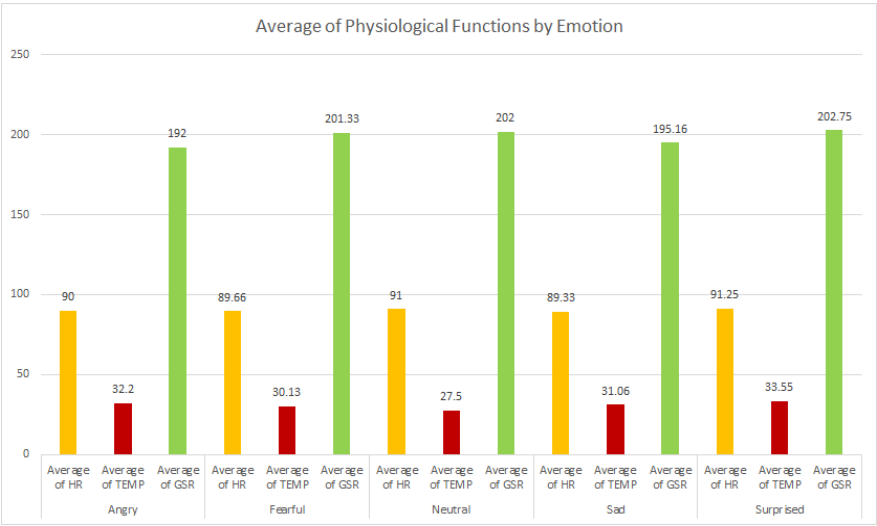

Figure 12
The average of physiological functions by emotions (own figure)

In Figure 12, it can be seen the average measurements of the physiological functions by emotions. Galvanic skin response was the highest while the user was surprised, while it was the lowest when he was angry. Average temperature was the lowest when the user was in neutral state and highest when he was surprised. Average heart rate was the lowest when the user was sad and highest when he was surprised. Results have shown that there are significant differences in the measured values for each emotion.

4.1 Usage of Results in Cognitive Infocommunications

Cognitive infocommunications investigate the relationship between several research areas such as cognitive sciences and infocommunications. Cognitive sciences often process inputs from psychology, computer science and artifical intelligence. An interdisciplinary field spanning computer science, psychology, and cognitive science is also affective computing. In the field of affective computing and human-computer interaction, the goal is to adapt intelligent systems to the emotional states of users.

The aim of the paper was to describe and create a sensory network to measure physiological functions. These physiological functions can be used in the field of machine learning to recognize the emotional state of the user. When the emotional state of the user is recognized, we can create softwares for a wide variety of devices to react to these emotions. For example, in smart homes, the users could define a set of actions by using their smartphones or web interface by using IF-THEN rules. One of the example rules can be that if they are afraid and its over 9 PM, the smart home should activate the alarm system.

4.2 Limitations and Future Directions

In this paper, we have presented the creation of an IoT device, with which we are able to classify the emotional states of a user. For the future there is a high demand for building a scalable, robust and efficient cost effective human emotion recognition systems. But in relation to these systems it is also worth noting that in some cases, it can also be difficult for people to accurately identify a facial expression, and different people may recognize different emotions in the same facial expression. This makes the classification difficult for the emotion recognition systems as well. The effective application of classification solutions requires a lot of training data. These data must contain images taken from different angles, with different backgrounds and the test subjects should be of different genders and nationalities. Improper pose, lighting, and changing contrast can cause problems when creating an image containing a facial expression prepared for image processing. The identification of facial expressions with lower intensity is more difficult and can be achieved with a much larger error. For this

reason, in the future we will use only physiological data to recognize the emotions.

Conclusions

In this article, we described the existing methods and solutions for classifying the emotional state of a person, based on available IoT devices and we created a system that is able to measure the physiological signals of a person and determine the current emotional state of that person.

The physiological functions, such as HR, GSR and temperature highly correlate with emotional reactions. At the same time when these physiological reactions were measured, an emotion recognition software was also used that is able to classify emotions based on the facial features of the user. With these information, we can use supervised machine learning algorithms, where the measured physiological reactions are the features and the label is the emotion classified from the facial recognition tool. This way, the predict method of the selected machine learning algorithm will be able to recognize emotions by only using the measured physiological data without the need to use the facial recognition tool.

The device we designed can monitor a person's physiological signals, as well as evaluate their condition. The measured data is stored on a server in a MariaDB database. This device is simple to use, affordable and does not require a special environment to function properly.

References

[1] C. Xiefeng, Y. Wang, S. Dai, P. Zhao, and Q. Liu, "Heart sound signals can be used for emotion recognition," *Sci. Reports 2019 91*, Vol. 9, No. 1, pp. 1-11, Apr. 2019, doi: 10.1038/s41598-019-42826-2

[2] A. Benedek, G. Molnar, Z. Szuts, and Ieee, "Practices of Crowdsourcing in relation to Big Data Analysis and Education Methods," in *Ieee 13th International Symposium on Intelligent Systems and Informatics*, New York: Ieee, 2015, pp. 167-172

[3] O. Vermesan, Friess, Peter, "Internet of things : converging technologies for smart environments and integrated ecosystems." 2013 [Online] Available: http://site.ebrary.com/id/10852704

[4] K. Nagy, G. Molnár, B. Szenkovits, J. Horvath-Czinger, and S. Zoltán, *Gamification and microcontent orientated methodological solutions based on bring-your-own device logic in higher education*. 2018

[5] P. Sethi and S. R. Sarangi, "Internet of Things: Architectures, Protocols, and Applications," *J. Electr. Comput. Eng.*, Vol. 2017, pp. 9324035:1-9324035:25, 2017

[6] A. Dzedzickis, A. Kaklauskas, and V. Bucinskas, "Human Emotion Recognition: Review of Sensors and Methods," *Sensors*, Vol. 20, No. 3.

2020, doi: 10.3390/s20030592

[7] S. Madakam, V. Lake, V. Lake, V. %J J. of C. Lake, and Communications, "Internet of Things (IoT): A literature review," Vol. 3, No. 05, p. 164, 2015

[8] G. Perrone, M. Vecchio, J. Del Ser, F. Antonelli, and V. Kapoor, "The Internet of Things: a Survey and Outlook." 2019

[9] O. Bello, S. Zeadally, and M. Badra, "Network layer inter-operation of Device-to-Device communication technologies in Internet of Things (IoT)," *Ad Hoc Networks*, Vol. 57, pp. 52-62, 2017, doi: https://doi.org/10.1016/j.adhoc.2016.06.010

[10] A. Aryal, F. Anselmo, and B. Becerik-Gerber, "Smart IoT Desk for Personalizing Indoor Environmental Conditions," 2018, doi: 10.1145/3277593.3277614

[11] J. Kim, S. Kwon, S. Seo, and K. Park, "Highly wearable galvanic skin response sensor using flexible and conductive polymer foam," in *2014 36th Annual International Conference of the IEEE Engineering in Medicine and Biology Society*, 2014, pp. 6631-6634, doi: 10.1109/EMBC.2014.6945148

[12] K. Zhang and W. Ling, "Health Monitoring of Human Multiple Physiological Parameters Based on Wireless Remote Medical System," *IEEE Access*, Vol. 8, pp. 71146-71159, 2020, doi: 10.1109/ACCESS.2020.2987058

[13] A. Silverio, A. Silverio, and A. Remot, "Low-Cost Elderly Healthcare Monitoring System," *J. Phys. Conf. Ser.*, Vol. 1529, p. 32061, 2020, doi: 10.1088/1742-6596/1529/3/032061

[14] M. Al-khafajiy *et al.*, "Remote health monitoring of elderly through wearable sensors," *Multimed. Tools Appl.*, Vol. 78, No. 17, pp. 24681-24706, 2019, doi: 10.1007/s11042-018-7134-7

[15] A. Moscaritolo, "The Best Smart Home Devices for 2021," 2021. https://www.pcmag.com/picks/the-best-smart-home-devices (accessed Jan. 20, 2022)

[16] A. S. Gillis, "DEFINITION What is internet of things (IoT)?," *2021*. https://internetofthingsagenda.techtarget.com/definition/Internet-of-Things-IoT (accessed Jan. 20, 2022)

[17] A. Coutts, T. Kempton, and S. Crowcroft, "Coutts, A. J., Crowcroft, S., & Kempton, T. (2018). Developing athlete monitoring systems: Theoretical basis and practical applications. In M. Kellmann & J. Beckmann (Eds.), Sport, Recovery and Performance: Interdisciplinary Insights (pp. 19-32) Abingdon," 2018, pp. 19-32

[18] A. G. R. Whitehouse and J. S. Haldane, "The dissolved constituents of

human sweat," *Proc. R. Soc. London. Ser. B - Biol. Sci.*, Vol. 117, No. 803, pp. 139-154, Mar. 1935, doi: 10.1098/rspb.1935.0020

[19] J. Nishida, K. Takahashi, and K. Suzuki, "A Wearable Stimulation Device for Sharing and Augmenting Kinesthetic Feedback," in *Proceedings of the 6th Augmented Human International Conference*, 2015, pp. 211-212, doi: 10.1145/2735711.2735775

[20] S. J. Qin, "Process data analytics in the era of big data," *AIChE J.*, Vol. 60, No. 9, pp. 3092-3100, Sep. 2014, doi: https://doi.org/10.1002/aic.14523

[21] G. Molnár, S. Zoltán, and K. Biró, "Use of Augmented Reality in Learning," *Acta Polytech. Hungarica*, Vol. 15, pp. 209-222, Nov. 2018, doi: 10.12700/APH.15.5.2018.5.12

[22] M. Chen, Y. Ma, Y. Li, D. Wu, Y. Zhang, and C.-H. Youn, "Wearable 2.0: Enabling Human-Cloud Integration in Next Generation Healthcare Systems," *IEEE Commun. Mag.*, Vol. 55, No. 1, pp. 54-61, 2017, doi: 10.1109/MCOM.2017.1600410CM

[23] V. Skorpil and J. Stastny, "Comparison of learning algorithms," in *24th Biennial Symposium on Communications, BSC 2008*, 2008, pp. 231-234, doi: 10.1109/BSC.2008.4563245

[24] J. Kim and E. André, "Emotion recognition based on physiological changes in music listening," *IEEE Trans. Pattern Anal. Mach. Intell.*, Vol. 30, No. 12, pp. 2067-2083, 2008, doi: 10.1109/TPAMI.2008.26

[25] C. L. Lisetti and F. Nasoz, "Using Noninvasive Wearable Computers to Recognize Human Emotions from Physiological Signals," *EURASIP J. Adv. Signal Process.*, Vol. 2004, No. 11, p. 929414, 2004, doi: 10.1155/S1110865704406192

[26] W. W. Bledsoe, "Some Results on Multicategory Pattern Recognition," *J. ACM*, Vol. 13, No. 2, pp. 304-316, Apr. 1966, doi: 10.1145/321328.321340

[27] T. Sakai, T. Kanade, M. Nagao, and Y. Ohta, "Picture processing system using a computer complex," *Comput. Graph. Image Process.*, Vol. 2, No. 3, pp. 207-215, 1973, doi: https://doi.org/10.1016/0146-664X(73)90002-6

[28] P. Ekman, E. R. Sorenson, and W. V Friesen, "Pan-Cultural Elements in Facial Displays of Emotion," *Science (80-.).*, Vol. 164, No. 3875, pp. 86 LP – 88, Apr. 1969, doi: 10.1126/science.164.3875.86

[29] D. Matsumoto *et al.*, "Mapping expressive differences around the world: The relationship between emotional display rules and individualism versus collectivism," *J. Cross. Cult. Psychol.*, Vol. 39, No. 1, pp. 55-74, 2008

[30] E. Røysamb, R. B. Nes, N. O. Czajkowski, and O. Vassend, "Genetics, personality and wellbeing. A twin study of traits, facets and life

satisfaction.," *Sci. Rep.*, Vol. 8, No. 1, p. 12298, Aug. 2018, doi: 10.1038/s41598-018-29881-x

[31] G. Songa, H. Slabbinck, and I. Vermeir, "How Do Implicit/Explicit Attitudes and Emotional Reactions to Sustainable Logo Relate? A Neurophysiological Study," *Food Qual. Prefer.*, Vol. 71, 2018, doi: 10.1016/j.foodqual.2018.04.008

[32] M. Magdin, Ľ. Benko, and S. Koprda, "A Case Study of Facial Emotion Classification Using Affdex," *Sensors*, Vol. 19, p. 2140, May 2019, doi: 10.3390/s19092140

[33] J. Francisti, Z. Balogh, J. Reichel, M. Magdin, Š. Koprda, and G. Molnár, "Application Experiences Using IoT Devices in Education," *Appl. Sci.*, Vol. 10, No. 20, pp. 1-14, 2020, doi: 10.3390/app10207286

[34] H. Lövheim, "A new three-dimensional model for emotions and monoamine neurotransmitters.," *Med. Hypotheses*, Vol. 78, No. 2, pp. 341-348, Feb. 2012, doi: 10.1016/j.mehy.2011.11.016

[35] B. Weiner, "A cognitive (attribution)-emotion-action model of motivated behavior: An analysis of judgments of help-giving.," *J. Pers. Soc. Psychol.*, Vol. 39, No. 2, pp. 186-200, 1980, doi: 10.1037/0022-3514.39.2.186

[36] P. Ekman, "Facial Expressions of Emotion: New Findings, New Questions," *Psychol. Sci.*, Vol. 3, No. 1, pp. 34-38, Jan. 1992, doi: 10.1111/j.1467-9280.1992.tb00253.x

[37] J. A. Russell, "A circumplex model of affect.," *J. Pers. Soc. Psychol.*, Vol. 39, No. 6, pp. 1161-1178, 1980, doi: 10.1037/h0077714

[38] P. Viola and M. J. Jones, "Robust Real-Time Face Detection," *Int. J. Comput. Vis.*, Vol. 57, No. 2, pp. 137-154, 2004, doi: 10.1023/B:VISI.0000013087.49260.fb

[39] M. Berkane, B. Kenza, and H. Belhadef, "Emotion Recognition Approach Using Multilayer Perceptron Network and Motion Estimation," *Int. J. Synth. Emot.*, Vol. 10, pp. 38-53, Jan. 2019, doi: 10.4018/IJSE.2019010102

[40] M. Colak and A. Varol, *Eyematch: An Eye Localization Method For Frontal Face Images*. 2019

[41] M. Besnassi, N. Neggaz, and A. Benyettou, "Face detection based on evolutionary Haar filter," *Pattern Anal. Appl.*, Vol. 23, Feb. 2020, doi: 10.1007/s10044-019-00784-5

[42] C. Oveis, E. J. Horberg, and D. Keltner, "Compassion, pride, and social intuitions of self-other similarity.," *Journal of Personality and Social Psychology*, Vol. 98, No. 4. American Psychological Association, Oveis, Christopher: Harvard University, Department of Psychology, William

James Hall 1418, 33 Kirkland Street, Cambridge, MA, US, 02138, oveis@wjh.harvard.edu, pp. 618-630, 2010, doi: 10.1037/a0017628

[43] J. L. Goetz, D. Keltner, and E. Simon-Thomas, "Compassion: An evolutionary analysis and empirical review.," *Psychological Bulletin*, Vol. 136, No. 3. American Psychological Association, Goetz, Jennifer L.: Department of Psychology, Middlebury College, McCardell Bicentennial Hall, Middlebury, VT, US, 05753, jgoetz@middlebury.edu, pp. 351-374, 2010, doi: 10.1037/a0018807

[44] R. M. Stern, W. J. Ray, and K. S. Quigley, *Psychophysiological Recording*. 2012

[45] P. J. Lang, M. K. Greenwald, M. M. Bradley, and A. O. Hamm, "Looking at pictures: affective, facial, visceral, and behavioral reactions.," *Psychophysiology*, Vol. 30, No. 3, pp. 261-273, May 1993, doi: 10.1111/j.1469-8986.1993.tb03352.x

[46] W. Boucsein, *Electrodermal activity, 2nd ed.* New York, NY, US: Springer Science + Business Media, 2012

[47] R. L. Mandryk and M. S. Atkins, "A fuzzy physiological approach for continuously modeling emotion during interaction with play technologies," *Int. J. Hum. Comput. Stud.*, Vol. 65, No. 4, pp. 329-347, 2007, doi: https://doi.org/10.1016/j.ijhcs.2006.11.011

[48] J. S. Hutchison *et al.*, "Hypothermia Therapy after Traumatic Brain Injury in Children," *N. Engl. J. Med.*, Vol. 358, No. 23, pp. 2447-2456, Jun. 2008, doi: 10.1056/NEJMoa0706930

[49] M. Ben Henia Wiem and Z. Lachiri, "Emotion recognition system based on physiological signals with Raspberry Pi III implementation," in *2017 3rd International Conference on Frontiers of Signal Processing (ICFSP)*, 2017, pp. 20-24, doi: 10.1109/ICFSP.2017.8097053

[50] Suchitra, S. P., and S. Tripathi, "Real-time emotion recognition from facial images using Raspberry Pi II," in *2016 3rd International Conference on Signal Processing and Integrated Networks (SPIN)*, 2016, pp. 666-670, doi: 10.1109/SPIN.2016.7566780

[51] A. Balaji, "Emotion detection," *GitHub repository*, 2018. https://github.com/atulapra/Emotion-detection (accessed Jun. 15, 2021)

[52] P. Ekman, "Basic emotions.," in *Handbook of cognition and emotion.*, New York, NY, US: John Wiley & Sons Ltd, 1999, pp. 45-60

[53] M. Piórkowska and M. Wrobel, "Basic Emotions," 2017

[54] I. J. Goodfellow *et al.*, "Challenges in representation learning: a report on three machine learning contests.," *Neural Netw.*, Vol. 64, pp. 59-63, Apr.

2015, doi: 10.1016/j.neunet.2014.09.005

[55] P.-L. Carrier and A. Courville, "The Facial Expression Recognition 2013 (FER-2013) Dataset," 2013. https://datarepository.wolframcloud.com/resources/FER-2013 (accessed Jun. 15, 2021)

[56] P. Viola and M. Jones, "Rapid object detection using a boosted cascade of simple features," in *Proceedings of the 2001 IEEE Computer Society Conference on Computer Vision and Pattern Recognition. CVPR 2001*, 2001, Vol. 1, pp. I–I, doi: 10.1109/CVPR.2001.990517

[57] A. Schaefer, F. Nils, X. Sanchez, and P. Philippot, "Assessing the effectiveness of a large database of emotion-eliciting films: A new tool for emotion researchers," *Cogn. Emot.*, Vol. 24, No. 7, pp. 1153-1172, Nov. 2010, doi: 10.1080/02699930903274322

[58] E. Vavrinsky, V. Stopjakova, M. Kopani, and H. Kosnacova, "The Concept of Advanced Multi-Sensor Monitoring of Human Stress," *Sensors*, Vol. 21, No. 10. 2021, doi: 10.3390/s21103499

Micro-Level Road Network Evaluation using Fuzzy Signature Rule Bases

Gergely Cs. Mikulai[1], László T. Kóczy[2, 3]

[1] Széchenyi István University, Doctoral School of Regional and Business Administration Sciences, Egyetem tér 1, 9026 Győr, Hungary, gergely.mikulai@ga.sze.hu

[2] Széchenyi István University, Department of Information Technology, Egyetem tér 1, 9026 Győr, Hungary, koczy@sze.hu

[3] Budapest University of Technology and Economics, Department of Telecommunication and Media Informatics, Műegyetem rkp. 3, 1111 Budapest, Hungary, koczy@tmit.bme.hu

Abstract: Nowadays, due to fast-increasing economic development, the current available road infrastructure is more and more crowded, which creates frustration for the people using them. In the current research, a model is proposed for authorities, companies and individuals, to choose the best available route(s) and road sections(s) for improvement measures, optimal delivery or commuting. In the proposed model, a fuzzy signature rule base, is introduced for commuters, which distinguishes all the relevant factors during commuting. The actual decision process is based on various input data, such as peoples' habits, assumptions and preferences and various other factors.

Keywords: fuzzy signature rule bases; personal preferences; route selection

1 Introduction

Traveling is an inevitable factor in modern societies. In order to decrease its negative effects, traveling itself and its side effects should be modelled properly. In this paper, such a model is proposed, which is built on the three levels, which were formulated first by Bjønskov and Svendsen [1]. These three levels are the following:

- Macro-level – governmental level
- Meso-level – group level
- Micro-level – personal level

This classification into three levels describes the entire problem area in a systematic way. A macro-level evaluation model was already introduced in [2]. That model

proposed a systematic overlook for governments, about which road sections should be renovated, expanded, or which one requires any special attention.

The meso-level may properly describe the decision-making process of a group of people, for example truck-drivers, or of individuals, such as commuters.

The currently evaluated micro-level describes the decision of individuals, how the choose their actual route in a concrete traffic situation. Nowadays, there are more and more tools available for the support of this decision, such as, mobile applications, or GPS aided devices. But these often do not offer the best solution, and there are always other factors to be taken in consideration, which may help the traveler choose the best option for a given route.

Behind these route selection algorithms, in many cases, there are learned habits, physical limitations, or simply assumptions, suggesting that one way is faster than the other.

The proposed model analyses these factors and helps categorize them and build up a fuzzy signature rule base in order to get a coherent result. In order to give a usable tool for commuters which route and which travel means should they choose. After creating the signature rule base, a decision with fuzzy elements is made, based on the individuals' specific inputs, in order to get them a personalized choice [3].

The currently proposed fuzzy signature rule base consists of multiple factors. One major group is formed by the objective factors, for example:

- The weather
- The congestion of the roads
- The available transportation options, etc.

The other major group contains the subjective factors, among others:

- Cognitive biases towards routes, or vehicles
- Personal preferences
- Travelling habits and beliefs, etc.

To sum up the model, it combines many currently difficultly measurable factors, makes them appreciable and by the fuzzy signature rule base it proposes an objective resolution for every route and selection, by evaluating objective and subjective factors as well.

2 Fuzzy Signature Rule Base Background

2.1 Problem Formation

Selecting the best potential route for a given trip is not an easy task. This selection is based on multiple inputs, which are difficult to evaluate manually within a short time.

The currently evaluated problem area is not describable by a linear, deterministic formula. In many cases, even complex correlation could be described by simple formulas, which help one to understand how the world works, for example the function of the gravity, which describes the uprising force by one single function.

However, the question area could be described with a non-deterministic, non-linear formula properly, since there are many flexible describing factors, such as the traffic, or the weather component. These factors could change extremely frequently.

First, it is important to identify the complex problem to be solved. To this end, several theoretical and empirical models have been created and validated up to now. Some of the models are based on technical approaches, while others are sociology-based. However, the realistic and multifaceted treatment of the issue needs a combined multidisciplinary approach, using the resources of both knowledge areas The substantial understanding of the phenomenon requires a wide scope and balanced work, taking all possible technical and societal aspects into account.

A clear and reliable model is needed, which can handle the uncertainties of several nonlinear and stochastic variables. Furthermore, it should reflect the foreseen individual preferences of the people involved.

2.2 Methodology

The phenomenon under our analysis is not deterministic: it is rather stochastic, rather complex, contains continuous subjective decisions. Therefore, there is no exact formula or model to find an explicit solution.

A fuzzy signature rule-based framework is proposed that can help to describe and analyze the relationship between the several factors. The proposed model, which has already been introduced in the article of our earlier article about Macro level road network evaluation [2], which proved to be suitable to produce clear results for highly complex and chaotic systems.

The method contains the following steps. First step, the problems and questions are listed and ordered in relevant sub-groups. Second step, the groups are weighted within the groups, that way the relative importance of the components within the subgroups is determined ($\Sigma = 1$). Third step, inside the groups, output scenarios are created, using the available data bases, evaluated by fuzzy methods. These scenarios simplify the possible outcomes and make the multiple inputs manageable. Fourth

step, the answers are aggregated with help of fuzzy aggregations and the thus cumulated information is "forwarded" one level higher, until the root, where a single fuzzy membership degree will express the overall evaluation. [4] The aggregations are continued level by level until the final recommendation forming the base of a decision is obtained. It is not necessary that the aggregations within the local roots of the subgroups are identical, not even in the type of operation, so, e.g. while a weighted average type aggregation may be rather common in some nodes, other mean type operations, max and min, and more complex ones, like t-norms or t-conorms may be applicable. The selection of these aggregations should be carefully done on the base of expert domain knowledge, or model fitting, using a significant number of known results for real cases [5].

Mathematically the fuzzy signatures are built up with logical relations. This means, there is a clearly described connection between attributes. It is mostly a below and above ordinance. From the below level originates the above level. This helps the model to systematically describe the issue and prepare for evaluation [6].

In order, to evaluate the fuzzy signature, an aggregation is needed. For this aggregation, each root receives an aggregation type. There are multiple types of these aggregation, for example, the arithmetic mean, the geometric mean, the harmonic mean, weighted average, or the minimum and maximum. In the current article mostly the weighted average is used, while in some cases the maximum type of aggregation. It is important to highlight, that the weighted average is a non-commutative aggregation operator [7].

Optimizing a route crossing several points (stops, shops, cities, etc.) is a very classical problem, who's most well-known prototype is the NP-complete travelling salesmen problem (TSP), which has a very wide literature where the following key publications may be mentioned [8] and [9]. Some recent alternative metaheuristic approaches may be found in [10] and [11]. A multitude of extended or modified TSP problems also has a very rich literature, however, here, we focused in the individual choice including subjective elements, such as preferences of the traveler and thus we omit a deeper analysis of the related route optimization literature.

3 Proposed Model

As mentioned above, based on the literature review, a three-level structure (macro, meso and micro levels) has been introduced. The highest level is the macro level, where the model focuses on the governmental level of road network evaluation, for example, about which routes or sections of a given region should be renovated, or extended. On the medium level, which is the "meso-level", the model focuses on the route selection preferences of a specific group, for example, the route selection preferences of international truck drivers, or families going on holiday. The lowest level, which is evaluated in the current article is the micro level, where the model

aims to evaluate the personal triggers of a specific route selection, why does a person select a given path between point A and B. Thus, the problem to be solved is to find a proper model and matching algorithm for describing the decision process by an individual traveler, including preferences and subjective components, where alternative routes and alternative means of traveling are considered. We are looking for a novel approach, where subjectivity and non-deterministic factors are modelled by non-probabilistic uncertainty, namely, a fuzzy approach. The multitude and partial interdependence of the components influencing the final decision are taken into consideration by a hierarchical, structured descriptor as explained in the next.

The model is using fuzzy aggregation by weighted factors, which makes it able, to combine 'hard' data from databases with 'soft' data, which are collected and estimated – or simply meant – by the participating people, reflecting their personal priorities and subjective experience.

The model proposes the structure described in Figure 1.

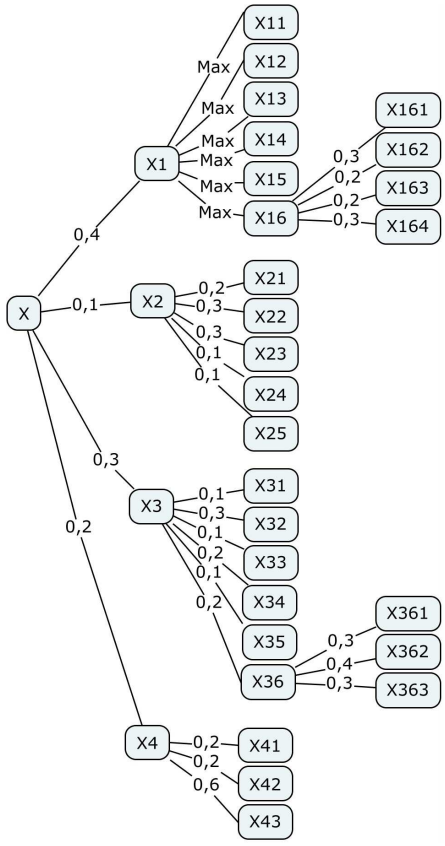

Figure 1
Micro level route selection graph for daily commute

The model consists of 26 + **4 variables**, where 24 variables are independent, forming 7 subgroups of membership degrees (recommendations), which together form a coherent model. These are the following:

X – Route selection (Which route should be used for daily commuting?) – In the current paper, the answer for an everyday commuter's route selection is evaluated, namely, which route should be taken, when a commuter has multiple options.

X1 – Infrastructure – The first big aggregation group is the evaluation of the infrastructural aspect of the route selection process. It describes the mostly objective aspects of the route, namely, what are the advantages, or disadvantages of the options [12].

X11 – Available transport options – It is important to see, what are the choices for the target person (the commuter), in order to evaluate, whether they have a choice, or the routing cannot be modified. The potential transport options could be walking, bicycle, car, local public transport (e.g.: bus, tram, etc.), distance public transport (e.g.: train, distance bus, etc.), taxi, self-driven car, or some other alternatives [13].

X12 – Available route alternatives – In most cases, there are alternatives for most of the commuters, despite the fact, that many people have habits, and tend to always use the same route alternative, and only modify it in case of some extreme circumstances, such as road closedowns, accidents, or other unavoidable barriers [14].

X13 – Accessibility – This variable describes how easily the given route can be accessed. In many cases, certain route options fall out because they are too far away from the person in question, or they are not accessible due to some unusual situation [15].

X14 – Economicality – It describes, how affordable is the given route option, both time- and cost-wise. Frequently it is one of the most important factors, since for many users, time and money are the most limited resources [16].

X15 – Environmental friendliness – Some users consider environmental friendliness as an important factor as well. In this case the user calculates with the ecological impact of their route and they try to minimize it [17].

X16 – Weather dependence – This describes to what extent the given route, especially the transport vehicle is weather dependent. For example, the option of riding a bike to the workplace is more weather dependent, than driving a car to there. This variable is an aggregated variable, which means, that the result of this is built up from the aggregation of X6, X7, X8 and X9 [18].

X161 – Temperature dependence – This variable describes whether the given route section is sensitive for the outside temperature, for example, whether there is any counter-indication of the route when the weather is too hot, or when it is too cold [18].

X162 – Rain dependence – It grades whether traveling the given section is affected by the rain. It could be that choosing a given section would be more dangerous in the sense of higher probability of traffic accidents in the case of e.g. a heavy rain shower [18].

X163 – Sunshine dependence – This attribute describes whether the section has a correlation with the grade of the sunniness of the weather. In some cases, it could be, for example, that the section is unusable by walk, or by bicycle, as the surface of the road is too hot due to the sun, or the tar is molten to some extent. [18].

X164 – Visibility dependence – It often happens, if the weather is foggy, some routes become uncomfortable, or even dangerous. There is a clear correlation between accidents and bad visibility. This could result in a strong tendency of choosing another way [19].

X2 – Social factors – The socio-demographic background of the commuter is clearly an important factor behind their route selection. Family/marital status often describes how many people intend to travel together, or whether there are any prestige aspects, etc. [20].

X21 – Age – The actual age of the commuter could be a significant factor, since often when people as get older, they tend to choose the more comfortable solution. the age could influence the person's flexibility of decisions and adaptability to changing circumstances [21].

X22 – Educational background – In general, the better the person is educated, the better they can evaluate their options and actually find the best route for the actual route. There is a clear negative correlation between education and prejudices, which concludes that better educated people can make better decisions [22].

X23 – Wealth – If a person has more available funds, than they can take more alternatives into account. For example, a user in a better financial situation could choose to buy a car, a motorbike, a bicycle and a public transport pass in the same time [23].

X24 – Preferences (determined by the life stage) – Every person has different transport selection preferences during their different life stages. During the beginning of their life, people (children, school pupils) are carried around. Later, young people tend to choose the best option optimizing the cost, during the time visiting school or college. Having the first job, people often change preferences and choose based on time. Once people have children, safety has a high influence, etc. [16] [24].

X25 – Gender – Men and women often have different views and preferences. Women usually tend to be more understanding and caring (e.g., taking environmental friendliness into consideration during route selection), while men tend to be more practical and more open for extreme solutions (e.g. riding a bike in heavy rain) [25].

X3 – Personal factors – In the end of the day, behind each and every decision, there is an actual person, who makes decisions not only based on raw data. People tend to take very personal, subjective parameters into account as well. In this variable, the most important parameters are collected, in order to have a holistic picture about one's personal motivations [26]. This is definitely the most subjective group of factors which necessitate the use of fuzzy variables in the model.

X31 – Mood – In case of a common daily route, the actual mood of the traveler may influence considerably the taken path. If a route is commonly known for frequent accidents, in some cases, it could influence the mood of the person in a way, that in the end, the commuter would consider other options, despite the fact, e.g., that the questionable route would be very likely the fastest, and/or cheapest [27].

X32 – Habits – As the English proverb states, "People do more from custom than from reason.". Most people are prisoners of their habits, which are difficult to get rid of from one day to another. In this respect, it is important to see, what people tend to do out of habit, as this could give answer for a couple of correlations which could be difficult to understand at first [28]. It is one of the most difficult tasks to transform the consequences of habits into fuzzy membership degrees.

X33 – Friends/family impact – People live in communities, in bigger, and smaller communities. This means that members of the same community have much stronger influence on each other than people outside of these communities do. It is important to have an overview, about the external influencing effects of the surrounding closer communities.

X34 – Time pressure – During the day of an average commuter, there could be bottlenecks in time, e.g., if the person in question has too many programs, close in time but located physically far from each other. If this is the situation, this could result in a rush, which pushes the user towards a faster traveling method [29].

X35 – Comfort – The quality of the commute could get more and more important for the users, as this journey could be a vital determining element of their choice. If the route has a more comfortable alternative, or vehicle, while they are completely, or at least almost equivalent to each other, the user tends to choose the more comfortable option. By psychologists it was observed that even, in case the shape of one of the alternative routes being more symmetric, or geometrically more "harmonic", users would often take that, in order to maximizing the aesthetics of the trip [30].

X36 – Daily program – Depending on the daily program of the commuter, e.g., if it contains evening sport, or leisure activities, it would require different equipment, time-frame, or transportation method. E.g. if there is a meeting with friends, it is quite a compromise, that the commuter person cannot drink alcohol because driving a car, or a bike.

X361 – Locations to visit – Whether the commuter has to go only to their workplace, it is a different scenario, then, if they have to make four or five different

appointments at different locations, the user would plan the route and the vehicle of travel in a completely different way than in the case of one single destination, and without any load to take with.

X362 – (Overall) Distance – This trigger is one of the most trivial factors. In some cases, distance clearly determines the route, or the vehicle. It is important to see in advance, how far the commuter should travel on the given day [31].

X363 – Equipment needed – On the daily commute, there could be an important factor what are the equipment or tools which should be taken for the given day's activity, especially, when a large amount of equipment is needed for these appointments. For example, if there is a training in the afternoon, the training equipment should often be carried around the entire day if the traveler has no more convenient solution.

X4 – Available information – In order to plan a proper route, there is certain information, which could help to decide in advance, whether it is worth to travel in a given direction, or it is better to choose another way of transportation. Many of these data inputs could arrive as live feed (e.g., radio traffic information, or GPS routing advice) in the model.

X41 – Accidents – This variable describes whether there is any information about unusual happening during the planned route. If there is any, that could result in extra journey time, which is better to avoid.

X42 – Close downs – If there are close downs, either of roads, or of metro or train stations, it could significantly increase the time of the given route. Live information about the actual obstacles is crucially important in order to optimize the route for the best outcome [32].

X43 – Traffic – This variable describes how many people, bikes, cars, or any other travelers are observed on the given route, in the given time. This observation is extremely important, since, for example, if there is a huge traffic jam along the route originally selected, the journey could become two or three times longer in total time, or if there are overcrowded trams, trains, or metros, the trip would be a lot less pleasant for the traveler, and could be considerably slower as well. If this is the observed situation, the best is to avoid the critical bottlenecks, as in the result, they would slow down the progress of the traveler.

The overall question for the current model is: Which route should be used for daily commuting? This question should be answered by evaluating the fuzzy signatures, by comparing the resulting degrees represented by the calculated root degrees of the fuzzy signature trees constructed from the above listed variables appearing on the leaves of the tree, with the various fuzzy membership degrees assigned to the more or less objective, or just on the contrary, rather subjective aspects listed, with help of the fuzzy aggregation operators forming also part of the model, which are assigned to the intermediate nodes of the fuzzy signature trees.

It should be remarked that similar problems, where similar structures and interrelationships of uncertain, vague and subjective components emerge, may be modelled in a similar way, thus, when constructing the new model proposed in this paper, the potential solution technique of a family of similar problems is also given. Setting up this model, we claim that it would be a useful framework for a large variety of further research topics with similar structure as well.

If the values for a concrete situation (task to choose a route) are filled in, the frame of the signature describing the current option is given. If all the leaves have been assigned membership degrees or functions (the latter, if building a fuzzy signature set) the values are given for further evaluation by calculation of the lower level values (intermediate nodes) as these are the input data for the next levels. After evaluating the actual values given to every variable, fuzzy aggregations are used, in order to sum up the problem area (e.g., a group of connected variables forming a sub-tree) into one single degree for each group. Selecting the proper aggregation in the model for every sub-tree root is essentially important for the adequate decision making. This way subjective and unexcitable decisions with ambivalent answers containing "on one hand, on the other hand" elements can be avoided. In the simplest way, the aggregations mentioned are often weighted means where the key question is to find the weights which are the most adequate for the elements of the given sub-groups. The integration of the partial results by proper aggregations, using realistic weights helps to transform the essentially uncertain system with multifold obscureness into relatively unambiguous and sound results, which are easy to understand and to communicate [7].

In the current research, we propose the use of the most widely applied fuzzy inference mechanism model described by Mamdani and Assilian. Their approach could be seen in Figure 2 [33].

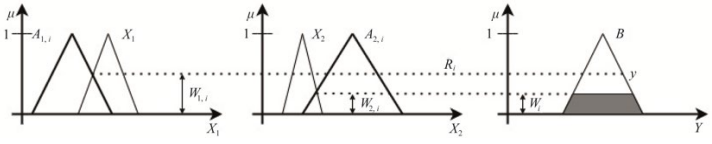

Figure 2
Schematic illustration of the Mamdani fuzzy inference [34]

This method could be used to build up generalized rules and based on these rules, to make consequent responses for the stated question, starting from more or less objective inputs. These generalized rules have the following general form:

$$If\ x_1 = A_{1,i}\ ,\ x_2 = A_{2,i}\ ,\ ...,\ and\ x_n = A_{n,i}\ then\ y = B_i \qquad /1/$$

where xi stand for the earlier mentioned variables, which represent the input to the fuzzy system. In the formula, y represents the output of the fuzzy system. $A_{n,i}$ and B_i are fuzzy sets (antecedents and consequents of the rules) defined by functions $\mu_{An,i}\ (x)$: $X \rightarrow [0,1]$ and $\mu_{Bi}\ (y)$: $Y \rightarrow [0,1]$, respectively [34].

In order to illustrate the way of the evaluation of the concrete problem, that may lead to a decision, a fuzzy signature set rule base will be introduced. In the next paragraphs, fuzzy linguistic values for the variables are proposed with some examples for the shapes of these membership functions representing the linguistic terms. We also present a very simple example, where we show that such a decision making is realistic and can be done with help of the proposed model.

The overall question is the ***X – Route selection***, which is:

Which route should be used for daily commuting (or, for today's trip)?

It is important, that the model is capable of comparing different routes, which means, that the user always needs to put in at least 2, or more route alternatives. Based on this, the one should be chosen, which requires less optimization. The following potential answers are expected after the evaluation:

- The given commuting route needs major optimization
- The given commuting route needs minor optimization
- The given commuting route is (more or less) optimal

In order to get an answer, the question was split into four major sub-questions, which help to organize a structured overlook of the problem. In case of each question, a membership function was proposed to describe and map all of the possible outcome possibilities. For example, in case of the ***X35 – Comfort***, the following membership function was proposed:

$$X35 \in \{Comfortable, Compromise, Uncomfortable\} \qquad /2/$$

In Figure 3 three actual membership function can be seen, which describe the uncertain boundaries between the personal preferences behind the route selection.

Figure 3
X3 (Personal factors) membership function

In Table 1, the potential values of *X*3 and three examples are reported.

Table 1
Linguistic value sets for X3, based on X31-X36

Attribute	**1. example**	**2. example**	**3. example**
*X*31 – Mood	Good	Good	Bad
*X*32 – Habits	Conventional	Ordinary	Innovative
*X*33 – Friends/family impact	Moderate	High	Minimal
*X*34 – Time pressure	High	High	High
*X*35 - Comfort	Compromise	Compromise	Uncomfortable
X36 – Daily program	One	Multiple	Multiple
*X*3 – Personal factor	Preferred	Compromise	Avoidable

A generalized if-then rule base is constructed using the actual values, in order to concretize the resulting values, and thus the final decision.

If X31 is A31, X32 is A32, X33 is A33, X34 is A34, X35 is A35 and X36 is A36 then X3 is D3 /3/

$$X31 \in \{Good, Average, Bad\} \quad /4/$$

$$X32 \in \{Conventional, Ordinary, Innovative\} \quad /5/$$

$$X33 \in \{Minimal, Moderate, High\} \quad /6/$$

$$X34 \in \{Minimal, Moderate, High\} \quad /7/$$

$$X35 \in \{Comfortable, Compromise, Uncomfortable\} \quad /8/$$

$$X36 \in \{One, Some, Multiple\} \quad /9/$$

$$D3 = \{Preferred, Compromise, Avoidable\} \quad /10/$$

Using this proposed structure, an adequate answer can be obtained for the major decision points, for *X*1, *X*2, *X*3 and *X*4, where the potential values are the following:

– for *X1* (Infrastructure)

$$D1 \in \{Good, Fair, Poor\} \quad /11/$$

– for *X2* (Social factors)

$$D2 \in \{Uninfluential, Neutral, Influential\} \quad /12/$$

– for X3 (Personal factors)

$$D3 \in \{Preferred, Compromise, Avoidable\} \quad /13/$$

– for *X4* (Available information)

$$D4 \in \{None, Some, Many\} \quad /14/$$

Based on the above stated decision parameters, an overall answer can be given for the original question (Which route should be used for daily commuting (or, for today's trip?), which could be the following:

$$D = \{Major\ change\ for\ optimization,\ Minor\ change\ for\ optimization,\ already\ optimal\} \quad /15/$$

After mergers and reductions of the various decision points in all dimensions and categories (technical vs. societal), the structure leads to a transparent and clear deduction.

It is important to mention, that the current model does not necessarily propose the exact point of potential optimization, but with multiple iterations, in any case, a far better route may be achieved, based on a comparison.

In fact, the proposed model contains several personal, subjective steps: for example, the selection of the problems, the chosen data sources, the methods to find and interpret the answers and also the weights of the factors. Interestingly, despite the pronounced presence of several subjective elements, the results show strong correlation with the intuitively better route selection. Users could objectively evaluate between two possible routes, including their subjective preferences. In this phase, the result can be compared to the expectations of the stakeholders: project participants, involved experts and decision makers.

In order to have a holistic overview about the membership functions, in Table 2 the exact functions could be found, which describes the potential end values.

Table 2
Membership function descriptions

Attribute	Value set	fX(y) value levels
X161	X161 ∈ {Low, Medium, High}	[1-30]={Low=1} [40-70]={Medium=1} [80-110]={High=1}
X162	X162 ∈ {Low, Medium, High}	[1-30]={Low=1} [40-70]={Medium=1} [80-110]={High=1}
X163	X163 ∈ {Low, Medium, High}	[1-30]={Low=1} [40-70]={Medium=1} [80-110]={High=1}
X164	X164 ∈ {Low, Medium, High}	[1-30]={Low=1} [40-70]={Medium=1} [80-110]={High=1}
X16	X16 ∈ {Low, Medium, High}	[1-33]={Low=1} [34-66]={Medium=1} [67-99]={High=1}
X11	X11 ∈ {Walk, Car, Bicycle, Public transport, Distance transport, other}	[0-1]={Walk=1} [1,01-2]={Car=1} [2,01-3]={Bicycle=1} [3,01-4]={Public transport=1} [4,01-5]={Distance transport=1} [5,01-6]={Other=1}

Attribute	Value set	fX(y) value levels
X12	X12 ∈ {None, Some, Many}	[1-30]={None=1} [40-70]={Some=1} [80-110]={Many=1}
X13	X13 ∈ {Low, Medium, High}	[1-30]={Low=1} [40-70]={Medium=1} [80-110]={High=1}
X14	X14 ∈ {Low, Medium, High}	[1-30]={Low=1} [40-70]={Medium=1} [80-110]={High=1}
X15	X15 ∈ {Not, Fair, Outstanding}	[1-33]={Not=1} [34-66]={Fair=1} [67-99]={Outstanding=1}
X1	X1 ∈ {Poor, Fair, Good}	[1-30]={Poor=1} [40-70]={Fair=1} [80-110]={Good=1}
X21	X21 ∈ {20-, 21-30, 31-40, 41-60, 61+}	[0-20]={20-=1} [21-30]={21-30=1} [31-40]={31-40=1} [41-60]={41-60=1} [61-120]={60+=1}
X22	X22 ∈ {Primary, Secondary, Higher education}	[0-1]={Primary=1} [1,01-2]={Secondary=1} [2,01-3]={Higher education=1}
X23	X23 ∈ {Poor, Average, Rich}	[1-30]={Poor=1} [40-70]={Average=1} [80-110]={Rich=1}
X24	X24 ∈ {Children, Student, Working, With children, Pensioner}	[0-1]={Children=1} [1,01-2]={Student=1} [2,01-3]={Working=1} [3,01-4]={With children=1} [4,01-5]={Pensioner=1}
X25	X22 ∈ {Male, Female}	[0-1]={Male=1} [1,01-2]={Female=1}
X2	X2 ∈ {Uninfluential, Neutral, Influential}	[0-1]={Uninfluential=1} [1,01-2]={Neutral =1} [2,01-3]={Influential =1}
X361	X361 ∈ {One, Some, Multiple}	[0-1]={One=1} [1,01-3]={Some =1} [3,01-20]={Multiple =1}
X362	X362 ∈ {10-, 11-20, 21-40, 41-100, 100+}	[0-10]={10-=1} [11-20]={11-20 =1} [21-40]={21-40 =1} [41-100]={41-100 =1} [100-∞]={100+ =1}

Attribute	Value set	fX(y) value levels
X363	X363 ∈ {None, Some, Many}	[0-0,99]={None=1} [1-3]={Some =1} [4-20]={Many =1}
X36	X36 ∈ {Easy, Moderate, Complicated}	[0-1]={Easy=1} [1,01-3]={Moderate =1} [3,01-20]={Complicated =1}
X31	X31 ∈ {Bad, Average, Good}	[1-30]={Bad=1} [35-65]={Average =1} [70-99]={Good =1}
X32	X32 ∈ {Conventional, Ordinary, Innovative}	[1-3]={Conventional=1} [4-7]={Ordinary =1} [8-10]={Innovative =1}
X33	X33 ∈ {Minimal, Moderate, High}	[1-30]={Minimal=1} [40-70]={Moderate =1} [80-110]={High =1}
X34	X34 ∈ {Minimal, Moderate, High}	[1-20]={Minimal=1} [30-50]={Moderate =1} [60-80]={High =1}
X35	X35 ∈ {Uncomfortable, Compromise, Comfortable},	[1-100]={Uncomfortable=1} [200-300]={Compromise=1} [400-500]={Comfortable=1}
X3	X3 ∈ {Avoidable, Compromise, Preferred }	[1-33]={Avoidable=1} [34-66]={Compromise=1} [67-99]={Preferred=1}
X41	X41 ∈ {None, One, Multiple}	[0-0,99]={None=1} [1-1,99]={One =1} [2-20]={Multiple =1}
X42	X42 ∈ {None, One, Multiple}	[0-0,99]={None=1} [1-1,99]={One =1} [2-20]={Multiple =1}
X43	X43 ∈ {Low, Medium, High}	[1-30]={Low=1} [40-70]={Medium=1} [80-110]={High=1}
X4	X4 ∈{None, Some, Many}	[0-0,99]={None=1} [1-9,99]={Some =1} [10-20]={Many =1}
X	X ∈{Major optimization, Minor optimization, Optimal}	[0-10]={Major optimization=1} [11-20]={Minor optimization =1} [21-30]={Optimal =1}

In the next, an illustrative example will be given. In Table 3 a theoretical route is evaluated based on the proposed model. In the model the same person would be evaluated for her daily commuting route. This way it can be determined, whether the given route with the given input parameters would require an optimization, or not and it can be decided, whether one, or the other requires less optimization.

In this example the commuter needs to travel 9.7 km from her home to her workplace. The location is in Budapest, Hungary. There is public transport, but a short walk needed in both ends. Other alternative would be taking the car.

Table 3
Route selection example for exact case

Attribute's name	**Alternative 1**	**Alternative 2**
X161 – Temperature dependence	fX161(25)={Low}, N(fX161(25))={Low}	fX161(50)={Medium}, N(fX161(50))={Medium}
X162 – Rain dependence	fX162(15)={Low}, N(fX162(15))={Low}	fX162(57)={Medium}, N(fX162(57))={Medium}
X163 – Sunshine dependence	fX163(26)={Low}, N(fX163(26))={Low}	fX163(34)={Low=0,6, Medium=0,4}, N(fX163(34))={Low}
X164 – Visibility dependence	fX164(38)={Low=0,2, Medium=0,8}, N(fX164(38))={Medium}	fX164(14)={Low}, N(fX164(14))={Low}
X16 – Weather dependence	fX16[0,3*fX161+0,2*fX162+ 0,2*fX163+0,3*fX164]={Low}, N(fX16(y))={Low}	fX16(0,3*fX161+0,2*fX162+ 0,2*fX163+0,3*fX164)= {Medium}, N(fX16(y))={Medium}
X11 – Available transport options	fX11[2]={Car}, N(fX11(2))={Car}	fX11[4]={Public transp.}, N(fX11(4))={Public transp.}
X12 – Available route alternatives	fX12[97]={Many}, N(fX12(97))={Many}	fX12[14]={None}, N(fX12(14))={None}
X13 – Accessibility	fX13[83]={High}, N(fX13(83))={High}	fX13[37]={Low=0,3, Medium=0,7}, N(fX13(83))={Medium}
X14 – Economicality	fX14[27]={Low}, N(fX14(27))={Low}	fX14[74]={Medium=0,6, High=0,4}, N(fX14(74))={High}
X15 – Environmental friendliness	fX15[19]={Not}, N(fX15(19))={Not}	fX15[57]={Fair}, N(fX15(57))={Fair}
X1 – Infrastructure	fX1[max(X11)+max(X12)+max(X13)+max(X14)+max(X15)+max(X16)]={Good}, N(fX1(y))={Good}	fX1[max(X11)+max(X12)+max(X13)+max(X14)+max(X15)+max(X16)]={Fair}, N(fX1(y))={Fair}
X21 – Age	fX21[34]={31-40}, N(fX21(34))={31-40}	fX21[34]={31-40}, N(fX21(34))={31-40}
X22 – Educational background	fX22[3]={Higher education}, N(fX22(3))={Higher education}	fX22[3]={Higher education}, N(fX22(3))={Higher education}

Attribute's name	Alternative 1	Alternative 2
X23 – Wealth	fX23[59]={Average}, N(fX22(59))={Average}	fX23[59]={Average}, N(fX22(59))={Average}
X24 – Preferences (determined by the life stage)	fX24[4]={With children}, N(fX24(4))={With children}	fX24[4]={With children}, N(fX24(4))={With children}
X25 – Gender	fX25[2]={Female}, N(fX25(2))={Female}	fX25[2]={Female}, N(fX25(2))={Female}
X2 – Social factors	fX2[0,2*fX21+0,3*fX22+0,3 *fX23+0,1*fX24+0,1*fX25] ={Influential}, N(fX2(y))={Influential}	fX2[0,2*fX21+0,3*fX22+0,3 *fX23+ 0,1*fX24+0,1*fX25]={Influe ntial}, N(fX2(y))={Influential}
X361 – Locations to visit	fX361[3]={Some}, N(fX361(3))={Some}	fX361[3]={Some}, N(fX361(3))={Some}
X362 – (Overall) Distance	fX362[19,4]={10-20 km}, N(fX362(19,4))={10-20 km}	fX362[19,4]={10-20 km}, N(fX362(19,4))={10-20 km}
X363 – Equipment needed	fX363[3]={Some}, N(fX363(3))={Some}	fX363[3]={Some}, N(fX363(3))={Some}
X36 – Daily program	fX36[0,3*fX361+0,4*fX362+ 0,3* fX363]={Easy}, N(fX36(y))={Easy}	fX36[0,3*fX361+0,4*fX362+ 0,3* fX363]={Easy}, N(fX36(y))={Easy}
X31 – Mood	fX31[78]={Good}, N(fX31(78))={Good}	fX31[32]={Bad=0,6, Average=0,4}, N(fX31(32))={Bad}
X32 – Habits	fX32[3]={Conventional}, N(fX32(3))={Conventional}	fX32[3]={Conventional}, N(fX32(3))={Conventional}
X33 – Friends/family impact	fX33[88]={High}, N(fX33(88))={High}	fX33[88]={High}, N(fX33(88))={High}
X34 – Time pressure	fX34[47]={Moderate}, N(fX34(47))={Moderate}	fX34[53]={Moderate=0,7, High=0,3}, N(fX34(53))={Moderate}
X35 – Comfort	fX35[452]={Comfortable}, N(fX35(452))={Comfortable}	fX35[139]={Uncomfortable= 0,6, Compromise=0,4}, N(fX35(139))={Uncomfortab le}
X3 – Personal factors	fX3[0,1*fX31+0,3*fX32+0,1 *fX33+0,2*fX34+0,1*fX35+ 0,2*fX36]= {Preferred}, N(fX3(y))={Preferred}	fX3[0,1*fX31+0,3*fX32+0,1 *fX33+0,2*fX34+0,1*fX35+ 0,2*fX36]= {Avoidable}, N(fX3(y))={Avoidable}
X41 – Accidents	fX41[1]={One}, N(fX41(1))={One}	fX41[1]={One}, N(fX41(1))={One}
X42 – Close downs	fX42[1]={One}, N(fX42(1))={One}	fX42[0]={None}, N(fX42(0))={None}

Attribute's name	Alternative 1	Alternative 2
X43 – Traffic	fX43[73]={Medium=0,7, High=0,3}, N(fX43(73))={Medium}	fX43[46]={Medium}, N(fX43(46))={Medium}
X4 – Available information	fX3[0,2*fX41+0,2*fX42+0,6*fX43]= {Many}, N(fX3(y))={Many}	fX3[0,2*fX41+0,2*fX42+0,6*fX43]= {Some}, N(fX3(y))={Some}
X – Route selection	fX[0,4*fX1+0,1*fX2+0,3*fX3+0,2* fX4]= {Optimal}, N(fX3(y))={Optimal}	fX[0,4*fX1+0,1*fX2+0,3*fX3+0,2* fX4]= {Minor optimization}, N(fX3(y))={Minor optimization}

Based on the model, when choosing public transport, minor optimization would be required, but choosing the car and the bike is optimal. The result was surprising, that public transport was not the preferred form of transportation. It is due to the fact, that there is a lot of compromise in this route, due to the long walks and not good weather dependencies.

Conclusions and Future Work

The main goal of this study was to propose a model, at a micro-level, that is suitable to integrate large numbers of uncertain and/or subjective input information and to create clear answers. A new model was proposed where the actual users could evaluate the commuting path for themselves, which could help them in choosing the most suitable route. This new approach contributes to establishing an efficient and reality-based model and evaluation algorithm, which offer a more adequate solution of the problem investigated, compared to all other approaches in the literature.

It is very hard to measure the efficiency of a decision, based on uncertain components, especially subjective elements. Validation of the decisions based on the new approach may happen by similarly subjective evaluation by human "experts", e.g. active participants of route selections experiments according to the original problem set. The observations we made on real life examples confirm and validate the quality of the decisions based on the proposed new model. Further validation could be carried out by extensive questionnaires and comparison of the replies to relevant questions. Construction of such a questionnaire and conducting such experiments may be an interesting continuation of the present research.

As a side-note, we have also proposed a novel, combined model, containing the fusion of fuzzy signatures and fuzzy rule based reasoning.

Under the umbrella of the study, we tested the system, with variable input data, with substantial deviations, and, despite that, the aggregated results show remarkable coherence. This demonstrates the power of the model.

Based on the categories of Bjørnskov and Svendsen (2003), the project covered three levels of social capital: macro level, meso level and micro level. Another paper (Mikulai-Kóczy, 2021, [2]) described the results achieved at a macro level. This paper focuses on the results at the micro level, using the same model. The next step is to carry out a similar study at the meso level, using the same model, making the three-part series complete. Thus, the third study will focus on the route selection habits of specific groups.

Acknowledgement

The research was supported by the National Research, Development and Innovation Office (Hungary) grant nr. K124055.

References

[1] Bjørnskov C., Svendsen G., Measuring social capital – Is there a single underlying explanation?, *Working Papers*, 2003

[2] Mikulai G. C., Kóczy T. L., Macro-level road network evaluation by fuzzy signature rule bases, *Hungarian Statistical Review*, Vol. 4, No. 1, 2021

[3] Long X., Zhao H., Zhou M., Hou C., Switching threshold of commuting Travelers' route choice under different patterns of information, *Travel Behaviour and Society*, Vol. 23, pp. 216-225, 2021

[4] Grabisch M., Orlovski S. A., Yager R. R., Fuzzy Aggregation of Numerical Preferences, 1998

[5] Mayne A. J., Klir G. J., Folger T. A., Fuzzy Sets, Uncertainty, and Information, *The Journal of the Operational Research Society*, 1990

[6] Kóczy L. T., Vámos T., Bíró G., *Proceedings of EUROFUSE -- SIC '99: Eurofuse '99, the Fourth Meeting of the EURO Working Group on Fuzzy Sets and SIC '99, the Second International Conference on Soft and Intelligent Computing*. University of Veterinary Science, Department of Biomathematics and Informatics, 1999

[7] Kóczy L. T., Cornejo M. E., Medina J., Algebraic structure of fuzzy signatures, *Fuzzy Sets and Systems*, Vol. 418, pp. 25-50, 2021

[8] Helsgaun K., Effective implementation of the Lin-Kernighan traveling salesman heuristic, *European Journal of Operational Research*, Vol. 126, No. 1, 2000

[9] Kóczy L. T., Földesi P., Tüű-Szabó B., An effective Discrete Bacterial Memetic Evolutionary Algorithm for the Traveling Salesman Problem, *International Journal of Intelligent Systems*, Vol. 32, No. 8, 2017

[10] Kóczy L. T., Földesi P., Tüű-Szabó B., Enhanced discrete bacterial memetic evolutionary algorithm - An efficacious metaheuristic for the traveling salesman optimization, *Information Sciences*, Vol. 460-461, 2018

[11] Tüű-Szabó B., Földesi P., Kóczy L. T., Analyzing the Performance of TSP Solver Methods, in *Studies in Computational Intelligence*, 2022, Vol. 955

[12] Winters M., Teschke K., Grant M., Setton E. M., Brauer M., How far out of the way will we travel? Built environment influences on route selection for bicycle and car travel, *Transportation Research Record*, No. 2190, 2010

[13] Bovy P. H., Stern E., *Route Choice: Wayfinding in Transport Networks*, 1st ed. Dordrecht: Kluwer Academic Publisher, 1990

[14] Tischler S., Finding the right way - A new approach for route selection procedures?, in *Transportation Research Procedia*, 2017, Vol. 25

[15] Bascom G. W., Christensen K. M., The impacts of limited transportation access on persons with disabilities' social participation, *Journal of Transport and Health*, Vol. 7, 2017

[16] Seliverstov Y. A., Seliverstov S. A., Lukomskaya O. Y., Nikitin K. V., Grigoriev V. A., Vydrina E. O., The method of selecting a preferred route based on subjective criteria, in *Proceedings of 2017 IEEE 2nd International Conference on Control in Technical Systems, CTS 2017*, 2017

[17] Leng R. B., Emonds M. V. M., Hamilton C. T., Ringer J. W., Holistic route selection, *Organic Process Research and Development*, Vol. 16, No. 3, 2012

[18] Böcker L., Priya Uteng T., Liu C., Dijst M., Weather and daily mobility in international perspective: A cross-comparison of Dutch, Norwegian and Swedish city regions, *Transportation Research Part D: Transport and Environment*, Vol. 77, 2019

[19] Hammad H. M. *et al.*, Environmental factors affecting the frequency of road traffic accidents: a case study of sub-urban area of Pakistan, *Environmental Science and Pollution Research*. 2019

[20] Handy S., Cao X., Mokhtarian P., Correlation or causality between the built environment and travel behavior? Evidence from Northern California, *Transportation Research Part D: Transport and Environment*, Vol. 10, No. 6, 2005

[21] Stinson M. A., Bhat C. R., Commuter Bicyclist Route Choice: Analysis Using a Stated Preference Survey, in *Transportation Research Record*, 2003, No. 1828

[22] Carvacho H. *et al.*, On the relation between social class and prejudice: The roles of education, income, and ideological attitudes, *European Journal of Social Psychology*, Vol. 43, No. 4, 2013

[23] Bocarejo S. J. P., Oviedo H. D. R., Transport accessibility and social inequities: a tool for identification of mobility needs and evaluation of transport investments, *Journal of Transport Geography*, Vol. 24, 2012

[24] Christiansen L. B., Madsen T., Schipperijn J., Ersbøll A. K., Troelsen J.,

Variations in active transport behavior among different neighborhoods and across adult life stages, *Journal of Transport and Health*, Vol. 1, No. 4, 2014

[25] Kronsell A., Rosqvist L. S., Hiselius L. W., Sustainability transitions and gender in transport sector decisions, *5th International Conference on Women's Issues in Transportation*, No. April, 2014

[26] Golledge R. G., Path selection and route preference in human navigation: A progress report, in *Lecture Notes in Computer Science (including subseries Lecture Notes in Artificial Intelligence and Lecture Notes in Bioinformatics)*, 1995, Vol. 988

[27] Kariryaa A., Veale T., Schöning J., Activity and mood-based routing for autonomous vehicles, *arXiv*, 2020

[28] Prato C. G., Bekhor S., Pronello C., Latent variables and route choice behavior, *Transportation*, Vol. 39, No. 2, 2012

[29] Hoogendoorn S. P., Bovy P. H. L., Pedestrian route-choice and activity scheduling theory and models, *Transportation Research Part B: Methodological*, Vol. 38, No. 2, 2004

[30] Papinski D., Scott D. M., Doherty S. T., Exploring the route choice decision-making process: A comparison of planned and observed routes obtained using person-based GPS, *Transportation Research Part F: Traffic Psychology and Behaviour*, Vol. 12, No. 4, 2009

[31] Wasiak M., Vehicle selection model with respect to Economic Order Quantity, *Archives of Transport*, Vol. 40, No. 4, 2016

[32] Walker N., Fain W. B., Fisk A. D., McGuire C. L., Aging and decision making: Driving-related problem solving, *Human Factors*, Vol. 39, No. 3, 1997

[33] Mamdani E. H., Assilian S., An experiment in linguistic synthesis with a fuzzy logic controller, *International Journal of Man-Machine Studies*, Vol. 7, No. 1, 1975

[34] Kóczy T. L., Tikk D., *Fuzzy Systems - Fuzzy rendszerek*. 2001

Leader of Digital Cooperation? – Scientific Mapping Engaging Leadership

Heléna Krén[1], Beatrix Séllei[2], György Molnár[3,4]

[1] PhD School in Business and Management, Faculty of Economics and Social Sciences, Budapest University of Technology and Economics, Műegyetem rkp. 3, H-1111 Budapest, Hungary, e-mail: kren.helena@edu.bme.hu

[2] Department of Ergonomics and Psychology, Faculty of Economics and Social Sciences, Budapest University of Technology and Economics, Műegyetem rkp. 3, H-1111 Budapest, Hungary, e-mail: sellei.beatrix@gtk.bme.hu

[3] Óbuda University, Kandó Kálmán Faculty of Electrical Engineering, Tavaszmező u. 17, H-1084 Budapest, Hungary, e-mail: molnar.gyorgy@uni-obuda.hu

[4] Széchenyi István University, János Csere Apáczai Faculty, Egyetem tér 1, 9026 Győr, Hungary, e-mail: molnar.gyorgy@sze.hu

Abstract: In this time of digitalization, leaders have to face new challenges and concentrate on engaging subordinates, due to the hybrid working conditions. One of these challenges is the Digital Competence Expectations for Public School Leaders, published in 2021, by the Digital Pedagogical Development Working Group. The emerging importance of engagement is supported by a great deal of scientific research. However, it is still questionable… what directly determines engagement and affects subordinates in the engaging process? Our review aims to analyze the characteristics of engaging leadership and leaders' behavior, which contributes to the engagement of coworkers. Taking the challenges of the digital world into consideration, we make some practical suggestions for future leaders and HR professionals, in order to strengthen their organizations and retain valuable employees.

Keywords: engaging leadership; engagement; digital workplace; empowerment; HR solutions; leadership practice

1 Introduction

Engagement and engaging leadership became essential topics in organizational settings, and in the changing digital world, these characteristics might gain more importance. We have to prepare to engage followers too, because engagement

seems to be a key determinant of success [1-3]. Engaging leadership is a complex term, and its effect depends on environmental factors [4] [5], job characteristics, and individual characteristics like personality [5] [6]. Leaders are part of an "engagement equation" [6] because they provide organizational and social resources [7-9], like a safe place, letting someone be oneself and valued part of a team [4], and they match the followers' personal needs and abilities to perform, perceive themselves essential and their job meaningful, and have control over the challenges one faces at work [6].

Engagement usually occurs naturally when conditions are met, so leaders can motivate and inspire subordinates and individuals can do their best [6]. But leaders can influence this process with practices oriented toward others [10] and engaging themselves because the first step for engaging others is engaging oneself [4]. In times of digital transformation, this engagement must be extended to digital platforms, new techniques, broader network and used to inspire coworkers and other leaders, for example, when working in the form of shared leadership [11].

We define engaging leadership with the help of previous theories and summarize the most important findings, leadership behaviors contributing to engagement via engaging leadership. Finally, we propose some steps to develop engagement through leaders' behavior in the middle of digital transformation.

2 Scientific Mapping Engaging Leadership

2.1 Selection of Relevant Literature

Engaging leadership is a pretty new construct among leadership theories. For our review, we checked available sources with the help of Scopus in November 2021. The keywords "engaging" and "leadership" were limited to final publications, considering articles in social sciences; business, management, and accounting; nursing; psychology; arts and humanities; environmental science; economics, econometrics, finance and decision sciences. The query resulted in 1427 records, published in between 1959 and 2021, with an increasing frequency in the last few years. We visualized the results with VOSviewer 1.6.17 and Figure 1 shows that engaging leadership has been investigated mainly, in the previous few years.

To narrow the scope to engaging leadership, we used "engaging leadership" as a keyword. We found 56 records in Scopus and a further 44 records in the database of Web of Science without any limitations to subjects. After reading the titles and abstracts of the 101 records, we found 69 records connected to leadership, organizations, or engagement. There were several duplicated articles that we removed.

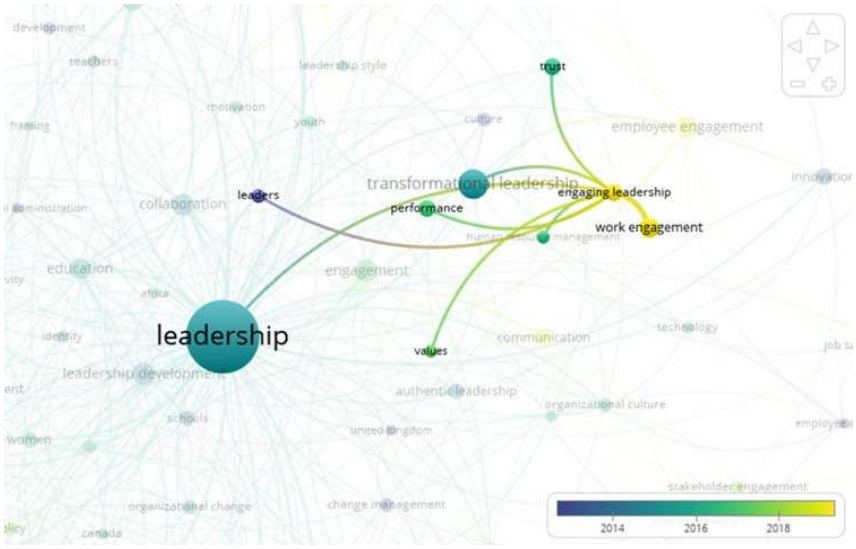

Figure 1
Visualization of engagement and leadership literature

To focus more on engaging leadership in peer-reviewed articles or conference papers, we excluded 2 Web of Science-indexed conference abstracts, one book and six book chapters. After all, 27 papers were chosen for further review: three conference proceedings and 24 articles.

2.2 Theoretical Frames of Engaging Leadership

Engaging leadership was approached from three different perspectives. First, Dulewicz and Higgs [12] conceptualized engaging leadership in association with effective leadership and varying organizational context. This is used, for example, in change and project management [3] [13]. Second, Alimo-Metcalfe and Alban-Metcalfe [1] defined performance as influencing leadership competencies and qualities. Among them, engaging leadership as a leadership quality seemed to determine goal achievement and positive affective outcomes [1]. Third, Schaufeli [8] formulated a new concept rooted in the motivational theory.

2.2.1 Engaging Leadership as an Effective Leadership Style

Transformational leadership theory dominated leadership theories when Dulewicz and Higgs [12] wanted to create a universal profiling instrument to determine leadership styles and effectiveness in a different context. Based on the that leader's personality defines how someone leads, and leadership must be fitted to the organizational context, Dulewicz and Higgs [12] identified cognitive,

behavioral, personality, and learning factors for a dynamic relationship between a leader and the organization. This means one change in a leader's behavior can lead to different strategies of an organization, and in contrast, an organizational step can also impact leadership [12]. This theory focuses on leaders' effectiveness in different contexts of change. Dulewicz and Higgs [12] found that intellectual, managerial, and social-emotional components reoccur in leadership models. Since these are the most important leadership dimensions, they built their Leadership Development Questionnaire on these. 15 leadership competencies were used to analyze differences between leadership behaviors in changing contexts. Three main leadership types were identified (goal-oriented, involving, and engaging) as leader profiles for change projects [12]. From this, we highlight engaging leadership style and related competencies.

The engaging leadership style is based on the engagement and commitment of others to find the right direction and achieve the desired goal. Leaders can support this through empowerment and involvement in complex contexts where a facilitative style is needed. This style was profiled with the help of the 15 leadership competencies based on transformational and change leadership theories. From the managerial dimension, engaging communication, empowering, and developing, from the social-emotional dimension, self-awareness, emotional resilience, motivation, interpersonal sensitivity, influencing, intuitiveness, and conscientiousness define the most engaging style based on typical high scores of leaders [12].

According to Dulewicz and Higgs [12], the ***characteristics of an engaging leader*** are:

- Communicates enthusiastically, focused, and inspiring and can engage others and win support because he or she is approachable and accessible in communication topics for the staff
- Empowers followers with autonomy and encourages them to challenge themselves personally and the existing practices of the organization; supports them to be innovative, creative, and critical in problem-solving and forming visions
- Strengthens the potential in others, believes in the capabilities of followers, and supports them to evolve and develop new skills through challenging tasks and roles with adequate support and critical feedback
- Is aware of emotions and able to recognize and control them and their impact on followers and the work environment
- Adapts behavior to situations and can keep consistent performance, balancing the need of the situation and the involved colleagues while focusing on the results even though he or she gets criticized and challenged
- Relies on rational and emotional perception or information in decision-making and uses intuition to decide and drive implementations even if the available information is incomplete or unclear

- Is aware and committed to the needs and perceptions of others and wants to stay open to others' solutions, listen actively and reflect on the reaction and inputs from others
- Convinces others about the relevance of changing views and the rationale of it by listening to their perspective and recognizing the needs behind them
- Is motivated to achieve results and make an impact through demanding goals, even if he or she faces with a negative attitude towards the goals
- Is committed to actions against problems and drives others towards a transparent, ethical solution to complex business situations

We introduce two articles from the review in Table 1, which used the conceptual model and tool, the Leadership Development Questionnaire.

Table 1
Summary of articles based on the theory of Dulewicz and Higgs [12]

Müller and Turner in 2010 [3]	
Purpose (P): To identify leadership competency profiles of successful project managers of different projects	Method (M): Two questionnaires: (1) reflecting on the last successful project, (2) Leadership Development Questionnaire (LDQ) and demographic questions Identified top-performing projects were statistically analyzed.
Sector (S): Project application area: engineering and construction, information and communication technology, and organizational change projects	Result (R): Indicators of success in all project types were critical thinking, influence, motivation, and conscientiousness. The more complex a project is, the more engaging leadership is needed to manage it. Therefore, emotional competencies as criteria of selection and development programs are suggested.
Lundy and Morin in 2013 [13]	
P: To analyze leaders' effect on management of resistance to change in projects	M: Qualitative method: semi-structured interviews and observation; data saturation and analysis of answers and keywords which were linked to LDQ dimensions
S: Canadian public service, a governmental organization specialized in information management	R: Leadership competencies, especially emotional dimensions, were found to be important in order to decrease resistance to change. Moreover, an engaging leadership style was perceived to be the most effective when facing resistance in change process.

2.2.2 Engaging Leadership as a Leadership Quality

The evolution of leadership theories brought a new perspective in the post-heroic era, namely, engaging leadership style [1]. Alimo-Metcalfe and Alban-Metcalfe [1] defined engaging leadership as a "nearby transformational" leadership style.

Engaging leadership is a style that places others' development and well-being in the focus of the leaders and emphasizes respect for others. An engaging leader unites different groups, fosters a shared vision, and supports a culture of development, empowerment, and critical thinking. "Engaging leadership is based on integrity, openness, and transparency, and genuinely valuing others, and their contributions, along with being able to resolve complex problems and to be decisive" [1, p. 587]. This style enables coping with change in a proactive way to achieve the shared vision with the guidance of ethical principles. Besides this, engaging leadership facilitates the contribution of employees and ensures productivity and profitability, while organizational culture also affects individual and organizational performance [1].

Alimo-Metcalfe and Alban-Metcalfe differentiated engaging leadership definitely from transformational leadership later, as they constructed a new scale assessing leadership capabilities and qualities [5]. The construct of engaging leadership was formulated using a grounded theory approach and measured by leadership style or quality, i.e., how leaders act, while leaders' competencies refer to what they do [5]. To measure the "what" and "how," Alban-Metcalfe and Alimo-Metcalfe [5] designed a 360-degree multi-rater diagnostic tool, Leadership competencies and engaging leadership scale (LCELS). One part of this scale assesses how leaders can engage individuals, organizations, and other stakeholders using their competencies and measures personal qualities and values connected to leadership competencies.

The other part reflects leadership qualities, and ***how engaging leaders behave***:

- Assessing engaging individuals through showing genuine concern, enabling
- Engaging organizations through supporting a developmental culture, focusing team effort
- Engaging other stakeholders through building a shared vision, facilitating change sensitively
- Considering personal qualities in behavior when measuring acting with integrity [5]

Three articles analyze engaging leadership in the theoretical framework of Alimo-Metcalfe and Alban-Metcalfe [1]. We introduce these studies in Table 2.

Table 2
Summary of articles based on the theory of Alimo-Metcalfe and Alban-Metcalfe [1]

Alimo- Metcalfe, and Alban-Metcalfe in 2008 [1]	
Purpose (P): To examine the relationship between leadership qualities and individual attitudes to work and well-being at work and how these affect organizational performance via individual performance	Method (M): Longitudinal study using two questionnaires: Leadership Climate and Change Inventory, leadership culture items from Transformational Leadership Questionnaire, leadership capability items collected and rated by managers in mental health care; organizational performance assessed by reaching the governmental target Results were statistically analyzed.
Sector (S): Health care, mental health crisis resolution/home treatment teams (Crisis Resolution Team - CRT)	Result (R): Engaging with others and shared vision as leadership quality and one leadership capability factor emerged. Engaging with others was rated higher in higher-performing teams and was significantly related to attitudes to work and well-being at work. Furthermore, engaging with others as a leadership quality is a significant predictor of goal achievement.
Alban-Metcalfe and Alimo-Metcalfe in 2013 [5]	
P: To strengthen the evidence of reliability and validity of the leadership competencies and engaging leadership scale	M: LCELS was used, and results were statistically analyzed
S: Public service, local government	R: Reliability and validity were supported, which means each scale measures different competencies and engaging leadership behaviors. Above this, leadership behavior affects employees' attitudes and well-being, and organizational performance.
Michalec, Veloski, Hojat and Tykocisnki in 2014 [10]	
P: To identify potential engaging leaders with the help of peer-assessed positive influence and engaging leadership behavior	M: Survey about demographic, relational aspects, academic performance, and performance in clinical clerkship, Jefferson Scale of Empathy, communication, and interpersonal scores from patient simulation; results from different time periods were statistically analyzed
S: Academic, private medical school	R: Peer-selection method seemed to be successful in identifying positive influencers who also presented leadership qualities, showing a genuine concern for others. This study supports that leadership skills and traits can be identified already in school.

2.2.3 Engaging Leadership as Work Engagement Increasing Leadership Behavior

Schaufeli [8] formulated the theory of a new, positive psychological leadership style, namely engaging leadership. The newest theoretical model is built-in into the model of job demands and resources and defined with the help of need

satisfaction, contributing to the motivational process toward work engagement and organizational outcomes [8].

Engaging leadership, especially some aspects of it, was considered as job resource. Since leaders have impact on employees, and they balance job demands and job resources for employees to stay productive, leadership should be a separately handled construct within the Job Demands and Resources theory defined by Bakker and Demerouti, [14 in 8]. Therefore, this leadership theory was integrated into the job demands-resources model based on the framework of the Self-Determination Theory defined by Deci and Ryan [15 in 8]. It means leaders balance job demands and resources and satisfy employees' basic psychological needs to foster work engagement [9].

Engaging leadership is a leadership behavior that inspires, strengthens and connects employees and has a positive effect on work engagement through the satisfaction of basic psychological needs [16]. The Engaging Leadership Scale (ELS) measures three aspects of engaging leadership, and all of them are based on the premises of psychological need satisfaction. In other words, innate psychological needs for autonomy, competence and relatedness need to be fulfilled in order to be engaged. These psychological needs mediate between job resources and engagement, so their satisfaction can contribute to the effect of leadership on work engagement. Inspiration from leaders can support employees' autonomy, strengthening employees through challenging tasks can contribute to their competencies, and encouragement of collaboration and team building enhance the feeling of belongingness which all result in a higher level of engagement [8].

Engaging leadership behavior is defined with the help of three aspects, inspiration, strength, and connection. Further, we describe ***what leaders practically do***:

1. **To inspire:**
    - Motivates employees with vision and plans
    - Acknowledge the contribution to an important mission
    - Stimulates others to contribute to important goals
    - Provides organizational resources and minimizes job demands
    - Highlights the importance of alignment, value and trust
    - Manages organizational change adequately
2. **To strengthen:**
    - Gives freedom to employees
    - Delegates tasks and responsibilities
    - Challenges the skills and competencies of employees with tasks appropriate for development

- Provides work and development resources
- Gives autonomy to control one's own job
- Ensures task variety
- Gives feedback and career perspectives
- Manages workload and supports work-life balance

3. **To connect:**
   - Supports collaboration
   - Facilitates interpersonal relations and bonding
   - Provides social resources
   - Clarifies roles
   - Creates good team spirit and maintains a good atmosphere [8]

Some researchers use a measure with four aspects, adding empowering as an engaging leadership factor [17] [18]. To empower, leaders provide learning opportunities and ensure knowledge sharing [17], partly contributing to strengthening competence and bonding through shared experiences and knowledge. Another research [18] defines empowering as a factor that satisfies the need for autonomy by letting someone articulate one's own opinion. As we see, it slightly overlaps with strengthening and connecting in the first case, and in the second case, it can refer to inspiration too.

Later, research confirmed the four-factor model of Engaging Leadership Scale [19] [20], therefore, we complete the original engaging leadership behavior described by Schaufeli [8] by describing ***what else engaging leaders do***:

4. **To empower:**
   - Creates space for freedom of choice and safety
   - Supports responsibility and accountability
   - Encourages communication without repercussion
   - Acknowledges the contribution and gives positive feedback
   - Involves employees in decision-making [21]
   - Let others make their own decisions freely [16]

Fifteen articles were published using the engaging leadership theory of Schaufeli [8] which we introduce in Table 3.

Table 3
Summary of articles based on the theory of Schaufeli [8]

Schaufeli in 2015 [8]	
Purpose (P): To integrate engaging leadership into the job demand-resources model based on the self-determination theory	Method (M): Measurement items were selected from a Questionnaire on the Experience and Evaluation of Work (QEEW), National Working Conditions Survey, Maslach Burnout Inventory, Utrecht Work Engagement Scale (UWES), and a self-constructed engaging leadership scale and items for team- and organizational commitment. The hypothetical model was tested with structural equation modeling.
Sector (S): National representative sample of the general working population	Result (R): Engaging leadership had a direct effect on organizational outcomes, but just an indirect effect on work engagement through job resources. This means leadership affected the stress process by decreasing job demands and burnout, and the motivational process by increasing job resources and engagement.
Basinska, Gruszczynska and Schaufeli in 2018 [17]	
P: To analyze the role of job-related affect mediating between engaging leadership as an organizational resource and work engagement	M: Cross-sectional study using ELS, Job-related Well-being Scale and UWES Multiple-mediation model was analyzed via structural equation modeling
S: Public administration	R: From the supposed parallel mediators, just positive affect was significant, which means higher engaging leadership leads to higher positive job-related affect which also leads to stronger work engagement.
Nikolova, Schaufeli and Notelaers in 2019 [7]	
P: To examine job resources mediating the relationship between engaging leadership and work engagement across time	M: Cross-lagged study using ELS, QEEW, UWES The hypothesized model was tested with structural equation modeling
S: Hospitality industry, hotel chain	R: Engaging leadership predicted autonomy and support from colleagues across time and the authors found that employee perception about engaging leadership is shaped by their own level of engagement. Engagement contributes also to the perception and access to job resources.
Rahmadani and Schaufeli in 2019 [10]	
P: To investigate engaging leadership and its impact on work engagement mediated by basic psychological need satisfaction over time	M: Longitudinal study using ELS, UWES, Basic Psychological Need Satisfaction Scale (BPNSS) The proposed model was tested with structural equation modeling
S: State-owned agricultural company, participation of	R: Engaging leadership predicted work engagement across time, and this relation is mediated indirectly by

blue-collar workers	basic need satisfaction. Fulfillment of basic needs can increase work-related well-being.
Rahmadani, Schaufeli, Ivanova and Osin in 2019 [18]	
P: To examine the mediating role of basic psychological need satisfaction between engaging leadership and work engagement	M: Quantitative study using ELS, BPNSS, UWES The hypotheses were tested with structural equation modeling
S: State-owned agricultural company's blue-collar workers and civil servants of regional government	R: It was supported that basic psychological need satisfaction mediates the relationship between engaging leadership and work engagement. This model was validated in a cross-national setting.
Rahmadani and Schaufeli in 2020 [19]	
P: To investigate engaging leadership and work engagement mediated by diuwongke and the difference between engaging and transformational leadership	M: Quantitative study using UWES, ELS, Global Transformational Leadership, self-constructed items measuring diuwongke Data were statistically analyzed, and the hypotheses were tested via structural equation modeling
S: State-owned agricultural company's blue-collar workers	R: Engaging and transformational leadership also predicts work engagement and diuwongke moderated this relationship in the case of engaging leadership. The lower diuwongke was, the stronger engaging leadership related to work engagement.
Rahmadani, Schaufeli, Stouten, Zhang and Zulkarnain in 2020 [22]	
P: To define a model about how engaging leadership perceived by employees enhances job outcomes mediated by work engagement both at individual and team level	M: Multi-level longitudinal study using ELS, UWES, Team Work Engagement Scale, Team Performance Scale, Team Learning Behavior Scale, Team Innovation Scale, Job Performance Scale, Employee Learning Scale, and Work Behavior Scale. After confirmatory factor analysis, data were aggregated to check proper team scores, then multi-level effects were tested statistically.
S: State-owned agricultural company, blue-collar workers	R: Team engaging leadership (T1) predicted team learning (T2) and team innovation (T2) moderated by team work engagement (T2); predicted individual job performance mediated by team work engagement (T2) and individual job performance, employee learning and innovative work behavior mediated by individual work engagement (T2).
Robijn, Euwema, Schaufeli and Deprez in 2020 [9]	
P: To examine the relationship between engaging leadership and open conflict norms in team settings and analyze how they affect work engagement via basic need satisfaction	M: Questionnaires were used: ELS, UWES, three adapted items for the measurement of open conflict norms, and need satisfaction items for meaningfulness The hypothesized model was tested with structural equation modeling

S: Public insurance company	R: Engaging leadership and open conflict norms have an indirect effect on work engagement and engaging leadership is also positively connected to open conflict norms in teams. This means open conflict norms and engaging leadership contribute to well-being.
van Tuin, Schaufeli, van Rhenen and Kuiper in 2020 [23]	
P: To measure the business impact of the engaging leadership development program, focusing also on psychological well-being to generate positive business outcomes	M: Quasi-experimental, pre-test-post-test control group design. The leadership intervention program consisted (1) a survey (2) 6 training sessions (3) between them coaching and peer consultations (4) a survey and evaluation. Measurements: Orders booked on time, ELS, items from Balanced Measure of Psychological Needs Scale and Multidimensional Work Motivation Scale (MWMS)
S: Health system multinational company, employees from the customer fulfillment center	R: The company experienced a significant increase in performance and a decrease in sick-leave absenteeism among leaders and team members. The control group setting showed a higher level of autonomy and motivation of trained team leaders. Furthermore, the intervention seemed to be sustainable and effective just in the case of the leaders, not in the case of team members.
van Tuin, Schaufeli and van Rhenen in 2020 [21]	
P: To test the mediation role of basic psychological need satisfaction and frustration between engaging leadership and work motivation and work engagement	M: Measurements were ELS, scales of basic psychological need satisfaction and frustration, MWMS, and UWES. Hypotheses were tested with partial least squares structural equation modeling.
S: Multinational, technical engineering organizations	R: Engaging leadership related to positive and negative outcomes and autonomy satisfaction predicted outcomes. The common-factor variable of need satisfaction showed partial mediation with positive outcomes, and need frustration mediated towards negative outcomes.
Independent author in 2021 [24]	
P: To summarize and analyze the paper of Robijn et al. [9]	M: Same as Robijn et al. [9]
S: Same as Robijn et al. [9]	R: The author commented, that the research opened the door to scale benefits of work engagement after the basic need is satisfied, and a leader is engaging.
Salas-Vallina, Alegre and López-Cabrales in 2021 [25]	
P: To better understand the connection between well-being-oriented human resources management (HRM) and performance, by investigating well-being	M: Quantitative study used items measuring Well-Being-Oriented Human Resources Management, ELS, Happiness at Work, and exhaustion, trust, and performance from different measurements. Data were statistically analyzed, and the hypothesized

factors (WBF) as mediators, and engaging leadership as meditator between HRM and WBF	model was tested with structural equation modeling.
S: Eight different organizations' employees and their line managers	R: The combined effect of well-being-oriented human resources management and work-related well-being measures predicted individual performance. The impact of well-being-oriented human resources management on work-related well-being and performance was moderated by engaging leadership.
Schaufeli in 2021 [16]	
P: To clarify the concept of engaging leadership and review empirical results on it	M: Conceptual analysis was made
S: No specific sector, conceptual analysis was made	R: Engaging leadership is a well-established construct, built on a theoretical foundation. It is measured with a statistically confirmed scale on individual and team levels, contributing to several processes in organizations.
van Tuin, Schaufeli and Van den Broeck in 2021 [26]	
P: To investigate the relationship between engaging leadership and employees' perception of organizational values, need satisfaction, and engagement.	M: Study 1: the cross-sectional study used measurements such as UWES, ELS, and items measuring psychological need satisfaction and perception of the organization's value orientation. Data were analyzed with structural equation modeling. Study 2: a longitudinal study using ELS, UWES, and items for intrinsic value orientation and autonomy satisfaction. Data were analyzed with longitudinal structural equation modeling.
S: Study 1: Health system, participants from back-office departments of an international manufacturing organization Study 2: automotive industry, technical function engineers of a manufacturer	R: Engaging leadership can predict work engagement via perceived intrinsic organizational values and satisfying the need for autonomy. This leadership is an antecedent of employees' intrinsic value perception, which positively affects need satisfaction and engagement, and showed a negative association with extrinsic organizational values, but this perceived value orientation did not affect need satisfaction measures negatively.
Xiaojun and Yiwen in 2021 [27]	
P: To examine the influence mechanism of engaging leadership on turnover intention	M: Applied measurements: ELS, Turnover Intention Scale, UWES, Cognitive trust, and Affective trust scale. Data were statistically analyzed.
S: Information technology, biomedical, insurance, and media industry	R: Engaging leadership had a negative effect on turnover intention, which relation was mediated by overall trust and work engagement, creating a chain mediating effect from engaging leadership towards decreased turnover intention.

2.2.4 Further Aspects of Engaging Leadership

Since engaging leadership is an actively researched and discussed topic from different aspects, some other approaches should be mentioned that appeared in our search.

Firouznia with her colleagues examined the relationship between engaging leadership and work engagement and summarized the findings in a holistic model. They presented a multi-faceted definition of engaging leadership within seven dimensions. According to their theory inspiration, integrity, autonomy granting, supportive coaching, role clarifying, team supporting, and participative decision-making describe and contribute to engaging leadership. Additionally, they emphasize the role of the work environment, determined by psychological resources and social support, and job characteristics, like job meaningfulness and job fit for employees [28]. Although they do not present statistically acceptable results, this hypothetical model might be worth further analysis.

Drewiske [29] approached engaging leadership from a unique perspective of safety maintenance. He highlighted the importance of engaging the leaders to get support while managing electrical safety programs. According to his view, employees can engage leaders to support their aims. Leaders can be involved and engaged through clear education about the important topic, communication about needs and needed steps, and persistent feedback and improvement. This way, Drewiske suggests everyone can win the leaders' support.

Finally, Mosley wrote a series of publications about her experiences with engaging leadership. She emphasized decision-making to balance demands and available resources and the effect of decisions on followers who might experience missing support which turns into higher turnover [30]. She outlined how innovations and innovative ideas can help to engage employees by involving them in evaluation, decision-making, planning, and execution. Furthermore, she pointed out that if one can engage open-minded colleagues, one might help engage other staff and catalyze change [31]. Mosley [32] made a distinction between titled leaders who got promoted and should be balanced, aware and thoughtful, and passionate leaders who overgrow their peers and became leaders through his or her capabilities. She mentioned several leadership behaviors which are needed to engage followers, such as standing for group thoughts, taking needs into consideration when making a decision, encouraging others to be a part of a solution, communicating effectively across situations, and facilitating a growth culture [32]. In the last paper, Mosley [33] discusses the term disengagement among employees. Leaders can suppose disengagement if an employee does not invest in work or underperforms. Another aspect of disengagement is disconnection which serves someone's recovery and makes him or her able to reengage with positive emotions [33].

From a practical aspect, Mosley and the above-mentioned authors can also contribute to the development of HR and management, suggesting numerous great aspects. In the next section, we summarize the practical implications of our literature review.

3 Practical Implications to Foster Engaging Leadership

After reviewing the literature, we can conclude that engaging leadership plays an important role in organizations, teams, and interpersonal relations because it effects work engagement, directly or indirectly. The authors made several suggestions for HR professionals and leaders to engage employees or maintain the level of their engagement. Since retention is getting harder with working from home, narrowed social interactions, and with business cooperation in the digital space, we summarize the most significant recommendations in this part.

The first step is to find the right candidate and the right leader. Someone can be called a project manager, and not be the real project leader. So, it is essential to identify the leader and help him or her develop leadership competencies [13]. Project managers' competencies need to match project types [3] and meet sector-specific needs too [5]. Therefore, the assignment should base on the characteristics of both the project and the possible leader [3]. Furthermore, HR professionals should recruit qualified candidates, who match the job expectations and suit the leader [28]. The leader who is competent and uses strengths and qualities to lead effectively [5].

Second, leaders and HR professionals have to create an organizational culture and provide resources to function well. The challenge is usually for them that people differ in what they like, and this is also right if we are speaking about leadership behavior. Different teams and employees can value different leadership behavior from the same leader. But a supportive environment, in which great concern for others' lives, can help to satisfy different needs [5].

Engagement is affected by organizational culture, therefore, engaging leadership behavior should be the basic behavioral norm to promote engagement in organizations [1]. Leaders must create a job environment in which organizational values are congruent with the values of employees [26], and are driven by inspiration to maintain a positive organizational culture [17]. In an engaging culture, open communication should facilitate conversation about basic needs and help leaders satisfy important needs [20] [25]. Furthermore, a dialogue between leader and employee can increase engagement and the quality of their relationship [25]. Learning from the Indonesian example, leaders should treat employees with dignity and respect [19], let others participate in decision-making [8] [25], propose

co-creation, and support autonomy [23] to create an open and mutually trusting climate [18] [27]. In such a milieu, employees will be more proactive and receptive to the intentions of a leader [20]. Additionally, promoting safe employment relationship and securing that the organization value its members can boost positive work effects [25].

The organization should create resourceful work environments [7] [28], invest in job resources [8] [28], and focus on the satisfaction of basic needs [20]. Resources are needed to enhance intrinsic motivation, engage employees, and enhance the positive affect of work on them. Because supporting others to feel less bad is not enough, using strength and fulfilling needs is what ensures a positive attitude and work engagement [17]. When balancing employees' job demands and job resources, leaders should choose specific job resources at different levels and types of engagement [22]. Leaders and HR professionals should be also aware of personal causation and internalization of extrinsic motives [21]. Moreover, employees should proactively seek opportunities to satisfy needs [18].

HR professionals can stay informed and engage employees if they foster employee involvement [1] [23] and check the learning and development needs of employees [18]. One of the main tasks is focusing on organizational achievement and supporting employees in pursuing their learning goals at the same time [18]. So, leaders must learn how to reflect on needs and how to detect the needs to increase engagement [25]. Leaders and HR professionals should understand the theoretical background of engaging leadership too and implement this kind of leadership style into their every day, for example in one-on-one sessions [18].

Support and a positive climate are important on the team and organizational levels too. An open and trustful climate is inevitable in team settings too. Leaders should facilitate sharing good news and expressing enthusiasm to enhance collective engagement by fostering emotional contagion [22]. Negative cognitive and emotional processes must be managed as soon as possible to prevent demotivation and disengagement [7]. A supportive team climate and coordination can rather stimulate teamwork engagement [22]. Supportive top management adds credibility to the values and behavior of leaders [26]. The whole company should cherish engaging leadership behavior and encourage management to implement it [28]. At the organizational level, HR professionals can take steps to maintain engagement [22]. First, they should set a goal and promote organizational engagement to reach it [22]. Second, they can ask for feedback and give feedback about performance [8]. Surveys could be useful to measure engagement within organizations [22]. Finally, HR must react to the feedback, redesign jobs, provide learning opportunities and invest in development programs, if needed [28].

Any development is useless unless the person uses his or her talent and incorporates into behavior what he or she has learned [1]. Authors agree that leadership development programs [7, 8, 23, 26, 27], training [19, 22, 25], and coaching [1, 8, 18, 19, 22] can be great tools to teach leaders how to engage

followers. Engagement is more important in challenging and hard times when leaders have to manage resistance to change on the side of employees or stakeholders. To overcome the resistance, leaders require upper managerial support and behavioral training where they can evolve [13].

Everyone in the organization needs developmental feedback to identify the needs for growth [18]. Leaders and subordinates are also recommended to participate in training [18]. Organizations should expand the opportunity of leadership development programs for those who are talented and can be future leaders [23]. Team members should also get trained to reach teamwork engagement because team engagement contributes to the effectiveness of individuals and teams [22]. Leaders should polish their engaging behavior with help of coaching [18]. And employees can also profit from coaching [25].

Team and leadership development programs should aim for several competencies and behaviors, like conflict management skills [9] or emotional competencies, such as self-awareness, interpersonal sensitivity, or motivation [3]. Leaders should create and support open conflict norms and be masters of conflict management [9] and develop skills that match a particular project [3]. Program objectives must be defined to inspire managers, followers, and HR professionals. Organizations are suggested to blend different types of developmental tools, classroom training, peer consultation, one-on-one coaching, and action learning [23].

Conclusions

Competencies can be developed and behavior can be formed through habits. So leaders can learn how to behave as engaging leaders. This was our aim, to define engaging leadership and the behaviors one should incorporate to engage others. The main message of the reviewed literature is, what van Tuin [26] summarized well, that leaders and organizations have to focus on employee needs and leaders must learn how to motivate and engage employees [26].

While the competency approach was focused on leadership capabilities, Alimo-Metcalfe [1] and Alban-Metcalfe [5] opened a door to a distributed process between individuals and organizations. Schaufeli [8] wanted to focus on employees, so he defined engaging leadership based on the need and satisfaction of employees. This theoretical framework dominated the latest few years in engaging leadership research. Proposing leadership behavior that aims to support leaders to create a resourceful environment and fulfill the basic psychological needs of employees [21]. Engaging leadership impacts why HR practices are effective. Leaders affect the individual and team level, and HR affect the organizational level [25]. Engaging leadership influences employees through positive culture, shared vision, trustful communication, individual development, and need satisfaction [17]. While HR practices increase happiness at work and trust, which contribute to the effectiveness of teams and the organization too. All in all, engaging leadership provides win-win solutions for employees and organizations [25].

The shift toward employees emerges in modern leadership forms, like agile methods, holocracy, or sociocracy, which promote autonomy-supporting and participative leadership [21], and theories like servant leadership and transformational leadership too [20]. Schaufeli [8] highlighted the overlapping parts of engaging and transformational leadership. Inspirational motivation enhances work engagement like inspiring leadership, and strengthening leadership reflects to individualized consideration [8]. Both types of leadership support employees, create a vision, empower and increase work engagement [19].

A rapidly changing business environment pushes organizations to perform effectively, learn fast and innovate continuously [22]. Digitalization brought further challenges with information overload, simultaneous use of digital channels and processing topics at the same time. It is certain, that leaders need IT skills and self-organization, but they also need to motivate and engage others, even at a distance [34]. Online communications are inevitable in this digital era, where we work from home or in an International setting. While parallel communication can affect positively job performance, it affects negatively work engagement, which means leaders must allocate more time and energy to retain employees [35]. Moreover, the digital generation requires extra support from leaders to reach the same level of engagement as older, more loyal coworkers [17].

Younger generations demand digital media and online communication, which influences their expectations in the workplace. To retain them, organizations must hone their learning and development techniques, ensuring constant learning in small units. Real-time feedback, grows in importance and contributes to growth-focused cultures to improve performance. “Digital leadership” creates new tasks and challenges for leaders. Digital leaders connect different groups and foster knowledge-sharing, in an inclusive environment [36]. New ways of working impact work engagement and the effects are mediated by transformational leadership [37]. Although engaging leadership is not examined in association with digitalization, to our best knowledge, engaging leadership can be effective and useful in “digital cooperation”. According to our review, leaders should master how to care for others and support employees by providing relevant resources. Additionally, future research needs to test how effective engaging leadership can be in the digital setting. There might be some “digital-specific” engaging leadership behaviors. To help managers navigate today's digital world, the Digital Competence Expectations, ratified by the Department for Education in 2021, are a concrete set of real-life examples, designed to help leaders prepare [38].

References

[1] Alimo-Metcalfe, B., Alban-Metcalfe, J., Bradley, M., Mariathasan, J., & Samele, C.: The impact of engaging leadership on performance, attitudes to work and wellbeing at work: a longitudinal study, Journal of health organization and management, Vol. 22, No. 6, 2008, pp. 586-598

[2] Alban-Metcalfe, J., & Alimo-Metcalfe, B.: (2009) Engaging leadership part one: competencies are like Brighton Pier, The International Journal of Leadership in Public Services, Vol. 5, No. 1, 2009, pp. 10-18

[3] Müller, R., & Turner, R.: Leadership competency profiles of successful project managers, International Journal of Project Management, Vol. 28, 2010, pp. 437-448

[4] Wildermuth, C. D., & Pauken, P. D.: A perfect match: decoding employee engagement – Part I: Engaging cultures and leaders, Industrial and Commercial Training, Vol. 40, No. 3, 2008, pp. 122-128

[5] Alban-Metcalfe, J., & Alimo-Metcalfe, B.: Reliability and validity of the "leadership competencies and engaging leadership scale", International Journal of Public Sector Management, Vol. 26, 2013, pp. 56-73

[6] Wildermuth, C. D., & Pauken, P. D.: A perfect match: decoding employee engagement – Part II: engaging jobs and individuals, Industrial and Commercial Training, Vol. 40, No. 4, 2008, pp. 206-210

[7] Nikolova, I., Schaufeli, W. B., & Notelaers, G.: Engaging leader – Engaged employees? A cross-lagged study on employee engagement, European Management Journal, Vol. 37, 2019, pp. 772-783

[8] Schaufeli, W. B.: Engaging leadership in the job demands-resources model, Career Development International, Vol. 20, 2015, pp. 446-463

[9] Robijn, W., Euwema, M. C., Schaufeli, W. B., & Deprez, J.: Leaders, teams and work engagement: a basic needs perspective, Career Development International, Vol. 25, 2020, pp. 373-388

[10] Michalec, B., Veloski, J. J., Hojat, M., & Tykocinski, M. L.: Identifying potential engaging leaders within medical education: The role of positive influence on peers, Medical Teacher, Vol. 37, 2015, pp. 677-683

[11] Cortellazzo, L., Bruni, E. T., & Zampieri, R.: The Role of Leadership in a Digitalized World: A Review, Frontiers in Psychology, Vol, 10, 2019

[12] Dulewicz, V., & Higgs, M.: Assessing leadership styles and organisational context, Journal of Managerial Psychology, Vol. 20, 2005, pp. 105-123

[13] Lundy, V., & Morin, P.: Project Leadership Influences Resistance to Change: The Case of the Canadian Public Service, Project Management Journal, Vol. 44, No. 4, 2013, pp. 45-64

[14] Bakker, A. B. and Demerouti, E.: The job demands-resources model: state of the art, Journal of Managerial Psychology, Vol. 22, No. 3, 2007, pp. 309-328

[15] Deci, E. L. and Ryan, R. M.: The 'what' and 'why' of goal pursuits: human needs and the self-determination of behavior, Psychological Inquiry, Vol. 11, No. 4, 2000, pp. 227-268

[16] Schaufeli, W. B.: Engaging Leadership: How to Promote Work Engagement? Frontiers in Psychology, Vol. 12, 2021

[17] Basinska, B. A., Gruszczynska, E., & Schaufeli, W.: Engaging leadership and work engagement in public servants: the indirect role of job-related affect, 11th Annual Conference of the EuroMed Academy of Business, 2018, pp. 126-137

[18] Rahmadani, V. G., Schaufeli, W. B., Ivanova, T., & Osin, E. N.: Basic psychological need satisfaction mediates the relationship between engaging leadership and work engagement: A cross-national study, Human Resource Development Quarterly, Vol. 30, 2019, pp. 453-471

[19] Rahmadani, V. G., & Schaufeli, W. B.: Engaging leadership and work engagement as moderated by "diuwongke": an Indonesian study, International Journal of Human Resource Management, 2020, pp. 1-29

[20] Rahmadani, V. G., & Schaufeli, W. B.: Engaging Leaders Foster Employees' Well-Being at Work, Proceeding of the 5th International Conference on Public Health, Vol. 5, 2019, pp. 1-7

[21] van Tuin, L., Schaufeli, W. B., & van Rhenen, W.: The Satisfaction and Frustration of Basic Psychological Needs in Engaging Leadership, Journal of Leadership Studies, Vol. 14, 2020, pp. 6-23

[22] Rahmadani, V. G., Schaufeli, W. B., Stouten, J., Zhang, Z., & Zulkarnain, Z.: Engaging Leadership and Its Implication for Work Engagement and Job Outcomes at the Individual and Team Level: A Multi-Level Longitudinal Study, International Journal of Environmental Research and Public Health, Vol. 17, No. 3, 2020

[23] van Tuin, L., Schaufeli, W. B., van Rhenen, W., & Kuiper, R. M.: Business Results and Well-Being: An Engaging Leadership Intervention Study, International Journal of Environmental Research and Public Health, Vol. 17, No. 12, 2020

[24] Rooting wellbeing and work engagement in basic human needs, Human Resource Management International Digest, Vol. 29, No. 2, 2021, pp. 26-28

[25] Salas-Vallina, A., Alegre, J., & López-Cabrales, A.: The challenge of increasing employees' well-being and performance: How human resource management practices and engaging leadership work together toward reaching this goal, Human Resource Management, Vol. 60, 2021, pp. 333-347

[26] van Tuin, L., Schaufeli, W. B., & van den Broeck, A.: Engaging leadership: Enhancing work engagement through intrinsic values and need satisfaction, Human Resource Development Quarterly, 2021, pp. 1-23

[27] Xiaojun, Z., & Yiwen, C.: A Study on the Chain Mediating Mechanism Effects of Reducing Employees' Turnover Intention Through Management, 2021 International Conference on Public Management and Intelligent Society (PMIS), 2021, pp. 66-70

[28] Firouznia, M., Allameh, S. M., & Hosseini, S. H.: Engaging leadership, engaging environment, engaging job, and engagement, International Journal of Process Management and Benchmarking, Vol. 11, No. 2, 2021, pp. 178-199

[29] Drewiske, G. W.: Engaging Leadership in Electrical Safety and Maintenance: Being the Advocate for Electrical and Safety Programs, IEEE Industry Applications Magazine, Vol. 27, 2021, pp. 24-28

[30] Mosley, P. A.: Bringing Back "Innovation", Library and Leadership Management, Vol. 27, No ½, 2013

[31] Mosley, P. A.: Engaging Leadership: Choices: You May Make More Than You Realize, Library and Leadership Management, Vol. 27, No. 4, 2013

[32] Mosley, P. A.: Leadership Writ Large, Beyond the Title, Library and Leadership Management, Vol. 28, No. 2, 2014

[33] Mosley, P. A.: Engaging Leadership: Knowing When to Disengage, Library and Leadership Management, Vol. 28, No. 4, 2014

[34] Klus, M. F., & Müller, J.: The digital leader: what one needs to master today's organisational challenges, Journal of Business Economics, Vol. 91, 2021, pp. 1189-1223

[35] Orhan, M. A., Castellano, S., Khelladi, I., Marinelli, L., & Monge, F.: Technology distraction at work, Impacts on self-regulation and work engagement, Journal of Business Research, Vol. 126, 2021, pp. 341-349

[36] Petrucci, T., & Rivera, M.: Leading Growth through the Digital Leader, Journal of Leadership Studies, Vol. 12, No. 3, 2018, pp. 53-56

[37] Gerards, R., Grip, A. D., & Baudewijns, C.: Do new ways of working increase work engagement, Personnel Review, Vol. 47, 2018, pp. 517-534

[38] Working Group on Digital Pedagogical Development (2021): digital competence expectations in public education, DigComp EU Recommendation

Validation of an Emotional Pattern Generator with an Eye-Tracking Research Experiment

Laura Trautmann[1], Attila Piros[1] and Bálint Szabó[2]

[1] Department of Machine and Product Design, Faculty of Mechanical Engineering, Budapest University of Technology and Economics, Műegyetem rkp. 3, 1111 Budapest, Hungary
trautmann.laura@gt3.bme.hu; piros.attila@gt3.bme.hu

[2] Department of Ergonomics and Psychology, Faculty of Economic and Social Sciences, Budapest University of Technology and Economics, Műegyetem rkp. 3, 1111 Budapest, Hungary, szabo.balint@gtk.bme.hu

Abstract: This article introduces the operation of a previously developed Emotional Pattern Generator and its user-centered validation, through the use of an emotion-driven design case study. As the primary work, various geometric patterns were generated by an in-house Emotional Pattern Generator (EmPatGen) that was successfully developed in MatLab to generate patterns based on user preferences. 33 individuals participated in this eye-tracking study, in order to fully comprehend the complexity of the fuzzy logic of the EmPatGen system. The participants were required to select a geometric pattern from a 3x3 palette, based on a situation, with the assistance of personas designed to indicate emotions during the tasks. Eye-tracking results contributed to a comprehensive understanding of the cognitive processes underlying pattern selection, allowing for the user-centric improvement of the applied pattern generator. For instance, it was discovered that female factors played a more significant role in the selection activities; therefore, the fuzzy logic of the generator presented in this article could be improved through a series of user-centered experiments.

Keywords: Eye-tracking; Emotional Design; Pattern Design; Interdisciplinary Research; Design for Experience

1 Introduction

The aesthetic appeal of a product is becoming increasingly significant in a variety of industries today. Theoretical psychological studies and researches [1] [2] have demonstrated that, in addition to a product's functionality, its aesthetic appearance is one of the most influential factors in the purchasing decision. The geometric properties - such as basic geometries and lines - of patterns that are simple structures consist typically of the repetition of simple elements or their mathematically described modifications. These are all associated with human emotions [3] [4].

The Emotional Pattern Generator (EmPatGen) is a previously developed system [5] [6] that assists product designers by generating patterns automatically based on user preferences. In the automotive industry, for instance, this program enables designers to create the most aesthetically pleasing car interiors and to more easily meet specific customer requirements.

Using the automotive industry as an example, until the 1930s, the focus of automotive technology was on meeting basic (mostly mechanical) functional requirements to produce durable vehicles. The shift at that time toward designing faster vehicles began with the development of the 1934 Chrysler Airflow automobile, which emphasized the importance of aerodynamics. Thus, the vehicles shrank and became more rounded. This resulted in efforts to redesign the entire cab layout to increase seating comfort in the passenger compartment while preserving the new outward visibility of automobiles [7] [8].

Prior to World War II, it was not necessary to consider human factors when adapting military technologies to make systems more effective and reliable. After World War II, the importance of human factor research expanded to the commercial aviation and automotive industries. This contributed to the fact that early automobile studies focused on human-centered design and crash-related injuries [9-11].

In recent years, the automotive industry has also placed a greater emphasis on emotion-driven design and the consumer's specific requirements [12]. In addition to meeting automotive standards and customer requirements, design customization is becoming an increasingly prevalent element in the design of twenty-first-century vehicles. During configuration, it is possible to specify the exterior and interior color, carpets, seat type, rev-counter, passenger display, wheels and calipers, and exhaust piper, among other options. As an example of the EmpatGen application, interior trim elements such as center console trims, instrument panels, and decoration panels were examined in depth.

Customization of interior trim elements is possible in two ways. On the one hand, customers could choose from a variety of materials (such as plastic, wood, aluminum, carbon fiber, piano black, stone, etc.), or it could be personalized with three-dimensional laser surface texturing [13]. Alternatively, consumers can achieve a unique appearance by using covered or wrapped components. They can create custom trims by applying foil stickers in a variety of colors and materials, including leather and marble.

Due to the importance of customization, the aim of this research is to validate the appropriateness of geometric patterns generated by the previously developed EmPatGen system, which enables consumers to participate in the design process and customize the interior elements of a vehicle according to their preferences. This concept satisfies the criterion of emotion-driven design, as the appearance of a unique interior could be created by providing particular moods. Examining the product experience, which is the user's overall experience with the product, one can conclude that the demand for products has shifted from pure functionality to

emotional satisfaction [14]. This study's findings could increase customer satisfaction, which is one of the primary goals, of many businesses [15].

2 Theoretical Background

As with colors and textures, geometries (triangle, rectangle, circle, etc.) affect human emotions, feelings, and moods. When repeated geometries are combined with a rule, patterns can be created. Patterns are utilized as an aesthetic element of a product, clothing, wall decoration, etc., but their meaning is rarely considered. Due to this deficiency, the relationships between pattern properties and emotions were investigated.

Literature studies reveal that while many industries are about to use patterns as an aesthetic feature on a product, only a few of them (such as the textile industry [16]) use patterns based on their emotional impact on humans. In the fields of interior design [17], jewelry manufacturing [18], packaging [19], and the textile and apparel industry [20], for instance, researchers use patterns on products without associating them with emotions.

It is also true for the auto industry, where only few relevant studies have focused on emotions. For instance, Jindo and Hirasago (1997) [21] focused on automobile interior design and its components (especially with speedometer and steering wheel). The researchers used computer graphics to create samples (speedometer, meter cluster, layout, etc.) for a subjective evaluation in which eight pairs of adjectives described the typical appearances of the devices. Participants assigned a numeric value to the eight pairs of adjectives with a 7-point semantic differential. Researchers used the following adjectives: playful, luxurious, elegant, retro-looking, likeable, sporty, clean-looking, and easy to understand.

Helander et. al (2013) [12] investigated the emotional intent of car purchasers and designers, demonstrating conclusively that car owners look beyond functionality to consider emotional design elements. A survey was conducted with 179 Asian and European car owners from ten nations. In the second experiment, seven car designers were instructed to include an affective feature in the design of their vehicle's dashboard, but they were given no further guidance. Since the results revealed emotional changes in the designers' designs, it was determined that designers must learn how to incorporate emotional design elements into the design process. In the study, the following adjectives were used: cute, cool, sexy, trendy, elegant, sporty, rugged, aggressive.

Further international studies [22] [23] have successfully measured the influence of emotion through the use of psycho-physiological tools (e.g. eye-tracking); however, the examination of the relationships between geometric patterns and emotions is novel in the fields of psychology, sociology, mathematics, and design.

In order to address this research gap, a study was conducted to determine the emotional impact of geometric patterns. In this research, geometric patterns were generated using the EmPatGen system, and an eye-tracking experiment series was designed to validate its proper operation.

3 Research Introduction

3.1 Research Preparation

Since both of the aforementioned studies being used *Elegant* and *Sporty* expressions, it was also utilized in this study. In addition to these, *Youthful* and *Classic* also represent a dimension, as both lists of adjectives contain similar phrases. The connected semantics for the word *Youthful* are *Cool*, *Trendy*, and *Playful*. *Classic* also appeared as a *Retro-looking* (and maybe *Rugged*) expression. In this research, the *Feminine* phrase is used for *Cute* and *Sexy*, and as an opposing pair, *Masculine* was also incorporated. The adjective *Luxurious* is related to *Elegant*, whereas *Aggressive* is linked to *Sporty*. *Clean-looking* and *Easy to understand* were excluded from this study because they are irrelevant in the context of decoration. Additionally, *Likeable* was not included because it is difficult to categorize.

To validate the relationships between the aforementioned expressions and the geometric elements, first the EmPatGen was developed [5] [6]. With EmPatGen, it is possible to create a pattern based on the desired emotions, which could also be of assistance to the designer. The mathematical model that runs in the background of the method connects two systems: the psychological relationships established between emotions and patterns and the algorithms of pattern development. The mathematical model must be able to account for human variables, language, and fuzzy boundaries. Fuzzy logic, a subset of artificial intelligence, is appropriate for this purpose. On the basis of the research findings, the input and output parameters, membership functions, and fuzzy rule system were defined in the MatLab environment as part of the development of the steps for the application of fuzzy logic.

The generic structure of a fuzzy system is illustrated in Figure 1. In essence, it is comprised of input data, a fuzzy rule base, an inference mechanism, and output data. Fuzzification and defuzzification refer to the transformation of data from crisp to fuzzy and from fuzzy to crisp [24].

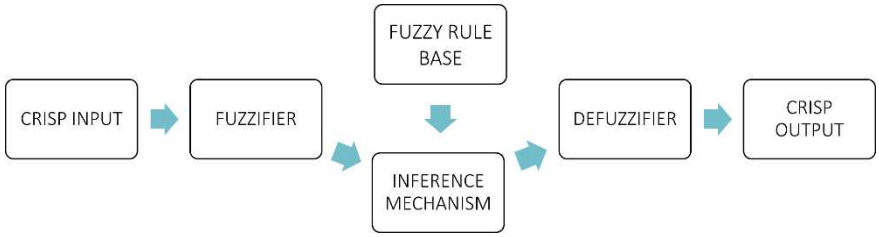

Figure 1
Generic structure of a fuzzy system (Source: own edition)

EmPatGen uses the following general form of a fuzzy rule with one input and one output:

$$R: If\ x\ is\ A, then\ y\ is\ B \tag{1}$$

In this equation, $x \in X$ is the input and $y \in Y$ is the output variable (X is the universe of discourse for the input variable, and Y is the universe of discourse for the output variable). In addition, parameters A and B are linguistic labels expressed using fuzzy sets. Rule R has fuzzy set A as its antecedent, and fuzzy set B as its consequent. The general form of a fuzzy rule with multiple inputs and a single output dimension is the so-called Mamdani form [25].

$$R: If\ x_1\ is\ A_1\ and\ ...\ and\ x_n\ is\ A_n\ then\ y\ is\ B \tag{2}$$

where $x = (x_1, \ldots, x_n)$ is the input vector; $x_j \in X_j$, $X = X_1 \times \ldots \times X_n$ is the n-dimensional universe; $A = (A_1, \ldots, A_n)$ is the antecedent vector; $y \in Y$ is the output variable; Y is the universe for the output; and B is the consequent set.

The fuzzy system's inference mechanism compares the given observation to the antecedent parts of fuzzy rules. On the basis of these comparisons, the degree to which each rule matches the observation will be determined. These degrees are utilized by the inference mechanism when considering the consequent parts of fuzzy rules. In the case of Mamdani inference [25], each rule's consequent fuzzy set is segmented based on the rule's degree of matching, which provides a subconclusion for the rule. The conclusion of the given observation for the entire rule base can be determined by combining the previously calculated subconclusions. This outcome is a fuzzy set, but in the majority of cases, a crisp value is expected. Consequently, the crisp value that best characterizes the conclusion fuzzy set should be determined. This process is referred to as defuzzification.

Other researchers have successfully linked mathematics and art using fuzzy logic [26], so the application of this method to the current task is appropriate. In this system, however, the pattern is determined by emotional inputs, whereas it was previously used to shape geometries.

Therefore, the three inputs of the used fuzzy system are dynamics, style, and orientation, while the eleven outputs cover the four variables of basic geometry and

seven variables of pattern space. The fuzzy logic consists of eight rules that encompass all input ranges based on Trautmann, Piros and Botzheim (2020) [5].

According to our perspective, Table 1 demonstrates the characteristics of the expressions used as input parameters in this study.

Table 1

Expressions used in EmPatGen and their characteristics

Expression (EmPatGen inputs)	**Characteristics**
Elegant	Luxurious, stylish, beautiful, sophisticated, business
Sporty	Aggressive, active, powerful, dynamic, exiting
Classic	Old, timeless, high class, serious, executive
Youthful	Bright, trendy, modern, active, dynamic
Feminine	Girly, curvy, round, attractive
Masculine	Strong, powerful, sporty

Trautmann and Piros (2017) [27] demonstrated that not only the Basic Geometry (circle, triangle, etc.) of a pattern has an effect on people, but also the Pattern Space, or the manner in which the pattern spreads. In consequence of this, the parameters are linked to these two main categories. These attributions are summarized in Table 2 and were explained in greater detail by Trautmann and Piros (2020) [6].

Table 2

Parameters of EmPatGen and their definitions

Related to	**Name**	**Definition**
Basic Geom.	r	Uniform scale: scale all sides of the geometry equally
	e	Non -uniform scale: scale sides of the geometry
	n	Side: number of sides of the geometry
	rot	Rotation: rotate the geometry
Pattern Space	VStS	Row distance: distance of the rows of the pattern
	A	Amplitude: the height of periodic waves in a row
	dRng	Dynamic Range: the number of varying pattern members
	dSft	Dynamic Shift: the distance between of same pattern members in neighboring rows
	dScU	Dynamic uniform scale: the value of uniform scale
	dSnU	Dynamic non-uniform scale: the value of non-uniform scale
	dRot	Dynamic rotation: the value of dynamic rotation

The definition of the various parameters (Table 2) reveals a few similarities between the parameters related to Basic Geometry and Pattern Space. There are pairs that modify the pattern similarly, but one pair modifies the Basic Geometry while the other defines the Pattern Space. As a result, the correlation between these columns will be identical. The pairs consist of r – dScU, e – dSnU, and rot – dRot.

In EmPatGen, nine expressions or characteristics listed in Table 1 could be quantified using the parameters in Table 2 based on research from the scientific literature. These are: *Dynamic, Exciting, Aggressive*, *Active; Calm*, *Stable, Feminine, Masculine* and *Strong*. These terms are all adjectives that could be used to describe emotions and feelings. Feelings are entirely mental, whereas emotions include behavioral and physiological components. *Stable, Aggressive*, *Calm* or *Strong* are feelings, whereas *Dynamic, Exciting, Active, Feminine*, or *Masculine* are behaviors. These emotions and feelings have been assigned to EmPatGen's inputs. The summarized values are shown in the green rows, while the combination of the inputs with their summarized values can be found at the bottom of Figure 2.

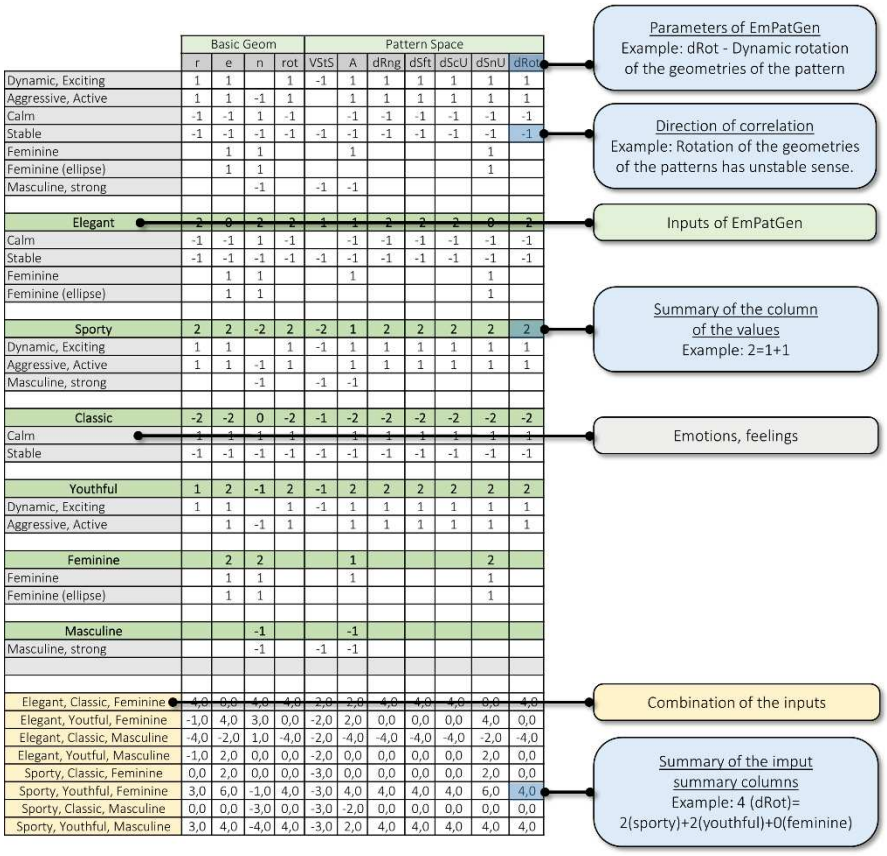

	Basic Geom				Pattern Space						
	r	e	n	rot	VStS	A	dRng	dSft	dScU	dSnU	dRot
Dynamic, Exciting	1	1		1	-1	1	1	1	1	1	1
Aggressive, Active	1	1	-1	1		1	1	1	1	1	1
Calm	-1	-1	1	-1		-1	-1	-1	-1	-1	-1
Stable	-1	-1	-1	-1	-1	-1	-1	-1	-1	-1	-1
Feminine		1	1			1				1	
Feminine (ellipse)		1	1							1	
Masculine, strong			-1		-1	-1					
Elegant	2	0	2	2	1	1	2	2	2	0	2
Calm	-1	-1	1	-1		-1	-1	-1	-1	-1	-1
Stable	-1	-1	-1	-1	-1	-1	-1	-1	-1	-1	-1
Feminine		1	1			1				1	
Feminine (ellipse)		1	1							1	
Sporty	2	2	-2	2	-2	1	2	2	2	2	2
Dynamic, Exciting	1	1		1	-1	1	1	1	1	1	1
Aggressive, Active	1	1	-1	1		1	1	1	1	1	1
Masculine, strong			-1		-1	-1					
Classic	-2	-2	0	-2	-1	-2	-2	-2	-2	-2	-2
Calm	-1	-1	1	-1		-1	-1	-1	-1	-1	-1
Stable	-1	-1	-1	-1	-1	-1	-1	-1	-1	-1	-1
Youthful	1	2	-1	2	-1	2	2	2	2	2	2
Dynamic, Exciting	1	1		1	-1	1	1	1	1	1	1
Aggressive, Active		1	-1	1		1	1	1	1	1	1
Feminine		2	2			1				2	
Feminine		1	1			1				1	
Feminine (ellipse)		1	1							1	
Masculine			-1			-1					
Masculine, strong			-1		-1	-1					
Elegant, Classic, Feminine	4,0	0,0	4,0	4,0	2,0	2,0	4,0	4,0	4,0	0,0	4,0
Elegant, Youtful, Feminine	-1,0	4,0	3,0	0,0	-2,0	2,0	0,0	0,0	0,0	4,0	0,0
Elegant, Classic, Masculine	-4,0	-2,0	1,0	-4,0	-2,0	-4,0	-4,0	-4,0	-4,0	-2,0	-4,0
Elegant, Youtful, Masculine	-1,0	2,0	0,0	0,0	-2,0	0,0	0,0	0,0	0,0	2,0	0,0
Sporty, Classic, Feminine	0,0	2,0	0,0	0,0	-3,0	0,0	0,0	0,0	0,0	2,0	0,0
Sporty, Youthful, Feminine	3,0	6,0	-1,0	4,0	-3,0	4,0	4,0	4,0	4,0	6,0	4,0
Sporty, Classic, Masculine	0,0	0,0	-3,0	0,0	-3,0	-2,0	0,0	0,0	0,0	0,0	0,0
Sporty, Youthful, Masculine	3,0	4,0	-4,0	4,0	-3,0	2,0	4,0	4,0	4,0	4,0	4,0

Figure 2

Summary of literature research related to basic geometry and pattern space attributions

(Source: own edition)

The associations between the EmPatGen parameters and the aforementioned emotions and feelings can take the values -1, 1, or empty (Figure 2). These numbers indicate the correlation's direction. According to studies [3] [4], the triangle is

associated with adjectives *Aggressive*, *Active*, *Masculine*, *Strong*, and *Stable*. In this instance, the correlation in the "n" column is -1, as the goal in terms of the number of sides of the geometry is to reduce the number of sides. For *Feminine* and *Calm* emotions, round shapes are required. Simonds and Starke (2013) [28] demonstrates that while *Calm*, *Stable*, and *Masculine* adjectives are associated with horizontal and vertical lines, the *Dynamic*, *Exciting*, and *Feminine* characteristics and expressions are associated with waves, which has an effect on the "A" column that generates waves. If "A" is 0 in the model, the pattern's rows will be horizontal. In addition, Trautmann, Piros and Hámornik (2019) [29] also provided information, such as the finding that when the distance between the rows of the pattern (VStS value) is smaller, people perceive the pattern to be more *Dynamic*.

Therefore, EmPatGen is a software product that was created to link the fundamental geometries with a variety of emotions and feelings. Figure 3 [27] depicts the EmPatGen user interface: when the user adjusts the rate of the slider on the program's interface, the software generates a 2D pattern as a DXF file automatically.

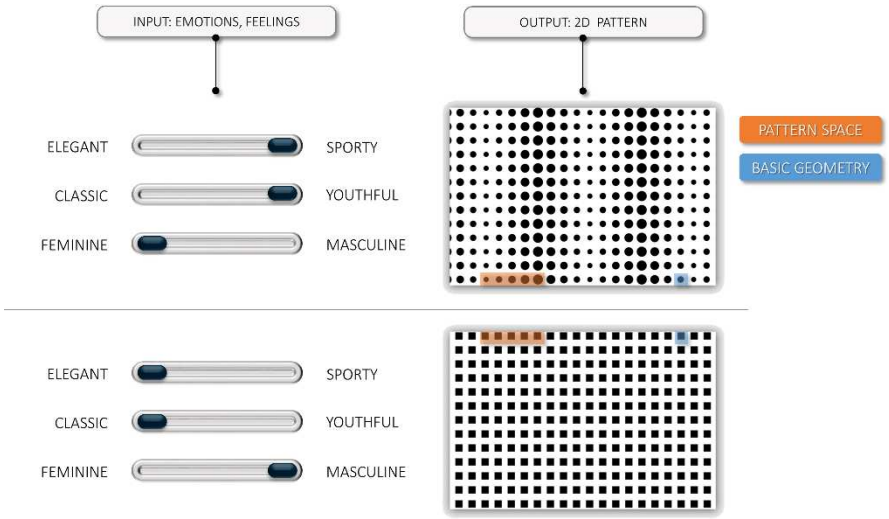

Figure 3
Concept of EmPatGen (Source: own edition)

3.2 Aim of the Research and Methodology

The aim of this research was to validate EmPatGen. For the validation, an eye-tracking system comprised of Tobii Studio software and a T120 monitor was utilized. With the use of the eye-tracking technology we were able to quantify the subject's responses and determine the location and frequency of the subject's focus on a particular pattern during this experiment by analyzing the subject's eye movement sequences [30].

Before the research design was developed, a hypothesis regarding the validation of EmPatGen was formulated. The hypothesis of this study is that human-centered findings will contribute to the improvement of the EmPatGen generator.

In this study, the initial step was to administer a brief questionnaire containing the following question-areas: gender, age, level of education, length of time with a driver's license, self-reported driving habits, etc. In the second phase, eye-tracking technology was applied in this research to quantify gaze location to understand human behavior. In this series of experiments, 33 subjects performed a total of eight tasks. Finally, participants were questioned in a structured interview regarding their perspective and inner motivation throughout the task selection procedure.

Figure 4 illustrates an example task from the experiment in which Vilmos was tasked with personalizing the Elegant-Classic-Masculine personality. In all of the tasks, the question was the same: *"For wrapping a present for the described person on the side, what type of pattern would you choose?"* Then, nine patterns were displayed, and the participants had to click on one of them to proceed. Using eye-tracking software, the selection processes of individuals could be observed, and the selected patterns could be easily compared to the expected (EmPatGen) outcomes.

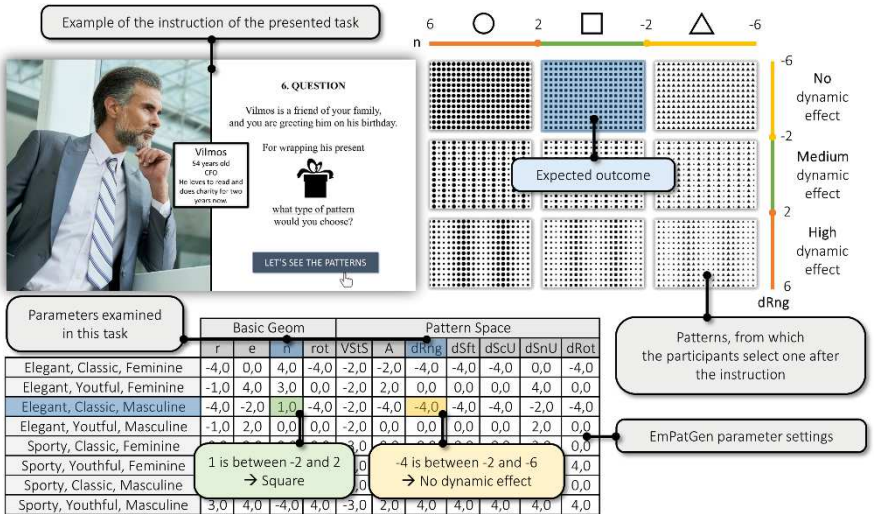

	Basic Geom				Pattern Space						
	r	e	n	rot	VStS	A	dRng	dSft	dScU	dSnU	dRot
Elegant, Classic, Feminine	-4,0	0,0	4,0	-4,0	-2,0	-2,0	-4,0	-4,0	-4,0	0,0	-4,0
Elegant, Youtful, Feminine	-1,0	4,0	3,0	0,0	-2,0	2,0	0,0	0,0	0,0	4,0	0,0
Elegant, Classic, Masculine	-4,0	-2,0	1,0	-4,0	-2,0	-4,0	-4,0	-4,0	-4,0	-2,0	-4,0
Elegant, Youtful, Masculine	-1,0	2,0	0,0	0,0	-2,0	0,0	0,0	0,0	0,0	2,0	0,0
Sporty, Classic, Feminine											0,0
Sporty, Youthful, Feminine											4,0
Sporty, Classic, Masculine											0,0
Sporty, Youthful, Masculine	3,0	4,0	-4,0	4,0	-3,0	2,0	4,0	4,0	4,0	4,0	4,0

Figure 4

Example task from the experiment. (Source: own edition).

Note: During the test, the participants have seen the instruction first (upper-left corner), and after that, the pattern palettes (upper-right corner)

Two parameters were included in the creation of the patterns. The number of sides of the geometry ("n") was selected from the Basic Geometry parameter group in every case. The other parameter belonged to the Pattern Space group, which was distinct for each task. In this instance, the "dRng" parameter was chosen, which specifies the number of pattern members that vary. Circle, square, and triangle

geometries were defined in relation to "n" in the tasks involving circle, square, and triangle geometries. On the vertical axis of the patterns, the parameter quantity for the selected Pattern Space grew from "No" to "High" dynamic effect.

In Figure 4, according to the result, the following borders were distinguished: from -6 to -2; from -2 to +2; from +2 to +6. The task's expected outcome was assigned according to the category where the number from the summary table belongs. For instance, in this specific example, "n" is in the middle category, which is considering the number of sides of the geometries, the square column. "dRng" in the -2 to -6 category, which indicates the "No dynamic effect" row. That is why, in this task, the expected outcome was the second pattern.

In the same manner, each of the remaining three personas (Anna, Elena, Zoli) had a unique personality and appeared twice (Figure 5). This concept originated from a design thinking process known as "persona," which is a modeling tool of human-centered design that is primarily utilized during the ideation phase of design [31]. The persona is a possible user archetype [32] that conveys a certain user requirement with their name, age, hobbies, etc. The other four examples (Sporty-Classic-Masculine, Elegant-Youthful-Feminine, etc.) were not examined in this test because participants' attention could wane throughout a lengthy examination.

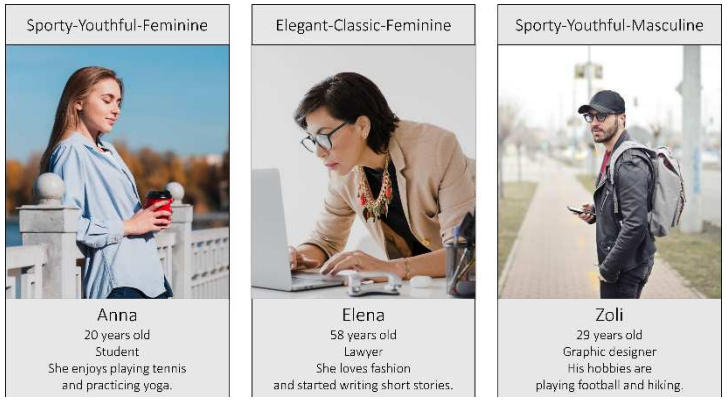

Figure 5

Personalized characters for the eye-tracking serious of experiments (Source: own edition)

Using eye-tracking technology, it is possible to determine where individuals are looking during a test. Figure 6 [33] illustrates the working mechanism of this technology, which consists of five major components: an eye tracker, the illuminator, the cameras, the image processing algorithms, and the position and gaze point of the eyes.

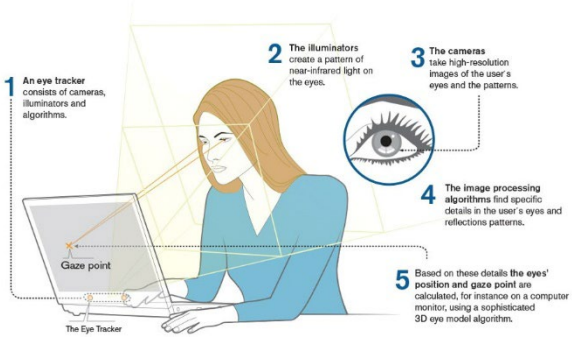

Figure 6

The operation of the used eye-tracking technology (Source: [33])

In addition to recording eye movements, the trackers also recorded the duration and sequence of the attention's location on the screen. Figure 7 illustrates a recording of the example task.

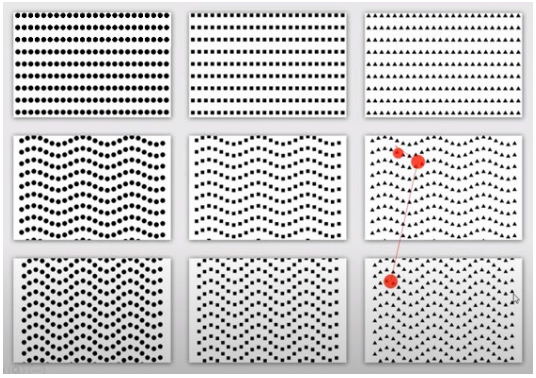

Figure 7

Sequence detection during the example task (gaze plot visualization) (Source: own edition)

Each pattern in this experiment indicated an area of interest (AOI). It is possible to define regions and assign all fixations that fall within them using the AOI tool [34]. Eye-tracking software allows researchers to manually select different AOI areas for further quantitative analyses. Length, number of fixations, and number of visits (returns to the area) were the most frequently employed indicators in AOI analyses, as they indicate the subjective importance of the given areas [35].

4 Results

This examination was taken by a total of 33 people. There were 60,6% men and 39,4% women in this group. Eighty percent of the participants had a college degree. The average age was 37.50 years (standard deviation, SD=15.18). The youngest attendee was 19 years old, and the oldest participant was 79 years old. 36,4% of the population used their license daily.

The interview revealed that on a 1 to 4 Likert scale, respondents liked cars an average of 3.34 (SD=0.7) and were receptive to the arts an average of 3.37 (SD=0.79). Pureness, harmony, color, excellent material quality, comfort, design, and clarity were deemed to be the most essential aesthetic characteristics of an automobile's interior, according to the respondents. Aside from these, participants also discussed the significance of specific car interior elements, such as the dashboard, seats, and steering wheel, which areas could be the most suitable for the application of the EmPatGen system.

It was discovered that people do not necessarily choose the pattern that they viewed for the longest amount of time (marked with red color), as shown on the Heat Map of the example task (Figure 8) [36]. Considering Figure 8, the central areas, particularly the fifth (middle) pattern in the 3x3 palette were examined for a considerable amount of time. Consequently, the middle patterns appear to be the most intriguing. However, the pattern that was chosen most frequently throughout the entire study was the second.

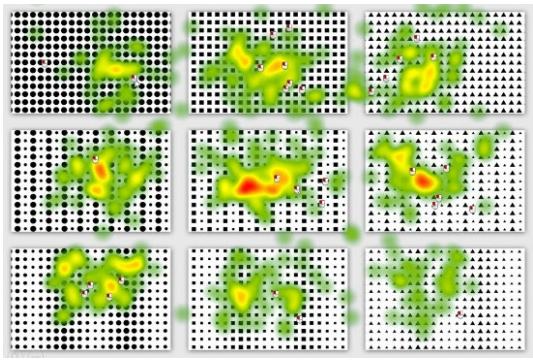

Figure 8

Heat Map based on fixation length of the example task (Source: own edition)

Each pattern indicated an area of interest (AOI) of the eye-tracking technology, as depicted in Figure 9. This was due to the use of statistical tools to identify the areas that were truly of most interest to the subjects. It is possible to retrieve the number of fixations as an indicator of the subjective significance of the pattern.

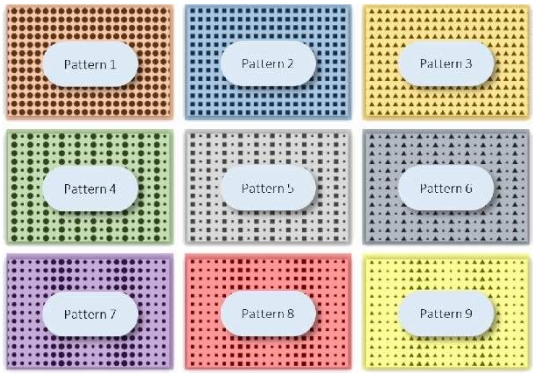

Figure 9
Area of interest (AOI) selection used in the current research for further statistical analysis
(Source: own edition)

The number of fixations for the example task is displayed in Table 3, and it can be seen that the fifth pattern (P5) has the highest summarized fixation value. There are a total of 93 fixations in this region, as reported by 33 participants. The maximum Fixation Count values occurred on the fifth pattern in seven out of eight instances, suggesting that the middle pattern was used as a starting point before moving on to examine the other patterns. Consequently, the fixation began and ended there.

Table 3
Number of fixations (eye tracking results from AOI selection)

Participant ID	P 1	P 2	P 3	P 4	P 5	P 6	P 7	P 8	P 9
1	4	4	1	2	2	1	1	1	-
2	-	2	1	2	9	3	2	2	2
3	1	2	5	1	6	3	1	5	1
4	4	2	1	2	1	1	1	-	1
5	1	-	3	-	1	11	-	1	3
6	1	1	-	2	8	1	1	1	-
7	-	1	3	-	2	8	-	2	3
8	1	2	2	-	-	-	-	-	7
9	1	-	-	-	-	-	1	-	-
10	-	3	-	-	1	-	-	-	-
11	1	2	1	3	9	2	-	4	-
12	1	6	1	1	10	2	3	3	1
13	5	6	2	26	4	2	32	5	1
14	3	5	4	2	-	1	-	-	-
15	1	-	1	2	1	1	1	-	-
16	-	2	2	1	1	5	1	1	4
17	1	1	2	2	1	7	1	1	1

18	-	-	-	-	2	-	-	-	-
19	-	3	1	1	10	3	-	-	1
20	2	2	2	3	5	1	14	1	3
21	2	6	2	1	3	1	1	3	-
22	-	1	1	-	3	1	1	13	1
23	5	6	1	6	3	1	-	-	-
24	-	-	4	1	1	1	-	-	-
25	-	-	1	1	-	-	-	-	-
26	-	-	-	-	-	-	-	-	-
27	-	2	1	-	-	-	-	-	-
28	3	10	4	2	2	1	-	1	2
29	1	1	3	1	-	1	2	1	-
30	1	7	1	2	5	-	1	2	3
31	2	3	4	1	3	6	1	-	1
32	1	1	-	-	-	-	1	1	-
33	1	-	6	1	-	2	-	1	-
All fixations	**43**	**81**	**60**	**66**	**93**	**66**	**66**	**49**	**35**

The Kolmogorov-Smirnov test can be used to determine if the variables under study have a normal distribution. Since neither set of generated data follows a normal distribution (all p-values were less than 0.05), the Wilcoxon test can be used to identify patterns that participants found significantly more interesting than the others. Comparing the obtained results, AOI 4, 7, 8, and 9 exhibited a significant difference from the middle pattern. For this reason, the 1, 2, 3, 5, and 6 patterns were significantly more significant than the others in this task (Table 4). 24 participants selected one of these patterns, and for this task, the expected result (pattern 2) was selected the majority of the time by 7 out of 33 participants.

Table 4
Wilcoxon Signed Ranks Test

Pattern pairs	1 - 5	2 - 5	3 - 5	4 - 5	6 - 5	7 - 5	8 - 5	9 - 5
Z	-1.883	-.266	-1.044	-2.056	-1.390	-2.370	-2.571	-2.639
Asymp. Sig. (2-tailed)	0.06	0.79	0.297	0.04	0.164	0.018	0.01	0.008

From the evaluation of the results, it can be concluded that participants most frequently selected patterns 5, 9, 2, and 4 for male personalities, while patterns 1 and 7 were chosen for female personalities (Table 5). In the elegant-classic case, the choice was made for 5, 7, 2 patterns, while in the sporty-youthful case, the 1, 9, 7, 4 patterns were selected. According to these results, it seems that feminine factors played a more significant role during the selection. Female personas fall every time into the first column of the palette. Those patterns are containing circle basic geometries, which indicates feminine attributes. Interestingly, masculine factors have not shown this kind of direction.

Moreover, it appears that changing the size of the geometry was the most dynamic change, and similar outcomes were chosen for these patterns. Where the perceived difference between patterns was smaller, such as when the size of the patterns did not change and only rotation was used, responses were much more dispersed.

As shown in Table 5, of the eight tasks, the expected outcome fell into the most interesting cases five times, and was identical to the most popular pattern twice.

Table 5
Results of the pattern selection

Task Number	1	2	3	4	5	6	7	8
Input: Elegant - Sporty	E	S	E	S	S	E	S	E
Input: Classic - Youthful	C	Y	C	Y	Y	C	Y	C
Input: Masculine-Feminine	M	F	F	M	F	M	M	F
Most interesting patterns by Heat Map Visualization	1,2,4,5,6	1,3,4,5,6,7,8,9	4,5,6,7,8,9	1,2,3,4,5,6,7,8,9	4,7	1,2,3,5,6	4,5,6,7	1,4,5,7,8
Pattern number of the expected outcome	2	8	1	9	8	2	9	1
The frequency of the expected outcome chosen by subjects (out of the 33)	5	4	3	7	3	7	1	4
Number of the most selected pattern	5	1	7	9	7	2	4	7

Discussion and Conclusion

Nowadays, the importance of customization and the investigation of any affected emotions caused by car design, is becoming increasingly important in the automotive industry. This study proposes a method for potential car owners to participate in the design process and obtain a unique car interior, based on their preferences, such as elegant, classic, sporty and so on. It is possible to provide emotions and feelings in this presented system, and the model automatically generates a geometric pattern based on the inputs, using fuzzy logic. This design could be applied to the desired car interior trim elements. This system is required to investigate more scientific areas; thus, in previous studies, the relationship between human emotions and geometric patterns was explored, through interviews and survey examination.

In this article, selection-based tasks were created to validate the EmPatGen with 33 participants. Using eye-tracking technology, where it is possible to monitor the participants' selection processes, the EmPatGen validation was conducted. The results indicate that feminine factors have a greater impact on individuals; therefore, the fuzzy logic should be imporved. If the weight of the Feminine input values is multiplied by three, the expected pattern moves much closer to the position of the most intriguing pattern, referred as "modified expected outcome" in Table 6.

Seven times out of eight tasks, the expected pattern fell within the most interesting patterns, and three times it was identical to the most chosen pattern.

Table 6
Summary of the results of the pattern selection used for the improvement of EmPatGen

Task number	**1**	**2**	**3**	**4**	**5**	**6**	**7**	**8**
Pattern number of the expected outcome	2	8	1	**9**	8	**2**	9	1
Pattern number of the modified expected outcome	2	7	4	**9**	**7**	**2**	9	1
Number of the most selected pattern	5	1	7	**9**	**7**	**2**	4	7
The expected outcome is in the most interesting cases?	**Yes**	**Yes**	No	**Yes**	No	**Yes**	No	**Yes**
The modified expected outcome is in the most interesting cases?	**Yes**	**Yes**	**Yes**	**Yes**	**Yes**	**Yes**	No	**Yes**

As can be seen, the human-centered research methodology performed admirably in validating EmPatGen, and thus the formulated hypothesis is accepted. The validation series of experiments produced superior results for the generator's further development. Future research could apply the findings to other disciplines such as exterior and interior architecture, textile, jewelry, decoration, stationery, package design industries or other product design segments.

Limitations

The research boundaries limited the possibilities for randomizing the positions of the patterns; however, this randomness will be considered in future research. Aside from that, it would be interesting to measure the effect of right and left-handed subjects, as this could also influence the outcome of the experiments. This specific research step, described in the article, was prepared to validate the model; however, more information is required with a larger subject number (60 people) and with different task types, taking into account the factors mentioned above.

Acknowledgments

The research reported in this paper is part of project no. BME-NVA-02, implemented with the support provided by the Ministry of Innovation and Technology of Hungary from the National Research, Development and Innovation Fund, financed under the TKP2021 funding scheme.

References

[1] Türkyilmaz, A.; Kantar, S.; Bulak, M. E.; Uysal, O.; others. User Experience Design: Aesthetics or Functionality? Managing Intellectual Capital and Innovation for Sustainable and Inclusive Society: Managing Intellectual Capital and Innovation; Proceedings of the MakeLearn and TIIM Joint International Conference 2015, ToKnowPress, 2015, pp. 559-565

[2] Norman, D. The design of everyday things: Revised and expanded edition; Basic books, 2013

[3] Fogelström, E. Investigation of Shapes and Colours as Elements of Character Design; Uppsala Universitet, 2013

[4] Frutiger, A. Signs and Symbols: Their Design and Meaning; Van Nostrand Reinhold, 1989

[5] Trautmann, L.; Piros, A.; Botzheim, J. Application of the Fuzzy System for an Emotional Pattern Generator. Applied Sciences 2020, 10, 6930

[6] Trautmann, L.; Piros, A. The concept of EmPatGen (Emotional Pattern Generator). SN Applied Sciences 2020, 2, 982

[7] Wells, R. Occupant Protection and Automobile Safety in the US since 1900; SAE, 2012

[8] Asmus, T.; Bragg, G.; Cowan, C.; Gibbs, L.; Johnston, R.; Ludvigsen, K.; Rinek, L.; Rinschler, G.; Rizvi, S.; Woehrle, W.; others. The automobile: a century of progress; Vol. SAE Order No. R-203, SAE, 1997

[9] Sinaiko, H. W. Selected papers on human factors in the design and use of control systems; Vol. 140, Dover Publications, 1961

[10] Chapanis, A.; Garner, W. R.; Morgan, C. T. Applied experimental psychology: Human factors in engineering design; John Wiley & Sons Inc, 1949

[11] National Research Council, C.o.U.W. A survey report on human factors in undersea warfare; Committee on Undersea Warfare, National Research Council, 1949

[12] Helander, M. G.; Khalid, H. M.; Lim, T. Y.; Peng, H.; Yang, X. Emotional needs of car buyers and emotional intent of car designers. Theoretical Issues in Ergonomics Science 2013, 14, 455-474

[13] Hase, C. Laser Texturing Adds Another Level of In-Mold Decoration Possibilities

[14] Yin, D.; Li, T.; Liao, Z. Research on the Evaluation Modeling Method of User Experience Quality under Uncertain Noise Environment. Mathematical Problems in Engineering 2020, 2020

[15] Ahmad, A.; Barukab, O. A Novel Approach to Identify the Categories of Attributes for the Three-Factor Structure in Customer Satisfaction. Complexity 2020, 2020

[16] Kim, N.Y.; Shin, Y.; Kim, E.Y. Emotion-based textile indexing using neural networks. International Conference on Human-Computer Interaction. Springer, 2007, pp. 349-357

[17] Saito, S.; Hiyama, A.; Tanikawa, T.; Hirose, M. Indoor marker-based localization using coded seamless pattern for interior decoration. 2007 IEEE Virtual Reality Conference. IEEE, 2007, pp. 67-74

[18] Gulati, V. Rapid tooling for producing stretch-formed jewelry. International Journal of Computer Applications 2011, 975, 8887

[19] Auttarapong, D. Package design expert system based on relation between packaging and perception of customer. Procedia Engineering 2012, 32, 307-314

[20] Rödel, H.; Schenk, A.; Herzberg, C.; Krzywinski, S. Links between design, pattern development and fabric behaviours for clothes and technical textiles. International Journal of Clothing Science and Technology 2001

[21] Jindo, T.; Hirasago, K. Application studies to car interior of Kansei engineering. International journal of industrial ergonomics 1997, 19, 105-114

[22] Bendall, R. C.; Mohamed, A.; Thompson, C. Emotional real-world scenes impact visual search. Cognitive processing 2019, 20, 309-316

[23] Li, M.; Cao, L.; Zhai, Q.; Li, P.; Liu, S.; Li, R.; Feng, L.; Wang, G.; Hu, B.; Lu, S. Method of Depression Classification Based on Behavioral and Physiological Signals of Eye Movement. Complexity 2020, 2020

[24] Hellendoorn, H.; Thomas, C. Defuzzification in fuzzy controllers. Journal of Intelligent & Fuzzy Systems 1993, 1, 109-123

[25] Mamdani, E. H.; Assilian, S. An experiment in linguistic synthesis with a fuzzy logic controller. International journal of man-machine studies 1975, 7, 1-13

[26] Feijs, L. M. A program for Victory Boogie Woogie. Journal of Mathematics and the Arts 2019, 13, 261-285

[27] Trautmann, L.; Piros, A. Identifying the Emotions in Order to Design the Patterns of Consumer Products. Proceedings of the 11th International Workshop on Integrated Design Engineering, 2017, pp. 61-68

[28] Starke, B. W.; Simonds, J. O. Landscape architecture: a manual of environmental planning and design; McGraw-Hill Education New York, 2013

[29] Trautmann, L.; Piros, A.; Hámornik, B. Handling Human Factors in Car Interior Design. Human Behaviour in Design, 2019, pp. 113-124

[30] Wang, X.; Zhao, X.; Ren, J. A New Type of Eye Movement Model Based on Recurrent Neural Networks for Simulating the Gaze Behavior of Human Reading. Complexity 2019, 2019

[31] So, C.; Joo, J. Does a persona improve creativity? The Design Journal 2017, 20, 459-475

[32] Pruitt, J.; Adlin, T. The persona lifecycle: keeping people in mind throughout product design; Elsevier, 2010

[33] Tobii. How do Tobii Eye Trackers work?

[34] Orquin, J. L.; Ashby, N. J.; Clarke, A. D. Areas of Interest as a Signal Detection Problem in Behavioral Eye-Tracking Research. Journal of Behavioral Decision Making 2016, 29, 103-115. doi:10.1002/bdm.1867

[35] Józsa, E.; Hámornik, B. Find The Difference! Eye Tracking Study on Information Seeking Behavior Using an Online Game. Journal of Eye Tracking, Visual Congnition And Emotion 2012

[36] Holmqvist, K.; Nyström, M.; Andersson, R.; Dewhurst, R.; Jarodzka, H.; Van de Weijer, J. Eye tracking: A comprehensive guide to methods and measures; OUP Oxford, 2011

Current Safety Legislation of Food Processing Smart Robot Systems – The Red Meat Sector

Kristóf Takács[1], Alex Mason[2], Luis Eduardo Cordova-Lopez[3], Márta Alexy[4], Péter Galambos[5], and Tamás Haidegger[6]

[1]Antal Bejczy Center of Intelligent Robotics, Óbuda University; kristof.takacs@irob.uni-obuda.hu
[2]Norwegian University of Life Science (NMBU), As, Norway; alex.mason@nmbu.no and also with the Research and Development Department, Animalia AS, Oslo 0585, Norway
[3]Norwegian University of Life Science (NMBU), As, Norway; luis.eduardo.cordova-lopez@nmbu.no
[4]University Research and Innovation Center (EKIK), Óbuda University; alexy.marta@uni-obuda.hu
[5]EKIK, Óbuda University and John von Neumann Faculty of Informatics, Óbuda University; peter.galambos@irob.uni-obuda.hu
[6]EKIK, Óbuda University; tamas.haidegger@irob.uni-obuda.hu

Abstract: Ensuring the safety of the equipment, its environment and most importantly, the operator during robot operations is of paramount importance. Robots and complex robotic systems are appearing in more and more industrial and professional service applications. However, while mechanical components and control systems are advancing rapidly, the legislation background and standards framework for such systems and machinery are lagging behind. As part of a fundamental research work targeting industrial robots and industry 4.0 solutions for completely automated slaughtering, it was revealed that there are no particular standards addressing robotics systems applied to the agri-food domain. More specifically, within the agri-food sector, the only standards existing for the meat industry and the red meat sector are hygienic standards related to machinery. None of the identified standards or regulations consider the safety of autonomous robot operations or human–robot collaborations in the abattoirs. The goal of this paper is to provide a general overview of the regulations and standards (and similar guiding documents) relevant for such applications, that could possibly be used as guidelines during the development of inherently safe robotic systems for abattoirs. Reviewing and summarizing the relevant standard and legislation landscape should also offer some instrumental help regarding the foreseen certification procedure of meat processing robots and robot cells for slaughterhouses in the near future.

Keywords: robotic meat processing, robot standardization, agri-food robotics

1 Introduction

In the EU (European Union), the CE mark (Conformité Européenne) is part of the EU's harmonised legislation, signifying that a product has been assessed to comply with the high safety, health and environmental protection requirements set by the EU. CE mark must be obtained for every new electrical product sold in the EEA (European Economic Area), that supports fair competition too, since all manufacturers have to fulfill the requirements of the same set of rules [1]. The approval procedure can be managed by the manufacturer (this way, the CEO bears all legal responsibility), or by an independent certification body (which is called a Notified Body, in case registered in the EU). Upon the system assessment (carried out by either a Notified Body or the manufacturer), the main goal is to ensure the conformity of the product with the regulations (legal requirements) before the product is put on the European market.

By default, standards are voluntary for product manufacturers. They should be based on a consensus between industrial and academic experts, codifying already existing good practices, methods and general requirements. Nevertheless, by definition, they are intended to be the best available set of requirements toward a certain field; for instance, the safety aspects of a type of system, standards often serve as the basis of regulations enacted by lawmakers. For example, the ISO/IEC 60601-1 standard (International Organization for Standardization, International Electrotechnical Commission) regarding medical electrical equipment became the basis of the EC MD (European Commission Machinery Directive) and the subsequent MDD (Medical Device Directive). When a Notified Body is dealing with a new system, it is usually considering the recommendations of some non-compulsory standards during the system assessment as well. Therefore, developers and manufacturers should consider those non-compulsory standards from the early periods of development too. After all, better compliance may increase competitiveness [2]. Until today, the agri-food domain has not seen such structured, specific standards. The increasing autonomy of robots and robotic systems used in the industry has reasonably enhanced certification challenges, only recently evolved standards have the potential to address the safety concerns of this new approach – in an application domain specific manner [3].

It is still an ongoing professional debate to unambiguously define what is a robot or a robotic system. However, efforts for standardization have been extensive in the robotics domain in the past three decades [4]. Traditionally, ISO standards have been providing guidance for safety of robots and robotic systems, and they have been forming the basis of the Machinery Directive [5]. The traditional ISO 8373 – Robots and robotic devices – Vocabulary standard under ISO was published first in 1996, only referring to robots as *Manipulating industrial robots*, but the document was later extended to all kinds of robots (in the ISO sense) [6]. To incorporate all new domains, forms and applications of robots, TC299, the Technical Committee of ISO responsible for this topic, has revised the official definition of robots numerous times in the past decades. The key factors distinguishing robots from other machinery are autonomy, mobility and task-oriented behaviour. The current ISO definition of a robot as per ISO 8373 is [7]:

> *Programmed actuated mechanism with a degree of autonomy to perform locomotion, manipulation or positioning.*

Wherein autonomy is defined as:

> *Ability to perform intended tasks based on current state and sensing, without human intervention.*

Another modern holistic definition of a *robot* from 2020 was given in the Encyclopedia of Robotics [8]:

> *A robot is a complex mechatronic system enabled with electronics, sensors, actuators and software, executing tasks with a certain degree of autonomy. It may be pre-programmed, teleoperated or carrying out computations to make decisions.*

Robotics is advancing rapidly in practically all professional service domains, entering recently to the agri-food industry and within that, the meat sector as well [9]. A prime example, the robot cell under development within the Ro-BUTCHER project (https://robutcher.eu) aims to carry out the primary cutting and manipulation tasks of a pig slaughtering [10, 11]. The general purpose industrial robots in the cell are supported by RGB-D cameras, Artificial Intelligence, Virtual Reality, intelligent EOAT (End of Arm Tooling), telemanipulation and Digital Twin technology [12–14]. Accordingly, the designed system will be unprecedented in complexity and autonomy from the safety and legislation aspects. The robots in the Meat Factory Cell (MFC) will handle raw meat products intended for human consumption autonomously, however the risk of contamination due to the presence of the gastrointestinal tract is high. On the other hand, the applied EOAT (grippers, knives and saws) are designed for meat and bone cutting and gripping, making them highly dangerous for humans. Under the current approach for classification within the related standards, the robot cell would be regarded as an industrial service robot application, meaning that it will still fall under the EC MD (2006/42/EC) when assessing the safety assurance of the system (Fig. 1).

This paper covers mainly the ISO standards, since they are commonly used in most sectors of the industry, practically world-wide accepted, and they have always been pioneers in the robotics field. Furthermore, ISO certification is often required by industrial customers due to its direct linkage to the EC MD. It is worth mentioning however, that ISO does not act as a Notified Body, meaning that they do not issue certificates, only participate in the process by developing the international standards. The two main options for conformity assessment – according to ISO – are the followings:

- **Certification** – the provision by an independent body in written assurance (a certificate) that the product, service or system in question meets specific requirements.
- **Accreditation** – the formal recognition by an independent body, generally known as an accreditation body that a certification body operates according to the international standards.

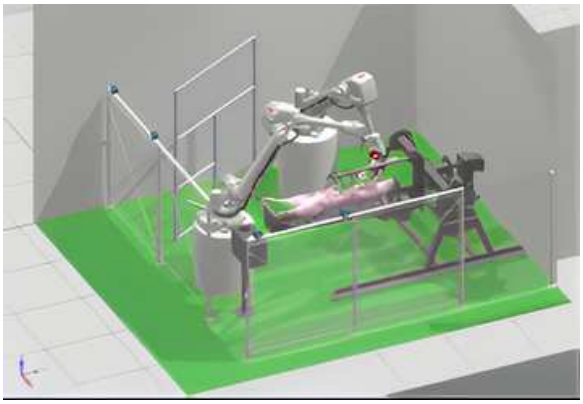

Figure 1
Conceptual setup of the autonomous pig processing cell in the RoBUTCHER project. The carcass is handled by the actuated CHU (Carcass Handling Unit), the intelligent EOATs (knife, gripper) are fixed on the industrial ABB robots along with an RGB-D camera. *Image credit: RoBUTCHER project, RobotNorge AS.*

The clear, unambiguous and consistent use of the frequently occurring words, technical terms and expressions in the robot industry is essential, especially when documents with potential legal force are concerned. ISO 8373 states that:

> *This International Standard specifies vocabulary used in relation with robots and robotic devices operating in both industrial and non-industrial environment.*

The standard was recently revised, the latest – third – version is ISO 8373:2021 that cancels and replaces the second edition originally from 2012) [7, 15]. Beside ISO standards, some important and relevant EU directives, guidelines and recommendations were also reviewed and will be summarized in this paper.

It is worth mentioning that a relevant Digital Innovation Hub (DIH), called agROBOfood was initiated in 2019, financed by the EU (https://agrobofood.eu/). Their motto being ”Connecting robotic technologies with the agri-food sector”, which means that they aim is to build a European ecosystem for adaptation of robotics and streamline standardization aspirations in Europe [16]. The agROBOfood consortium consists of 7 Regional Clusters involving 49 DIHs and 12 Competence Centers (as of late 2022), actively accelerating the agri-food sector’s digital transformation and robotization.

2 Industrial robotics applied in the meat sector

The automation in the meat industry has started long ago, however its pace is significantly slower compared to other industries. Machines dedicated to accomplish single tasks during the cutting processes were introduced in larger slaughterhouses

relatively early, however only some simple, straightforward cuts could be automated by these machines. Several examples of such machinery were used and published world-wide in the late 20th century, such as [17] about the modern lamb and beef industry solutions at plants at New Zealand, or the world-wide review of machinery and level of automation of the meat industry by G. Purnell [18].

Broader utilization of industrial robots and robot systems in the meat sector required the development of cognitive systems as well [19]. Nowadays several manufacturers sell commercial intelligent systems for slaughterhouses (e.g., Frontmatec, Marel, Mayekawa, etc.) and the related research activity is significant as well. Mark Seaton from Scott Technology Limited published their experience gained in the last decades in [20]. Their key finding is that product consistency is the paramount advantage of the implementation of their robotised solutions, but shelf life, general product quality and workers' safety can improve as well. Their solutions include, e.g., X-ray based cutting prediction, de-boning with industrial robots and bladesaw that stops under a millisecond. Several review papers were published about the current stage and possibilities of meat industry automation e.g., the paper of Romanov et al. about collaborative robot cells [21], or more general reviews by Khodabandehloo [22] or Esper et al. [12].

2.1 The RoBUTCHER project

The RoBUTCHER research project is funded by the EU, and aims to develop the first entirely automated pig processing robot cell [23]. Therefore, it has been a priority for the study project to establish the framework of guiding documents [24]. The robot cell will carry out all primary steps of the pig-slaughtering with industrial robot arms (according to the EC MD), including the cutting of all four legs, the splitting of the carcass and the evisceration process [10]. Beside the two robots, the cell consists of a motorized carcass handling unit (CHU), intelligent cutting and gripping tools, an RGB-D camera (fixed on one of the robots as well) and some other supplementary equipment (Fig. 1).

Modern image processing techniques are widely used in the meat sector to handle the natural variability of animals [25, 26]. The autonomous cutting begins with an imaging sequence, one of the robots moves the RGB-D camera (which is fixed on the shaft of the "smart knife" [27]) to pre-defined positions around the carcass. In a simulation environment (powered by Ocellus: *www.bytemotion.se*) a digital twin of the carcass is constructed from the images, where artificial intelligence (a set of image processing deep neural networks) calculates the desired gripping points and cutting trajectories on the carcass. Although the RoBUTCHER concept strictly rules out all kinds of collaborative behaviour between the machinery and humans, at this point, the supervising operator checks the predicted trajectories on the digital twin using Virtual Reality glasses [28]. They may accept the predicted cutting trajectories, request a new imaging and prediction, or may draw a 3D trajectory in the virtual environment that will be executed by the cutting robot. Thus – in optimal case – the cutting is performed completely without any interaction from human operators. Furthermore, even when the operator chooses to draw new trajectories there is no direct physical interaction, the robots and the operator never share the

same workspace. In case of maintenance or any issue within the MFC that requires physical intervention, protective fencing with sensors will ensure that all machinery shuts down while anyone is working inside the cell.

This fundamental approach in abattoir-automation introduces several different challenges, not only from the engineering and developing aspects, but also from the safety and legislative side of the development. Automation and generally the robot industry are especially fast evolving and ever-changing fields, and since working together (in a collaborative way) at any level with robots and/or machines is always potentially dangerous, several directives and strict standards apply to robotized solutions [21].

2.2 Guidance documents for safe industry applications

Since the employment of general-purpose robot arms in cell-based automated raw-meat handling or animal slaughtering is unprecedented, no single standard exists that would regulate all aspects of this scenario. To have a thorough view on this domain's standardization, the complete list of Robotistry was scanned for relevant standards, along with traditional online search engines (e.g., Google Scholar, IEEExplore etc.) [29].

An important document covering almost all aspects of robotics in the EU is the Robotics Multi-Annual Roadmap (MAR), which was also reviewed. However, automated slaughtering seems to be such a special part of robotics, that even the Robotics 2020 MAR does not cover it in detail [30]. The closest to slaughterhouse automation is the "Agriculture Domain" (Chapter 2.4), defined as:

> *Agriculture is a general term for production of plants and animals by use of paramount natural resources (air, water, soil, minerals, organics, energy, information).*

However, slaughtering itself does not appear in any of the subcategories (Fig. 2), animals are barely mentioned within the document. The only appearance of the meat sector is in the *Food* section under the *Manufacturing* sub-domains, where automation and machinery used for deboning and raw-meat handling are mentioned. This lack of recognition of the sector makes solution developers' task especially difficult.

In spite of not addressing the meat sector in depth, the recommendations in the "Safety design and certification" section are worth considering. Most of the statements and suggestions can be interpreted to the red meat domain too, although animal rights and animal welfare should always be kept in mind. The *Hardware in Loop* and the *Semantic Environment Awareness* sections contain interesting farming-related recommendations as well. The practical and beneficial application of simulations, planning systems, virtual models and semantic environment-representations are discussed, many of which are used in meat sector automation as well (and being used in the RoBUTCHER project).

The MAR document, however, only provides general guidelines, suggestions and best practises, while the certification is most crucial in the food industry. Therefore,

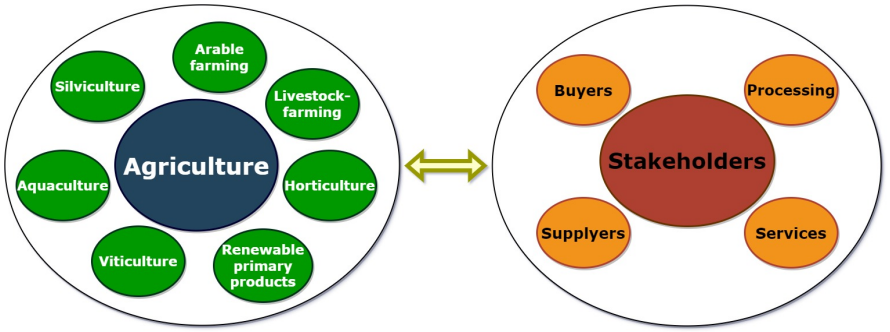

Figure 2
Simplified structure of agricultural production categories and stakeholders according to the Robotics 2020 MAR. Although the document mentions the meat sector within the agriculture section, it is not presented as a subcategory [30].

in this section, the relevant robot industry-related standards will be discussed.

ISO/IEC started to work on the integration of the new robotic application domains (e.g., collaborative robotics, medical robotics, self-driving cars) more than a decade ago. Numerous working groups (WGs) are active within the ISO/TC 299 Robotics Technical Committee, dealing with specific fields of robotics; e.g., *Electrical interfaces for industrial robot end-effectors* (WG 9), *Modularity for service robots* (WG 6) or *Validation methods for collaborative applications* (WG 8). One of the most important and fundamental standards for practically every modern industrial automation project is the ISO 12100 Safety of machinery – General principles for design – Risk assessment and risk reduction standard, its latest version is the ISO 12100:2010 [31]. The primary purpose of this standard is to provide engineers and system developers with an overall framework. The document acts as a guidance for decisions during the development of machinery, helping developers to design machines and whole systems that work safely while fulfilling their intended tasks. In spite of all this, at the beginning of the standard in the *Scope* section it is highlighted that:

> *It does not deal with risk and/or damage to domestic animals, property or the environment.*

It is, therefore, clear that this comprehensive standard does not encompass specific information or advice tailored for meat sector automation projects.

ISO 12100:2010 offers a classification of the related safety standards that helps the identification of more specific, relevant ISO standards. This classification of standard-types is used in this paper as well [31]:

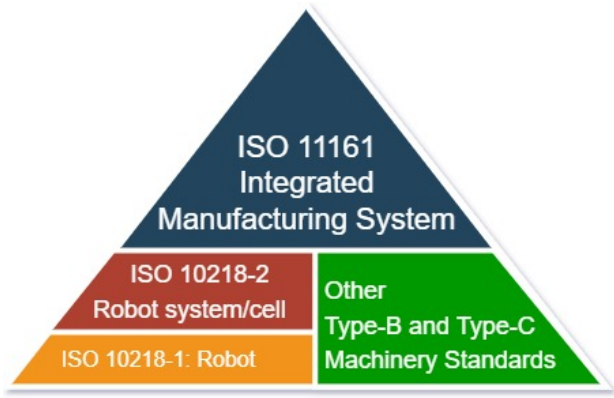

Figure 3
Graphical representation of hierarchy between standards related to robot system/cell. ISO 11161 as a Type-A standard is on the top level relying on several different Type-B and Type-C standards.

- **Type-A standards** (basic safety standards) giving basic concepts, principles for the design and general aspects that can be applied to machinery;
- **Type-B standards** (generic safety standards) dealing with one safety aspect or one type of safeguard that can be used across a wide range of machinery:
  - **Type-B1 standards** on particular safety aspects (e.g., safety distances, surface temperature, noise);
  - **Type-B2 standards** on safeguards (e.g., two-hand controls, interlocking devices, pressure-sensitive devices, guards);
- **Type-C standards** (machine safety standards) dealing with detailed safety requirements for a particular machine or group of machines.

In this sense, ISO 12100 is not specifically robotics-standard, rather a more comprehensive one (a type-A standard), covering a wide range of machinery design safety – including robotic applications too. It is, however, intended to be used as the basis for preparation of type-B and type-C safety standards as well, that should be more specific to a given application.

Regarding the given domain, presumably the most relevant type-B (more precisely type-B1) standard is the ISO11161:2007 Safety of machinery – Integrated manufacturing systems – Basic requirements [32]. As explained in its introduction, Integrated Manufacturing Systems (IMS) are very different in size, complexity, components, and they might incorporate different technologies that require diverse or specific expertise and knowledge, thus usually more specific (type-C) standards should be identified as well for a given application. As a consequence, this standard mainly describes how to apply the requirements of ISO 12100-1:2003, ISO 12100-2:2003 (and ISO 14121 Safety of machinery, which is currently inactive, due to its integration into ISO 12100) in specific contexts.

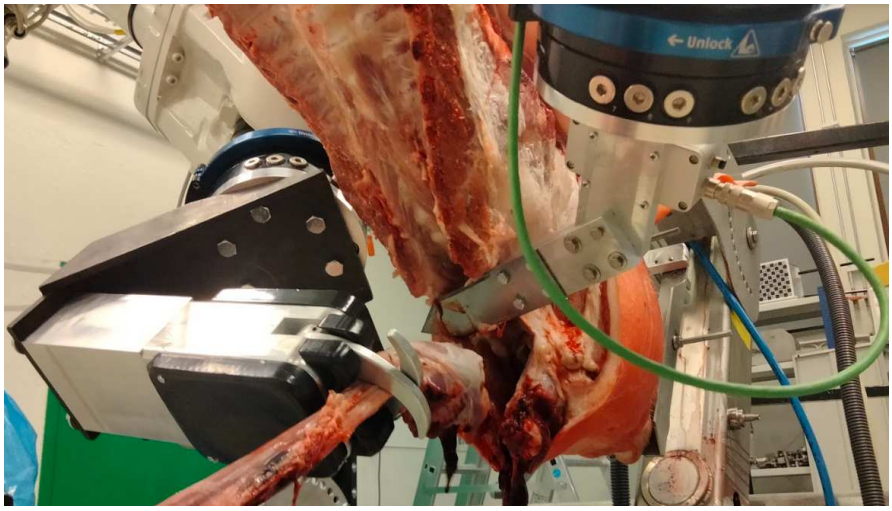

Figure 4
Typical intelligent EOAT for meat industry automation. The reinforced gripper with pointed claws and the sharp knife are ”by design” dangerous robotic tools, even when the robot is not moving. *Image credit: RoBUTCHER Project, Óbuda University & NMBU*

The ISO10218:2011 Robots and robotic devices – Safety requirements for industrial robots is a type-C standard, meaning that this document contains specific requirements and guidelines for system safety design that can potentially be used in meat sector automation projects. ISO10218:2011 consists of two main parts:

1. Part 1: Robots [33];
2. Part 2: Robot systems and integration [34].

While Part 1 only refers to the application of a single robot, Part 2 includes the peripheral elements connected to or working together with the robot(s) too. Part 2, in this sense, is typically more suitable for food-industry projects, since handling of carcasses and meat products usually requires complex EOAT and other external devices (e.g., sensors). Having more robots working together and/or employing external devices results in a “robot system”, thus the robot system specific problems (e.g., electrical connection between devices, overlapping workspaces, etc.) shall be considered too [35, 36]. Nevertheless, Part 2 of ISO10218:2011 naturally relies on information presented in Part 1, thus that should also be taken into consideration in all cases when Part 2 is being used. The relationship between the aforementioned ISO standards is shown in Fig. 3.

Another type-C standard, ISO/TR 20218-1:2018 Robotics – Safety design for industrial robot systems – Part 1: End-effectors should also be relevant. Meat-industry automation projects typically mean automated deboning and/or meat-cutting, both requiring sharp knives, saws and strong grippers, “potentially dangerous end-effectors” in the wording of the standard (Fig. 4.). Part 2 of ISO/TR 20218-1:2018 is about

manual load/unload stations. This standard offers suggestions for applications where hazard zones are established around the robot(s). In such cases, access restriction to hazard zones and ergonomically suitable work spaces might be important, however, this is not the case in the described autonomous scenario [37].

ISO/TR 20218-1:2018 Part 2 covers collaborative applications too, where human operators and robot systems share the same workspace. However, the recent increase of importance of collaborative robotics resulted in standalone standards for this new special field of robotics, the most significant ISO documents are ISO/TR 15066:2015 Robots and robotic devices – Collaborative robots and ISO/TR 9241-810:2020 Ergonomics of human–system interaction [38, 39]. Beside these specific standards there are several projects and activities offering new solutions and assistance for collaborative robot system development, such as the EU funded *COVR* project (https://safearoundrobots.com) [40].

Nevertheless, meat processing generally requires high payload robots, strong automated tools and single purpose machines that are intended to process and cut human-like tissues. The basic purpose of these devices self-evidently mean unacceptably high risk for any operator within the reach of the robots and the tools (the general workspace), regardless of how strict the safety regulations in place. Therefore, this paper (and the RoBUTCHER project) focuses on the completely automated slaughtering, telepresence of operators and strict physical perimeter guarding, excluding any type of collaborative work.

2.3 ISO 10218: Robots and robotic devices — Safety requirements for industrial robots

ISO 10218:2011 is arguably still the most important ISO standard in relevance of abattoir automation [33, 34]. The latest version of the standard was published in 2011 (more than 10 years ago), but a new version (with a new title: Robotics — Safety requirements) is currently under development and should be published soon. ISO 10218:2011 mainly offers guidelines and requirements for inherent safe design of machinery (focusing on robots), presenting protective measures, foreseeable hazards and suggestions to eliminate, or at least reduce the risks associated with them. In the standards' terms *hazards* are possible sources of harm, while the term *risk* refers to hazard exposure.

ISO 10218:2011 Part 1: Industrial robots focuses on individual industrial robots, while Part 2: Robot systems and integration discusses the safety of robot systems and their integration into a larger manufacturing system. The most crucial statement in the standard is that any robot application (or robot system) should be designed in accordance with the principles of ISO 12100 for relevant and predictable hazards. It is worth mentioning as well that the standard emphasizes the fact that – beside the several common and typical hazardous scenarios mentioned in the document – task-specific sources of additional risk are present in most applications that should be examined in detail by the developers as well.

ISO 10218 includes important annexes. Annex A presents a list of common significant hazards, classified by their types (mechanical, electrical, etc.). For better

understanding examples and potential consequences are presented along with the relevant clause in the standard for each hazard. According to the standard, a suitable hazard identification process should include risk assessment on all identified hazards. Particular consideration shall be given during the risk assessment to the followings:

- The intended operations of the robot, including teaching, maintenance, setting and cleaning;
- Unexpected start-up;
- Access by personnel from any directions;
- Reasonably foreseeable misuse of the robot;
- The effect of failure in the control system;
- Where necessary, the hazards associated with the specific robot application.

Risks shall be eliminated, or at least reduced mainly by substitution or by design. If these preferred methods are not feasible, then safeguarding or other complementary methods shall be employed. Any residual risks shall then be reduced by other measures (e.g., warnings, signs, training).

ISO 10218 also suggests solutions in many relevant topics, such as:

- robot stopping functions;
- power loss;
- actuating controls;
- singularity protection;
- axis limiting;
- safety-related control system performance.

Furthermore, the standard has a dedicated chapter (Information for use) to help preparing a useful and comprehensive documentation (called instruction handbook), using the suggested standard expressions, markings, symbols, etc.

Further lists, specific instructions and specific detailed descriptions can be found in the appendix of ISO 10218:

- Annex A: List of significant hazards;
- Annex B: Stopping time and distance metric;
- Annex C: Functional characteristics of three-position enabling device;
- Annex D: Optional features;
- Annex E: Labelling;
- Annex F: Means of verification of the safety requirements and measures.

Part 2 (Robot systems and integration) of ISO 10218 states that:

> *The design of the robot system and cell layout is a key process in the elimination of hazards and reduction of risks [34].*

Correspondingly, this part offers fundamental robot cell layout design principles, referring to different types of workspaces, physical limitations, perimeter safeguarding, manual intervention, human interfacing, ergonomics, etc.

Different components of typical robot systems might fall under the scope of other standards too, thus Part 2 of ISO 10218 provides a useful list of those:

- Equipotential bonding/earthing requirements (grounding): IEC 60204-1;
- Electric power: IEC 60204-1;
- Hydraulic power: ISO 4413;
- Pneumatic power: ISO 4414;
- Actuating control: IEC 60204-1;
- Emergency stop function: IEC 60204-1, ISO 13850, IEC 61800-5-2;
- Enabling devices: ISO 10218-1-Annex D.

2.4 ISO/TR 20218-1:2018 Robotics — Safety design for industrial robot systems — Part 1: End-effectors

ISO 20218-1:2018 is a relatively new TR (Technical Report) providing guidance for safe design and integration of EOATs. The standard covers end-effector design, suggested manufacturing principles, integration of an EOAT into a robot system, and necessary information for operation. Part 2 of ISO 20218 is dealing with manual load and unload stations that is out of scope for the red meat sector.

The standard's main suggestion is to avoid dangerous structures by design on EOAT, e.g., sharp edges and pointed corners. Nonetheless, knives and saws are indispensable tools of meat-processing robot systems, thus the only option is risk-minimization. Risk reduction in such cases is mostly solved by physical protective devices and built-in safety-related control systems. Commonly used examples for the latter include capabilities for force sensing, speed monitoring, presence sensing, emergency stop. Besides covering sharp and pointed EOAT, ISO 20218 has a dedicated section for grippers, highlighting grasp-type grippers (force closure and form closure types), magnetic grippers and vacuum grippers. Grasp-type and vacuum grippers are commonly used in the meat-industry too, the RoBUTCHER project employs smart grasp-type grippers as EOAT and arrays of vacuum grippers as part of the robot system as well [41].

ISO 20218 contains annexes as well, including references to potentially relevant other standards and presenting real risk assessment scenarios. Furthermore, there are suggestions with examples for safety-rated monitored stopping, gripper safety performance assessment and a table about potential hazards, their possible origins and consequences.

3 Food-safety standards

In food industry automation projects, hygiene aspects and general food-safety are almost as important concerns as the safety of operators and machinery. Despite the fact that this article focuses on the safety regulations of food-sector robotics, food-safety should be mentioned as well, since the two topics are obviously strongly related [42]. ISO 22000:2018 Food safety management defines food safety as [43]:

> *Assurance that food will not cause an adverse health effect for the consumer when it is prepared and/or consumed in accordance with its intended use.*

This comprehensive standard suggests the adoption of a Food Safety Management System (FSMS), claiming that it has a great potential in helping to develop a system's performance regarding food safety [44]. The most important benefits of introducing an FSMS are:

- The organization improves its ability to consistently provide safe products and food-related services that meet customer needs and satisfy all regulatory and statutory requirements;
- Identifying and addressing hazards associated with its products and services;
- The ability to demonstrate conformity to specified FSMS requirements.

The most general ISO standard in this topic is the ISO 22000:2018 Food safety management systems – requirements for any organization in the food chain [43]. The standard introduces a practical plan-do-check-act (PDCA) cycle in details, that shall be used at the development process of an FSMS. The PDCA should also be able to help with improving the FSMS's efficiency to achieve safe production and services along with fulfilling relevant requirements.

The technical segment of ISO 22000 specifies the implementation of the PDCA cycle, offers suggestions about the tasks of the organization, and clarifies the communication, operation and documentation that is required to preserve the safety operation. The standard also covers hazard control, analysis and assessment, emergency response, monitoring and measuring. Its last sections offer possibilities and methods for internal auditing, review of management systems and continuous long-term improvement.

As ISO 22000 is a comprehensive standard, it suggests potentially relevant more specific standards, as well as other important official documents, such as:

- ISO/TS 22002 Prerequisite programmes on food safety;
- ISO/TS 22003 Food safety management systems — Requirements for bodies providing audit and certification of food safety management systems;
- CAC/RCP 1-1969 General Principles of Food Hygiene;

4 Discussion

Although the number of machinery safety related standards for industrial robotics applications became rather large in the past decades, the selection for the fast growing domain of service robots is significantly smaller. Furthermore, there is no technically comprehensive standard for agri-food robotics applications, that would cover all safety aspects, and no specific standard that would cover meat industry automation. Regarding the automated meat processing applications with industrial robots (e.g., the Meat Factory Cell developed within the RoBUTCHER Project, see Fig. 1), the general suggestion of the ISO standards is to follow the minimum hazard principle by methodically identifying and eliminating (or at least reducing) the risk factors.

The most relevant ISO standard that was identified in this review is the ISO 10218, which is more than 10 years old, yet a new version is currently under development. According to this type-C standard, a systematic solution for safe design based on the existing relevant ISO standards should be possible to be given, even to novel, innovative robotic systems and applications. However, the Notified Body chosen to certify a new system might propose different or additional requirements. The adoption of already existing safety related guidelines from other domains e.g., from medical robotics, where safety requirements has been linked to the level of autonomy of a robotic system, to the food sector is currently the best-practise, and could be a beneficial method [3, 45]. Generally, the maximum safety control principle of a robot cell (e.g., development of advanced teleoperated systems instead of collaborative operations, especially when the robot cell contains remarkably dangerous tools) most likely will increase the applicability and deployability of such developments in the future.

It is also worth mentioning that despite the general public (and official bodies as well) increasing support for sustainability in development of robotic applications with regulations [46, 47], the appropriate guidelines for streamlined implementations are still missing [48]. Similarly, in spite of robot ethics becoming a general discussion topic, the establishment of proper standards and guidelines was just launched in the robotics and automation domains [49, 50].

5 Conclusion

Nowadays, it is clear that automation and robotization mean the long-term solutions for many services and industrial applications. However, due to the complexity of the tasks in the food industry (agriculture and meat-processing as well), in many cases, it is still necessary to have human operators in the workplace too. This new kind of collaboration between humans and autonomous robots has elevated need for new and adapting safety features, thus for associated safety guidelines and standards too. The development of such regulations are in their early stages yet, however – derived from the existing standards – implementation of safety features will remain the manufacturer's responsibility, as s*afety by design* is still the preferred design principle.

Acknowledgment

This work has received funding from the European Union's Horizon 2020 research and innovation programme under grant agreement No 871631, RoBUTCHER (A Robust, Flexible and Scalable Cognitive Robotics Platform).
P. Galambos's work is partially supported by Project no. 2019-1.3.1-KK-2019-00007, provided by the National Research, Development and Innovation Fund of Hungary.
T. Haidegger is a Bolyai Fellow of the Hungarian Academy of Sciences.
We acknowledge the assistance of RobotNorge AS with this topic as a partner in the RoBUTCHER project.

Abbreviations

The following abbreviations are used in this article:

CE	Conformité Européenne
CEO	Chief Executive Officer
DIH	Digital Innovation Hub
DoF	Degrees of Freedom
EC MD	European Commission Machinery Directive
EOAT	End of Arm Tooling
EU	European Union
FSMS	Food Safety Management System
IEC	International Electrotechnical Commission
IMS	Integrated Manufacturing System
ISO	International Organization for Standardization
MAR	Multi-Annual Roadmap
PDCA	Plan-Do-Check-Act
RGB-D camera	Red-Green-Blue-Depth camera
TC	Technical Committee
TR	Technical Report

References

[1] European Commission. CE marking, 2014. Accessed: 2022-10-29.

[2] A. Okanovic, B. T. Jokanovic, V. Dakovic, S. Vukadinovic, and J. S. Jesic. Innovating a model for measuring competitiveness in accordance with the challenges of industry 4.0. *Acta Polytechnica Hungarica*, 17:67–88, 2020.

[3] K. Chinzei. Safety of surgical robots and IEC 80601-2-77: The first international standard for surgical robots. *Acta Polytechnica Hungarica*, 16:171–184, 2019.

[4] T. Jacobs, J. Veneman, G. Virk, and T. Haidegger. The flourishing landscape of robot standardization. *IEEE Robotics & Automation Magazine*, 25:8–15, 03 2018.

[5] Directive 2006/42/EC of the European Parliament and of the Council of 17 May 2006 on machinery, and amending Directive 95/16/EC. Directive, European Parliament, Council of the European Union, 17/05/2006.

[6] ISO 8373:1994/COR Manipulating industrial robots — Vocabulary — Technical Corrigendum 1. ISO, International Organization for Standardization, 1996.

[7] ISO 8373:2021 Robots and robotic devices — Vocabulary. ISO, International Organization for Standardization, 2021.

[8] T. Haidegger. Taxonomy and standards in robotics. In O. K. Marcelo H. Ang and B. Siciliano, editors, *Encyclopedia of Robotics*, pages 1–10. Springer Nature, 2021.

[9] A. Khamis, J. Meng, J. Wang, A. T. Azar, E. Prestes, Á. Takács, I. J. Rudas, and T. Haidegger. Robotics and intelligent systems against a pandemic. *Acta Polytechnica Hungarica*, 18(5):13–35, 2021.

[10] O. Alvseike, M. Prieto, P. H. Bjørnstad, and A. Mason. Intact gastro-intestinal tract removal from pig carcasses in a novel meat factory cell approach. *Acta Veterinaria Scandinavica*, 62(1):1–5, 2020.

[11] European Comission. Horizon 2020 Project Information: A Robust, Flexible and Scalable Cognitive Robotics Platform , 2020, Accessed: 2022-09-05. *https://cordis.europa.eu/project/id/871631*.

[12] I. de Medeiros Esper, P. J. From, and A. Mason. Robotisation and intelligent systems in abattoirs. *Trends in Food Science Technology*, 108:214–222, 2021.

[13] I. de Medeiros Esper, O. Smolkin, M. Manko, A. Popov, P. J. From, and A. Mason. Evaluation of rgb-d multi-camera pose estimation for 3d reconstruction. *Applied Sciences*, 12(9), 2022.

[14] B. Takács, K. Takács, T. Garamvölgyi, and T. Haidegger. Inner organ manipulation during automated pig slaughtering—smart gripping approaches. In *2021 IEEE 21st International Symposium on Computational Intelligence and Informatics (CINTI)*, pages 97–102, 2021.

[15] ISO 8373:2012 Manipulating industrial robots — Vocabulary — Technical Corrigendum 1. ISO, International Organization for Standardization, 2012.

[16] C. Lokhorst, E. Pekkeriet, and G. Chatzikostas. agrobofood: A pan-european digital innovation hub network for robotics in agri-food systems, February 2020.

[17] G. Longdell. Advanced technologies in the meat industry. *Meat science*, 36(1-2):277–291, 1994.

[18] G. Purnell. Robotic equipment in the meat industry. *Meat science*, 49:S297–S307, 1998.

[19] N. Echegaray, A. Hassoun, S. Jagtap, M. Tetteh-Caesar, M. Kumar, I. Tomasevic, G. Goksen, and J. M. Lorenzo. Meat 4.0: Principles and applications of industry 4.0 technologies in the meat industry. *Applied Sciences*, 12(14):6986, 2022.

[20] M. Seaton. Lessons in automation of meat processing. *Animal Frontiers*, 12(2):25–31, 2022.

[21] D. Romanov, O. Korostynska, O. I. Lekang, and A. Mason. Towards human-robot collaboration in meat processing: Challenges and possibilities. *Journal of Food Engineering*, pages 111–117, 2022.

[22] K. Khodabandehloo. Achieving robotic meat cutting. *Animal Frontiers*, 12(2):7–17, 2022.

[23] A. Mason, I. Esper, O. Korostynska, T. Haiddegger, A. Popov, L. Christensen, and O. Alvseike. The meat factory cell: A new way of thinking for meat producers. In *2021 IEEE 21st International Symposium on Computational Intelligence and Informatics (CINTI)*, pages 91–96. IEEE, 2021.

[24] O. Alvseike, M. Prieto, K. Torkveen, C. Ruud, and T. Nesbakken. Meat inspection and hygiene in a meat factory cell – an alternative concept. *Food Control*, 90:32–39, 2018.

[25] S. Szabo and M. Alexy. Practical aspects of weight measurement using image processing methods in waterfowl production. *Agriculture*, 12(11):1869, 2022.

[26] M. Alexy and T. Horváth. Tracing the local breeds in an outdoor system–a hungarian example with mangalica pig breed. *IntechOpen*, 2022, DOI: 10.5772/intechopen.101615.

[27] A. Mason, D. Romanov, L. Cordova-Lopez, and O. Korostynska. Smart knife: Integrated intelligence for robotic meat cutting. *IEEE Sensors Journal*, 22(21):20475–20483, 2022.

[28] L. I. N. Hansen, N. Vinther, L. Stranovsky, M. P. Philipsen, H. Wu, and T. B. Moeslund. Collaborative meat processing in virtual reality: Evaluating perceived safety and predictability of robot approach. In *International Conference on Human Robot Interaction (HRI 2018)*. VAM-HRI, 2018.

[29] Robotistry.org. Aggregated standards list, 2015, Accessed: 2022-09-05. *http://robotistry.org/standards/StandardsList.html*.

[30] Robotics 2020 Multi-Annual Roadmap. Horizon 2020 Call ICT-2016 (ICT-25 & ICT-26).

[31] ISO 12100:2010 Safety of machinery — General principles for design — Risk assessment and risk reduction. ISO, International Organization for Standardization, November 2010.

[32] ISO 11161:2007 Safety of machinery — Integrated manufacturing systems — Basic requirements. ISO, International Organization for Standardization, May 2007.

[33] ISO 10218-1:2011 Robots and robotic devices — Safety requirements for industrial robots — Part 1. ISO, International Organization for Standardization, July 2011.

[34] ISO 10218-2:2011 Robots and robotic devices — Safety requirements for industrial robots — Part 2: Robot systems and integration. ISO, International Organization for Standardization, July 2011.

[35] M. Turanli and H. Temeltas. Multi-robot workspace allocation with hopfield networks and imprecise localization. *Acta Polytechnica Hungarica*, 17:169–188, 01 2020.

[36] S. Ross, O. Korostynska, L. Cordova-Lopez, and A. Mason. A review of unilateral grippers for meat industry automation. *Trends in Food Science Technology*, 119:309–319, 2022.

[37] ISO 20218-1:2018 Robotics — Safety design for industrial robot systems — Part 1: End-effectors. ISO/TR 20218-1:2018, International Organization for Standardization, August 2018.

[38] ISO 15066:2016 Robots and robotic devices — Collaborative robots. ISO, International Organization for Standardization, February 2016.

[39] ISO 9241-810:2020 Ergonomics of human-system interaction — Part 810: Robotic, intelligent and autonomous systems. Iso/tr, International Organization for Standardization, September 2020.

[40] J. Bessler, L. Schaake, C. Bidard, J. Buurke, A. Lassen, K. Nielsen, J. Saenz, and F. Vicentini. *Towards Simplified Evaluation and Validation of Collaborative Robotics Applications Across a Wide Range of Domains Based on Robot Safety Skills*, pages 123–126. 01 2019.

[41] K. Takács, A. Mason, L. B. Christensen, and T. Haidegger. Robotic grippers for large and soft object manipulation. In *2020 IEEE 20th International Symposium on Computational Intelligence and Informatics (CINTI)*, pages 133–138, 2020.

[42] M. Sødring, T. Thauland Håseth, E. Rasten Brunsdon, P. Bjørnstad, R. Sandnes, O. Røtterud, A. Mason, I. de Medeiros Esper, E. Hallenstvedt, P. Agerup, et al. Effects of meat factory cell on pork qualities, sensory characteristics and carcass hygiene: an exploratory study. *Acta Agriculturae Scandinavica, Section A—Animal Science*, pages 1–16, 2022.

[43] ISO 22000:2018 Food safety management systems — Requirements for any organization in the food chain. ISO, International Organization for Standardization, June 2018.

[44] A. Panghal, N. Chhikara, N. Sindhu, and S. Jaglan. Role of food safety management systems in safe food production: A review. *Journal of food safety*, 38(4):e12464, 2018.

[45] T. Haidegger. Autonomy for Surgical Robots: Concepts and Paradigms. *IEEE Transactions on Medical Robotics and Bionics*, 1(2):65–76, 2019.

[46] V. Mai, B. Vanderborght, T. Haidegger, A. Khamis, N. Bhargava, D. B. Boesl, K. Gabriels, A. Jacobs, A. Moon, R. Murphy, et al. The Role of Robotics in Achieving the United Nations Sustainable Development Goals. *IEEE Robotics & Automation Magazine*, 29(1):92–107, 2022.

[47] D. B. Boesl, T. Haidegger, A. Khamis, V. Mai, and C. Mörch. Automating the achievement of SDGs: Robotics enabling & inhibiting the accomplishment of the SDGs. pages 122–126, 2021.

[48] A. Mason, O. Korostynska, L. Cordova-Lopez, I. Esper, D. Romanov, S. Ross, K. Takács, and T. Haidegger. Meat factory cell: Assisting meat processors address sustainability in meat production. In *2021 IEEE 21st International Symposium on Computational Intelligence and Informatics (CINTI)*, pages 103–108, 2021.

[49] E. Prestes, M. A. Houghtaling, P. J. Gonçalves, N. Fabiano, O. Ulgen, S. R. Fiorini, Z. Murahwi, J. I. Olszewska, and T. Haidegger. The first global ontological standard for ethically driven robotics and automation systems. *IEEE Robotics and Automation Magazine*, 28(4):120–124, 2021.

[50] A. Khamis, H. Li, E. Prestes, and T. Haidegger. AI: a key enabler of sustainable development goals, part 1. *IEEE Robotics & Automation Magazine*, 26(3):95–102, 2019.

2022 Reviewers

Ádám, Norbert
Ameer, Iqra
Andoga, Rudolf
Andrieiev, Volodymyr
Antal, Attila
Antunović, Ranko
Arbuzov, Maxim
Ari, Lajos
Bago, Peter
Bains, Robert
Balas, Valentina Emilia
Balogh, Gábor
Baracskai, Zoltan
Baranyi, Aranka
Baranyi, Peter
Bárdos, Krisztina
Battyányi, Péter
Batyrshin, Ildar
Bednar, Peter
Bencsik, Andrea
Béres, Gábor
Berki, Borbála
Bilan, Yuriy
Biró, Piroska
Bodnár, Éva
Borgulya, Istvan
Borisov, Vadim
Brito, Pedro
Bucha, Jozef
Butka, Peter
Castro-Sánchez, Noé Alejandro
Chatterjee, Prasenjit
Chmielewska, Katarzyna
Chovancova, Eva
Costaguta, Rosanna
Csapo, Adam
Csernoch, Maria
Csiszárik-Kocsir, Ágnes
Cveticanin, Livija
Danaj, Adela
Dedera, Lubomir
Deveci, Muhammet
Dhir, Krishna
Dli, Maksim
Dobeš, Marek
Dobrilovic, Dalibor
Dömötör, Ferenc
Dubrovskaya, Tatsiana
Dudas, Laszlo
Eigner, György
Eremeyev, Victor A.
Esposito, Anna
Fábián, Enikő Réka
Fanfara, Peter
Farkas, Gabriella
Ferenci, Tamas
Filatov, Denis
Fischer, Szabolcs
Főző, Ladislav
Franklin, Francis
Garai-Fodor, Mónika
Gazdagh, Zoltan Gabor
Gelbukh, Alexander
Gomide, Fernando
Gonda, Viktor
Gonzalez-Mendoza, Miguel
Gyenge, Balázs
Hanka, Laszlo
Havrylov, Maksym
Herisanu, Nicolae
Hmelevska, Nelya
Holcsik, Peter
Horváth, Balázs
Horváth, Ildikó

Horváth, László
Horváth, Richárd
Hrabovsky, Jan
Hubar, Oleksii
Hurtuk, Ján
Iantovics, Laszlo Barna
Illyes, Laszlo
Ito, Atsushi
Izonin, Ivan
Jain, Amit
Jeremic, Dejan
Joós, Antal
Juhász, Erika
Kadar, Peter
Karácsony, Péter
Kasanicky, Tomas
Katai, Zoltan
Katona, Ferenc
Katona, Jozsef
Kelemen-Erdős, Anikó
Khabazian, Masoud
Kirpluks, Mikelis
Klyus, Oleh
Kocsis, Imre
Korcsmáros, Enikő
Kou, Lei
Koutsombogera, Maria
Kovács, László
Kovacs, Szilveszter
Kovács, Tünde
Kővári, Attila
Krajci, Stanislav
Kreinovich, Vladik
Kurhan, Dmytro
Kurhan, Mykola
Kyrarini, Maria
Labeckas, Gvidonas
Lakatos, István
Lámer, Géza
Lazanyi, Kornelia
Ledeneva, Yulia
Lendvai, László
Leško, Jakub
Lórencz, Róbert
Machová, Kristína
Machova, Renata
Máhr, Tamás
Majláth, Melinda
Marciniak, Mariola
Marinkovic, Dragan
Massel, Aleksei
Máté, Márton
Méndez-Gurrola, Iris Iddaly
Mikhailov, Mikhail
Milic, Dejan
Miranda, Sabino
Molnár, Bálint
Moreau, Erwan
Movahedi Rad, Majid
Nagy, Tamás
Neduzha, Larysa
Németh, Attila
Nemeth, Balazs
Németh, Szilárd
Nguyen, Phuong
Okstad, Eivind H.
Pavlovičová, Jarmila
Pekár, Adrián
Peter, Tamas
Péter, Tamás
Pintér, Éva
Pinter, Istvan
Pittman, Russell
Podvesovskii, Aleksandr
Pogatsnik, Monika
Pokorády, Károly
Popovics, Anett
Purgic, Sanel